CARDIOVASCULAR OUTCOMES OF NEONATAL RESPIRATORY DISEASE IN INFANTS AND CHILDREN

A thesis submitted in candidature for the degree of

Doctor of Philosophy

by

Chuen Yeow Poon

Department of Child Health

Cardiff University

Cardiff, Wales

UK

October 2015

To my wife, Ivy,

for your unconditional love, support and unwavering belief

Table of Contents

CARDIOVASCULAR OUTCOMES OF NEONATAL RESPIRATORY DISEASE IN INFANTS AND CHILDREN

Acknowledgements

I would like to thank my supervisors, Professor Sailesh Kotecha, Professor Alan Fraser and Professor Richard Wise, for their continued support, advice and encouragement, without which completion of this project would have been impossible. I am extremely grateful to Professor Kotecha for his advice and knowledge, and many insightful discussions and suggestions. He is my primary resource for getting my many questions answered and was instrumental in helping me crank out this thesis.

I am also very grateful to Dr Mark Drayton (University Hospital of Wales, Cardiff) and Dr Siddhartha Sen (Royal Gwent Hospital, Newport) for providing the list of prematurely born children and for writing to the families on behalf of the research team.

I would like to reserve a special thanks to my colleague, Mrs Julie Edwards for her help in recruiting subjects for both projects, performing the echocardiograms on the subjects and helped analysing the MRI images for the inter-observer variability of PA PWV analysis in children. I am very grateful for her help, patience and sacrificing her free time to ensure we complete our scanning during the weekends.

My knowledge in paediatric cardiology at the start of the research project was limited. Without the help of several colleagues from the Department of Paediatric Cardiology at University Hospital of Wales and the Wales Heart Research Institute at Cardiff University, I would never have learnt the art and science of echocardiography. I am immensely grateful to Dr Amos Wong and Dr Dirk Wilson for teaching me the practical skills of echocardiography from scratch and for allowing me to gain practical experience in their clinics, and to Dr Suchita Joshi and Professor Alan Fraser for

patiently teaching me everything I know about tissue Doppler echocardiography. I would also like to extend my gratitude to Suchita for her efforts in obtaining the research project and ethics approvals, and developing the research protocol for the 'Neonatal tissue Doppler study' prior to my starting my research project.

Professors Sailesh Kotecha and John Cockcroft have provided me with numerous ideas during the development of the research protocol for the 'PuSH MRI study' and I would like to thank them both for that. I was very fortunate to have had the opportunity to work with the Cardiff University Brain Research Imaging Centre (CUBRIC) team – Professor Richard Wise, Dr John Evans, Mr Peter Hobden, Dr Kevin Murphy, Dr Ashley Harris and Mrs Angela Reardon. I am very thankful to Professor Richard Wise, Dr Beverly Tsai-Goodman and Dr John Evans for their help with developing the MRI scanning protocol for the 'PuSH MRI study'. I am grateful to Mr Peter Hobden for his help with scanning the subjects and also ensuring that we scanned as many subjects as possible during the allocated time slots. Without the help of Dr Kevin Murphy and Dr Ashley Harris with the respiratory circuit and CO_2 monitoring for the 'PuSH MRI study', I would not have been able to perform and complete the project. I am very thankful for their help.

I would also like to thank Mrs Ann Russell for her help in recruiting subjects for the term-born control group. I am very grateful to Dr William Watkins for providing statistical advice whenever I need his help. I was very lucky to have Mrs Melanie Bullen, Mrs Nuri Karim, Mrs Nicola Benallick and all the wonderful administrative staff who were ever so helpful. I had truly wonderful office mates, Dr Suchita Joshi, Dr

Nicole Pickerd, Dr Sarah Kotecha, Dr Lesley Lowes, Mr John Lowe, Dr William Watkins and Dr Martin Edwards with whom I shared three and a half memorable years.

I especially thank my mother, father and brother. My hardworking parents have sacrificed their lives for my brother and myself and provided unconditional love and care. I love them so much, and I would not have made it this far without them.

The best outcome from these past years is finding my best friend, soul-mate, and wife. Ivy has been a true and great supporter and has unconditionally loved me during my good and bad times. She has been non-judgmental of me and instrumental in instilling confidence. She has faith in me and my intellect even when I don't. These past several years have not been an easy ride, both academically and personally. I truly thank Ivy for sticking by my side, even when I was irritable and depressed. I thank God for her.

I would also like to extend my gratitude to Mason Medical Research Grant and Children and Young People's Research Network Research Development Group for partly funding my studies.

Last but not the least I am sincerely grateful to all the children and their parents who participated in this study. Without the help of these families, this thesis would not have been completed.

Publications arising from this research

Poon CY, Kotecha S. Research in Practice: Assessment of pulmonary arterial haemodynamics by MRI in children born preterm. *Welsh Paed J* 2010;33:6-8

Poon CY, Edwards JM, Joshi S, Kotecha S, Fraser AG. Optimisation of myocardial deformation imaging in term and preterm infants. *Eur J Echocardiogr* 2011;12(3):247-254

Poon CY, Edwards MO, Kotecha S. Long term cardiovascular consequences of chronic lung disease of prematurity. *Pediatr Respir Rev* 2012;12(4):242-249

Poon CY, Edwards JM, Evans CJ, et al. Assessment of pulmonary artery pulse wave velocity in children: an MRI pilot study. *Magn Reson Imaging* 2013;31(10):1690-1694

Poon CY, Watkins WJ, Evans CJ, et al. Pulmonary arterial response to hypoxia in survivors of chronic lung disease of prematurity. (Accepted for publication to Archives of Disease in Childhood Fetal and Neonatal in Oct 2015)

Abstracts presented

Poon CY, Tsai-Goodman B, Wise RG, Cockcroft JR, Kotecha S. Pulmonary and systemic haemodynamics in children born preterm: an MRI study. Poster presentation. Children and Young People's Research Network meeting (Cardiff, 2 November 2009).

Poon CY, Evans J, Bolton CE, Cockcroft JR, Wise RG, Kotecha S. Pulmonary artery stiffness assessment in children born preterm using velocity encoded MRI. Poster presentation. British Association of Perinatal Medicine meeting (Cardiff, 10 August 2012)

Poon CY, Tsai-Goodman B, Wise RG, Cockcroft JR, Kotecha S. Main PA stiffness assessment in children born preterm using velocity-encoded MRI. Oral presentation. Children and Young People's Research Network / Academic Paediatrics Association Annual Conference (Cardiff, 8 October 2012).

Poon CY, Wise RG, Cockcroft JR, Kotecha S. Pulmonary arterial reactivity to hypoxia in survivors of chronic lung disease of prematurity. Oral presentation. Welsh Paediatric Society 40th Anniversary Autumn meeting (Wales, 6 November 2013)

List of commonly used abbreviations

AT	Acceleration time
bl	basal lateral
BPD	Bronchopulmonary dysplasia
bs	basal septal
CD	Computational distance
CI	Cardiac index
CLD	Chronic lung disease of prematurity
CO	Cardiac output
CO_2	Carbon dioxide
CV	Coefficient of variation
CYP	Chuen Yeow Poon
Ds’	Annular displacement measured using tissue tracking
ε	Myocardial strain
ET	Ejection time
FiO_2	Concentration of inhaled Oxygen
fps	frames per second
IVC	Inferior vena cava
IVRT	Isovolumic relaxation time
JME	Julie M Edwards
LA	Left atrium
LMA	Lateral mitral annulus
LV	Left ventricle
LVOT	Left ventricular outflow tract
Mitral E	Early diastolic flow through the mitral valve

Mitral A	Late diastolic flow through the mitral valve
MMA	Medial mitral annulus
MRI	Magnetic resonance imaging
MVI	Myocardial velocity imaging
NS	Not significant
O_2	Oxygen
PA	Pulmonary artery
PAH	Pulmonary arterial hypertension
PaO_2	Partial pressure of Oxygen
PAP	Pulmonary arterial pressure
PEP	Pre-ejection period
PR	Pulmonary regurgitation
PT	Preterm
PVR	Pulmonary vascular resistance
PWV	Pulse wave velocity
RA	Right atrium
RDS	Respiratory distress syndrome
ROI	Region of interest
RV	Right ventricle
SaO_2	Oxygen saturation measured by pulse oximetry
SD	Standard deviation
sPAP	Systolic pulmonary arterial pressure
SRa	Myocardial diastolic strain rate during atrial contraction
SRe	Myocardial early diastolic strain rate
SRs	Myocardial systolic strain rate

Ss	End-systolic strain at the middle segment of the wall
Ssl	End-systolic strain at the middle segment of the lateral wall
Sss	End-systolic strain at the middle segment of the septum
SVR	Systemic vascular resistance
TDI	Tissue Doppler imaging
TR	Tricuspid regurgitation
Vabl	Late diastolic velocity at the basal segment of the lateral wall
Vabs	Late diastolic velocity at the basal segment of the septum
Ve’	Annular velocity measured by real time pulsed tissue Doppler
Vebl	Early diastolic velocity at the basal segment of the lateral wall
Vebs	Early diastolic velocity at the basal segment of the septum
Vsbl	Systolic velocity at the basal segment of the lateral wall
Vsbs	Systolic velocity at the basal segment of the septum
VTI	Velocity time integral
wks	weeks

Symbols used to indicate significant differences between groups in Neonatal TDi study

$p < 0.05$ †(PT RDS V PT control), ††(PT RDS V Term control), †††(PT control V Term control)

$p < 0.01$ ‡(PT RDS V PT control), ‡‡(PT RDS V Term control), ‡‡‡ (PT control V Term control)

$p < 0.001$ §(PT RDS V PT control), §§(PT RDS V Term control), §§§(PT control V Term control)

List of tables

List of figures

Figures **Page No**

List of appendices

Abstract

The aim of this thesis is to compare effects of respiratory distress syndrome (RDS) on the myocardial function of newborn preterm infants and the later effects of chronic lung disease of prematurity on pulmonary artery stiffness in school age children.

The first study in this thesis compared global and regional myocardial function in preterm infants with respiratory distress syndrome (RDS) with preterm and term-born controls (30 with RDS, 30 preterm control ≤34 weeks, 60 term control) using conventional and tissue Doppler echocardiography at birth, at term, one month, and one year of age. The second study compared the pulmonary artery stiffness, an early preclinical marker of pulmonary hypertension, in children (aged 8-12 years) who had chronic lung disease of prematurity (CLD) with preterm and term-born controls. Pulmonary artery pulse wave velocity (PA PWV) was assessed in 59 children: 13 with CLD, 21 preterm (≤ 32 weeks gestation) and 25 term controls) using velocity encoded MRI technique while breathing room air and after 20 minutes of breathing 12% oxygen.

At birth, infants with RDS had lower pulmonary artery AT:ET ($p<0.001$), long axis shortening ($p<0.01$), RV systolic velocity ($p<0.001$) and higher TR ($p<0.01$) compared to preterm and term control groups. The preterm groups was also noted to have diastolic dysfunction (lower mitral E:A) at birth ($p<0.001$). At term corrected age, pulmonary artery AT:ET was still lower in the RDS group but no differences detected in TR between the groups. There were no differences in all parameters measured between the groups at one month and one year.

PA PWV was similar in all three groups at baseline when assessed at school age. However, following hypoxic challenge, PA PWV in children who had CLD increased significantly compared to preterm ($p=0.025$) and term controls ($p=0.042$).

The findings in this thesis suggest that infants with RDS had mildly elevated pulmonary arterial pressure as a result of milder respiratory disease with improvement in antenatal and neonatal care. The RV global dysfunction in infants with RDS resolved with resolution of the respiratory condition. Both preterm groups underwent postnatal maturation of myocardial function and caught up with the term control group by one month corrected age. At school age, children who had CLD displayed increased pulmonary vascular reactivity to hypoxia and are at greater risk of developing pulmonary hypertension earlier.

(Word count: 381)

Chapter One:

General Introduction

My thesis focused on the effects of neonatal lung disease secondary to surfactant deficiency as a result of extreme prematurity on the cardiovascular system during the neonatal period, in infancy and later on at school age. In my studies, I used conventional and the novel myocardial velocity imaging to assess the effects of respiratory distress syndrome on the myocardial function and pulmonary pressure in preterm infants. In addition to using echocardiography, I have also used velocity-encoded magnetic resonance imaging to study the stiffness and reactivity of the pulmonary artery in children aged 8-12 years who had chronic lung disease of prematurity.

Therefore, discussed below are the developments of the cardiorespiratory systems, haemodynamic changes following delivery, effects of preterm births on the cardiorespiratory systems, review of different echocardiographic parameters and the use of magnetic resonance imaging in the assessment of pulmonary hypertension.

1.1 Development of the cardiopulmonary system

1.1.1 Lung growth and development

The human lungs go through five different stages in their developments (Table 1.1); embryonic (3-7 weeks), pseudoglandular (7-16 weeks), canalicular (16-26 weeks), saccular (26-36 weeks) and alveolar (36 weeks to 2 years) (Burri 1984, Zeltner 1987). The primary respiratory acini consisting of respiratory bronchioles, alveolar ducts and rudimentary alveoli develop during the late canalicular stage of lung development. During the saccular stage, the airspaces branch and expand to form saccules, surfactant is synthesized by type II cells and capillaries becomes closely associated with type I cells. Alveolar formation, maturation and proliferation occur during the alveolar stage resulting in a significant increase in the surface area for gas exchange (Zeltner 1987, DiFiore 1994).

The formation of primary respiratory acini is the critical period of lung development when gas exchange can occur and determines the limit of viability of preterm birth. Infants born extremely preterm (≤28 weeks gestation) are at the late canalicular or early saccular stages of lung development, where gas exchange is inefficient, and are at risk of dysregulated alveolarisation. Antenatal corticosteroids administration accelerates lung maturation and increases surfactant production (Ballard 1972, Liggins 1972) but caution is required for their long term consequences on lung growth and neurodevelopment especially after repeated courses of treatment antenatally (Johnson 1981).

Table 1.1 - Stages of lung growth

Stage	Time	Events
Embryonic	0-7 wks	Formation of trachea, right and left main bronchi and segmented bronchi; vasculogenesis around airway buds
Pseudoglandular	7-17 wks	Differentiation of epithelial cells, formation of conduction airway and terminal bronchioles, formation of pulmonary arteries and veins
Canalicular	17-26 wks	Formation of respiratory bronchioles, alveolar ducts and primitive alveoli, differentiation of type I and type II pneumocytes and formation of alveolar capillary barrier
Saccular	26-36 wks	Increment in gas exchange areas, further differentiation of type I and type II cells
Alveolar	36 wks- 2 yrs	Septation and multiplication of alveoli
Microvascular	Birth to 2-3 yrs	Fusion of double alveolar capillary network into single layer

(Joshi 2007)

1.1.2 Development of the heart and pulmonary vessels

The heart and the two great vessels develop from the third week of conception and are fully formed by week ten of pregnancy. The fetal heart first develops as a tubular structure before undergoing morphological changes to form the final four chamber structure and the inflow and outflow tracts (Moorman 2003). By week five of pregnancy, the fetal heart begins to beat.

The developing tubular heart consists of three areas; the cranial, caudal and bulbus cordis, which develop into different parts of the aorta and the ventricles (van den Hoff 2001). As the heart rapidly expands, it assumes an S shape as it loops over on itself and bends to the right, known as d-looping, creating a primitive area where the ventricle will grow (van den Hoff 2001). In the two-chambered stage, the endocardial cushion acts as a valve between the atria and ventricular areas. The atria, which are formed from the dilation of the heart tube, divide first, creating a three-chambered heart consisting of two atria, the top chambers and one ventricle, the lower chamber (Anderson 1999). By week ten of pregnancy, the heart has formed, with two atria and two ventricles and two great blood vessels to carry the blood from the heart, the aorta and pulmonary artery.

The pulmonary vessels develop at the same time as the airways and grow by outgrowth from the existing vessels, a process called angiogenesis (Hislop 2002). Around each lung bud there is a capillary network that connects cranially to the aortic sac of the heart and caudally to the prospective left atrium (deMello 1997). The peripheral arteries grow along the newly formed airways by new vessel formation or vasculogenesis in the pulmonary mesenchyme (Hislop 2005). The increase in cell multiplication within the

mesenchyme is influenced by the growth factor, vascular endothelial growth factor (VEGF).

Animal studies have shown that VEGF, an angiogenic growth factor that is essential for vascular development, plays an important role in normal alveolar development (Jakkula 2000). Decreased levels of VEGF protein have been found in lung tissues of infants who died from chronic lung disease of prematurity (CLD) but not consistently (Bhatt 2001b, Currie 2001, Lassus 2001b). These findings lead to the hypothesis that disruption of normal lung angiogenesis may contribute to dysregulated alveolarisation as observed in CLD; the "vascular hypothesis" of lung development (Abman 2001).

During the canalicular phase of lung development, the mesenchyme around the airways thins and the capillaries become closely or intimately apposed to the epithelium, which will later differentiate into type I and II pneumocytes (DiFiore 1994). This reduction in distance between the future air-blood interfaces is vital for gas transfer postnatally. During the alveolar development, alveoli are formed from the developing septa within a double capillary network which then coalesce to form a single capillary sheet (DiFiore 1994). This process continues postnatally and can continue well into childhood, albeit at a decreased rate. Once the capillary network fuses into a single layer, new alveoli cannot be formed.

There are other factors that influence the pulmonary vessel development. Besides VEGF, other angiogenic growth factors and cytokines such as transforming growth factor β1, connective tissue growth factor, interferon-γ, platelet endothelial cell adhesion molecule-1, interleukin-6 and interleukin-8 can either suppress or promote

pulmonary vessel and alveolar development (Chakraborty 2010). Hyperoxia and pulmonary inflammation have been found to influence the abnormal alveolar development in preterm infants developing CLD (Jobe 1999).

1.1.3 Myocardial development during the second and third trimester

After the formation of the heart by the tenth week of pregnancy, the heart grows in weight and size through hyperplasia of the myocytes. A study of sheep showed that the normal growth of the fetal heart is accomplished by hyperplasia as the increase in myocardial mass was associated with minimal increase in myocyte diameter (Smolich 1989). This is in stark contrast to the increase in myocardial mass that is achieved exclusively by hypertrophy during the postnatal period (Smolich 1989). There is little evidence for myocyte hyperplasia beyond the first month of life (Oparil 1984). A preterm infant would have less myocytes, the contractile elements of the heart, at birth compared to the term infant (Friedman 1972). During the postnatal myocardial development of a preterm infant, if the heart weight increases normally in relation to the body weight, the increase in myocardial mass would be the result of a greater increase in hypertrophy of the myocytes than normal (Rudolph 2000). If the myocytes were already hypertrophied, there would be a limitation in the reserve for further increase in myocyte size in response to stimuli, such as increased pulmonary or systemic vascular resistance and increased volume load, which would invoke cardiac hypertrophy (Rudolph 2000).

The neonatal heart is less compliant compared to the adult heart. This is due to the relatively high content of total collagen in relation to the myocytes and also the increased ratio of type I collagen to type III collagen within the heart (Marijianowski

1994). This combination results in a more rigid and a less compliant ventricle in immature and preterm infants (Marijianowski 1994). In view of this, preterm infants are less able to cope with excessive volume load as the ventricles are not able to stretch and accommodate the extra volume, predisposing them to heart failure (Marijianowski 1994).

The combination of reduced myocyte numbers and decreased compliance of the preterm infants heart predisposes them to impaired cardiac function should they encounter the complications of extreme prematurity such as RDS, PDA, sepsis and intraventricular haemorrhage.

As the fetus approaches term, the overall amount of collagen decreases in relation to the total heart mass (Marijianowski 1994). The ratio of type I to type III collagen within the myocytes also decreased with gestation although the ratio does reach adult level until the age of 12 years (Marijianowski 1994).

1.2 Haemodynamic changes from fetal to neonatal life

1.2.1 Haemodynamics in fetal life

In the fetus, gas exchange occurs in the placenta. Deoxygenated blood from the fetus arrives at the placenta via the umbilical arteries and the umbilical vein carries oxygen rich blood back into the fetal circulation. The fetal circulation has multiple adaptations to divert the oxygenated blood from the less functioning organs such as lungs, liver, kidney and intestine as the placenta performs their functions, to the brain and heart. This

is achieved through the three vascular shunts within the fetal cardiovascular system and a tissue flap known as the Eustachian valve.

Approximately 50-60% of the oxygen rich blood from the placenta is diverted from the liver circulation into the inferior vena cava (IVC) via the ductus venosus (Bellotti 2000). In the IVC oxygenated blood from the umbilical vein (80-90% oxygen saturation) and the desaturated blood (25-40% oxygen saturation) from the lower limbs and abdominal organs including the liver stream separately towards the right atrium (RA) (Dawes 1954). At the junction of the IVC and the RA, the Eustachian valve directs the more oxygenated blood that was streaming in the dorsal aspect of the IVC across the foramen ovale into the left atrium (LA) (Edelstone 1979). This blood is mixed with deoxygenated blood from the lung circulation in the LA and the oxygen saturation is around 65% (Dawes 1954). The blood then enters the left ventricle (LV) to be ejected into the ascending aorta. The brain and heart receive the majority of the blood from the LV. The preferential shunting via the foramen ovale ensures oxygen rich blood is delivered to the vital organs.

The desaturated blood from the IVC and superior vena cava flows into the RA and is directed into the right ventricle (RV) through the tricuspid valve (Dawes 1954). The pulmonary circulation only receives 12% of the blood ejected out from the RV due to the high pulmonary vascular resistance (PVR) (Rudolph 1979). The high muscle resting tone and low oxygen tension within the collapsed alveoli all contribute to the high PVR. The remaining RV output is shunted across the ductus arteriosus into the descending aorta to supply relatively desaturated blood to the lower half of the body and eventually return to the placenta (Rasanen 1996, Mielke 2001). (Figure 1.1)

The fetal circulation is capable of transporting oxygen at lower saturation levels due to the presence of high levels of fetal haemoglobin (HbF) (Rudolph 1979). Fetal haemoglobin has a greater affinity for oxygen than normal haemoglobin. This leftward shift of the oxygen dissociation curve enhances oxygen uptake despite low placental oxygen levels. In addition to the presence of HbF, the fetus also has a high haemoglobin concentration, between 16 – 18 g/dL at term to ensure maximum oxygen carrying capacity.

Figure 1.1 - The fetal circulation

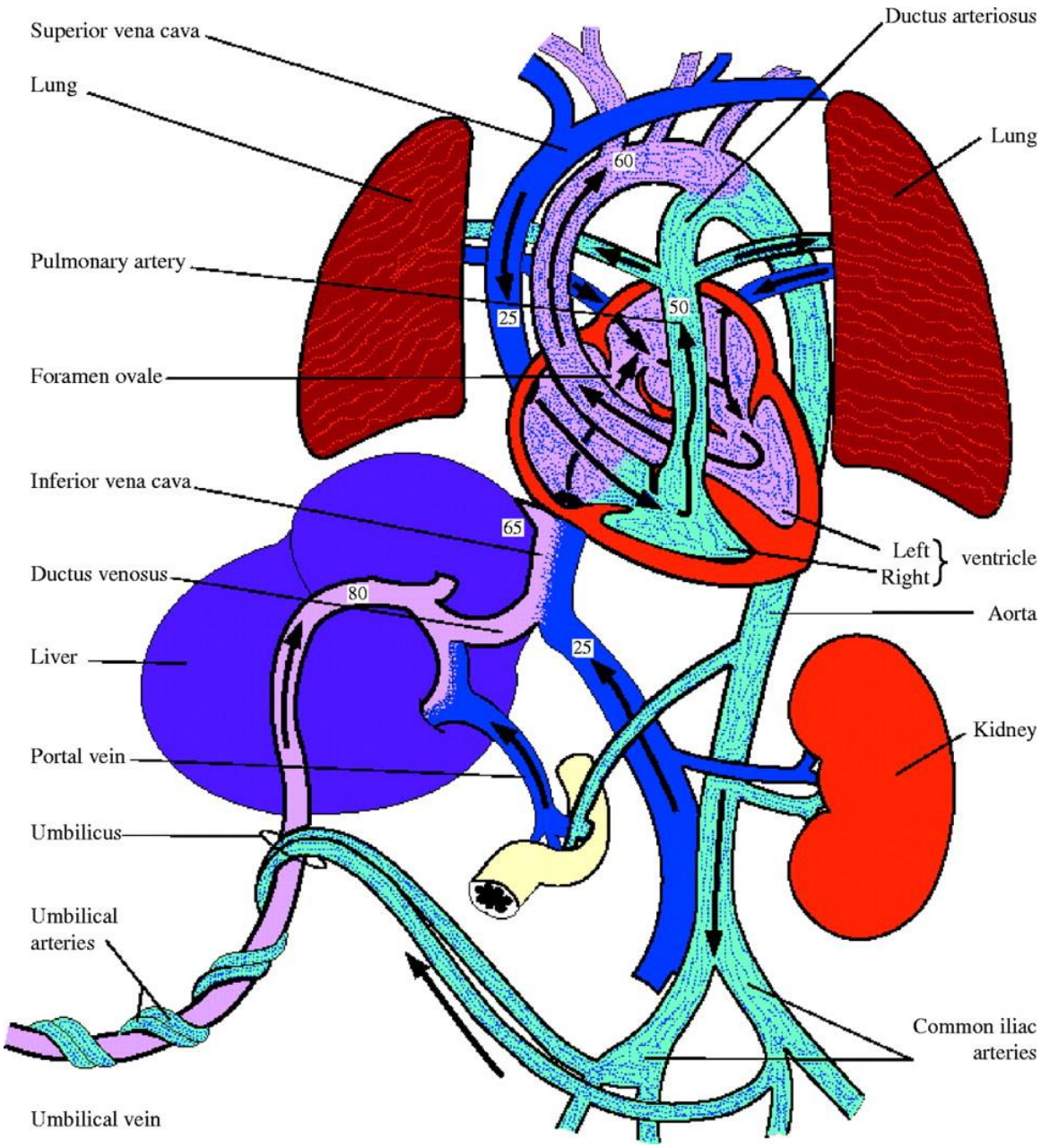

The fetal circulation – this diagram shows the circulation of the fetus highlighting oxygen rich blood delivered from the umbilical vein into the right atrium via the ductus venosus. The numbers within the vessels represent the estimated oxygen saturations of the blood within the blood vessels

(Murphy 2005)
(Reprinted with permission of Oxford University Press)

1.2.2 Transition from fetal circulation to neonatal circulation

Several cardiovascular adaptations have to occur as the fetus begins the transition into postnatal life. The fetal lungs have to take over the gas exchange role from the placenta, the fetal circulatory shunts must close and the left ventricular output must increase. At birth, the placental circulation is interrupted with the clamping of the umbilical cord. As a result, blood flow through the ductus venosus falls dramatically and the ductus eventually closes within one week after birth. The venous return to the RA is reduced significantly as a result.

The lungs become expanded and aerated with the first breath and these result in a dramatic fall in PVR with up to ten-fold increase in pulmonary blood flow (Saunders 1978, Hooper 2005). The fall in PVR is attributed to lung expansion opening up pulmonary vessels and reversal of pulmonary vasoconstriction due to improved oxygenation of the neonatal blood (Teitel 1990, Hooper 2005, te Pas 2008). The increase in pulmonary blood flow leads to an increase venous return to the LA (Rudolph 1979). The concurrent rise in LA pressure and fall in RA pressure described above leads to a physiological closure of the foramen ovale within minutes to hours after birth (Rudolph 1979). The anatomical closure occurs later via fusion of the septum primum and septum secundum.

As a result of the fall in PVR, flow across the ductus arteriosus becomes bi-directional. The high oxygen tension in the neonatal blood and the fall in placental produced prostaglandin results in smooth muscle constriction within the duct. Similar to the foramen ovale, the functional closure of the ductus arteriosus occurs by 96 hours and

anatomical closure occurs later through endothelial and fibrous proliferation. (Figure 1.2)

However, in the event where the ductus fails to close as seen in up to 50% of extremely low birth weight infants (Schmidt 2001b), the direction of shunting of blood between the systemic and pulmonary circulations depends on the size of the duct and the differences in the pressures and impedances of the respective circulations. Data indicate that a large ductal diameter is associated with decreased SVC flow at 5 hours of postnatal life; however, this effect is no longer observed at 24–48 hours after delivery (Kluckow 2000b). To compensate for the decreased systemic blood flow resulting from the left-to-right shunting via the PDA, the preterm myocardium adapts with a limited increase in contractility and left ventricular output (LVO). Due to the limited compensatory increase in LVO, decreased systemic perfusion in the lower body, indicated by reversed diastolic flow in the descending aorta, has been demonstrated in preterm neonates with a large PDA (Groves 2008). This effect was observed starting at 4 hours after delivery, with nearly half of the neonates being affected by 24 hours of age. Similar findings were reported in preterm neonates with RDS (Shimada 2003). As discussed in previously, the preterm ventricle is not very compliant and therefore, will not be able to increase the left ventricular end-diastolic volume significantly to compensate for the increased venous return from the pulmonary circulation (Schmitz 2004a). Consequently, the left atrial pressure increases with subsequent increase in pulmonary venous pressure.

The increased shunting of blood from the systemic circulation to the pulmonary circulation would increase the right ventricular afterload. This would have a detrimental

effect on the right ventricle of the preterm infant with RDS as this would have increased the workload of an already strained ventricle.

Figure 1.2 - The neonatal circulation

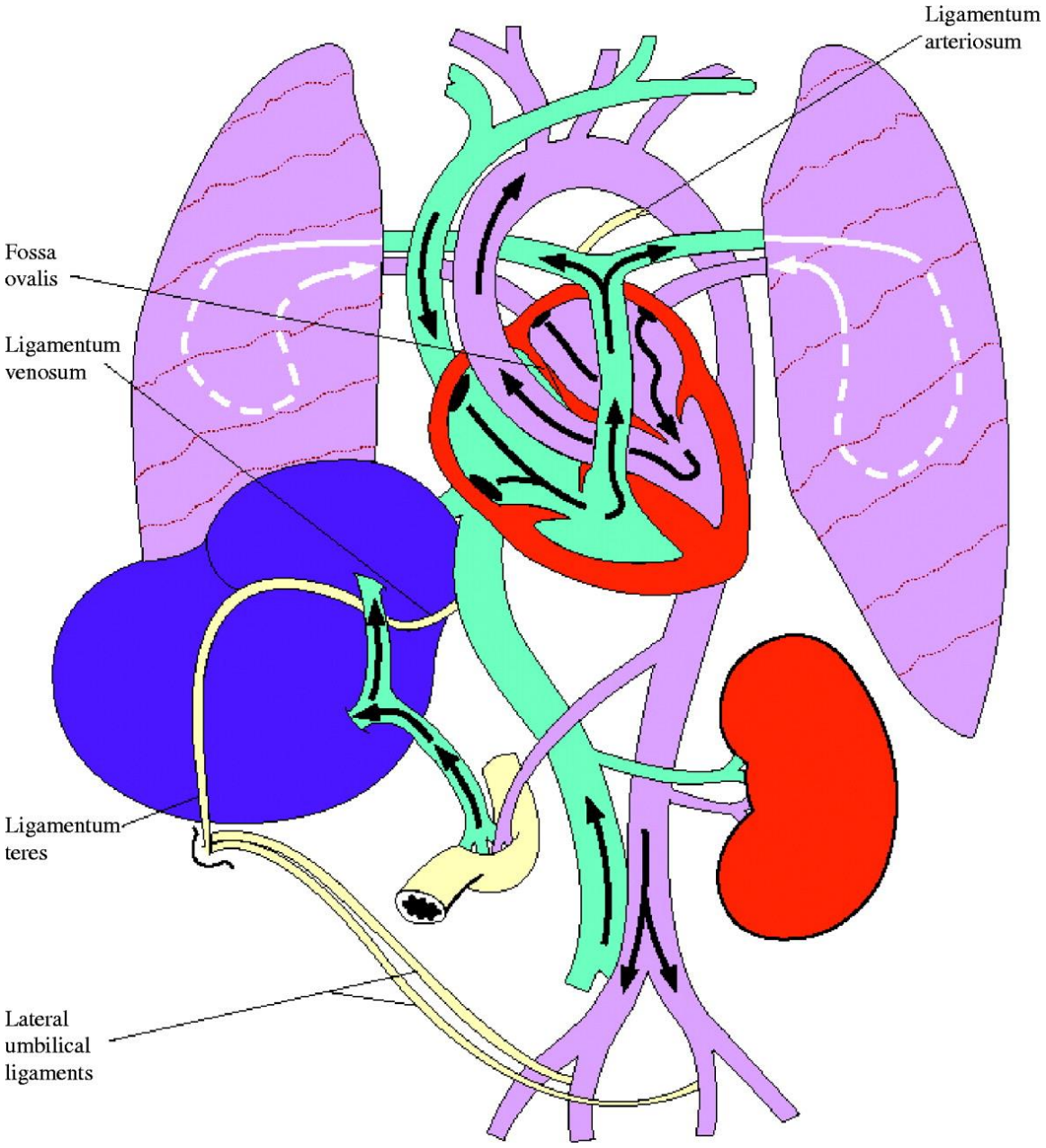

The neonatal circulation – this diagram shows the postnatal circulation highlighting the change from a paralell to serial circulation as a result of the closure of the three vascular shunts that were present in-utero.

(Murphy 2005)
(Reprinted with permission of Oxford University Press)

1.2.3 Failure of postnatal adaptation in preterm infants

1.2.3.1 Haemodynamics in postnatal life of preterm infants

In a healthy term infant, the pulmonary vascular resistance normally falls precipitously during the first day after birth (Skinner 1991). This coincides with the significant increase in systemic vascular resistance following clamping of the umbilical cord, disconnecting the placenta from the circulation. These infants do not have any significant right to left ductal shunt after 12 hours of age (Walther 1992) and physiological closure of the duct occurs at 24 hours of age (Walther 1993). The left ventricular output peaks between 30 minute and 2 hours after birth as a result of increased pulmonary blood flow. After peaking at 2 hours, the left ventricular output then decreases steadily and stabilizes at 8 hours postnatally (Walther 1993) to approximate the values seen in one week old term infants (Walther 1985).

In the preterm infants, the time taken to transition between fetal to postnatal circulation varies and differs from those of healthy term infants. The timing for ductus arteriosus constriction and subsequent closure also varies. The ductus remains open for longer in the majority of preterm infants and during the early postnatal period, the ductus actually increases in size in infants following surfactant treatment (Sehgal 2010). The increase in ductal shunting results in increased pulmonary blood flow, pulmonary oedema, increased ventilatory requirements and an increase in systolic but a reduction in diastolic blood pressure (Kluckow 2000a).

Preterm infants are particularly susceptible to haemodynamic instability and hypotension in the first 24 hours postnatally, in addition to the reduction in systemic

blood pressure secondary to ductal shunting (Kluckow 2000a). The immature myocardium of preterm infants has very limited capacity to increase ventricular output due to decreased compliance of the ventricle and decreased proportion of contractile elements (Friedman 1972).

1.2.3.2 Postnatal adaptation failure in preterm infants

Newborn infants undergo significant haemodynamic changes during the transition from fetal to neonatal life. At birth, the aeration of the lungs and improved oxygenation of neonatal blood result in a dramatic fall in pulmonary vascular resistance (Rudolph 1979). The pulmonary vascular resistance in preterm infants with neonatal or respiratory distress syndrome (RDS) remains elevated and there is evidence of right to left shunting across the ductus arteriosus (Walther 1992). Preterm neonates with severe respiratory disease have near systemic pulmonary artery pressures, reduced lung vascular perfusion and large right-to-left shunts at 12 hours of age. For those with mild to moderate RDS, the pulmonary pressure falls following surfactant therapy with improvement of pulmonary blood flow at 24 hours following birth (Walther 1992).

Preterm infants have a higher surface area to body mass ratio and are at higher risk of developing hypothermia. Hypothermia, along with hypoxia, hypercarbia, acidosis, and failure of lung expansion, will disrupt or reverse the normal transition from fetal to neonatal circulation (Toubas 1978, Abman 1989, Cornish 1994). Surfactant deficiency and immature pulmonary parenchyma and vessel development will exacerbate the situation. Failure of this postnatal adaptation of the circulation can lead to pulmonary arterial hypertension with echocardiographic evidence of right to left shunting across the ductus arteriosus and foramen ovale, severe tricuspid regurgitation, inter-ventricular

septal bowing at systole and an enlarged right ventricular chamber (Galie 2009). The decreased pulmonary blood flow results in shunting of deoxygenated blood back into the systemic circulation creating a vicious cycle of worsening hypoxia, acidosis and eventual cardiac failure.

In the systemic circulation, preterm infants are also susceptible to haemodynamic instability and low systemic blood flow in the first 24 hours postnatally (Kluckow 2000b). The inability of the immature myocardium to cope with the sudden increase in peripheral vascular resistance of the extrauterine circulation during the transition period is associated with low systemic and cerebral blood flow, intraventricular haemorrhage and adverse neurodevelopmental outcome (Osborn 2003, Hunt 2004). In addition to the above, low systemic blood flow which is associated with low gestational age, can be secondary to patent ductus arteriosus, high ventilation pressure resulting in reduced preload, peripheral vasodilatation in infants born to mothers with chorioamnionitis, sepsis and relative adrenal insufficiency.

1.3 Preterm births, respiratory distress syndrome, chronic lung disease of prematurity and pulmonary hypertension

1.3.1 Neonatal or respiratory distress syndrome

1.3.1.1 Introduction

RDS of the newborn is an acute lung disease which presents at birth and is most common in preterm infants. RDS is manifested by an increased respiratory rate (>60 breaths/min) and heart rate (>150 beats/min), chest wall retractions (subcostal, intercostal and sternal recessions), expiratory grunting, nasal flaring and cyanosis (Northway 1967). The incidence and severity of RDS are related inversely to the gestational age of the newborn infant. The incidence of RDS is around 60-80% in infants born at 26-28 weeks gestation whereas only 15-30% of those born at 32-36 weeks have RDS (Stoelhorst 2005, Ventolini 2008). Male infants are more likely to develop RDS compared to female infants (male:female ratio = 1.3:1) and this is thought to be due to the androgen hormone acting on type II pneumocytes resulting in delayed production of mature surfactant (Nielsen 1985). Other predisposing factors for the development of RDS include Caucasian race, elective Caesarean section, intrapartum asphyxia, hypothermia, maternal diabetes, twin pregnancy, intra-uterine growth retardation and genetic defects affecting production of different components of surfactant. Table 1.2 show a more extensive list of risk factors for RDS.

Table 1.2 - Risk factors for respiratory distress syndrome

Maternal factors	Infant factors
Multiple pregnancy	Prematurity
Elective Caesarean section	Male gender
Gestational diabetes	Familial predisposition
Gestational intrahepatic cholestasis	Hypothermia
	Caucasian ethnicity
	Intrapartum asphyxia
	Pulmonary infections
	Pulmonary haemorrhage
	Meconium aspiration syndrome
	Congenital diaphragmatic hernia
	Pulmonary hypoplasia

(Pickerd 2009)

1.3.1.2 Pathophysiology and pathology of RDS

RDS is caused by developmental insufficiency of surfactant production and function, as well as by structural immaturity of the lungs (Avery 1959). Surfactant is a complex system of lipids, proteins and glycoproteins which are produced by type II pneumocytes during the canalicular stage of lung development at around 24 weeks gestation (Yu 1990). Surfactant decreases surface tension and prevents the alveoli from completely collapsing on exhalation (Baum 1971). In addition, the decreased surface tension allows re-opening of the alveoli with a lower amount of force. However, in infants born extremely preterm (≤28 weeks gestation), the amount of surfactant produced by the immature lungs (with reduced numbers of type II pneumocytes) is insufficient to lower the surface tension within the alveoli causing them to collapse (Baum 1971). This gives a typical chest radiograph appearance of uniform "ground glass" appearance, air bronchograms and in severe cases, a 'white-out' appearance (Reynolds 1970). Structural immaturity, as manifested by a decreased number of gas-exchange units and thicker walls, also contributes to the disease process.

Macroscopically, the surfactant deficient lung is poorly inflated, and submerges under water (Avery 1959). Microscopically, alveolar epithelial necrosis develops within half an hour of birth. The epithelial cells become detached from the basement membrane leaving patches of hyaline membrane on the denuded area (Avery 1959). Hyaline membranes, composed of fibrin, cellular debris, neutrophils and macrophages, line and fill up the alveolar spaces, affecting gas exchange (Reynolds 1970). After 24 hours, the repair phase begins with macrophages appearing within the airways. After 5-7 days, the repair is complete with resolution of the hyaline membrane and normalisation of the lung architecture (Reynolds 1970). However, the inflammatory process is often

prolonged or the course is usually complicated by infection, prolonged mechanical ventilation, pulmonary oedema secondary to patent ductus arteriosus in infants born extremely preterm and the disease may progress to chronic lung disease of prematurity (Northway 1967).

1.3.1.3 Cardiovascular consequences of RDS

Respiratory distress syndrome is the commonest cause of respiratory failure and pulmonary hypertension in extremely preterm infants. The pulmonary arterial (PA) pressure usually falls with the improvement of respiratory function. Surfactant administration, optimal ventilation management and maintenance of good alveolar and arterial oxygenation are essential in the management of acute RDS (Jobe 1987), also resulting in decreased PA pressure. Hypoxia, sepsis, pneumonia, hypothermia, pulmonary oedema secondary to patent ductus arteriosus or fluid overload are among other risk factors can trigger a pulmonary hypertensive crisis in these infants (Toubas 1978, Skinner 1992).

Preterm lambs exposed to intrauterine infection have vascular dysfunction as a result of the loss of the pulmonary vasodilator response to inhaled nitric oxide, which is attributed to diminished abundance of endothelial nitric oxide synthase (MacRitchie 2001) and soluble guanylate cyclase (Bland 2003) in the pulmonary circulation (Kallapur 2004). The resultant increase in pulmonary vascular resistance and pressure increases the workload (afterload) of the right ventricles. As elucidated in section 1.1.3 discussing fetal myocardial development, the preterm myocardium has reduced contractile units and therefore will be less able to cope with the increase in afterload seen in RDS (Reiser 1994). The increase in afterload decreases the velocity and amount

of muscle shortening (Friedman 1972). The decreased myocyte cross-sectional area of the immature myocardium shortens more slowly and by a smaller amount than the adult myocardium when both are subjected to the same afterload (Anderson 1996). The right and left ventricles are affected in a different manner by afterload (Thornburg 1983, Thornburg 1986).The right ventricle is less able to cope with the increased afterload as compared to the left ventricle due to the difference in ventricular geometry and larger end-diastolic volume (Friedman 1972). In addition to the impaired contractility, infants with continuing RDS have significant increase in troponin T levels suggesting a level of myocardial damage that may further affect the contraction and relaxation of their heart (Trevisanuto 2000).

The increase in pulmonary vascular resistance causes a reduction in pulmonary blood flow with right to left shunting of blood at the ductus arteriosus level and in severe pulmonary hypertension, at the foramen ovale. The complications from the acute increase in right ventricular workload and the resultant hypoxaemia include impairment of the left and right cardiac output. Additionally, the increased PAP and PA resistance leads to higher right ventricular diastolic pressure which in turn reduces the left ventricular filling pressure due to ventricular interaction (Romero 1972, Bove 1981, Slinker 1986). The impediment of left ventricular filling and increased left atrial pressure leads to decreased left ventricular stroke volume and left ventricular output.

1.3.2 Chronic lung disease of prematurity

1.3.2.1 Introduction

Chronic lung disease of prematurity (CLD), often also called bronchopulmonary dysplasia (BPD), is one of the most common sequelae in preterm births. Despite the

improvements in neonatal care, the incidence of CLD has remained unchanged, although the incidence of severe CLD has decreased (Smith 2005). It has been reported that up to a fifth of infants born ≤ 32 weeks gestation progress to develop CLD (Zeitlin 2008). The incidence of CLD is up to 40% of very low birth weight survivors and the incidence increases with decreasing birth weight affecting especially those born at less than 1 kg in birth weight (Darlow 2003, Farstad 2011).

The definition of BPD has continued to evolve since Northway et al first reported lung damage as a result of prolonged mechanical ventilation in preterm infants with severe RDS in 1967 (Northway 1967). Subsequent definitions of clinical CLD have included supplemental oxygen requirement at 28 days postnatal age (Sinkin 1990) and 36 weeks postmenstrual age (Marshall 1999). The National Institutes of Child Health and Human Development (NICHD) workshop established the diagnostic criteria for CLD in 2001 that included the gestational age and the disease severity (Jobe 2001) (Table 1.3). Using this definition, the incidence of CLD in infants born preterm was reported to be around 23% (Lemons 2001).

Table 1.3 - Diagnostic criteria for CLD

Gestational age	<32 weeks	>32 weeks
TPA	36 wks PMA or discharge to home, whichever comes first	> 28 days but <56 days PNA or discharge home, whichever comes first
	Treatment with oxygen >21% for at least 28 days plus	
Mild CLD	Breathing room air at TPA	Breathing room air at TPA
Moderate CLD	Need for <30% Oxygen at TPA	Need for <30% Oxygen at TPA
Severe CLD	Need for ≥ 30% Oxygen and/or positive pressure, (PPV or CPAP) at TPA	Need for ≥ 30% Oxygen and/or positive pressure, (PPV or CPAP) at TPA

TPA=Time point of assessment, PMA= Post menstrual age, PNA= Post natal age, PPV= Positive pressure ventilation, CPAP= Continuous positive pressure ventilation

(Jobe 2001)

1.3.2.2 Pathology of CLD

When Northway and colleagues first described CLD in 1967, the infant population describe was very different from the current infant population. These pre-surfactant era infants were born moderately preterm and were exposed to aggressive mechanical ventilation and high concentrations of oxygen (Northway 1967). Histological characteristics of this classic or old CLD were alternating areas of atelectasis and hyperinflation, severe airway epithelial lesions with squamous metaplasia, airway smooth muscle hyperplasia, prominent pulmonary vascular hypertensive lesions, extensive fibroproliferation and decreased internal surface area and total number of alveoli (Coalson 2003).

The introduction of surfactant treatment has improved the survival of smaller and more preterm infants and changed the pathology and clinical course of CLD (Jobe 2001). In post mortems of infants born in the surfactant era, an impairment of acinar development as evidenced by fewer and larger alveoli seen on examination has been described (Husain 1998).

Animal studies have shown that vascular endothelial growth factor (VEGF), an angiogenic growth factor that is essential for vascular development, plays an important role in normal alveolar development (Jakkula 2000, Le Cras 2002). Decreased levels of VEGF protein have been found in lung tissues of infants who died from CLD but not consistently (Bhatt 2001a, Currie 2001, Lassus 2001a). These findings lead to the hypothesis that disruption of normal lung angiogenesis may contribute to dysregulated alveolarisation as observed in CLD; the “vascular hypothesis” of lung development (Abman 2001). The impairment of angiogenesis results in a reduction in the number and

size of intra-acinar pulmonary arteries and total cross-sectional area of the pulmonary vascular bed, thus increasing pulmonary vascular resistance (Bush 1990, Stenmark 2005). In addition, there is also evidence of increased muscularisation of the pulmonary arteries, along with a reduction of alveoli numbers, in infants who died from CLD (Hislop 1990, Margraf 1991). Extremely preterm infants are at high risk of developing pulmonary arterial hypertension (PAH) due to the combination of an increase in pulmonary arterial medial thickness and pulmonary vascular resistance as a result of dysregulated angiogenesis.

1.3.2.3 Factors contributing to the development of CLD

CLD is a complex disorder with multiple factors contributing to the onset and progression of the disease. In a prospective study of 86 infants with birth weights less than 1500g, Cunha and colleagues found that prematurity, birth weight, high oxygen requirement, high peak inspiratory pressure ($\geq$ 21cmH_2O), fluid overload and the presence of patent ductus arteriosus are associated with an increased risk of CLD (Cunha 2005).

Prolonged exposure to high oxygen concentration leads to reduction of alveolar formation with structural changes (Hislop 1987). Oxygen toxicity is mediated through reactive oxygen species which have potent pro-inflammatory effects on the alveoli (Rozycki 2002, Wagenaar 2004). Preterm infants are more susceptible to volutrauma due to their compliant chest wall which allows uncontrolled expansion from mechanical ventilation. Repeated expansion and collapse of the alveoli causes shear stress resulting in injury with disruption of structural elements leading to release of inflammatory mediators with subsequent pulmonary inflammation and macrophage infiltration

(Muscedere 1994, Kotecha 1996a, Tremblay 1997). Infants who develop CLD have elevated levels of interleukin-8 and several other neutrophil chemoattractants (Groneck 1995, Kotecha 1995). There are suggestions from a rat lung model that moderate volume ventilation with high PEEP causes significantly less production and release of pro-inflammatory cytokines compared to high volume ventilation without PEEP (Muscedere 1994).

Antenatal exposure to chorioamnionitis (Young 2005) and postnatal infection with cytomegalovirus (Sawyer 1987), *Ureaplasma urealyticum* (Benstein 2003), and Mycoplasma (Bhandari 1998) are associated with a significant risk of developing severe CLD. Chorioamnionitis and postnatal infections have been found to amplify the inflammatory response of the preterm lung to ventilation as reflected by a marked infiltration of inflammatory cells and increased expression of pro-inflammatory chemokines (Schmidt 2001a, Speer 2006). It has been reported that neonatal neutrophils have a prolonged survival due to suppression of natural apoptosis (Kotecha 2003, Koenig 2005). These activated neutrophils adheres to the endothelium of the pulmonary vascular system thereby initiating a sequence of injurious events and causes extravasation of neutrophils and macrophages into the alveolar spaces leading to pulmonary oedema (Speer 2006). The injury to the pulmonary capillary endothelium promotes neutrophil and platelet activation to induce pulmonary as well as systemic inflammation and activation of the clotting system (Sitaru 2005). In addition, vasoactive prostaglandin mediators released during sepsis prevent patent ductus arteriosus closure or induce re-opening of the duct leading to increased risk of developing pulmonary oedema and affecting gas exchange (Gonzalez 1996). In addition to the lung parenchymal effects, circulating pro-inflammatory cytokines, IL-6 and TNF-α, can

affect myocardial function. IL-6 has been shown to depress papillary muscle contraction and is negatively inotropic in cardiomyocyte cultures (Joulin 2007). TNF-α induces a relatively short duration of early positive inotropic effect followed by a delayed and prolonged phase of profound systolic and diastolic dysfunction (Murray 1996).

Inflammation-induced tissue injury is normally followed by a phase of repair (Grande 1997). Transforming growth factor-β (TGF-β) plays a key role in mediating tissue remodelling and repair (Bartram 2004). In preterm infants with BPD, increased concentration of TGF-β has been detected in the airways resulting in exaggerated repair and lung fibrosis (Kotecha 1996b). The combination of over-expression of TGF-β and suboptimal pulmonary and vascular growth factors contribute to the dysmorphic microvasculature and disrupted alveolarisation (Abman 2001, Bhatt 2001a, Lassus 2001a).

1.3.2.4 Cardiovascular consequences of CLD

Infants with CLD are at risk of developing pulmonary arterial hypertension (PAH) due to disruption of the pulmonary vasculature and a rise in pulmonary vascular resistance due to alveolar injury and inadvertent periods of hypoxia. PAH is defined as a mean PA pressure ≥ 25 mmHg at rest measured by cardiac catheterization or an estimated systolic PA pressure ≥ 40 mmHg on echocardiography (Haworth 2008). Although the true prevalence of PAH in infants with CLD is unknown, a range between 17% - 25% has been reported in individual studies (An 2010, Bhat 2012).

Supplemental oxygen reverses hypoxic pulmonary vasoconstriction, improving oxygen saturation, decreasing pulmonary vascular resistance and improving right ventricular

performance (Kotecha 2002). Long term supplemental oxygen therapy is considered the standard treatment for PAH associated with CLD (Stenmark 2005). It is assumed that the gradual fall in PA pressure in CLD infants is reflected indirectly by the gradual weaning of supplemental oxygen, guided by oxygen saturation monitoring and that PA pressure normalises once the infants are successfully weaned to breathing in room air. Evans and Archer refuted this assumption by showing that up to a third of preterm infants recovering from hyaline membrane disease when discharged home in air had evidence of raised PA pressure as assessed by Doppler echocardiographic (Evans 1991b). Another study noted that PA pressure in infants with CLD remained persistently raised until the end of the first year of life using Doppler-derived pulmonary arterial flow acceleration time to ejection time ratio (PA AT:ET ratio) (Subhedar 2000).

Fitzgerald et al studied the PA pressure of survivors of CLD (defined as oxygen dependence at 28 days with or without chest radiograph abnormalities in the study) in early childhood by measuring the PA AT:ET ratio (Fitzgerald 1994). They noted that nearly one quarter of CLD survivors had raised PA pressure, which was demonstrated across the range of severity of CLD children in early childhood. These survivors of CLD from the pre-surfactant era with raised PA pressure often did not exhibit any clinical features of PAH; hence they may have been exposed to subclinical hypoxaemia. This study also noted an improving PA AT:ET ratio with increasing age in these children, suggesting improvement during childhood. Another study of CLD in the pre-surfactant era of children less than 2.5 years of age showed that up to one third of children have raised PA pressure assessed using PA AT:ET ratio and TR jet velocity, which were found to be inversely correlated (Benatar 1995). Eight of 11 subjects with PAH responded to oxygen challenge with a decrease in PA pressure by at least 5 mmHg

and it was postulated that increased muscularisation of the pulmonary arterioles may be the cause for the lack of response to the oxygen challenge (Abman 1985).

Pre-school survivors of CLD from the post-surfactant have been noted to have higher PA pressures, estimated by TR jet velocity, compared to control subjects (30.4±6.9 mmHg vs 23.3±5.3 mmHg) (Gurses 2013). In the same study, CLD survivors had subclinical ventricular dysfunction using the myocardial performance index (also known as Tei index). A Finnish study on school-aged CLD survivors from the surfactant era did not find any evidence of raised PA pressure using echocardiographic Doppler assessment of the TR jet and the PA AT:ET ratio when compared to the term and preterm controls without CLD (Korhonen 2005). The findings from this study suggest that the increased pulmonary vascular resistance associated with CLD resolved by school age.

Although pulmonary vascular resistance and PA pressures in CLD survivors appear to normalise by school age, pulmonary vascular reactivity to changes in oxygen tension and inhaled nitric oxide may persist into adolescence (Mourani 2004) (Figure 1.3). Sartori et al found that term-born adults who were diagnosed with transient perinatal hypoxic pulmonary hypertension have significantly greater increases in their PA pressures at high altitude when compared to normal controls (Sartori 1999) but it is unknown whether children who had CLD in infancy have similar PA hyper-reactivity. Mourani et al found that acute hypoxia increased mean pulmonary artery pressure by more than 20% suggesting that the risk for pulmonary vasoconstriction due to hypoxia persist in children older than 5 years of age who had severe CLD (Mourani 2004). In these children, inhaled nitric oxide significantly augmented the vasodilator response of

the PA to oxygen suggesting a marked reversible component (Figure 1.3). The responsiveness to inhaled nitric oxide may indicate a likely response to a mechanistically similar agent such as sildenafil in the treatment of pulmonary artery hypertension associated with CLD (Mourani 2009b, Farquhar 2010).

Figure 1.3 - Individual effects of hypoxia (A), hyperoxia (B), hyperoxia + iNO (C), and calcium channel blockers (CCB) (D) on mean pulmonary artery pressure (PAP) compared with normoxic baseline measurements in children with CLD.

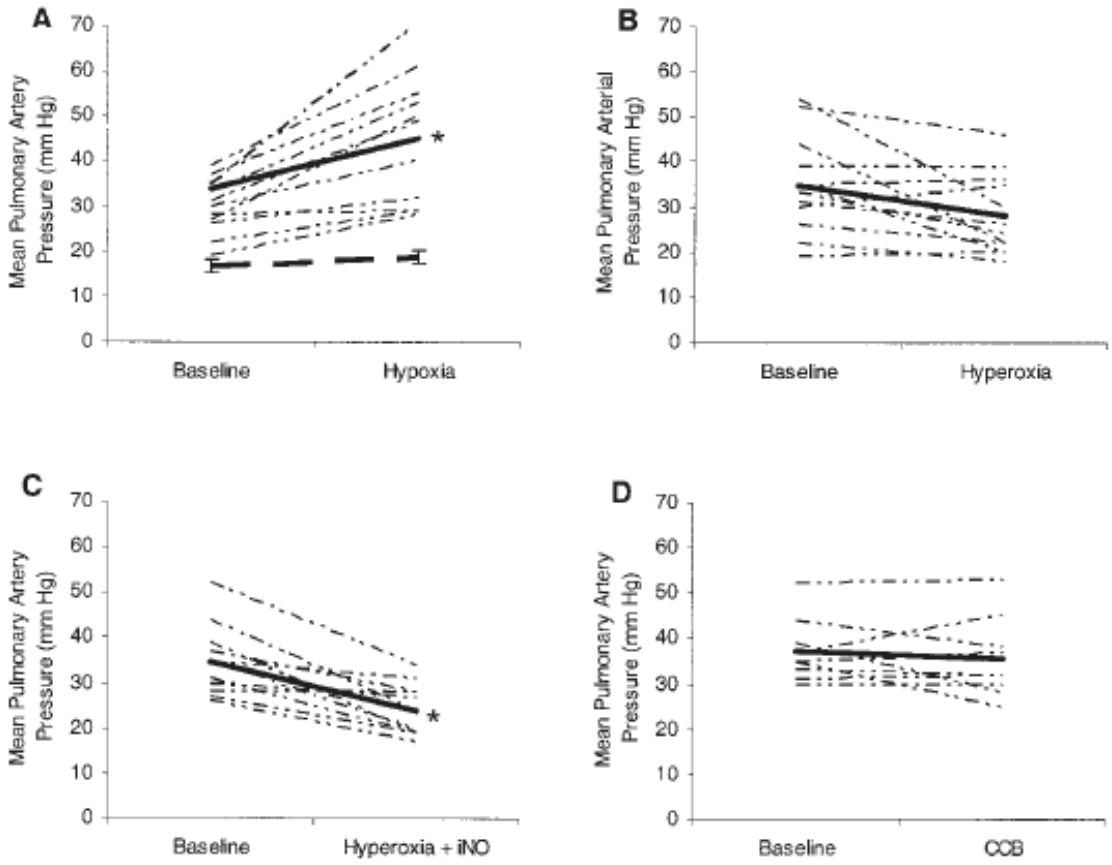

The mean pulmonary arterial pressure (PAP) increased and decreased significantly ($p<0.01$) in response to hypoxia and hyperoxia + iNO, respectively, from normoxic baseline value. There was no change in mean PAP to either oxygen alone or CCB.

Light dashed lines represent measurements made in individual patients. The solid line displays mean values for the study group.

(Mourani 2004)

1.4 Echocardiography in the assessment of pulmonary hypertension

The gold standard method for evaluating pulmonary haemodynamics and the measurement of pulmonary arterial pressure is invasive right heart catheterisation. However, this procedure carries significant risk to sick ventilated preterm infants or infants with CLD. Echocardiographic signs such as right atrial enlargement, right ventricular hypertrophy and/or dilatation, septal flattening and pulmonary dilatation can also be used qualitatively to detect PAH but their predictive values are relatively poor (Mourani 2009a). Other echocardiographic indices have been explored to measure pulmonary arterial pressure quantitatively and are discussed below.

1.4.1 Pulsed Doppler methods

1.4.1.1 Tricuspid regurgitation peak velocity

Systolic pulmonary artery pressure (sPAP) is considered equal to right ventricular systolic pressure in the absence of pulmonary valve stenosis or outflow obstruction (Galie 2009). Right ventricular systolic pressure can be determined by addition of the right atrial pressure to the pressure gradient between the right chambers. Therefore, sPAP can be estimated from the tricuspid regurgitant (TR) jet velocity, measured by continuous wave Doppler ultrasound, by using the modified Bernoulli equation (4 x TR jet peak velocity^2 + right atrial pressure). The European guidelines for the diagnosis and treatment of PAH consider the echocardiographic diagnosis of PAH 'likely' when the TR jet velocity is >3.4 m/s (or sPAP >50 mmHg) and 'possible' when the TR jet velocity is between 2.9 and 3.4 m/s (or sPAP between 37 and 50 mmHg) (Galie 2009).

This technique has been validated against right heart catheterisation in both adults and children. Skjaerpe and Hatle measured pulmonary arterial pressure using the TR jet in 70 adults and found sPAP to correlate well with catheter measurements (r=0.97) (Skjaerpe 1986). In infants with congenital heart disease, the TR jet velocity appears to have a high correlation with cardiac catheterization (r=0.95) (Skinner 1993).

However, estimation of sPAP from TR jet flow is not always possible as only between 44% and 61% of infants and young children respectively with CLD have a measurable TR jet (Benatar 1995, Mourani 2008). The precision of sPAP estimation using TR jet velocity has been questioned in studies comparing echocardiographically estimated values and true values measured by right heart catheterisation where the mean difference between the two methods ranged from 3 to 38 mmHg and sPAP was underestimated by the echocardiographic method by >20 mmHg in 31% of all patients studied (McGoon 2004). In view of its poor precision, TR jet velocity is not suitable to be used as a diagnostic tool in asymptomatic PAH (Galie 2009). Despite the above, TR jet velocity measurement remains a feasible and reliable screening method for suspected PAH.

1.4.1.2 Pulmonary regurgitation end diastolic velocity

End diastolic pulmonary regurgitant flow measurement using pulsed-wave or continuous-wave Doppler echocardiography enables the calculation of the pressure gradient between the right ventricle and the pulmonary artery at end diastole using the modified Bernoulli equation. The calculated pressure gradient added to right atrial pressure estimates diastolic pulmonary arterial pressure. This method has a high correlation with invasive diastolic and mean pulmonary arterial measurements (r=0.94

for both measurements) in the adult population (Masuyama 1986, Ge 1992). Similar to TR jet flow, pulmonary regurgitation flow was only successfully obtained in 18 of the 21 patients with pulmonary hypertension and in 13 of the 24 patients without pulmonary hypertension (Masuyama 1986).

1.4.1.3 Right ventricular systolic time intervals

Right ventricular systolic time intervals, along with TR jet velocity, are the most studied surrogate markers of PAH in preterm infants and infants with CLD. The pulmonary blood flow is visualised using a pulsed-wave Doppler signal. The pulmonary arterial flow acceleration time (AT) is defined as the time interval from the onset of forward flow in the pulmonary artery to the peak velocity of this flow and ejection time (ET) is measured from the onset to the end of systolic pulmonary flow. (Figure 3.9) Good quality pulsed-wave Doppler signals of the right ventricular outflow tract or pulmonary artery can be measured in the vast majority of patients, unlike TR and pulmonary regurgitant flows.

In 1983, Kitabatake et al reported that AT or the ratio of AT to ET measured from the pulsed-wave Doppler signal in the right ventricular outflow tract decreased with increases in mean pulmonary artery pressure in adults. A very strong inverse correlation between AT:ET ratio and log mean pulmonary artery pressure was found ($r = -0.90$) (Kitabatake 1983). A similar study performed on older infants and children by Akiba et al also showed a close negative correlation between AT:ETc and directly measured PAP (Akiba 1988). The lower limit of AT:ETc corresponding to normal PAP is 0.54 (Akiba 1988). AT:ETc is calculated by dividing AT:ET by the square root of the R-R interval

from a simultaneous electrocardiogram tracing. The reason Akiba and others used a corrected ratio is AT, ET and AT:ET are all shortened as heart rate increases.

In a study involving children with congenital cardiac disease, Kosturakis et al noted a good correlation between the AT:ET ratio and mean PAP (r = -0.76) (Kosturakis 1984). This group also defined the normal values for healthy paediatric patients where an AT:ET ratio of 0.35 approximates to a mean PAP of 20 mmHg and a ratio of 0.25 approximates to a mean PAP of 50 mmHg. Fitzgerald et al measured PAP in 76 children aged 1-7 years (mean age 4 years) with CLD along with 21 sibling controls and found that 24% of children who had CLD had subclinical PAH (Fitzgerald 1994). This group defined an AT:ET ratio of ≥0.35 as normal, between 0.31 and 0.35 as possibly low and <0.31 as definitely low ratio suggesting increased PAP (Fitzgerald 1994).

1.4.2 Myocardial velocity imaging / Tissue Doppler methods

Myocardial velocity imaging (MVI) is now established as a tool for quantifying regional myocardial function in adults. The technique has been validated and established in children, infants, and neonates (Harada 2000, Kapusta 2000, Frommelt 2002, Mori 2004, Nestass 2009, Pena 2009). Reference values of parameters measured using MVI in healthy children and neonates have been published (Weidemann 2002, Ekici 2007, Roberson 2007). MVI has also been used to assess regional myocardial function in different neonatal conditions (Patel 2009, Wei 2009). It has been shown to be both feasible and reproducible in preterm infants (Joshi 2010), thus permitting the assessment and monitoring of regional myocardial function which can be affected by various respiratory and congenital cardiac conditions prevalent in preterm-born subjects.

MVI allows the measurements of velocities at any point in the ventricular wall during the cardiac cycle. Myocardial strain (ε), a measure of local contractile function, is a one-dimensional measurement of relative deformation of myocardial fibres. Strain rate is the rate by which deformation occurs and this is derived from the instantaneous velocity gradient between adjacent points of the myocardium. The instantaneous data on deformation (or ε) are then obtained by integrating the strain rate curve with time (Marwick 2006) (Figure 3.13 and Figure 3.14)

1.4.2.1 Right ventricular relaxation time (IVRT)

Myocardial pulsed Doppler imaging of the tricuspid annulus can be used to measure RV relaxation time (IVRT). In adults, IVRT correlates well (r = 0.74 - 0.87) with simultaneously measured PAP by RV catheterization (Lindqvist 2006, Bréchot 2008). RV relaxation time was longer in patients with PAH, compared to those who did not have PAH. RV relaxation time 'IVRT' ≤ 40 ms has been shown to exclude PAH with 100% negative predictive value (Bréchot 2008). Although prolonged IVRT is suggestive of elevated PAP, this cannot confirm the diagnosis of PAH by itself. At present, there is a lack of normal values and validation of this technique in infants and children. Joshi et al showed poor inter-observer reproducibility in measuring IVRT in term and preterm infants (Joshi 2010), thus suggesting using IVRT as a surrogate marker of elevated PAP in this cohort may not be appropriate for the time being.

1.4.2.2 Right ventricular systolic strain and strain rate

Strain is the percent magnitude of myocardial deformation during the cardiac cycle. Systolic strain is the percentage shortening of myocardium within a region of interest during systole (Figure 3.13). Strain rate represents the rate of myocardial deformation.

Longitudinal ventricular strain rate assessment gives a negative value when the ventricle shortens at systole and a positive value when the ventricle lengthens at diastole due to directional changes (Figure 3.14). RV systolic strain and strain rate have been explored as a promising new technique for the diagnosis of PAH. RV systolic strain had a significant correlation with PAP (r = 0.59; p<0.001) and pulmonary vascular resistance (r = 0.6; P< 0.001), giving it the potential to be a surrogate marker of PAH (Rajagopalan 2008). Lopez-Candales et al studied 111 patients with PAH and 35 controls using both tissue Doppler myocardial imaging and cardiac catheterization and reported that RV systolic strain of less than -20% has a sensitivity of 60% and a specificity of 87% to predict PAP of > 40 mmHg (Lopez-Candales 2008). RV systolic strain rate also had a significant correlation with mPAP (r = 0.57; p=0.001) and pulmonary vascular resistance (r = 0.62; P< 0.001) (Naderi 2013). Both RV systolic strain and strain rate are powerful predictors of outcome in adult patients with known or suspected pulmonary hypertension (Sachdev 2011, Fine 2013). In view of these promising results in the adult population, RV systolic strain and strain rate may be useful surrogate markers for the diagnosis of PAH in infants and children as well. Normal values for RV strain and strain rates have been described in children (Weidemann 2002, Kutty 2008) but the studies included children from 1 year up to 16 years. Although strain and strain rate imaging has been proved to be feasible and reliable in infants (Nestaas 2007) and preterm infants (Joshi 2010), there are only a few small studies assessing strain and strain rates using tissue Doppler echocardiography in healthy newborn infants (Nestass 2009, Pena 2009) and in infants who suffered perinatal asphyxia (Nestaas 2011, Nestaas 2012). The inter-observer reproducibility of myocardial deformation imaging in the neonatal population is 30% (Joshi 2010) compared with 10 – 15% in children (Weidemann 2002) and adults (Serri 2006). This is

likely caused by the size of the heart in this population which presents additional technical challenges in the acquisition and analysis of myocardial deformation images.

1.5 Magnetic Resonance Imaging (MRI) in the assessment of pulmonary hypertension

Cardiac MRI (CMRI) has been used routinely for non-invasive assessment of ventricular volumes, mass, function and flow with high accuracy and repeatability. Recent interest in arterial stiffness and compliance has resulted in the development of CMRI techniques that allow non-invasive measurements of distensibility, stiffness index and pulse wave velocity (PWV) of both major pulmonary and systemic arteries thus providing detailed information on physiological arterial function and subsequent effects on ventricular loading conditions.

1.5.1 Relationship between pulmonary artery compliance and resistance

Lankhaar et al have reported an inverse relationship between resistance and compliance from which the RC-time can be calculated (Lankhaar 2008). It characterises the decay of pulmonary artery pressure in diastole. RC-time is the same in patients with and without pulmonary hypertension implying that resistance and compliance are inversely related as shown in Figure 1.4 (Lankhaar 2008). Resistance is calculated as the ratio of mean pulmonary artery pressure and mean flow and compliance as the ratio of stroke volume and pulse pressure. For RC-time it then holds:

$$\text{RC-time} = R \times C = \frac{mPAP - PCWP}{SV/T} \times \frac{SV}{PP} = T\left(\frac{mPAP - PCWP}{PP}\right)$$

T = heart period, SV = stroke volume, mPAP= mean pulmonary artery pressure, PCWP = pulmonary capillary wedge pressure, PP = pulmonary artery pulse pressure

(Lankhaar 2008) (Reprinted with permission of Oxford University Press)

Thus, an inverse relationship implies that loss of pulmonary arterial compliance (or increased pulmonary arterial stiffness) is an early sign of pulmonary hypertension. A new screening method in assessing pulmonary arterial compliance non-invasively offers the opportunity to detect pulmonary arterial hypertension or even detect changes of pulmonary arterial compliance well before clinical and echocardiographic features manifest.

Figure 1.4 - The graph showing the constant relationship between compliance and resistance

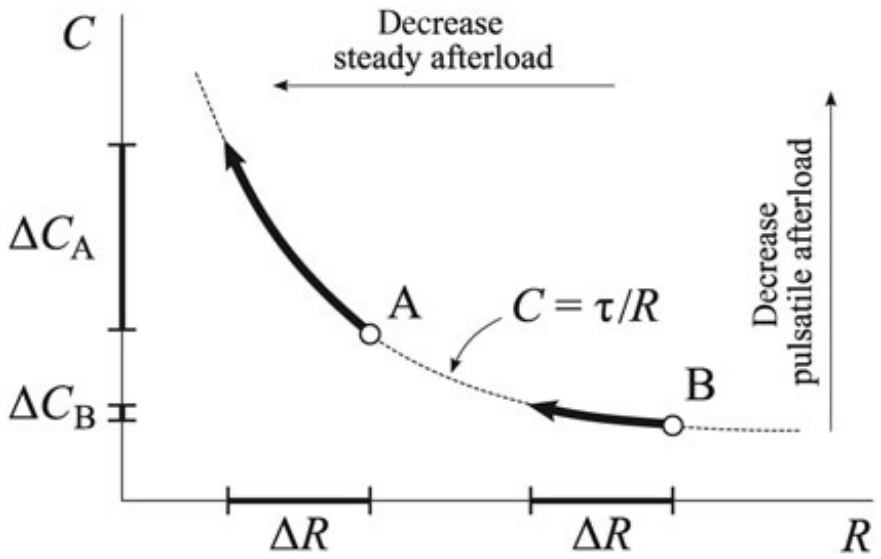

The consequence of a constant RC-time *t* during therapy for patients A and B. At baseline, **patient A** has a low resistance R (mild PH) and **patient B** a high resistance (severe PH). If the RC-time is constant, patients will always move along the dashed line and a change in resistance ΔR will be accompanied by a change in compliance ΔC. If the resistance R of both patients decreases with the same amount ΔR, **patient A** will improve much more in compliance than **patient B**. Thus, **patient A** will improve substantially in both steady and pulsatile afterload, while patient B will improve in steady afterload only.

(Lankhaar 2008)

1.5.2 MRI assessment of PA compliance, distensibility, stiffness

Velocity-encoded phase-contrast MRI can be used to study haemodynamic changes associated with pulmonary arterial hypertension reliably and with good reproducibility, by estimating PWV in the main pulmonary artery (Peng 2006). In adult patients with pulmonary arterial hypertension, mean pulmonary artery peak flow velocity, pulmonary artery blood flow, and pulmonary distensibility/compliance were noted to be significantly lower than in matched volunteers (Ley 2007). Sanz et al compared right heart catheterisation and phase-contrast MRI and showed a strong correlation between average blood velocity and mean PAP and pulmonary vascular resistance index ($r = -0.73$ and -0.86, respectively; $p<0.001$), thus potentially allowing non-invasive diagnosis of pulmonary arterial hypertension (Sanz 2007).

Vulliémoz et al proposed a MRI technique to measure PWV in aorta non-invasively without the need to measure arterial pulse pressure by proposing the complex calculation of obtaining PWV value from local arterial early systolic flow and cross sectional area, derived from the Bramwell-Hill equation (Vulliémoz 2002). This is shown in Figure 1.5 below. Peng et al then applied the QA method to measure PA PWV and compared PA PWV of patients with pulmonary hypertension against normal subjects (Peng 2006). The PA flow is calculated by multiplying the vessel cross-sectional area by the mean velocity inside the vessel cross section, which is performed by the analysis software. A line is then fitted to the flow versus area data during early systole using the least-squared error method, from which PWV is calculated (Peng 2006). As shown in the derivation of PWV in Figure 1.5, PWV is associated with PA resistance and flow. As this is a novel method, there are no studies on correlating PA PWV with PA pressure, compliance or resistance as yet.

Figure 1.5 – The derivation of PWV as demonstrated by Vulliémoz

For unidirectional waves, the ratio between pressure variation (ΔP) and flow variation (ΔQ) is then equal to the characteristic impedance Z_C:

$$Z_C = \frac{\Delta P}{\Delta Q}. \quad [1]$$

By definition, the local area compliance C_A is given by

$$C_A = \frac{\Delta A}{\Delta P} \quad [2]$$

where ΔA stands for the variation of cross-sectional area. C_A is related to Z_C through the following formula:

$$Z_C = \sqrt{\frac{\rho}{A}\frac{1}{C_A}} \quad [3]$$

where ρ stands for the blood density and A for the cross-sectional area at the end diastole. Eliminating ΔP from the above expressions yields the following expression for C_A:

$$C_A = \left(\frac{\Delta A}{\Delta Q}\right)^2 \frac{A}{\rho}. \quad [4]$$

C_A is related directly to PWV (PWV_{QA}) by

$$PWV_{QA} = \sqrt{\frac{A}{\rho}\frac{1}{C_A}}. \quad [5]$$

Therefore, by substituting Eq. [4] for C_A we obtain:

$$PWV_{QA} = \frac{\Delta Q}{\Delta A}. \quad [6]$$

(Vulliémoz 2002)
(Reprinted with permission of John Wiley & Sons, Inc.)

1.5.3 PA stiffness and mortality in PAH patients

Chronic PAH is associated with loss of elasticity in the pulmonary vascular bed. Stiffening of the vasculature results in greater reflection of pressure waves from bifurcations in the pulmonary vessels during pulsatile ejection of blood from the right ventricle. In a study involving 70 patients with PAH and 16 non-PAH controls, Gan et al reported that the proximal PA of patients with PAH are more distended, less distensible and have a small relative area change during the cardiac cycle compare to healthy controls. Relative area change showed an inverse curvilinear relation with mean pulmonary artery pressure (R^2 = 0.47) (Gan 2007). During the 48 months follow up period, patients with a relative area change value ≤16% were more likely to die from cardiopulmonary causes (Gan 2007). The authors concluded that non-invasive measurement of PA relative area change, a marker of arterial stiffness, using MRI is a good predictor of mortality in patients with PAH.

Mahapatra et al studied the relationship between pulmonary arterial capacitance and mortality in patients with idiopathic PAH (Mahapatra 2006). Pulmonary arteriolar capacitance measures how much the total pulmonary arteriolar tree will dilate with each contraction of the right ventricle. During the four year follow-up study, 21 out of 104 patients died and it was noted that the capacitance index was a strong independent predictor of mortality in patients with idiopathic PAH (Mahapatra 2006).

1.6 Cardiopulmonary effects of hypoxia

1.6.1 Hypoxic effects of altitude

The percentage of oxygen in inspired air is constant at different altitudes, which is 21% of dry air. The fall in atmospheric pressure at higher altitude decreases the partial pressure of inspired oxygen and hence the driving pressure for gas exchange in the lungs. The weight of air above us up to 10000 metre high is responsible for the atmospheric pressure, which is normally about 100 kPa at sea level. This atmospheric pressure is the sum of the partial pressures of the constituent gases, oxygen and nitrogen, and also the partial pressure of water vapour (6.3 kPa at 37°C). As oxygen is 21% of dry air, the inspired oxygen pressure is $0.21\times(100-6.3)=19.6$ kPa at sea level (Peacock 1998).

Atmospheric pressure and inspired oxygen pressure fall roughly linearly with altitude. At 3500m and 5500m, the inspired oxygen is equivalent to 13% oxygen and 10% oxygen at the sea level respectively. A fall in inspired oxygen pressure reduces the driving pressure for gas exchange in the lungs and causes the effects of hypoxaemia. The use of air travel for business and leisure purposes is progressively increasing. Similarly, as society becomes more affluent, increasing number of healthy lowland adults and children are holidaying in high altitude skiing resorts or hiking up the high mountains (Yaron 2008). Many of these resorts are about 8000ft / 2438m above sea level. The once remote Everest base camp is 5500m where only few non-natives would visit has become increasingly more accessible. Many adults, children and infants are exposed to the risk of hypoxia and its consequences in this modern lifestyle.

Commercial airlines fly at high altitude of 30,000 to 40,000ft to avoid turbulence and minimize fuel costs. The partial pressure of oxygen at such high altitudes is <5kPa, which is lethal. Commercial aircrafts are pressurized to an altitude of 8000ft / 2438m, which is equivalent to breathing 15% oxygen at sea level (Samuels 2004). There are limited reports of the hypoxic response of healthy children to air travel. In a study measuring the oxygen saturations of 80 healthy children aged 0 – 15 years in an eight to ten hours flight from Taiwan to Hawaii, the mean oxygen saturations fell to 95.7% (± 1.7%) after 3 hours and 94.4% (± 1.8%) after 7 hours of flight (Lee 2002). A similar study that included 10 healthy children found that five children desaturated to <94% during flight (Humphreys 2005). Although oxygen saturations decrease in healthy children and adults at cruising altitudes, the desaturations are not thought to result in clinically relevant hypoxia unless there is an underlying disease that compromises respiratory or cardiovascular reserve (Dillard 1989, Samuels 2004, Bossley 2008, Coker 2008, Winck 2008).

1.6.2 Hypobaric versus normobaric hypoxia

Two methods used in flight simulation testing to predict hypoxic response at altitude are hypobaric hypoxic chambers and inhalation of diluted gas mixture. Whilst a hypobaric hypoxic chamber is ideal to simulate the conditions of aircraft cabin pressure and oxygen tension, the limited availability of this facility limits it use. Therefore, the commonest method used for pre-flight hypoxic challenge is the normobaric hypoxia test using a 15% oxygen nitrogen admixture delivered by face mask or body box.

The Young Everest Study compared oxygen saturations of nine healthy children aged 6-13 years (median 8 years) during a normobaric hypoxic challenge breathing 15%

oxygen for 20 minutes (via a modified body plethysmograph) against hypobaric hypoxia during flight and at high altitude (2500m) (Scrase 2009). The mean oxygen saturations decreased from 98.5% at sea level down to 93% in all three hypoxic conditions. The oxygen saturation at normobaric hypoxic challenge was 93.4% (SD 1.7) versus 93.2% (SD 2.2) at 2600m. The exact oxygen saturation value for in-flight testing was not reported. There are no paediatric studies comparing PaO_2 between normobaric and hypobaric hypoxic challenges and there are conflicting reports on the measured PaO_2 between these two methods in the adult population. In a study on adult patients with chronic obstructive airway disease comparing PaO_2 15% normobaric hypoxia inhalation test against hypobaric hypoxia delivered by hypoxic chamber at 2438m, there was no difference in the PaO_2 relationships between the two methods (Dillard 1995). However, when healthy adults were subjected to more significant hypoxic challenge at 12% oxygen, oxygen saturations and PaO_2 was found to be significantly lower following hypobaric hypoxia challenge (4500m) compared to normobaric hypoxic challenge (12% oxygen) (Sartori 1999, Savourey 2003). Despite this, the use of the normobaric hypoxia inhalation test is still a good method to simulate hypobaric hypoxia.

1.6.3 Hypoxic pulmonary vasoconstriction

Hypoxic pulmonary vasoconstriction is an adaptive mechanism in which pulmonary arteries constrict in the presence of hypoxia without hypercapnia, redirecting blood flow to alveoli with a higher oxygen content, thereby optimizing the ventilation-perfusion match and thus reducing shunting. The effect of global hypoxia on the pulmonary circulation is dramatic resulting in pulmonary hypertension caused by an increase in pulmonary vascular resistance. The onset has been shown in man to be very rapid,

reaching a maximum within 5 minutes (Talbot 2005). Zhao et al demonstrated that breathing 11% oxygen for 30 minutes increased mean pulmonary artery pressure by 56%, from 16 to 25 mmHg in healthy volunteers (Zhao 2001). In another study, inhalation of 12.5% oxygen at sea level has been shown to decrease systemic PaO_2 to below 50 Torr (6.6kPa) and increase of pulmonary vascular resistance by 100% -150% in normal adult volunteers (Naeije 1987). The mechanism of pulmonary artery vasoconstriction following acute exposure of hypoxia has been shown to involve inhibition of O_2 sensitive K^+ channels leading to depolarization of pulmonary artery smooth muscle cells and activation of voltage gated Ca^{2+} channels. This causes Ca^{2+} influx and vasoconstriction (Moudgil 2005). This process is immediately reversed by breathing oxygen. Hypoxia also invokes a hyperventilation response attempting to improve oxygenation by increasing minute volume (Scrase 2009).

1.6.4 Hypoxic effects on children with neonatal hypoxic pulmonary arterial hypertension

I have discussed the acute effects of hypoxia causing pulmonary vasoconstriction and pulmonary hypertension. However, there is little evidence to prove that hypoxia in the perinatal period leads to susceptibility for hypoxic pulmonary arterial hypertension (PAH) in childhood and adulthood. Mourani et al assessed pulmonary arterial pressure (PAP) and other parameters on 10 patients with bronchopulmonary dysplasia (BPD) age between 4 months – 27 years via right heart catheterisation (Mourani 2004). The PAP at baseline for the group was 34.1 mmHg (SE 2.6). Following hypoxic challenge, 16% oxygen for non-oxygen dependent subjects and room air for oxygen dependent subjects, PAP and pulmonary to systemic vascular resistance ratio (PVR/SVR) increased by 50 ± 8% and 82 ± 14% respectively ($p<0.01$). Hyperoxia and inhaled nitric oxide given

together decreased PAP and PVR/SVR by 29 ± 5% ($p < 0.01$) and 45 ± 6% ($p < 0.05$) from baseline values, respectively (Mourani 2004).

In a separate study, Sartori et al measured systolic PAP by echocardiography on 15 adults (mean age 21 years), who had transient hypoxic pulmonary hypertension in the first week of life (Sartori 1999). These volunteers had their systolic PAP measured at sea level and then at a high altitude research laboratory at 4559m (4600 m ~ inhalation of 12% oxygen at sea level). They also had their PAP measured after inhalation of nitric oxide for 20 minutes at high altitude. The results were compared with that of 10 healthy volunteers who were born at full term and had a normal perinatal period. The results showed that at sea level, PAP between the two groups was similar but 24-36 hours after arrival at 4559m, the mean increase in PAP in the group who had neonatal pulmonary hypertension was significantly higher compared to the control group ($p< 0.01$). In this experiment, the decrease in PAP after inhalation of nitric oxide at high altitude was also significantly higher in the neonatal pulmonary hypertension group compared to the control group. The group also found that hypoxic breathing at low altitude (12% oxygen for 20 minutes) increased PAP similarly in patients and controls; at the end of hypoxic breathing the values for systolic PAP were 50.2 mmHg (5.6) and 47.6 mmHg (7.9), respectively.

Post mortem studies on infants who died from neonatal chronic lung disease showed thickening of the pulmonary vascular smooth muscle (Bush 1990, Margraf 1991). Similar findings were also noted in those infants who died from pulmonary hypertension (Haworth 1988, Stenmark 1988). Whether this early life pathology persists

in children who survive neonatal chronic lung disease is not known. If it does, it could predispose to an exaggerated vasoconstrictor response to acute hypoxia.

In view of the observations made by Sartori et al, it would be prudent to look for evidence of pulmonary arterial hypertension in response to acute hypoxia in the surviving children with chronic lung disease of prematurity. It is also not known if children with CLD of prematurity are at risk of developing subclinical right ventricular dysfunction and pulmonary arterial hypertension secondary to impaired lung function, especially if they are exposed to hypoxic conditions.

1.7 Hypothesis and study aims

1.7.1 Hypotheses

Since preterm infants with RDS are at risk of raised PAP, I hypothesised that the global and regional myocardial function of both left and right ventricles in preterm infants with RDS:

1a. are impaired compared with healthy term and preterm infants without RDS at birth

1b. will mature and improve during the first year of life of the preterm infants

School-aged children who had chronic lung disease of prematurity in infancy would have:

2a. Reduced pulmonary artery compliance compared to healthy term controls and preterm controls who did not have CLD in infancy at baseline

2b. An exaggerated response (more dramatic increase in pulmonary artery stiffness) to hypoxia (12% oxygen) compared to term and preterm controls who did not have CLD in infancy

1.7.2 Specific aims

My specific aims were:

1a. to assess longitudinal global and regional myocardial function of both ventricles using new echocardiographic parameters in ventilated preterm infants with RDS, in preterm infants without RDS and healthy term infants.

1b. to assess the changes in longitudinal global and regional myocardial function of both ventricles using new echocardiographic parameters during the first year of life in ventilated preterm infants with RDS, in preterm infants without RDS and healthy term infants.

2a. to measure pulmonary arterial stiffness (PWV) using velocity-encoded MRI at baseline in children who had chronic lung disease of prematurity in infancy, healthy term controls and preterm controls who did not have CLD in infancy.

2b. to measure pulmonary arterial stiffness (PWV) using velocity-encoded MRI under hypoxic condition (12%) in children who had chronic lung disease of prematurity in infancy, healthy term controls and preterm controls who did not have CLD in infancy.

Chapter Two:

Optimisation of myocardial deformation imaging in term and preterm infants – a technical study

2.1 Introduction

The assessment of regional myocardial function using myocardial velocity imaging (MVI) has been validated in children, infants, and neonates (Harada 2000, Kapusta 2000, Frommelt 2002, Mori 2004, Nestass 2009, Pena 2009). This technique has been used to assess regional myocardial function in different neonatal conditions (Patel 2009, Wei 2009) and shown to be both feasible and reproducible in preterm infants (Joshi 2010).

MVI allows the measurement of local contractile function using strain and strain rate. The relationship between these two parameters has been discussed previously in the Introduction section. The accuracy of these parameters depends on the technical settings used in the post-processing analysis but there is only one study using MVI to assess myocardial function in the preterm population (Joshi 2010).Using inappropriate computational distances, region of interest size and placement or inadequate frame rates would affect the measurements.

The distance between two adjacent points used to calculate the velocity gradient is known as the computation distance (CD). A shorter CD is associated with greater noise since the gradient is estimated from fewer velocities. Regional ε is the average ε from all the points within a sample area or the region of interest (ROI). A larger ROI will include more points within that area to be averaged. Therefore, a longer CD and a larger ROI will give a better signal-to-noise ratio, hence a more consistent ε estimation.

There are only two published studies on the technical aspects of offline tissue Doppler deformation analysis in the neonatal population (Nestaas 2007, Nestaas 2008). Nestaas

et al (Nestaas 2007) recommended the ROI size of 1mm long by 3mm wide with a strain length (or CD) of 10mm in a two-segment ε analysis of the term neonatal population. Pena et al (Pena 2009), who used a computation length of 6mm, suggested measuring ε in the middle segment of each wall as an initial screening parameter of local systolic function in the neonatal population but no data are available for preterm infants.

The inter-observer coefficient of variation (CV) of myocardial deformation measurements in the neonatal population is 30% (Joshi 2010) compared with 10 – 15% in children (Weidemann 2002) and adults (Serri 2006). Joshi et al (Joshi 2010) used a CD of 10mm for their population that consist of both term and preterm neonates. This could be the reason for their high inter-observer CV in myocardial deformation measurements. The reproducibility of myocardial deformation measurement would need to be improved considerably if it was to be used in the clinical setting. However, the size of the heart in this population presents additional technical challenges in the acquisition and analysis of myocardial deformation images.

The aim of the study was to establish the parameters that improve the reproducibility of measuring ε in both term and preterm infants.

2.2 Methods

The myocardial deformation data from infants who were recruited for the main study 'Regional and global myocardial assessment in preterm neonates with respiratory distress syndrome at birth and maturation of myocardial function during the first year' were used for this study. Fifty eight healthy term infants (≥38 weeks gestational age) (Group A), 24 preterm infants (≤34 weeks gestational age) without respiratory distress

syndrome (Group B), and 26 preterm infants with respiratory distress syndrome (Group C)] had been recruited from the postnatal wards and the Neonatal Unit of University Hospital of Wales when this technical study was conducted. The echocardiograms were performed by Mrs Julie M Edwards (JME) and Dr Suchita Joshi (SJ), who started this research project prior to my taking over the study.

The study was approved by the South East Wales Regional Ethics Committee (REC reference number: 07/WSE02/80) and Cardiff and Vale NHS Trust Research and Development department (R&D study reference: 07/RPM/3992). Written informed consent was obtained from parents.

All infants were scanned within 72 hours after birth. The infants were screened for congenital cardiac defects and excluded from the study if there was any abnormality other than patent ductus arteriosus or patent foramen ovale.

Out of 108 sets of digitally stored echocardiographic images, 20 recent sets of images [recorded in 7 healthy term infants (Group A), 7 preterm infants without respiratory distress syndrome (Group B), and 6 preterm infants with respiratory distress syndrome (Group C)] were studied. It was felt that 20 sets of images (a total of 60 wall segments) with almost equal numbers from each group would be sufficient to examine the effect of heart size, the image quality and the frame rates of the image acquisitions. As this was sole a study to examine the reproducibility of repeated measures of strain using different computational distance and not comparing the strain between the groups, a formal sample size calculation was not performed. Details of the infants are given in Table 2.1.

2.2.1 Echocardiographic protocol

Images were obtained from infants in a supine or left lateral position using a standard commercial ultrasound machine (Vivid 7, GE Vingmed Ultrasound AS, Horten, Norway) with a 10 MHz or a 7.0 MHz transducer by a single operator (JME).

Pulsed Doppler recordings of flow in the left ventricular outflow tract (LVOT) and the proximal pulmonary trunk were acquired from apical 4-chamber and parasternal short-axis views, and used to determine the timing of the opening and closure of the aortic and pulmonary valves. Ventricular chamber lengths were measured from the apical four-chamber image.

Colour tissue Doppler images of the left ventricle (LV), right ventricle (RV) and septum were acquired separately using the apical four-chamber view. The sector width and depth of each image were adjusted to obtain for the highest frame rate possible with the optimum Nyquist limit to avoid aliasing. All images were stored as three-beat loops on magneto-optical disks for post-processing.

2.2.2 Offline analysis

Images were analysed using the commercial EchoPac software (GE Vingmed Ultrasound EchoPac 7.00, Horten, Norway) by the same operator (CYP). The heart rates and frame rates of each loop were recorded. The LV and RV chamber lengths in end-diastole and end-systole were measured from the midpoint of each atrioventricular junction (between the lateral mitral or tricuspid annulus and the septum) to the apex of the left or right ventricular cavity respectively (Figure 3.6).

Myocardial longitudinal strain (ε) was measured in the middle segment of the LV and RV free walls and the septum (Figure 2.1). Maximal negative ε during systole was measured, using the timings of opening and closure of the aortic and pulmonary valves (Figure 3.13). All parameters were measured in three beats and averaged, unless the signal from an individual beat was too noisy, in which case only two beats were averaged. Linear drift compensation and the default 40ms Gaussian smoothing were used for all ε analyses.

In order to test the optimal technical settings for measuring ε in term and preterm infants, the maximal end-systolic ε was analysed using five different computational distances (CDs) (also called strain length) (2mm, 4mm, 6mm, 8mm, and 10mm) with the same ROI size (10 x 5mm), in two ways. First, the stored loop from each subject was analysed by positioning the ROI within the middle segments of the septum, LV and RV free walls, at sites that gave similar strain waveforms for each beat. This process was performed for all subjects, using the same CD for all walls, and then repeated in all subjects using the other CDs; the order in which the CDs were tested was determined randomly. In the second method, a CD of 10mm was used while selecting the position within the middle segment of the RV free wall that gave the least noisy strain curve. The maximal ε for this CD was determined. Without changing the ROI position, the CD was then reduced to 8mm, 6mm, 4mm, and 2mm and the maximal end-systolic longitudinal ε for the different CDs were documented. The same process was repeated separately on the LV free wall and septal wall. These methods were used in all subjects, twice, at an interval of 2 weeks.

Table 2.1 – Subject demographics, heart rate, frame rate and ventricular chamber lengths

Variable	Group A (Term infants)	Group B (Preterm infants without RDS)	Group C (Preterm infants with RDS)	P value
Number of infants	7	7	6	
Gestational age (wk)	40.04 ± 0.83	33.02 ± 0.57	26.98 ± 2.65	$p^{\S} = <0.001^{*, +, \#}$
Birth weight (kg)	3.67 ± 0.31	1.87 ± 0.23	1.06 ± 0.37	$p^{\ddagger} = <0.001^{*}, 0.001^{+}, 0.005^{\#}$
Heart rate (beats/min)	120 ± 10	113 ± 24	144 ± 11	$p^{\S} = 0.703^{*}, 0.046^{+}, 0.009^{\#}$
Frame rate (frames/sec)	201 ± 56	219 ± 53	256 ± 72	$p^{\ddagger} = 0.097^{*}, 0.022^{+}, 0.073^{\#}$
Ventricular length (mm)				
LV at systole	21.7 ± 2.3	16.7 ± 1.8	13.2 ± 2.5	$p^{\S} = <0.001^{*, +}, 0.025^{\#}$
LV at diastole	29.6 ± 3.0	22.8 ± 2.1	17.5 ± 2.4	$p^{\S} = <0.001^{*, +}, 0.004^{\#}$
RV at systole	20.3 ± 2.5	13.9 ± 2.2	12.4 ± 2.3	$p^{\S} = <0.001^{*, +}, 0.467^{\#}$
RV at diastole	27.5 ± 2.7	19.3 ± 1.8	16.3 ± 2.5	$p^{\S} = <0.001^{*, +}, 0.082^{\#}$

Data expressed as numbers or as mean ± standard deviation.
RDS=respiratory distress syndrome, LV=left ventricle, RV=right ventricle
§Denotes ANOVA test and ‡denotes Mann-Whitney U-test.
* A vs B; $^{+}$ A vs C; $^{\#}$ B vs C

Figure 2.1 - Comparison of longitudinal strain in midwall sites.

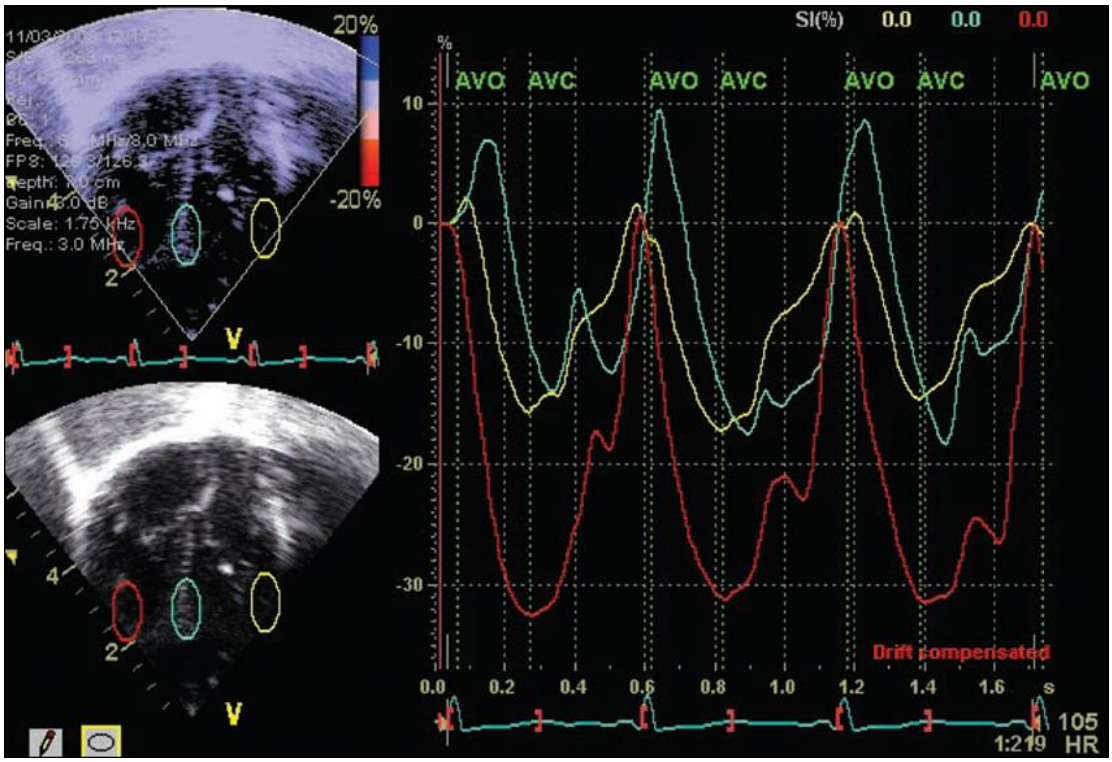

Position of the ROI in the middle segments of each wall displaying the ε curves of each wall. Note the heterogeneity in the ε between the walls.

2.2.3 Statistical analysis

Data were analysed using SPSS version 16.0 (SPSS Inc., Chicago, IL, USA). Values are presented as mean ± 2 SD. The Shapiro-Wilk test was used to test the normality of the measured parameters. Measurements between the three groups were compared by one-way ANOVA for normally distributed parameters and Tukey HSD was used for post-hoc multiple comparison. For parameters that were not normally distributed, measurements between the groups were compared by the Mann-Whitney U-test.

Two sets of longitudinal ε measurements on 20 sets of images were obtained on all three walls using five different CD by each method. The two methods were analysed separately. For each method, the mean ε, standard deviation (SD) and coefficients of variation (CV, in %) were calculated for each CD. The CV was calculated using the formula: CV = (SD / arithmetic mean of measurements) x 100, where SD is the standard deviation of the differences between the two sets of measurements. The CD with the smallest CV represents the highest reproducibility between measurements. ANOVA test was not used to compare the different CD because the objective was to check for the most reproducible strain results using different CD rather than comparing the results between the different CD. Therefore, CV was used instead.

The influences of other parameters such as frame rate, birth weight, and heart size (measured as ventricular length) on the reproducibility of measurements were also analysed by one-way ANOVA, where the means between groups were compared.

2.3 Results

As expected, infants who were born at an earlier gestational age weighed less at birth and had smaller hearts (Table 2.1). With increasing prematurity, there was a trend for the echocardiographic colour tissue Doppler loops to be recorded at higher frame rates, but the number of frames per heart beat was relatively constant (Group A 100 frames/beat, Group B 116 frames/beat, and Group C 107 frames/beat).

A total of 59 segments (20 RV free wall, 20 LV free wall, and 19 septum) were analysed, excluding only the septum in one infant in Group C. Measurements of these segments were averaged from three successive beats except for 7 / 59 (11.9%) (3 LV free wall, and 4 septum).

Systolic ε was highest in the RV free wall, followed by the LV and then the septum, in all 20 infants. Longitudinal ε increased proportionally with the size of the infants: the average ε values for Group A (mean birth weight 3.7kg), Group B (1.9kg), and Group C (1.1kg) were -23.5 ± 5.6%, -20.4 ± 7.4% and -14.4 ± 5.8%, respectively, at CD of 6mm (Table 2.2).

Using the first method (resampling the colour tissue Doppler loop for each measurement, to optimize each trace), the CD that gave the lowest CV was 6mm (CV 11.7%). The least reproducible CD was 2mm (CV 18.3%). Using the second method (when the ε measurements were done by reducing the CD without altering the position of the ROI within each wall, and without resampling the colour tissue Doppler loop), the differences in CV were minimal from CD of 2mm to 10mm (13.7 and 12.6%,

respectively). Further analyses were done using data obtained by the first method as this is a more realistic test of repeated measurements in clinical practice.

Table 2.2 - Reproducibility of longitudinal systolic strain with each computation distance resampled within each wall

Computation distance	RV		LV		Septum		Combined (LV, RV, Septum)	
	Mean ε ± SD (%)	CV (%)	Mean ε ± SD (%)	CV (%)	Mean ε ± SD (%)	CV (%)	Mean ε ± SD (%)	CV (%)
All groups								
2mm	-21.4 ± 6.3	10.9	-21.1 ± 9.6	22.5	-18.7 ± 6.7	15.7	-20.4 ± 7.7	18.3
4mm	-22.2 ± 5.8	8.8	-19.8 ± 8.5	19.3	-18.6 ± 7.0	11.7	-20.2 ± 7.2	14.0
6mm	-21.6 ± 5.3	9.8	-19.3 ± 9.1	15.1	-18.3 ± 6.8	6.3	-19.6 ± 7.2	11.7
8mm	-21.7 ± 5.4	8.8	-18.4 ± 8.6	16.5	-17.9 ± 6.3	14.5	-19.3 ± 7.0	13.8
10mm	-21.1 ± 5.3	10.7	-17.0 ± 7.7	13.6	-17.4 ± 6.2	12	-18.5 ± 6.6	12.9
Group A (Term infants)								
2mm	-25.3 ± 6.8	12.2	- 26.7 ± 11.6	22.8	-22.5 ± 5.9	11.4	-24.8 ± 8.2	20.0
4mm	-25.8 ± 5.5	11.5	-24.6 ± 6.7	25.4	-22.9 ± 5.5	6.3	-24.4 ± 5.8	17.1
6mm	-24.5 ± 5.2	12.8	-23.9 ± 6.8	19.5	-22.0 ± 5.3	7.4	-23.5 ± 5.6	14.8
8mm	-25.2 ± 5.3	11.3	-23.4 ± 6.1	16.7	-21.6 ± 4.8	12.2	-23.4 ± 5.4	14.2
10mm	-24.7 ± 5.3	12.0	-22.8 ± 5.5	15.0	-21.3 ± 5.1	8.4	-22.9 ± 5.3	13.2
Group B (Preterm infants without RDS)								
2mm	-21.0 ± 5.3	9.8	-21.4 ± 6.1	20.7	-19.2 ± 6.7	20.7	-20.5 ± 5.8	17.5
4mm	-21.8 ± 4.6	3.2	-21.1 ± 9.0	8.2	-18.8 ± 7.3	17.7	-20.6 ± 6.9	10.5
6mm	-21.4 ± 4.7	5.0	-20.7 ± 10.1	9.7	-19.0 ± 7.3	4.8	-20.4 ± 7.4	8.2
8mm	-21.1 ± 4.4	6.2	-19.5 ± 9.1	16.3	-18.1 ± 6.8	19.6	-19.5 ± 6.8	15.6
10mm	-20.6 ± 5.3	9.1	-16.9 ± 6.6	11.2	-17.4 ± 6.6	17.3	-18.3 ± 5.8	13.6
Group C (Preterm infants with RDS)								
2mm	-17.3 ± 4.5	10.4	-14.2 ± 6.6	5.6	-12.6 ± 3.5	17.0	-14.8 ± 5.2	11.2
4mm	-18.3 ± 5.3	8.4	-12.8 ± 5.9	4.6	-12.5 ± 4.1	8.3	-14.7 ± 5.6	7.3
6mm	-18.4 ± 4.9	3.0	-12.2 ± 6.4	3.9	-12.2 ± 3.8	4.9	-14.4 ± 5.8	3.6
8mm	-18.3 ± 4.8	4.2	-11.3 ± 6.2	5.0	-12.5 ± 3.3	5.9	-14.1 ± 5.7	4.9
10mm	-17.3 ± 4.6	9.5	-10.4 ± 6.1	8.0	-12.2 ± 3.1	9.6	-13.4 ± 5.5	9.2

RV=right ventricle, LV=left ventricle, *ε*=strain, SD=standard deviation, CV=coefficients of variation, RDS=respiratory distress syndrome

2.3.1 Influence of computation distance (CD)

When the measurements were analysed collectively, ε was most reproducible when the CD was 6mm. In the analysis between groups, a CD of 10mm gave the most reproducible measurements (with CV 13.2%) in the infants who were heaviest at birth and had the largest ventricular chambers (Group A). In the preterm infants (Groups B and C), the ε measurements were most reproducible using a CD of 6mm (CVs 8.2% and 3.6%, respectively). In the preterm groups, the poorest reproducibility was observed using CDs of 2mm and 10mm (Figure 2.2).

2.3.2 Influence of frame rate

In order to examine the influence of frame rate on the reproducibility of ε measurements, the data were sorted according to tertiles of frame rate, and within each tertile the CV for each CD was calculated. The average frame rate for all loops recorded in our study was 223 ± 63 frames per second (fps) and the mean for each group was >200 fps. There was an inverse relationship between frame rates and CV which decreased from 17.3% in the lowest tertile to 11.7% in the middle and 9.6% in the highest tertile (one-way ANOVA) (Table 2.3). At rates above 179 fps, in the middle and upper tertiles, repeated measurements of ε using a CD of 6mm gave CVs of only 7.0% and 8.0%, respectively.

2.3.3 Influence of heart size (diastolic ventricular length)

The longitudinal ε measurements obtained from images with frame rates >180 fps were sorted according to tertiles of diastolic length of the respective ventricles where each ε measurement was derived. Repeated measurements of systolic ε were most reproducible for infants in the first, second, and third tertiles of diastolic ventricular lengths (smallest,

average, and biggest hearts respectively) using CDs of 4mm (5.8%), 6mm (4.8%) and 8mm (8.4%) (Table 2.4).

Figure 2.2 - Reproducibility of longitudinal strain for different computation distance.

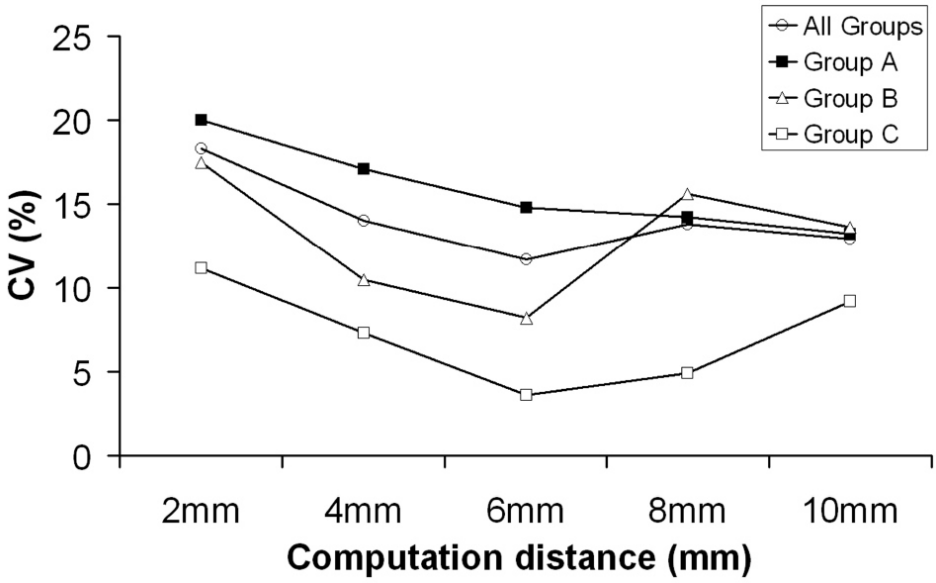

Graph of coefficients of variation (CV) versus computation distance (CD) according to groups. Computational distance of 6mm was the most reproducible for the preterm infant groups and 10mm in the larger term infants. However, the difference in CV between 6mm or 10mm in the term infants group is very small.

Table 2.3: Reproducibility of longitudinal strain sorted according to tertiles of frame rate

	1st (135 – 178 fps)		2nd (179 – 247 fps)		3rd (248 – 423 fps)	
Computation distance	Mean ε ± SD (%)	CV (%)	Mean ε ± SD (%)	CV (%)	Mean ε ± SD (%)	CV (%)
2mm	-23.3 ± 8.6	22.2	-17.1 ± 5.6	16.4	-20.5 ± 7.4	11.0
4mm	-22.7 ± 7.6	17.5	-18.1 ± 6.6	10.7	-19.7 ± 7.0	9.5
6mm	-22.4 ± 7.8	15.3	-17.2 ± 6.2	7.0	-19.4 ± 6.9	8.0
8mm	-21.7 ± 7.3	16.6	-17.2 ± 6.0	11.6	-18.9 ± 7.1	9.7
10mm	-20.4 ± 6.4	14.9	-16.5 ± 5.8	12.8	-18.5 ± 7.4	10.0
Mean CV		17.3 ± 2.9*		11.7 ± 3.4		9.6 ± 1.1

fps=frames per second, ε=strain, SD=standard deviation, CV=coefficients of variation
* $p < 0.05$ ANOVA test, first vs. second tertiles and first vs. third tertile

Table 2.4 – Reproducibility of longitudinal strain sorted according to tertiles of diastolic ventricular length (FR>180fps)

	1st (13.0 – 17.4mm)		2nd (17.5 – 23.0mm)		3rd (23.1 – 31.7mm)	
Computation distance	Mean ε ± SD (%)	CV (%)	Mean ε ± SD (%)	CV (%)	Mean ε ± SD (%)	CV (%)
2mm	-16.0 ± 5.1	12.6	-18.5 ± 6.1	10.3	-25.0 ± 5.7	9.2
4mm	-16.5 ± 6.2	5.8	-18.8 ± 6.4	7.9	-24.8 ± 4.2	9.6
6mm	-16.0 ± 6.4	6.6	-17.9 ± 6.4	4.8	-23.8 ± 4.1	9.8
8mm	-15.7 ± 6.8	13.2	-17.4 ± 6.0	10.9	-24.0 ± 4.9	8.4
10mm	-14.8 ± 6.6	10.9	-16.5 ± 5.8	12.0	-23.5 ± 4.8	10.0
Mean CV		9.8 ± 3.4		9.2 ± 2.9		9.4 ± 0.6

n = 25. No statistical differences between all three mean CV on ANOVA testing.
FR=frame rate, fps=frames per second, *ε*=strain, SD=standard deviation, CV=coefficients of variation

2.4 Discussion

I have confirmed that myocardial strain imaging is both feasible and reproducible even in preterm neonates. The overall CV of 11.7% for repeated measurements of ε in this study compares very well with the intra-observer reproducibility in another study (Joshi 2010).

The heterogeneity in the ε values seen between the three walls in our study is very similar to other studies (Nestass 2009, Pena 2009), albeit the mean RV ε values are lower. This may be explained by the inclusion in our study of preterm infants with respiratory distress syndrome, in whom RV function may be impaired.

I used two different methods to test the reproducibility of different CDs for measuring systolic ε in neonatal hearts. In the first method, repeated measurements were made by the same observer who resampled the same digitally stored myocardial velocity loops; each new measurement was made using slightly different data because of the slightly different sampling site (or ROI) as well as the altered CD. The second method was employed with the aim to eliminate the intra-observer's inconsistencies of placing the ROI in different positions for the best ε curve. The differences in the measured ε values in the second method were related only to variations in the CD, and showed that there were no consistent variations resulting from the processing algorithm. In this study, a total of 590 offline measurements were taken, consisting of 295 paired measurements from 59 different segments in 20 infants, repeated 2 weeks apart, and used to test the reproducibility of five different computational distances.

This study did not test the variability of repeated acquisitions or measurements by different observers, nor did it consider the variability that can occur if different machines or echocardiographic systems were used. Each of these factors in clinical practice introduces more variability.

2.4.1 Determinants of the reproducibility of myocardial strain

I have found that 6mm is the most appropriate CD to be used when measuring myocardial longitudinal ε in preterm infants. Shorter CDs gave worse reproducibility, probably because of increased noise in the signals. Longer CDs were expected to be more reproducible because of more averaging and smoothing, but they gave poorer reproducibility in repeated measurements, probably because the ROI included adjacent structures such as the papillary muscles, the mitral and tricuspid annuli and atria (Figure 2.3). In the larger term infants with a mean birth weight 3.7kg, increasing the CD to 10mm improved the reproducibility between measurements. This suggests that the CD to be used for measuring ε should be tailored to the size of the ventricle or infant.

Nestaas et al (Nestaas 2007) investigated the influence of different strain lengths (or CD) and ROI on two-segment ε and strain rate measurement in neonatal hearts. They found that the ROI size of 1mm long by 3mm wide with a CD of 10mm have the lowest beat-to-beat variation in a two-segment analysis of infants born at term. This is in keeping with our findings in the term infants. However, in the smaller preterm infants, 6mm would be the optimal CD to be used in a single segment longitudinal ε analysis.

Figure 2.3 - Variation of strain by sampling sites.

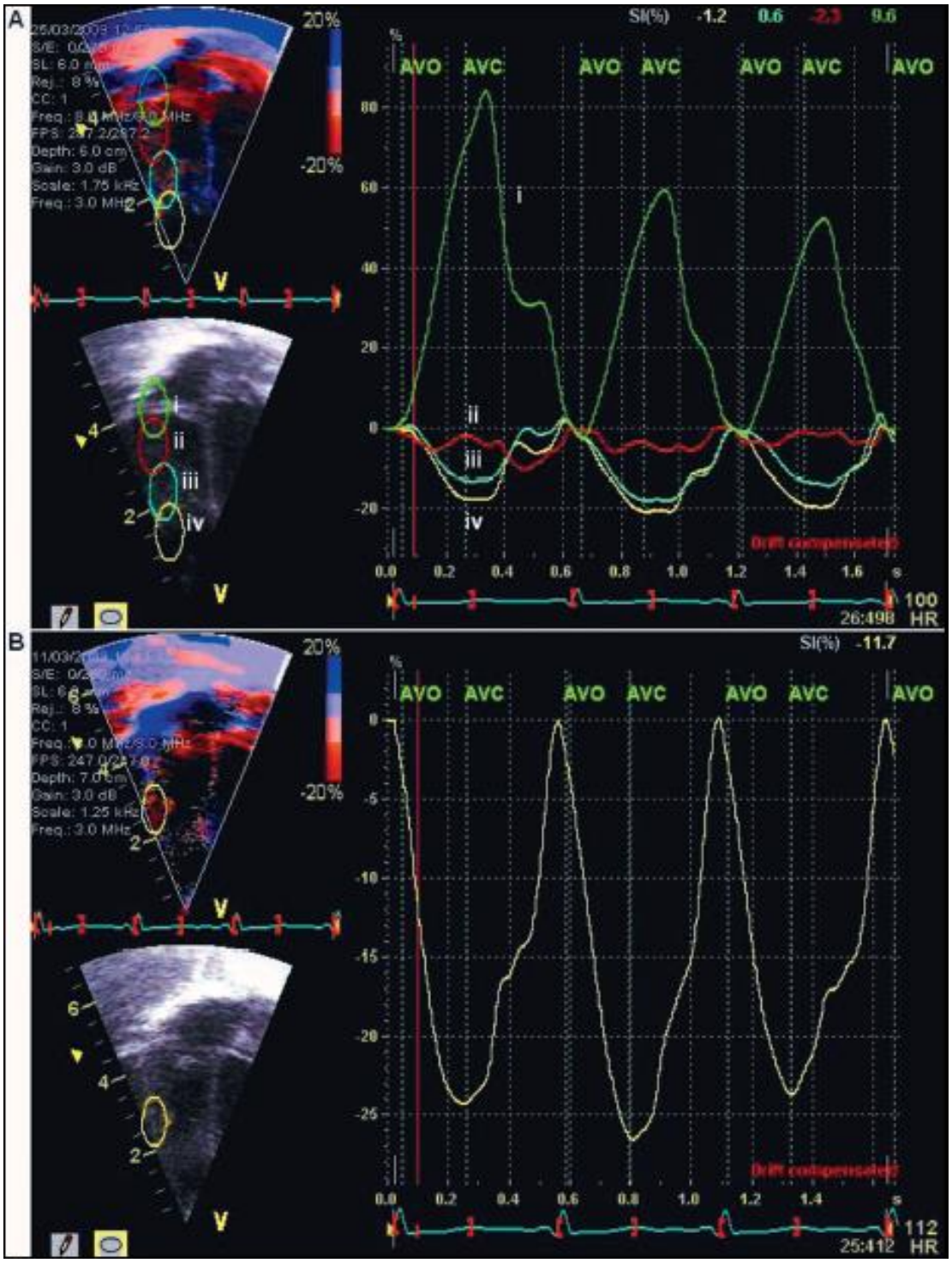

(A) Examples of strain curves obtained at different sampling sites, all using a strain length (computation distance) of 6mm. At site (i), longitudinal strain is positive because of the influence of the lateral wall of the right atrium, which elongates during systole. Sites (iii) and (iv) in mid and apex of the right ventricular free wall respectively, give good-quality traces, whereas a sampling site at the base of the right ventricular wall (ii) show an intermediate pattern presumably because of contributions from both atrial and ventricular myocardium. (B) A good-quality strain curve obtained from the middle portion of the right ventricular free wall, as used in this study.

I have shown conclusively that the reproducibility of repeated measurements improved with higher frame rates, across all the CD tested. I think this is the most likely explanation for improvements in the reproducibility of measurements in the smaller ventricles seen in my study as images were acquired from the smaller infants at higher frame rates. I recommend acquiring tissue Doppler images at frame rates >180 fps, in order to optimize the reproducibility of myocardial deformation imaging, in keeping with the general consensus that frame rates ≥200 fps help reduce the random noise component of the post-processing of myocardial strain and strain rate (Sutherland 2004). It is particularly important to obtain high frame rates in neonates whose heart rates are higher than in the children and adults. The average frame rates in other neonatal myocardial deformation studies were between 190 fps and 300 fps (Nestaas 2007, Pena 2009).

In conclusion, myocardial deformation imaging is a practical and reproducible echocardiographic technique for assessing regional longitudinal LV and RV function in both term and preterm neonates. I recommend using a CD (strain length) of 6mm for the off-line analysis of segmental strain in preterm infants. In term infants with larger hearts, although CD of 10mm is most reproducible, using a CD of 6mm in this population is also appropriate given the small difference in CV between the two CDs. All myocardial velocity loops should be acquired at frame rates above 180 fps.

This study has been published in European Journal of Echocardiography (Poon 2011) (Appendix H1) The above recommendations were used in the main study described in the next chapter.

Chapter Three

Regional and global myocardial assessment in preterm neonates with respiratory distress syndrome at birth and maturation of myocardial function during the first year (Neonatal TDi study)

3.1 Introduction

Myocardial velocity imaging (MVI) or tissue Doppler imaging (TDI) allows assessment of regional and global left and right ventricular function and thus helps detection of sub-clinical ventricular dysfunction. MVI has also been used to assess regional myocardial function in different neonatal conditions (Patel 2009, Wei 2009). Many studies assessed myocardial velocities or deformation separately and performed these either on term or preterm infants but did not compare with preterm infants with RDS (Schmitz 2004b, Ekici 2007, Pena 2009, Ciccone 2011). Negrine et al measured the left and right ventricular myocardial velocities using TDI in the first 24 hours of life in term, preterm and very preterm neonates (Negrine 2012). The group did not assess the myocardial deformation or study the effects of RDS on myocardial function. Table 3.1 summarises the MVI or TDI studies performed on neonates up to 2012.

In this chapter, I assessed for evidence of increased PAP in ventilated preterm infants with RDS and also assessed new TDI parameters (myocardial velocities, systolic strain and strain rate) in detecting the regional myocardial functions of both ventricles in three different groups of infants; ventilated preterm infants with RDS, preterm infants without RDS and term controls and compared them with established conventional global myocardial function. In addition to this, I have also assessed the changes in regional and global myocardial functions during the first year of life in these infants.

I hypothesised that the regional and global myocardial function of both ventricles in preterm infants with RDS:

(a) are impaired compared with healthy term and preterm infants

(b) would mature and improve during the first year of life

Table 3.1 Summary of literature review on tissue Doppler, myocardial velocity and deformation imaging in neonates (term and preterm)

Reference	Study population (N)	Age	Methods & Parameters measured	Results
Negrine, Birmingham, UK ADCFN 2012;97:F304-306	Very preterm (VPT), <30wks (15) Preterm (PT), 30-36 (12) Term (16)	Day 1 of life	PWD – MV, TV inflow velocity TDi – LMA, LTA ANOVA, t test used	HR decreased with increasing gestation. Trans-tricuspid E and A - NS between groups. Significant difference between groups – trans-mitral E (T52.8, PT56, VPT 40.5) and A flow (T47.3, PT58.6, VPT51.7) Mitral E/A ratio increased with increasing gestation. In all groups – higher velocities in RV than LV, and S' & E' increased with increasing gestation ($p<0.0001$) RV & LV E/E' ratio decreased with increasing gestation.
Schmitz, Berlin, Germany Pediatr Cardiol 2004;25:482-491	Healthy infants (280)	1day – 2yrs Cross-sectional study	LV filling - Doppler flow parameters	MV E & A peak velocities climax within 2 months after birth. E – 46.1(wk1) – 63.1(wk3-4) – 82 (mth 2) A – 42.1(wk1) – 57.3 (wk3-4) – 70 (mth2) Conclusion – maturation process in diastolic function mainly completed by 3 months of age.
Ciccone, Bari, Italy Early Hum Dev 2011	Term (33) Preterm, 31-36wks (20)	Within 3-4 days of life	PWD – MV, TV inflow vel TDi – LMA, LTA Myocardial tissue vel – LV, RV, IVS	Mitral E – T53.4, PT 45.3 (<0.01), Mitral A – T46.7, PT45.6 (NS) Mitral E/A – T 1.16, PT 1 (<0.01) LV Vs – T5.0 v PT4.1 (<0.01), LV Ve – T6.8 v PT5.8 (<0.01), LV Ve/Va – T1.2 v PT0.9 (<0.05) RV Vs – T7.2 v PT6.6 (<0.05), RV Ve – T7.9 v PT7.1 (<0.05), RV Ve/Va – T0.9 v PT0.7 (<0.05)
Ekici, Turkey Echocardiography 2007;24:61-67	Term (50) Children (54)	1 – 5 days 5 – 16 yrs	TDi – MMA, MLA, LVLW, IVS	LVLW (mid) – Vs4.8, Ve6.5, Va 6.0, IVS (mid) Vs4.3, Ve5.9, Va5.6cm/s MLA – S'6.6, E'8.2, A'8.6cm/s, MMA – S'6.1, E'6.8, A'8.2cm/s
Pena & Sutherland, Brazil &UK J Am Soc Echocard 2009;22:369-375	Term neonates (55)	Within 24 hours	CDMI – LV, RV Strain and SR (base, mid, apex) 300±50fps Longitudinal and radial ε	RV longitudinal deformation inhomogeneous – significant difference between basal and apical segments. Longitudinal ε higher in RV compared to LV. Mid segment LV ε -24.36%, LV SRs -1.67, SRe 2.96, SRa 2.04/s Mid segment RV ε -33.2%, RV SRs -1.91, SRe 3.00, SRa 2.57/s Recommend measuring SR and ε in each wall's middle segment as screening parameter.

Pena & Sutherland, Brazil &UK J Am Soc Echocard 2010;23:294-300	Term neonates (30)	Within 24 hours and 31 days old	CDMI – LV, RV Strain and SR (base, mid, apex) Longitudinal and radial ε	LV longitudinal peak systolic ε decreased at 1mth scan c.f. 1st scan. LV SRs, SRe, SRa - no difference. LV ε -25.58% vs -23.1% (<0.001), LV SRs -1.9 vs -1.85, SRe2.97 vs 3.29, SRa 2.16 vs 2.62/s RV systolic SR and ε significantly higher at 1 month. RV ε -33.21 vs -42.56 (<0.001), RV SRs -1.95 vs -2.25 (p=0.002), SRe 3.07 vs 5.03 (<0.001), SRa 254 vs 3.94 (<0.001) LV ε decrease at 1 month due to afterload increase and decrease in preload
Nestaas & Stoylen, Oslo, Norway Pediatr Res 2009;65:357-362	Term neonates (48)	First 3 days (scanned every day)	CDMI – LV, RV, IVS Strain and SR Multiple segments, multiple walls	High variations within segments, between segments and bet individuals – feasible to measure between segment groups and patient groups. Values highest in RV, intermediate in LV and lowest IVS. Basal left ε (D1-D3) -20.5% vs -18.6% vs -21.1 Basal anterior IVS ε (D1-D3) -14.5% vs -16.3% vs -13.2% Basal right lateral ε (D1-D3) -22.0% vs -26.0% vs -24.4% Basal LV SRs (D1-D3) -1.68/s vs -1.41/s vs -1.62/s Basal RV SRs (D1-D3) -1.85/s vs -2.26/s vs -2.33/s
Pauliks, Boston, USA Abstract (poster)	Preterm, 28 wks (12) Fetus, 25 wks (13)	4.5 ± 5.2 days	Colour myocardial Doppler imaging – Myocardial IVS peak systolic velocity, peak systolic SR	Similar S velocities – 2.2±0.6cm/s (PT) vs 2.0±0.5cm/s (Fetus). S velocity correlated with gestational age and septal length (R=0.89; p<0.001). SR similar -1.7±0.4/s (PT) vs -1.7±0.3/s (Fetus). Suggests somatic growth a major determinant of myocardial velocities early in life
Chan, HK, China Am Heart J 2005;150:750-755	302 fetus 19 – 37 weeks	-	Peak myocardial velocities – systolic (Sm), early diastole (Em) and late diastole (Am) PWD – MV, TV inflow vel	Sm, Em, Am, Em/Am, MV E/A and TV E/A all increased with increasing gestation. Fetal diastolic function predominantly contributed by atrial contraction at mid trimester. Ventricular relaxation becomes more mature with increasing gestation

3.2 Methods

A total of 120 infants were recruited into the study from the postnatal wards and the Neonatal Unit of the University Hospital of Wales. Sixty healthy term infants (≥37 weeks gestational age) (Group A - Term control), 30 preterm infants (≤34 weeks gestational age) without respiratory distress syndrome (Group B – PT Control), and 30 preterm infants with respiratory distress syndrome (Group C – PT RDS) were studied and followed up until one year of age.

The following criteria were used for selecting subjects for the different groups:

a) Term Control (Group A) – Healthy newborn infant born at term (≥37 weeks gestation)
b) PT Control (Group B) – preterm infant born ≤34 week gestation who did not have any clinical signs respiratory disease and did not require any respiratory support at first echocardiographic assessment
c) PT RDS (Group C) – preterm infant born ≤34 week gestation who has clinical and radiological evidence of respiratory distress syndrome and required mechanical ventilation support at first echocardiographic assessment.

Prior to contacting the parents for the 3-6 weeks and 1 year follow up studies, the infant's General Practitioner was contacted by letter or telephone by JME to ensure suitability of the infant for the follow up studies.

The study was approved by the South East Wales Regional Ethics Committee (REC reference number: 07/WSE02/80) and Cardiff and Vale NHS Trust Research and

Development department (R&D study reference: 07/RPM/3992). Written informed consent was obtained from parents.

3.2.1 Demographics and clinical observation data collection

The history proforma used is shown in Appendix B1.1. The clinical details, anthropometric data and clinical data (baseline pulse oximetry, heart rate and blood pressure measurements, invasive if available) were gathered by both JME and CYP, in addition to a cardiovascular examination by CYP.

3.2.2 Echocardiographic assessment

All infants were scanned within 72 hours after birth, at corrected term age for the preterm infants, at one month post term and at one year corrected age. The infants were screened for congenital cardiac defects and excluded from the study if there was any abnormality other than patent ductus arteriosus or patent foramen ovale. Images were acquired as 3-beat loops using a standard commercial ultrasound machine (Vivid 7, GE Vingmed Ultrasound AS, Horten, Norway) with a 10 MHz or a 7.0 MHz transducer. The echocardiograms were performed by Mrs Julie M Edwards (JME) and Dr Suchita Joshi (SJ).

A baseline echocardiography was performed to rule out structural cardiac defects prior to assessment of left and right ventricular function. Blood flow and tissue Doppler images were also acquired to measure the surrogate markers of pulmonary hypertension. The echocardiography acquisition protocol is given in Appendix A1.2.

A 2-D image of the long axis view of the LVOT was obtained to measure the LVOT diameter (Figure 3.3). Pulsed wave Doppler of the left ventricular outflow tract (LVOT) in the apical 4-chamber view was acquired to measure the LVOT velocity time integral (Figure 3.4). Conventional pulsed wave Doppler of mitral (Figure 3.5) flow was acquired from the apical 4-chamber view whereas pulmonary flow (Figure 3.9) and patent ductus arteriosus flow, if present, were acquired from the parasternal short axis view. The LV and RV chamber lengths in end-diastole were measured from the apical 4-chamber view (Figure 3.6).

Continuous wave Doppler image of the tricuspid flow (Figure 3.7) and pulsed wave Doppler of the pulmonary flow (Figure 3.8) were acquired to measure tricuspid regurgitation systolic velocity and pulmonary regurgitation end-diastolic velocity respectively, if present.

For lateral and medial mitral annular velocities (Figure 3.10) real-time pulsed tissue Doppler velocity profiles were acquired from the mitral annulus. Colour tissue Doppler images were acquired separately of the septum, left and right ventricles. The Nyquist limit was optimised to avoid aliasing, and the depth of imaging and the sector angle were adjusted to obtain high frame rates. The Nyquist limit, which is 50% of the sampling frequency, is the highest frequency that can be coded at a given sampling rate in order to be able to fully reconstruct the signal.

All images were stored as 3-beat loops in magneto-optical disks for post- processing.

Figure 3.1 Photograph of GE Vivid 7 equipment used in the study

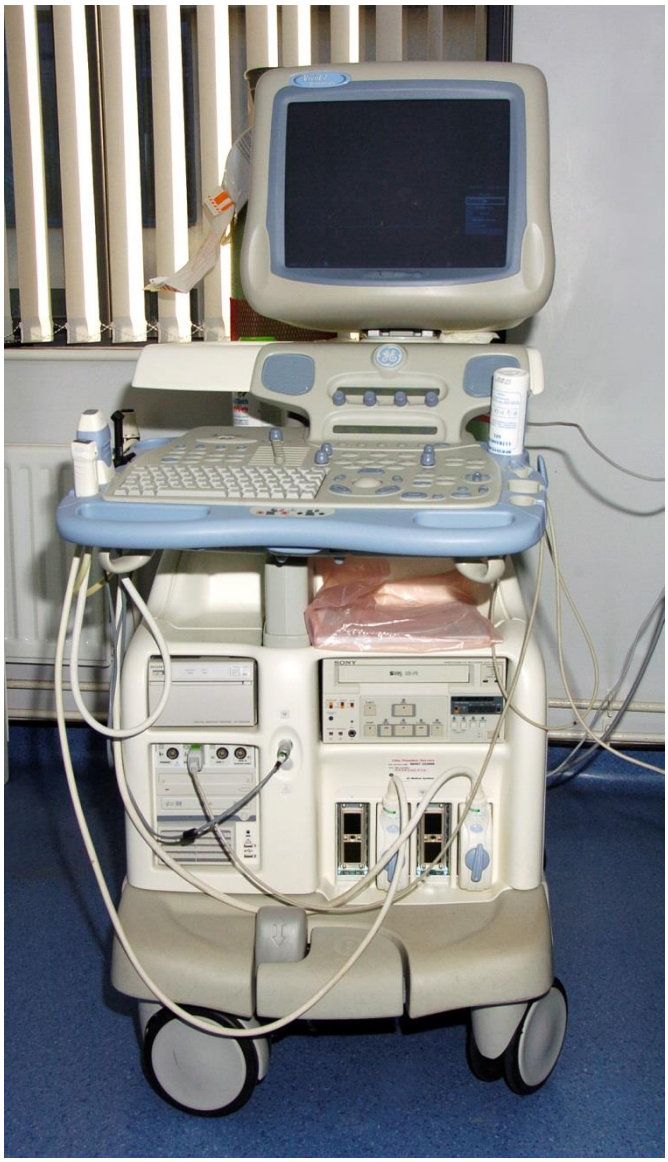

Figure 3.2 Photographs of infants having echocardiography at birth and at one year of age

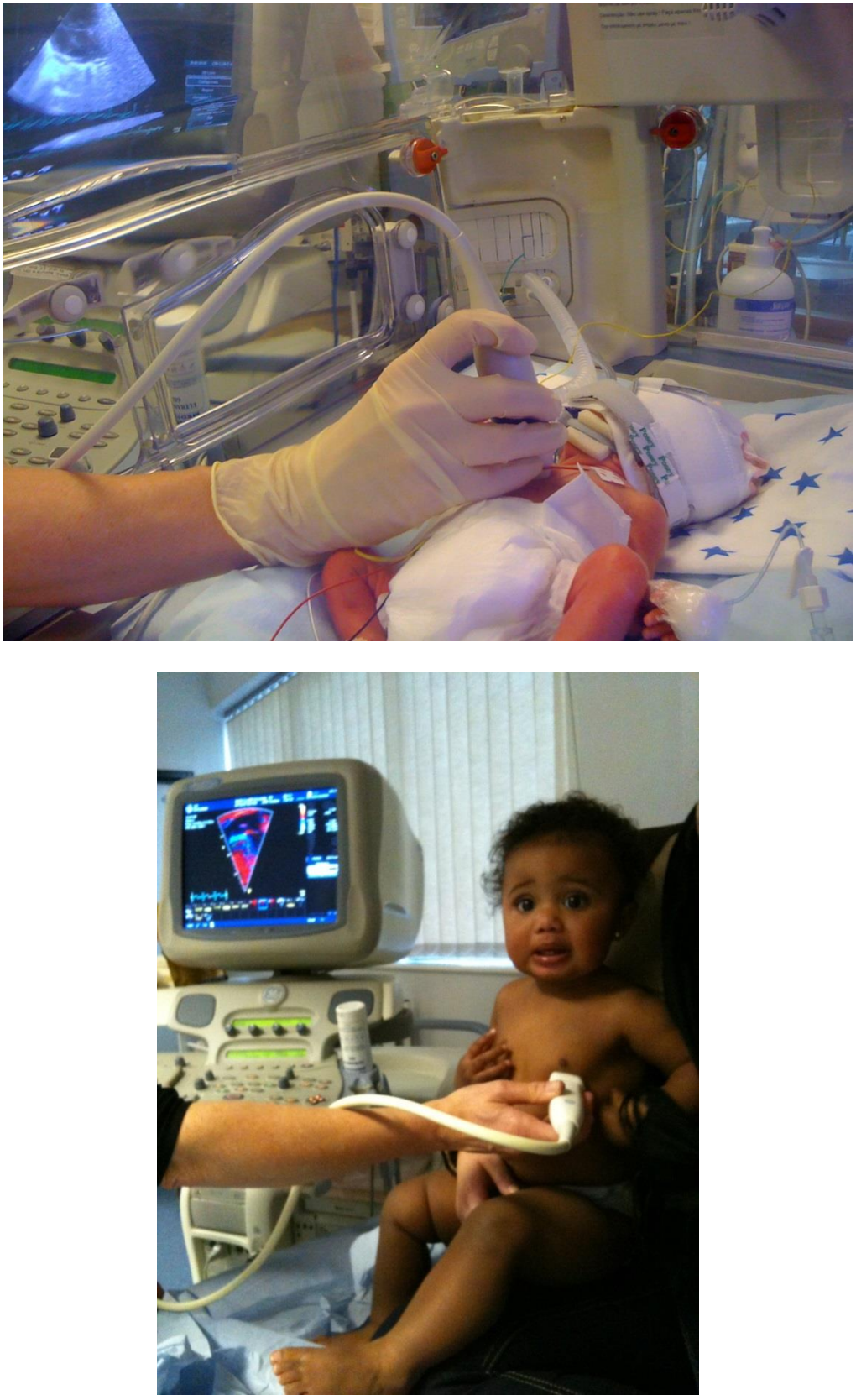

(Informed consent was obtained for the reproduction of this photograph in this thesis)

3.2.3 Analysis of the echocardiography images

Images were analysed solely by CYP using commercially available EchoPac software (GE Vingmed Ultrasound EchoPAC 7-00, Horten, Norway). Images were stored only with coded identity so that I was blinded to the clinical status of the subjects while analysing the images.

Forty parameters (Tables 3.2 and 3.3) were measured from each study, including 11 blood flow Doppler parameters, 2 tissue Doppler parameters from real-time tissue Doppler images and 24 post-processed parameters from LV and RV tissue Doppler loops.

Left ventricular pre-ejection period (PEP) was measured as the time interval between the onset of the QRS complex and the onset of the left ventricular outflow (Figure 3.4).

The velocity time integral of LV outflow (VTI) (Figure 3.4), the mitral E and A velocities (Figure 3.5), tricuspid regurgitation (Figure 3.7) and pulmonary regurgitation (Figure 3.8) velocities, patent ductus arteriosus flow velocity, and the pulmonary artery acceleration time (Figure 3.9) were measured conventionally from blood pool Doppler.

The area of the LV outflow tract was calculated as πr^2 where r is the radius of the LV outflow tract (r = diameter of LV outflow tract/2) (Figure 3.3). Stroke volume was calculated by multiplying the velocity time integral (VTI) by LV outflow tract area. Multiplying stroke volume by heart rate yields cardiac output (Thomas 2006). In order to correct cardiac output for body size, cardiac index (CI) was calculated as cardiac

output (L/min)/(length in m)^2. The LV and RV chamber lengths in end-diastole were measured from the apical 4-chamber view (Figure 3.6).

Right ventricular pre-ejection period (PEP) was measured as the time interval between the onset of the QRS complex and the onset of the right ventricular outflow. Pulmonary artery acceleration time (AT) was measured as the time interval between the onset of flow to the peak velocity and the ejection time (ET) was measured as the time interval between the onset of pulmonary flow to the end of flow (Figure 3.9). The ratio of the acceleration time to the ejection time (AT:ET) was calculated.

The mitral annular early diastolic velocity (Ve') was measured at both the medial and lateral mitral annulus (Figure 3.10) and averaged.

Myocardial systolic velocity (Vs), early diastolic velocity (Ve) and diastolic velocity during atrial contraction (Va) were measured at the basal segments (Figure 3.11) of the septum, LV and RV lateral walls. The cursor was positioned within each segment so that it did not encroach upon the annulus during systole. When myocardial Ve and Va were fused due to rapid heart rate, a single diastolic velocity was recorded and noted as Ve.

Annular displacement (Ds') was measured at the mitral (medial and lateral) and tricuspid valves using tissue tracking (Figure 3.12).

Longitudinal peak systolic strain at end-systole (S or ε) was measured within the middle segment of the septum, left and right ventricular walls (Figure 3.13). For computation,

strain length or computational distance of 6 mm was used as this was found to be the most reproducible strain length in this population as described in the previous chapter. Using the same sample area or region of interest (ROI) of 6mm x 3mm, systolic, early diastolic and late diastolic strain rates were measured for the septum, left and right ventricles (Figure 3.13). Myocardial systolic strain rate (SRs), early diastolic strain rate (SRe) and diastolic strain rate during atrial contraction (SRa) were measured within the middle segment of the septum, left and right ventricular walls (Figure 3.14). To ensure correct measurements of end-systolic strain during systole and the strain rate values, event timing was superimposed from left ventricular outflow tract and right ventricular outflow tract blood flow Doppler recordings for the LV and RV respectively.

All of the above parameters were measured in 3 beats and averaged.

Appendix A1.3 shows the analysis protocol and proforma used in this study.

Figure 3.3 2-D image of the left ventricular outflow tract diameter

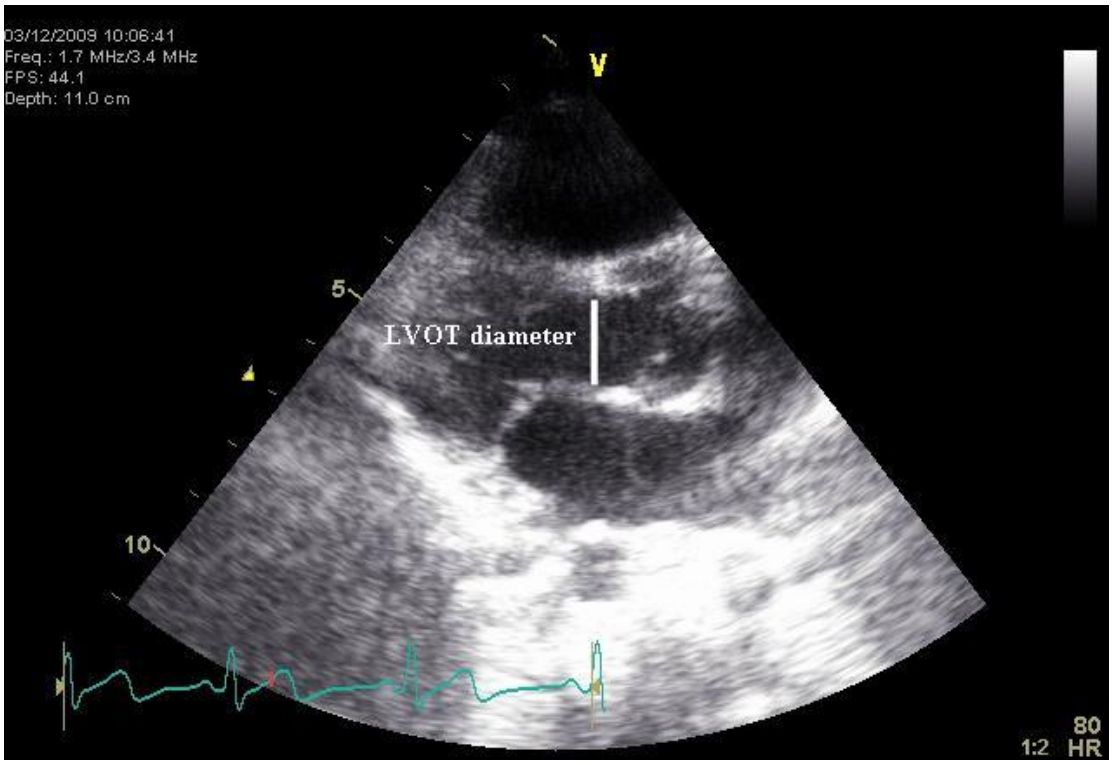

2-D parasternal long axis view of the left ventricular outflow tract. The vertical white line shows the measurement of the left ventricular outflow tract diameter when the aortic valve is open.

Figure 3.4 Pulsed wave velocity of the left ventricular outflow tract, LVOT

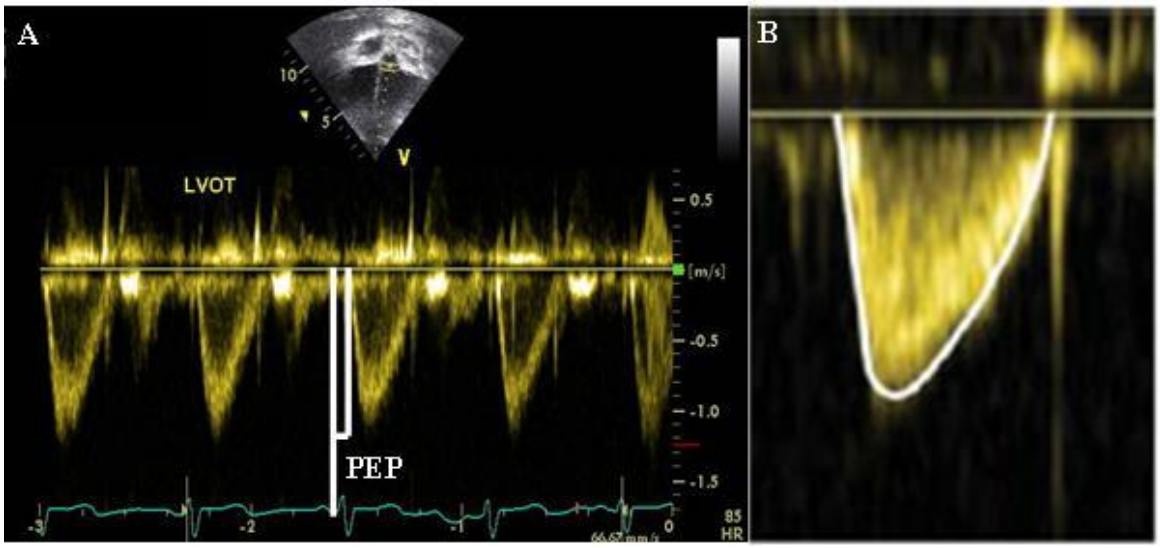

A. LV Pre-ejection period, PEP is the interval between the beginning of QRS complex and the start of left ventricular outflow.

B. Enhanced view of the left ventricular outflow velocity with thick tracing of the LVOT flow to measure the velocity time integral, VTI.

Figure 3.5 Pulsed wave Doppler of the mitral valve showing early (E) and late (A) diastolic velocities

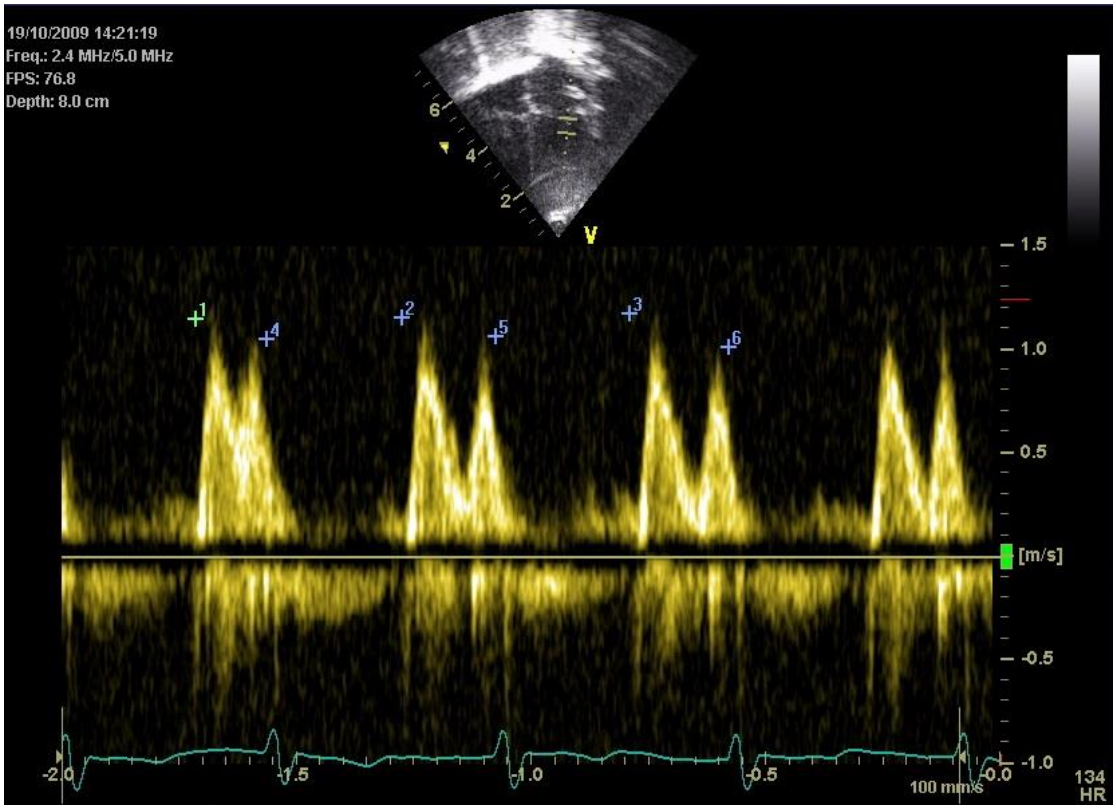

1, 2, & 3 = Mitral early diastolic velocity, E; 4, 5, & 6 = mitral late diastolic velocity during atrial contraction, A

Figure 3.6 Left ventricular chamber length measurement

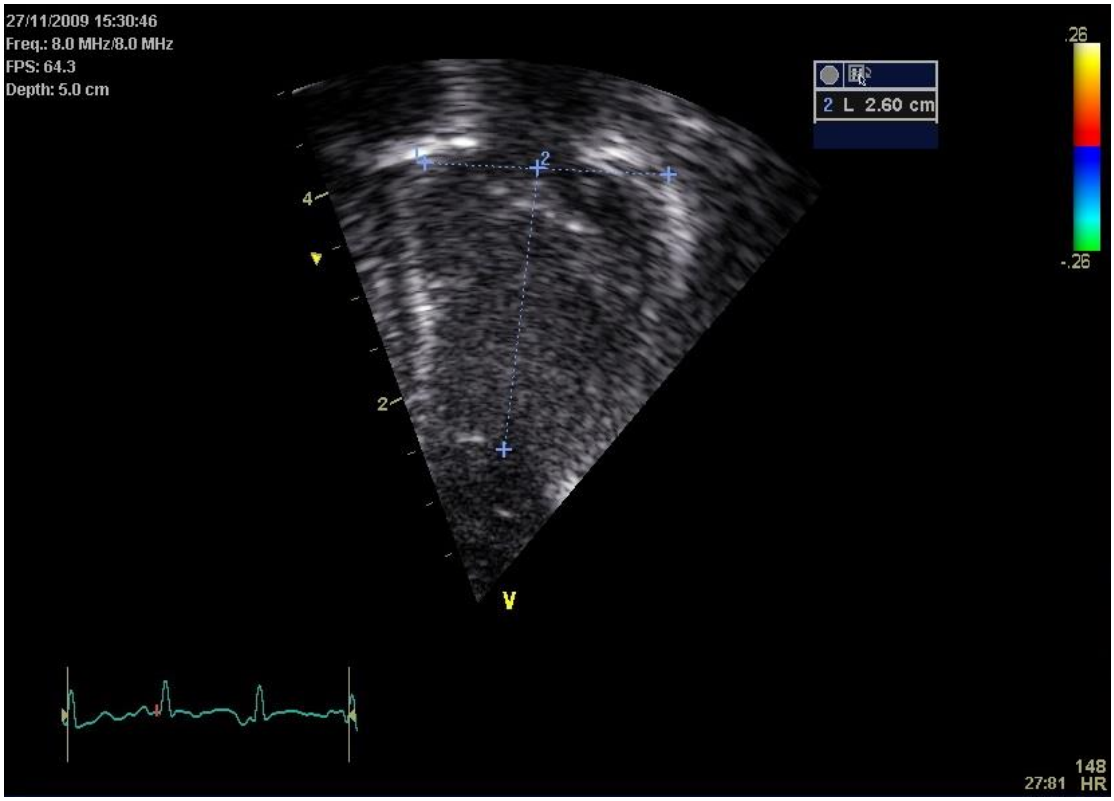

The chamber length, 2 is measured from the midpoint of atrioventricular junction (between the lateral mitral or tricuspid annulus and the septum) to the apex of the left or right ventricular cavity respectively.

Figure 3.7 Continuous wave Doppler of the tricuspid valve showing tricuspid regurgitation

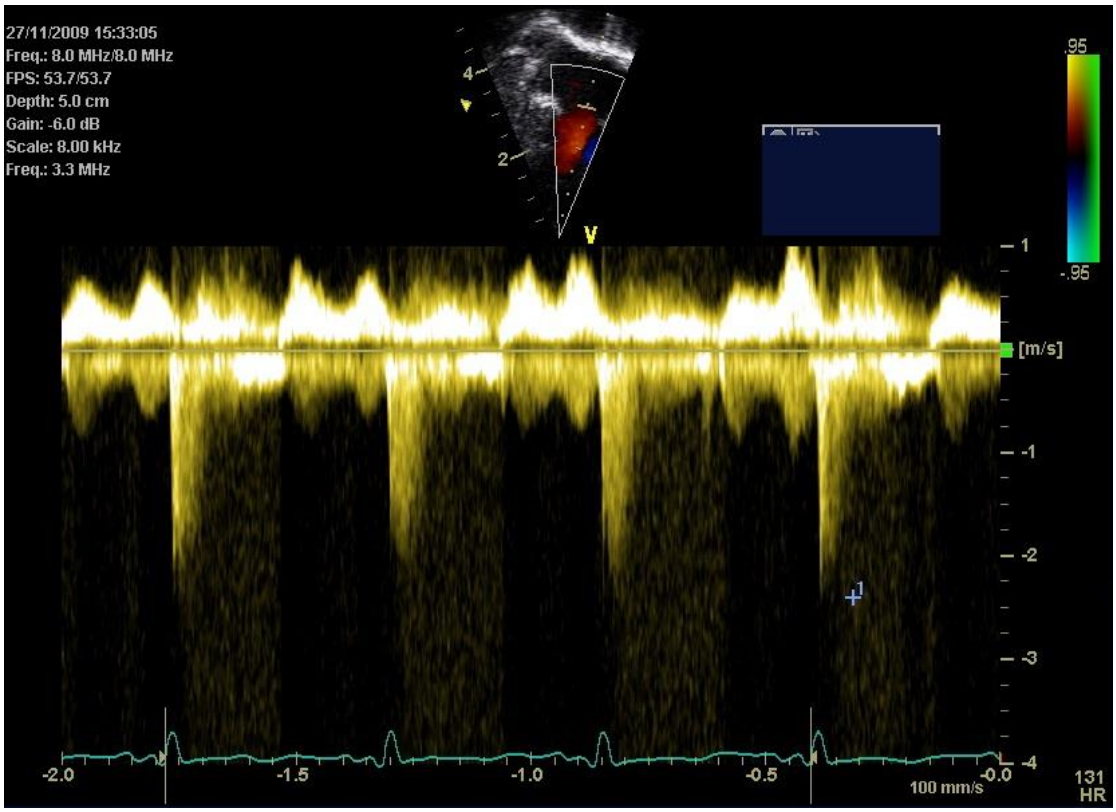

The marker, 1 marks the peak tricuspid regurgitation velocity

Figure 3.8 Pulsed wave Doppler of the pulmonary valve showing pulmonary regurgitation

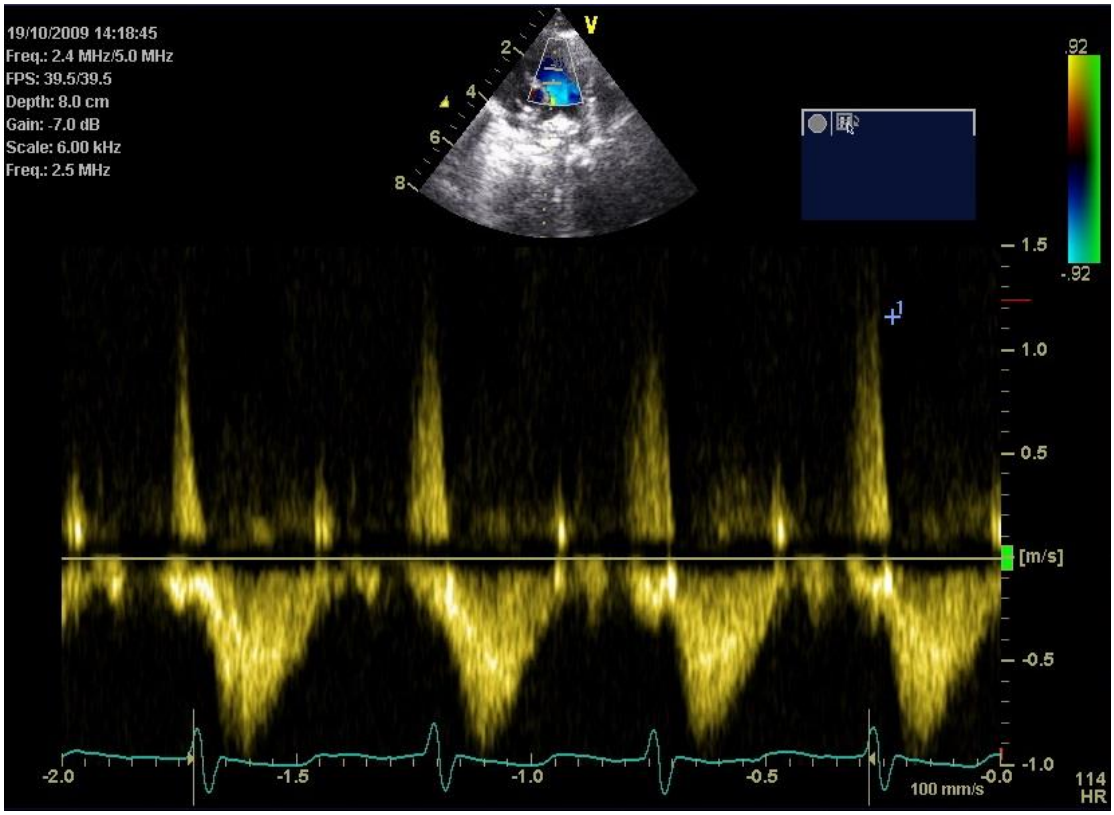

The marker, 1 marks the pulmonary regurgitation end-diastolic velocity

Figure 3.9 Pulsed wave Doppler of the pulmonary valve illustrating measurements of acceleration time and ejection time

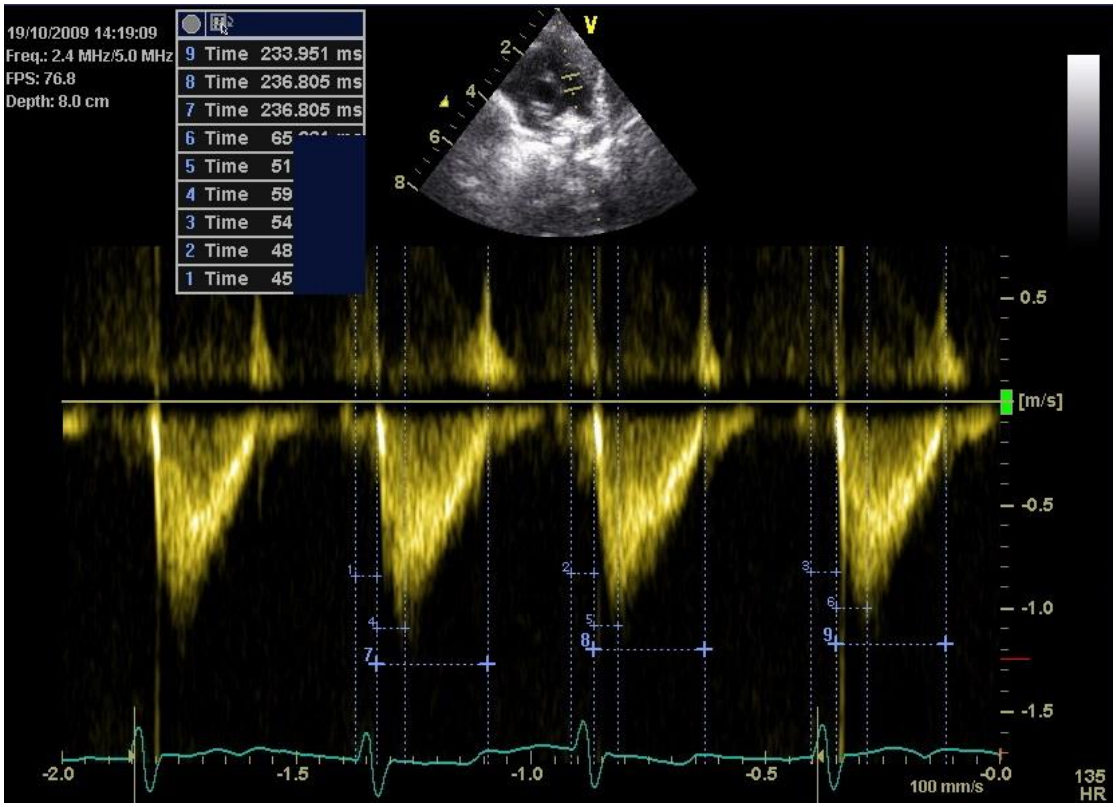

1, 2, & 3 = Right ventricular pre-ejection period, RV PEP, measured as the interval between the beginning of QRS complex and the start of right ventricular outflow.

4, 5, & 6 = Pulmonary arterial acceleration time, AT, measured as the interval between the onset of flow and the peak flow.

7, 8, & 9 = Pulmonary arterial ejection time, ET, measured as the interval between the onset of flow and the end of flow.

Figure 3.10 Real time pulsed tissue Doppler at the lateral mitral annulus

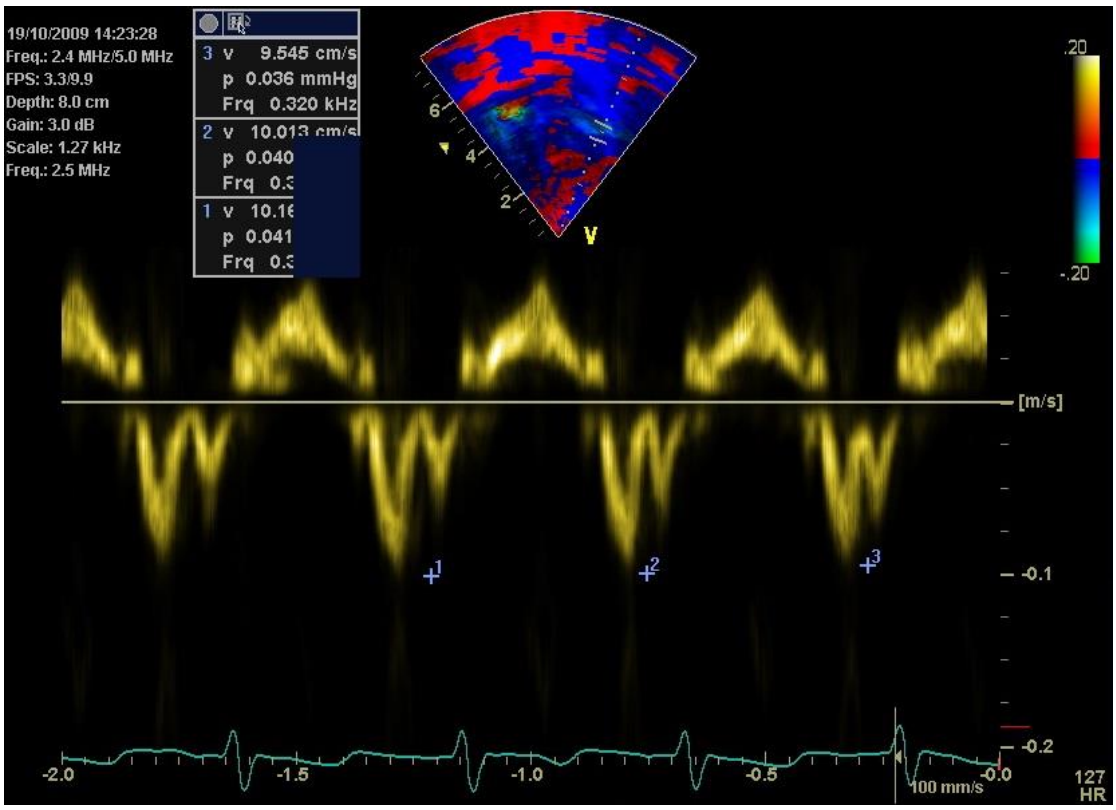

1, 2, & 3 mark the lateral mitral annular early diastolic velocity (Ve'). Ve' was measured at lateral and medial mitral annulus and the mean Ve' is reported.

Figure 3.11 Example of a myocardial velocity trace at the basal segment of the left ventricular free wall

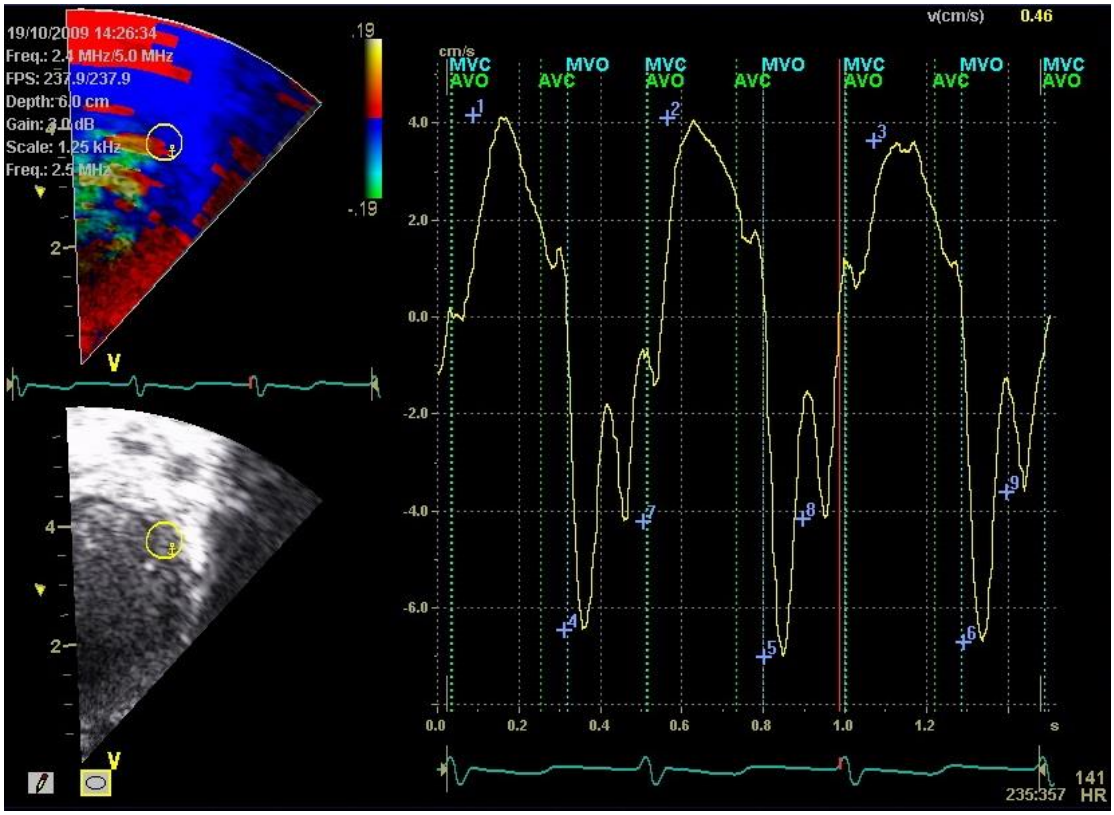

Figure showing the post-processed regional myocardial velocities of the left ventricle. A circular sample volume is placed at the base of the lateral wall.

AVO= Pulmonary valve opening and AVC= Pulmonary valve closure. AVO and AVC were measured from blood-flow Doppler traces of pulmonary flow.

MVO= Mitral valve opening and MVC= Mitral valve closure. MVO and MVC were measured from blood-flow Doppler traces of mitral flow.

1, 2, &3 = Peak systolic velocity (Vs); 4, 5, &6 = Early diastolic velocity (Ve); 7, 8, & 9 = Late diastolic velocity due to atrial contraction (Va).

Figure 3.12 Illustration of annular displacement at the lateral mitral annulus

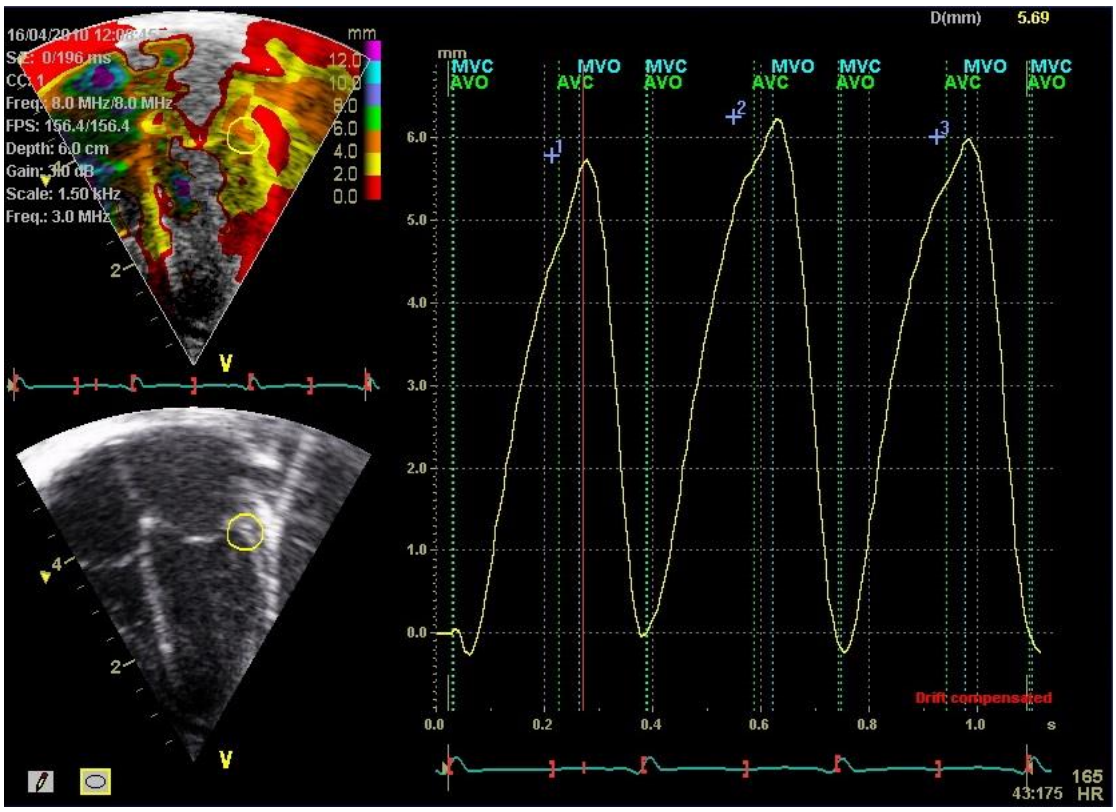

Figure showing the measurement of left ventricular annular displacement using tissue tracking. The numbers 1, 2, & 3 point to the annular displacements measured in millimetres.

Figure 3.13 Illustration of strain imaging at the middle segment of the left ventricular free wall

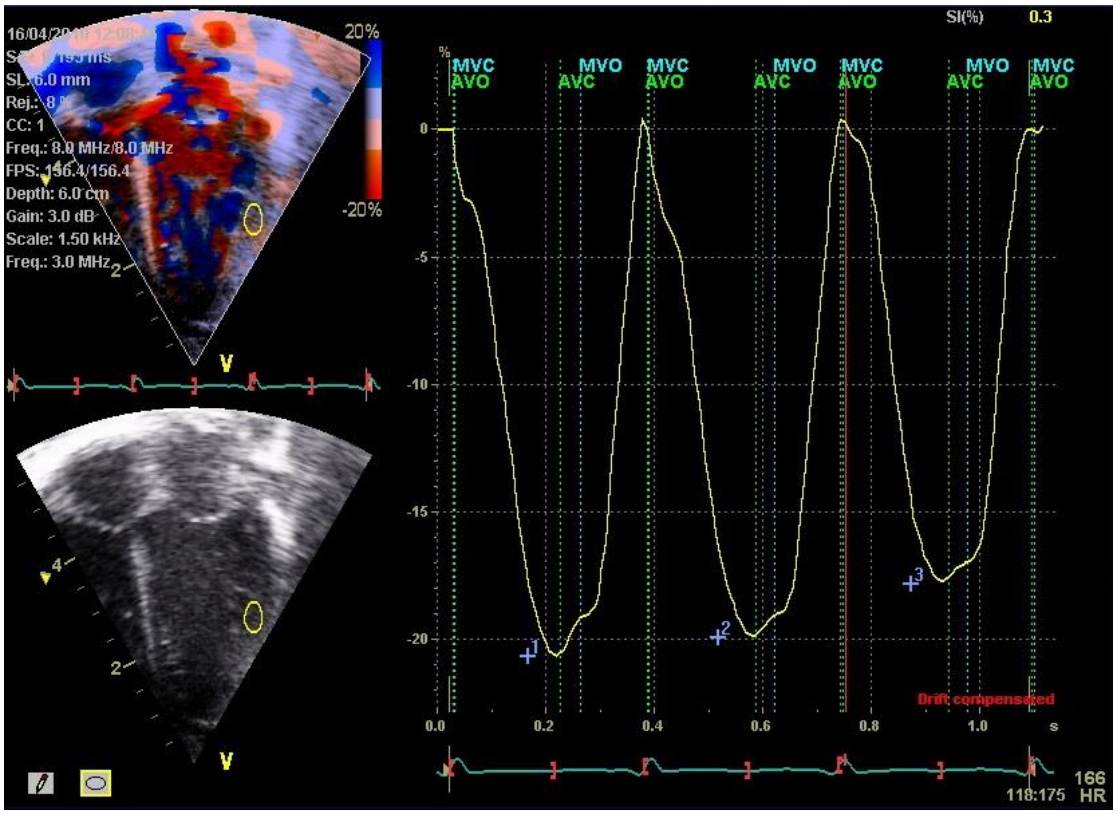

Figure showing left ventricular systolic strain at the middle segment of the left ventricle. AVO = Aortic valve opening, AVC = Aortic valve closure, MVO = Mitral valve opening and MVC = Mitral valve closure. Aortic valve closure marks the end of systole.

The numbers 1, 2, &3 point to the end-systolic strain.

Figure 3.14 Illustration of strain rate imaging at the middle segment of the left ventricular free wall

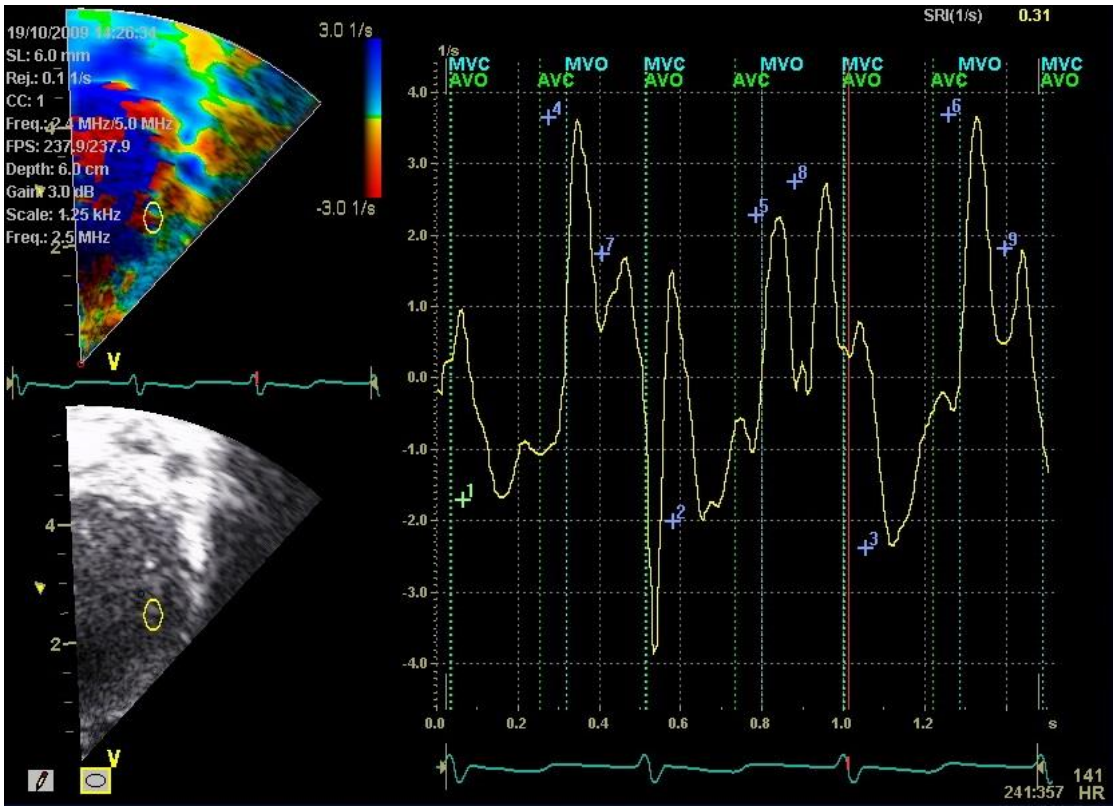

Figure shows the post-processed regional myocardial strain rates of the left ventricle. An elliptical sample volume is placed at the middle segment of the lateral free wall.

AVO= Pulmonary valve opening and AVC= Pulmonary valve closure. AVO and AVC were measured from blood-flow Doppler traces of pulmonary flow.

MVO= Mitral valve opening and MVC= Mitral valve closure. MVO and MVC were measured from blood-flow Doppler traces of mitral flow.

1, 2, &3 = Peak systolic strain rate (SRs);
4, 5, & 6 = Early diastolic strain rate (SRe);
7, 8, & 9 = Late diastolic strain rate due to atrial contraction (SRa).

3.2.4 Echocardiographic indices of left and right ventricular function

The echocardiographic indices that were used to assess left and right ventricular function are summarised in Table 3.2. Both systolic and diastolic function were assessed using 2-D, conventional blood flow Doppler and tissue Doppler methods also known as myocardial velocity imaging.

Cardiac index and LV pre-ejection period (LV PEP) were used as markers of LV systolic function. The ratio of the mitral inflow velocities E:A was measured to assess the LV filling pattern and diastolic function. The mitral annular Ve' velocity measured by myocardial velocity imaging was used to calculate E:Ve' ratio, which gives an estimate of mean LV filling pressure.

Myocardial velocity imaging was used to quantify both LV and RV global and regional long-axis function. Mitral and tricuspid annular displacements (Ds') are annular excursions, which in turn correlate with the left and right global myocardial systolic function, respectively. Ventricular long axis shortening, another measure of global myocardial function and presented as a percentage (%), was calculated from respective left and right annular displacements (Ds') divided by respective left and right end-diastolic ventricular chamber lengths multiplied by 100. The myocardial function at the basal segments of the septum, LV and RV lateral walls were quantified by myocardial systolic velocity, Vs, early diastolic velocity, Ve, and the late diastolic velocity, Va. RV, LV and septal systolic strains are indices of regional myocardial deformation.

Echocardiographic evidence of increased pulmonary arterial pressure (PAP) was also assessed using standard blood-flow Doppler methods and myocardial velocity imaging

as summarised in Table 3.3. Standard Doppler methods were used to measure tricuspid regurgitant velocity, and RV systolic pressure was calculated by applying the modified Bernoulli equation ($\Delta P = 4V^2$).

Pulmonary arterial acceleration time, AT, and ejection time, ET, and the ratio of AT: ET, were also used to assess pulmonary arterial systolic pressure.

RV free wall strain was measured as a surrogate of PA hypertension (Dambrauskaite 2007).

3.2.5 Statistical Analysis

Evans et al found the ratio of pulmonary artery time to peak velocity to right ventricular ejection time (another nomenclature for PA AT:ET) in infants with RDS to be significantly lower than the infants without lung disease (Evans 1991a). The mean PA AT:ET ratio for infants with RDS and the control group were 0.26 and 0.35 respectively. This gives an approximately 30% difference in PA AT:ET ratio, a surrogate marker of PAP, between the groups. Based on this data, I calculated that I would need to study at least 30 children in each arm to be 90% certain of a difference of 30% in pulmonary arterial pressure at a $p < 0.05$ between the groups.

Data were analysed using SPSS version 16.0 (SPSS Inc, Chicago, IL, USA). Results are presented as mean ± 2 SD. The Shapiro-Wilk test was used to test the normality of the measured parameters. For parameters that were not normally distributed, measurements between the groups were compared by the Mann-Whitney U-test. One-way ANOVA with Tukey HSD post-hoc multiple comparisons was used for normally distributed

parameters to test the differences between the three groups at individual time points. Since the term control group only had three echocardiographic assessments while the preterm groups had four assessments, it would be inappropriate to use repeated measures ANOVA to compare the differences in parameters across time as well. I am also aware of the possibility of a high dropout rate in follow up which may further influence the results from the repeated measures ANOVA test. $P<0.05$ will be considered significant.

Table 3.2 Echocardiographic markers of left and right ventricular function

Markers of LV function	Markers of RV function
Pulsed-Doppler parameter	
LV velocity time integral (VTI)	
LV pre ejection period (LV PEP)	
Mitral early diastolic velocity (E)	
Mitral late diastolic velocity (A)	
Real-time annular myocardial velocity imaging	
Medial mitral annular velocity (MMA Ve')	
Lateral mitral annular velocity (LMA Ve')	
Colour processed myocardial velocity imaging	
LV annular displacement (LV Ds')	RV annular displacement (RV Ds')
LV basal systolic velocity (LV Vsbl)	RV basal systolic velocity (RV Vsbl)
LV basal e velocity (LV Vebl)	RV basal e velocity (RV Vebl)
LV basal a velocity (LV Vabl)	RV basal a velocity (RV Vabl)
LV peak systolic strain (LV Ss)	RV peak systolic strain (RV Ss)
LV peak systolic strain rate (LV SRs)	RV peak systolic strain rate (RV SRs)
LV early diastolic strain rate (RV SRe)	RV early diastolic strain rate (RV SRe)
LV late diastolic strain rate (RV SRa)	RV late diastolic strain rate (RV SRa)
Septal annular displacement (LV Ds')	
Septal systolic velocity (LV Vsbs)	
Septal basal e velocity (LV Vebs)	
Septal basal a velocity (LV Vebs)	
Septal end systolic strain (Sep Ss)	
Septal end systolic strain rate (Sep SRs)	
Septal early diastolic strain rate (RV SRe)	
Septal late diastolic strain rate (RV SRa)	

Table 3.3 Surrogate markers of pulmonary arterial pressure

Blood pool Doppler markers	Tissue Doppler markers
Tricuspid regurgitation velocity (TR)	RV systolic strain (RV Ss)
Pulmonary regurgitation end-diastolic velocity (PR)	
Pulmonary artery acceleration time (AT)	
Pulmonary artery ejection time (ET)	
Pulmonary AT:ET ratio	

3.3 Results

3.3.1 At birth (within 72 hours old)

3.3.1.1 Demographics and general characteristics

General characteristics of the infants including baseline heart rate, blood pressure and ventricular end-diastolic lengths are summarised in Table 3.4. As expected, the preterm RDS group had the lowest gestation, birth weight and body surface area. Their smallest size is also reflected by having the shortest left and right ventricular chamber lengths. Term controls had the highest systolic and diastolic blood pressures; whereas preterm RDS group's systolic and diastolic blood pressures were the lowest. The opposite was true with regards to heart rate.

3.3.1.2 Left ventricular global systolic and diastolic functions

Table 3.5 and 3.6 summarise the echocardiographic parameters of left ventricular global systolic and diastolic functions between the groups. LV outflow tract diameter (LVOT d), LV outflow tract velocity time integral (LVOT VTI), stroke volume (SV), cardiac output (CO) and cardiac index (CI) were highest in the term group compared to the two preterm groups. Both LV basal lateral and basal septal annular displacements were highest in the term group compared to the preterm groups. However, LV pre-ejection period (LV PEP) and LV long axis shortening was only significantly different between the term group and the preterm RDS groups.

Mitral early diastolic flow velocity, mitral E:A ratio and mitral annular velocity were highest in the term group compared with the preterm groups. However, there were no differences in mitral late diastolic flow velocity and mitral E:Vé between the groups.

Table 3.4: General characteristics and clinical data at birth

	Term Control (A)	**PT Control (B)**	**PT RDS (C)**	**ANOVA p value**
Demographics				
Male : Female	31:29	18:12	21:9	-
Gestation (wks)	39.8 (1.2)	32.7 (1.4)	28.2 (2.7)	**<0.001**$^{§, §§, §§§}$
Birth wt (kg)	3.4 (0.5)	1.8 (0.4)	1.2 (0.4)	**<0.001**$^{§, §§, §§§}$
BSA (m^2)	0.21 (0.22)	0.15 (0.02)	0.11 (0.03)	**<0.001**$^{§, §§, §§§}$
Physiological measurements				
Heart rate (/min)	115 (19)	136 (15)	143 (16)	**<0.001**$^{§§, §§§}$
Systolic BP (mmHg)	66.9 (11.7)	65.1 (10.8)	49.3 (7.8)	**<0.001**$^{§, §§}$
Diastolic BP (mmHg)	41.3 (9.9)	37.1 (7.8)	30.8 (7.5)	**<0.001**$^{§§, †}$
Oxygen saturation (%)	98.9 (1.8)	99.1 (1.1)	96.1 (3.0)	**<0.001**$^{§, §§, §§§}$
End-diastolic ventricular chamber lengths				
LV length (cm)	2.8 (0.3)	2.1 (0.2)	1.8 (0.3)	**<0.001**$^{§, §§, §§§}$
RV length (cm)	2.7 (0.3)	2.0 (0.2)	1.8 (0.3)	**<0.001**$^{§, §§, §§§}$
Ventilation / respiratory parameters				
Highest peak pressure (cmH_20)	-	-	21.8 (3.9)	-
Duration of ventilation (days)	-	-	14.0 (17.5)	-
Duration of O_2 dependency (days)	-	-	57.9 (83.6)	-
Chronic lung disease (n)	-	-	10	-
Patent ductus arteriosus (n)	27	7	19	-

Results are presented as mean (SD).
§ p <0.001 (PT RDS V PT control), §§ p <0.001 (PT RDS V Term control), §§§ p <0.001 (PT control V Term control), † p <0.05 (PT RDS V PT control)
Chronic lung disease definition used – oxygen dependency at ≥36 weeks corrected gestational age

Table 3.5: LV global systolic function at birth

	Term Control (A)	PT Control (B)	PT RDS (C)	ANOVA p value
LVOT d (cm)	0.66 (0.07)	0.53 (0.06)	0.45 (0.08)	**<0.001**[§, §§, §§§]
LVOT VTI (cm)	12.5 (2.4)	10.2 (2.3)	8.6 (2.5)	**<0.001**[†, §§, §§§]
Stroke volume (ml)	4.3 (1.2)	2.3 (0.8)	1.4 (0.6)	**<0.001**[‡, §§, §§§]
Cardiac output (L/min)	0.49 (0.13)	0.31 (0.11)	0.19 (0.08)	**<0.001**[‡, §§, §§§]
Cardiac index (L/min/m2)	2.23 (0.55)	2.09 (0.61)	1.82 (0.61)	**0.002** [‡‡]
PEP (ms)	55.1 (10.7)	50.7 (10.9)	47.9 (14.0)	0.018 [‡‡]
PEP:ET ratio	0.27 (0.06)	0.26 (0.05)	0.26 (0.09)	0.725
LV Ds'bl (mm)	4.6 (1.0)	3.4 (0.8)	2.6 (1.0)	**<0.001**[‡, §§, §§§]
LVbl long axis shortening (%)	16.3 (3.6)	15.7 (3.5)	14.0 (5.1)	0.047[††]
LV Ds'bs (mm)	5.2 (0.8)	4.1 (0.8)	3.1 (0.9)	**<0.001**[§, §§, §§§]
LVbs long axis shortening (%)	18.6 (3.4)	19.0 (3.8)	17.3 (5.5)	0.249

Results are presented as mean (SD).
[§] *p* <0.001 (PT RDS V PT control), [§§] *p* <0.001 (PT RDS V Term control), [§§§] *p* <0.001 (PT control V Term control), [‡] p <0.01 (PT RDS V PT control), [‡‡] p <0.01 (PT RDS V Term control), [†] p <0.05 (PT RDS V PT control), [††] p <0.05 (PT RDS V Term control)

Table 3.6: LV global diastolic function at birth

	Term Control (A)	PT Control (B)	PT RDS (C)	ANOVA p value
Mitral E (m/s)	0.64 (0.12)	0.52 (0.11)	0.47 (0.14)	**<0.001**[§§, §§§]
Mitral A (m/s)	0.57 (0.11)	0.56 (0.11)	0.52 (0.13)	0.081
Mitral E:A	1.13 (0.23)	0.95 (0.18)	0.92 (0.22)	**<0.001**[§§, §§§]
LMA Vé (cm/s)	7.9 (1.5)	6.9 (1.1)	5.0 (1.0)	<0.001
MMA Vé (cm/s)	6.6 (1.5)	5.6 (1.1)	5.1 (1.4)	<0.001
Mitral Vé (cm/s)	7.3 (1.3)	6.3 (0.9)	5.1 (0.9)	**<0.001**[§, §§, §§§]
Mitral E:Vé	9.0 (1.8)	8.4 (1.9)	9.3 (2.5)	0.226

Results are presented as mean (SD).
[§] *p* <0.001 (PT RDS V PT control), [§§] *p* <0.001 (PT RDS V Term control), [§§§] *p* <0.001 (PT control V Term control)

3.3.1.3 Left ventricular regional function

Left ventricular myocardial systolic and early diastolic velocities were highest in the term group and lowest in the preterm RDS group (Table 3.7). This was seen in both basal lateral and basal septal walls. LV basal lateral myocardial late diastolic velocity was higher in the term compared to the preterm RDS group ($p=0.004$). The LV basal septal myocardial late diastolic velocity was lowest in the preterm RDS group compared to the term and preterm control groups, $p=0.02$ and $p=0.03$ respectively.

Myocardial peak systolic strains of both septal and lateral free walls were lowest in the preterm RDS group compared to term and preterm groups. The strain measurements in both walls were similar between the two control groups.

There were no differences in the myocardial strain rate measurements in both septal and lateral free walls between the groups.

Table 3.7: LV regional function at birth

	Term Control (A)	PT Control (B)	PT RDS (C)	ANOVA p value
Basal myocardial velocity				
Vsbl (cm/s)	3.0 (0.8)	2.1 (0.7)	1.7 (0.8)	**<0.001**[§§,§§§]
Vebl (cm/s)	4.5 (1.1)	3.5 (1.1)	2.52 (1.2)	**<0.001**[‡,§§,§§§]
Vabl (cm/s)	3.7 (1.4)	3.1 (1.1)	2.8 (1.2)	**0.003**[‡‡]
Vsbs (cm/s)	3.0 (0.7)	2.6 (0.8)	1.9 (0.6)	**<0.001**[‡,§§,†††]
Vebs (cm/s)	3.8 (0.9)	3.4 (1.5)	2.8 (1.0)	**<0.001**[§§]
Vabs (cm/s)	3.7 (1.1)	3.8 (0.8)	3.1 (0.9)	**0.016**[†,††]
Mid-segment myocardial peak systolic longitudinal strain				
Ssl (- %)	22.8 (3.9)	21.2 (3.8)	18.9 (4.9)	**<0.001**[§§]
Sss (- %)	19.8 (3.8)	19.5 (3.2)	17.5 (3.9)	**0.027**[††]
Mid-segment myocardial strain rate				
SRsl (/s)	2.2 (0.8)	1.9 (0.5)	2.0 (0.8)	0.116
SRel (/s)	2.7 (0.9)	3.1 (0.9)	2.6 (0.9)	0.172
SRal (/s)	2.4 (1.0)	2.5 (0.8)	2.8 (0.9)	0.188
SRss (/s)	2.0 (0.7)	2.0 (0.6)	2.0 (1.0)	0.952
SRes (/s)	2.2 (0.7)	2.1 (0.6)	2.3 (0.9)	0.6
SRas (/s)	2.0 (0.7)	2.3 (0.9)	2.6 (0.8)	0.014[††]

Results are presented as mean (SD), (- %) negative value of peak systolic strain denotes longitudinal shortening of myocardial fibres

SRsl = systolic strain rate of the lateral free wall, SRel = early diastolic strain rate of the lateral free wall, SRal = diastolic strain rate during atrial contraction, SRss = systolic strain rate of the septal wall, SRes = early diastolic strain rate of the septal wall, SRas = diastolic strain rate during atrial contraction

[§§] p <0.001 (PT RDS V Term control), [§§§] p <0.001 (PT control V Term control), [‡] p <0.01 (PT RDS V PT control), [‡‡] p <0.01 (PT RDS V Term control), [†] p <0.05 (PT RDS V PT control), [††] p <0.05 (PT RDS V Term control), [†††] p <0.05 (PT control V Term control)

3.3.1.4 Right ventricular global and regional function

Table 3.8 summarises the echocardiographic parameters of right ventricular global and regional functions. Right annular displacements were highest in the term group compared to the preterm groups. Right ventricular long axis shortening was lowest in the preterm RDS group compared to both term and preterm control groups.

Myocardial systolic and early diastolic velocities were highest in the term group and lowest in the preterm RDS group. Late diastolic velocity and peak systolic strain were lowest in the preterm RDS group compared to both term and preterm groups. The peak systolic, early and late diastolic strain rates were similar between the groups.

3.3.1.5 Surrogate markers of PA pressure

Table 3.9 summarises the results of surrogate markers of PA pressure at birth. Tricuspid regurgitation was present in 25/30 (83.3%) preterm infants with RDS, 12/30 (40%) preterm controls, and 29/60 (48.3%) term controls. Pulmonary regurgitation end-diastolic velocity was measurable in 8 (26.7%) in the RDS, 12 (40%) in the preterm control and 8 (13.3%) in the term control groups. The non-measurable TR and PR jets were assumed to be zero in the analysis.

There was no difference in PR end-diastolic velocity between the groups. RV pre-ejection period and PA ejection time were longest in term group. Maximum TR jet velocity was highest in the preterm RDS group along with the shortest PA acceleration time and lowest PA acceleration ejection time ratio compared to the control groups indicating highest PA pressure in the preterm RDS group at birth.

Table 3.8: RV global and regional function at birth

	Term Control (A)	**PT Control (B)**	**PT RDS (C)**	**ANOVA p value**
Global function				
RV Ds' (mm)	7.6 (1.3)	5.9 (1.1)	4.4 (1.3)	**<0.001**[§, §§, §§§]
RV long axis shortening (%)	28.7 (4.5)	29.2 (4.4)	25.1 (6.6)	**0.003**[‡,‡‡]
Regional function (Myocardial velocities, strain and strain rate)				
RV Vsbl (cm/s)	4.3 (0.9)	3.7 (0.8)	2.7 (0.8)	**<0.001**[§,§§,‡‡‡]
RV Vebl (cm/s)	6.1 (1.8)	4.4 (1.8)	4.3 (2.3)	**<0.001**[§§,§§§]
RV Vabl (cm/s)	5.7 (1.2)	5.3 (1.2)	4.5 (1.4	**0.002**[‡‡]
RV Ss (- %)	27.6 (5.8)	25.0 (5.5)	23.2 (6.7)	**0.004**[‡‡]
RV SRs (/s)	2.4 (0.7)	2.3 (0.7)	2.2 (0.8)	0.49
RV SRe (/s)	2.7 (0.9)	2.4 (0.8)	2.8 (1.2)	0.182
RV SRa (/s)	2.9 (0.9)	3.1 (0.8)	3.0 (1.3)	0.556

Results are presented as mean (SD), (- %) negative value of peak systolic strain denotes longitudinal shortening of myocardial fibres

[§] *p* <0.001 (PT RDS V PT control), [§§] *p* <0.001 (PT RDS V Term control), [§§§] *p* <0.001 (PT control V Term control), [‡] p <0.01 (PT RDS V PT control), [‡‡] p <0.01 (PT RDS V Term control), [‡‡‡] p <0.01 (PT control V Term control)

Table 3.9: Surrogate marker of PA pressure at birth

	Term Control (A)	**PT Control (B)**	**PT RDS (C)**	**ANOVA p value**
TR (m/s) [n/total]	1.0 (1.1) [29/60]	0.8 (1.1) [12/30]	1.7 (1.0) [25/30]	**0.005**[‡,††]
PR (m/s) [n/total]	0.1 (0.2) [8/60]	0.3 (0.5) [12/30]	0.2 (0.3) [8/30]	**0.008**[‡‡‡]
RV PEP (ms)	53.7 (13.1)	46.2 (12.3)	45.7 (12.4)	**0.005**[††,†††]
PA AT (ms)	70.3 (11.9)	64.2 (15.1)	52.6 (11.3)	**<0.001**[‡,§§]
PA ET (ms)	224.6 (20.7)	208.2 (19.7)	198.1 (26.3)	**<0.001**[§§,‡‡‡]
AT:ET ratio	0.31 (0.04)	0.31 (0.06)	0.27 (0.04)	**<0.001**[‡,§§,]

Results are presented as mean (SD)
[§§] *p* <0.001 (PT RDS V Term control), [‡] p <0.01 (PT RDS V PT control), [‡‡‡] p <0.01 (PT control V Term control), [††] p <0.05 (PT RDS V Term control), [†††] p <0.05 (PT control V Term control),

3.3.2 At term, 3-6 weeks and 1 year follow up

3.3.2.1 Demographics and general characteristics

At term, a total of 41 preterm infants (22 preterm controls, 19 preterm with RDS) were studied. 77 infants (45 term controls, 17 preterm controls, 15 preterm with RDS) and 67 infants (33 term controls, 18 preterm controls, 16 preterm with RDS) were studied at the planned follow-up at one month corrected age and one year corrected age respectively.

Infants in the preterm groups were assessed at a slightly younger age compared to their term counterparts at term, one month and one year corrected age. Correspondingly, infants weight, LVOT d and ventricular chamber lengths of the preterm groups were significantly smaller compared to the term control group at term. All infants cardiac size increased (measured in ventricular chamber lengths and LVOT d) along with their body weight with time. However, differences in infants weight, LVOT diameter and ventricular chambers lengths between the groups disappeared at one month and one year follow up, with only a difference in weight between preterm infants with RDS and term control noted at one year corrected age. (Table 3.10 and Figure 3.14)

Blood pressure of the preterm RDS group was significantly lower than the control groups at birth and at term gestational age. However, the differences disappeared at one month and one year corrected age.

Table 3.10: Subject characteristics at follow up scans

	Term Control (A)	PT Control (B)	PT RDS (C)	ANOVA p value
Numbers				
Birth	60	30	30	-
At term	"	22	19	-
1 month	45	17	15	-
1 year	33	18	16	-
Age (wks)				
Birth	-0.2* (1.2)	-7.3* (1.4)	-11.8* (2.7)	**<0.001**[§, §§, §§§]
At term	"	-2.7* (1.9)	-3.3* (1.4)	<0.001[§§, §§§]
1 month	5.3 (1.0)	4.6 (1.8)	3.8 (1.6)	**0.002**[‡‡]
1 year	53 (2.3)	51.9 (3.5)	49.2 (4.2)	**0.001**[§§, §§§]
Weight (kg)				
Birth	3.4 (0.5)	1.8 (0.4)	1.2 (0.4)	**<0.001**[§, §§, §§§]
At term	"	2.5 (0.7)	2.3 (0.4)	<0.001[§§, §§§]
1 month	4.5 (0.6)	4.3 (0.8)	4.1 (0.5)	0.064
1 year	9.8 (1.1)	9.5 (1.2)	8.8 (1.4)	0.041[††]
Systolic BP (mmHg)				
Birth	66.9 (11.7)	65.1 (10.8)	49.3 (7.8)	**<0.001**[§, §§]
At term	"	65.8 (10.1)	49.1 (6.7)	<0.001[§, §§]
1 month	95.6 (14.0)	95.3 (14.5)	99.1 (20.7)	0.765
1 year	106.3 (21.2)	107.8 (18.7)	92.2 (14.1)	0.058
Diastolic BP (mmHg)				
Birth	41.3 (9.9)	37.1 (7.8)	30.8 (7.5)	**<0.001**[†,§§]
At term	"	37.2 (8.3)	29.1 (6.0)	<0.001[†, §§]
1 month	60.7 (11.0)	57.7 (13.4)	58.6 (13.3)	0.688
1 year	70.1 (14.4)	71.5 (13.3)	61.5 (10.9)	0.095
End-diastolic left ventricular chamber lengths (cm)				
Birth	2.8 (0.3)	2.1 (0.2)	1.8 (0.3)	**<0.001**[§, §§, §§§]
At term	"	2.5 (0.4)	2.6 (0.4)	<0.01[††,‡‡‡]
1 month	3.1 (0.2)	3.1 (0.2)	3.0 (0.2)	0.263
1 year	4.0 (0.2)	3.9 (0.3)	3.9 (0.2)	0.340
End-diastolic right ventricular chamber lengths (cm)				
Birth	2.6 (0.3)	2.0 (0.2)	1.8 (0.3)	**<0.001**[§, §§, §§§]
At term	"	2.3 (0.4)	2.4 (0.3)	<0.001[‡‡,‡‡‡]
1 month	3.0 (0.2)	3.1 (0.3)	2.9 (0.2)	0.420
1 year	3.9 (0.2)	3.9 (0.3)	3.8 (0.2)	0.636

Results are presented as mean (SD)
* negative value denotes number of weeks before due date at term (40 weeks gestation)
[§] p <0.001 (PT RDS V PT control), [§§] p <0.001 (PT RDS V Term control), [§§§] p <0.001 (PT control V Term control), [‡] p <0.01 (PT RDS V PT control), [‡‡] p <0.01 (PT RDS V Term control), [‡‡‡] p <0.01 (PT control V Term control), [††] p <0.05 (PT RDS V Term control),

3.3.2.2 Left ventricular global systolic functions

LVOT VTI at birth was significantly different between the groups at birth. However, this difference disappeared when the preterm groups were assessed at term, at one month and one year. LVOT d was significantly smaller in the preterm RDS group at term compared to the term group; hence LV SV is also significantly lower. LV SV increased with age and growth within the groups as expected. There was no difference in LV SV between preterm controls and term control and preterm RDS groups at the term scan. There was no difference in LV SV between the groups at one month and one year follow up except between preterm RDS group and term control group at year follow up ($p<0.05$).

Cardiac output increased from 0.31 ± 0.11 L/min and 0.19 ± 0.08 L/min at birth to 0.62 ± 0.20 L/min and 0.54 ± 0.14 L/min in preterm control and preterm RDS groups respectively at term. The cardiac output of the preterm groups was significantly lower than term control group at birth but when these were assessed at term, their cardiac output was significantly higher than the term control group's at birth. Cardiac output within the groups increased with age when assessed at one month and one year but there were no differences between the groups at these two time frames. Similar changes were seen in cardiac index in the groups where CI increased from birth to peak at one month and decreased at one year.

LV PEP decreased from 50.7 ± 10.9 ms and 47.9 ± 14.0 ms at birth to 42.4 ± 8.2 ms and 44.7 ± 7.9 ms at term corrected age in preterm control and preterm RDS groups respectively. LV PEP in the preterm groups was significantly lower when compared to term infants LV PEP at birth. However by one month corrected age, LV PEP is only

significantly different between term control and preterm RDS groups (43.2 ± 7.2 ms vs 49.1 ± 9.0 ms, $p<0.05$). At one year old corrected, there was no difference in LV PEP. Similar findings were observed in LV ET except that there were no differences in LV ET between the groups at one month and one year corrected age. (Table 3.11)

Left ventricular basal lateral and basal septal systolic displacements (LV Ds'bl and LV Ds'bs of the preterm groups were significantly lower than the term control group at birth. However, the preterm groups' LV Ds'bl and LV Ds'bs at term were significantly higher than those of the term control group's displacement at birth. Both LV Ds'bl and LV Ds'bs in all groups increased at one month and one year with the term control group's systolic displacements found to be significantly higher than the preterm groups. LVbl and LVbs long axis shortening is the normalised value of LV Ds'bl and LV Ds'bs (divided by LV chamber length). There was no difference in both LVbl and LVbs long axis shortening at birth. LVbl and LVbs long axis shortening values increased from birth and peaked at one month. (Table 3.12).

In summary:

- Global systolic function (LVOT d, LVOT VTI, LV SV, cardiac output, cardiac index, LV Ds'bl and LV Ds'bs) was lowest in the smallest and lowest gestation infants at birth. This increased with increasing age and by 1 month and 1 year, there was no difference between the groups.
- LV PEP was highest in the term control group and lowest in PT RDS group. LV PEP decreased with age and at one year, there was no difference detected between the groups.

Table 3.11 Left ventricular global systolic parameters at follow up scans

	Term Control (A)	PT Control (B)	PT RDS (C)	ANOVA p value
LVOT d (cm)				
Birth	0.66 (0.07)	0.53 (0.06)	0.45 (0.08)	**<0.001**[§, §§, §§§]
At term	"	0.62 (0.06)	0.58 (0.06)	<0.001[§§]
1 month	0.77 (0.07)	0.75 (0.06)	0.73 (0.07)	0.109
1 year	0.98 (0.07)	0.96 (0.07)	0.92 (0.08)	0.097
LVOT VTI (cm)				
Birth	12.5 (2.4)	10.2 (2.3)	8.6 (2.5)	**<0.001**[†, §§, §§§]
At term	"	12.7 (2.9)	13.2 (2.0)	0.583
1 month	13.9 (2.2)	15.0 (2.0)	14.5 (1.6)	0.206
1 year	17.2 (1.7)	16.9 (2.0)	16.8 (2.8)	0.870
Stroke volume (ml)				
Birth	4.3 (1.2)	2.3 (0.8)	1.4 (0.6)	**<0.001**[‡, §§, §§§]
At term	"	2.5 (0.7)	2.3 (0.4)	0.014[††]
1 month	4.5 (0.6)	4.3 (0.8)	4.1 (0.5)	0.314
1 year	9.8 (1.1)	9.5 (1.2)	8.8 (1.4)	0.043[††]
Cardiac output (L/min)				
Birth	0.49 (0.13)	0.31 (0.11)	0.19 (0.08)	**<0.001**[‡, §§, §§§]
At term	"	0.62 (0.20)	0.54 (0.14)	<0.01[††,‡‡‡]
1 month	0.99 (0.25)	1.07 (0.25)	0.91 (0.15)	0.151
1 year	1.60 (0.29)	1.59 (0.26)	1.42 (0.22)	0.081
Cardiac index (L/m^2/min)				
Birth	2.28 (0.54)	2.09 (0.60)	1.82 (0.61)	**0.002** [‡‡]
At term	"	3.52 (0.82)	3.22 (0.75)	<0.001[§§, §§§]
1 month	3.69 (0.80)	4.27 (0.94)	3.72 (0.51)	**0.036**[†††]
1 year	3.55 (0.58)	3.58 (0.55)	3.38 (0.50)	0.529
LV PEP (ms)				
Birth	55.1 (10.7)	50.7 (10.9)	47.9 (14.0)	**0.018** [‡‡]
At term	"	42.4 (8.2)	44.7 (7.9)	<0.001[§§, §§§]
1 month	43.2 (7.2)	47.9 (7.1)	49.1 (9.0)	**0.012**[††]
1 year	46.1 (9.1)	44.7 (7.2)	44.5 (9.0)	0.777
LV PEP:ET				
Birth	0.27 (0.06)	0.26 (0.05)	0.26 (0.09)	0.725
At term	"	0.24 (0.05)	0.24 (0.04)	0.041
1 month	0.23 (0.04)	0.26 (0.05)	0.27 (0.05)	**0.008**[††,†††]
1 year	0.21 (0.05)	0.21 (0.04)	0.21 (0.04)	0.643

Results are presented as mean (SD)
[§] p <0.001 (PT RDS V PT control), [§§] p <0.001 (PT RDS V Term control), [§§§] p <0.001 (PT control V Term control), [‡] p <0.01 (PT RDS V PT control), [‡‡] p <0.01 (PT RDS V Term control), [‡‡‡] p <0.01 (PT control V Term control), [††] p <0.05 (PT RDS V Term control), [†††] p <0.05 (PT control V Term control),

Table 3.12 LV Ds'bl, LV Ds'bs, LVbl and LVbs long axis shortening at follow up scans

	Term Control (A)	PT Control (B)	PT RDS (C)	ANOVA p value
LV Ds'bl (mm)				
Birth	4.6 (1.0)	3.4 (0.8)	2.6 (1.0)	**<0.001**$^{‡, §§, §§§}$
At term	"	5.8 (1.3)	5.0 (1.1)	<0.001†,§§§
1 month	7.5 (1.2)	7.2 (0.8)	6.6 (0.9)	**0.037**††
1 year	9.5 (1.2)	8.7 (1.1)	8.5 (1.0)	**0.007**††,†††
LVDs'bs (mm)				
Birth	5.2 (0.8)	4.1 (0.8)	3.1 (0.9)	**<0.001**$^{§, §§, §§§}$
At term	"	6.2(0.9)	5.9 (0.9)	<0.001‡‡,§§§
1 month	7.2 (1.0)	7.1 (0.6)	7.2 (0.7)	0.949
1 year	9.3 (0.8)	8.5 (1.0)	8.4 (0.7)	**<0.001**‡‡,‡‡‡
LVbl long axis shortening (%)				
Birth	16.3 (3.6)	15.7 (3.5)	14.0 (5.1)	**0.047**††
At term	"	22.6 (3.0)	18.8 (3.1)	<0.001‡,††,§§§
1 month	23.7 (3.8)	23.0 (2.6)	21.9 (2.6)	0.200
1 year	24.0 (3.0)	22.2 (2.3)	21.9 (2.3)	**0.022**††
LVbs long axis shortening (%)				
Birth	18.6 (3.4)	19.0 (3.8)	17.3 (5.5)	0.249
At term	"	24.4 (3.1)	22.8 (2.9)	<0.001§§,§§§
1 month	22.9 (3.1)	22.8 (2.2)	23.7 (2.6)	0.552
1 year	23.6 (2.0)	21.8 (1.8)	21.8 (1.4)	**0.001**‡‡,‡‡‡

Results are presented as mean (SD)
§ *p* <0.001 (PT RDS V PT control), §§ *p* <0.001 (PT RDS V Term control), §§§ *p* <0.001 (PT control V Term control), ‡ p <0.01 (PT RDS V PT control), ‡‡ p <0.01 (PT RDS V Term control), ‡‡‡ p <0.01 (PT control V Term control), † p <0.05 (PT RDS V PT control), †† p <0.05 (PT RDS V Term control), ††† p <0.05 (PT control V Term control)

3.3.2.3 Left ventricular global diastolic functions

The mitral early diastolic flow velocity (mitral E) in the preterm groups was significantly lower than the term control group at birth but when assessed at term, this was significantly higher in the preterm groups compared to the term control group's value at birth. By one month and one year, mitral E was very similar between the groups. Similar changes were observed in the mitral late diastolic flow velocity (mitral A) at term, one month and one year. Mitral E in all groups increased from birth to the highest at one year of age, whereas mitral A peaked at one month. Mitral E:A was significantly higher in the term control group at birth. This difference disappeared when the groups were assessed at term and at one month of age. At one year, mitral E:A ratio of the preterm RDS group was highest but the difference was only significant between the preterm RDS and preterm control group ($p=0.024$). The mitral E:A increased with postnatal age in all groups.

Mitral annular early diastolic velocity (Vé) was highest in the term control group followed by preterm control group and lowest in the preterm RDS group at birth. At term, mitral Vé of the preterm was noted to be higher than term control group at birth. Mitral Vé of the preterm control group was significantly higher than the term control and preterm RDS groups. By one month and one year, the mitral Vé were similar between the groups. Mitral Vé increased with postnatal age in all groups with the highest values seen at one year.

There was no difference in mitral E: Vé ratio between the groups at birth. The mitral E: Vé was highest in the preterm RDS group followed by the preterm control group at term and both were significantly higher than the term group at birth. The difference in mitral

E: Vé between the groups narrowed at one month where only the preterm RDS group was significantly higher than the term group and by one year, there was no difference between the groups.

In summary:

- Preterm infants (both PT control and PT RDS groups) had diastolic dysfunction at birth which improved and attained the values similar to the term control group at one month and one year old.

Table 3.13 Left ventricular global diastolic parameters at follow up scans

	Term Control (A)	PT Control (B)	PT RDS (C)	ANOVA p value
Mitral E (m/s)				
Birth	0.64 (0.12)	0.52 (0.11)	0.47 (0.14)	**<0.001**[§§, §§§]
At term	"	0.96 (0.24)	0.94 (0.20)	<0.001[§§, §§§]
1 month	1.04 (0.21)	1.08 (0.18)	1.09 (0.16)	0.649
1 year	1.18 (0.15)	1.16 (0.19)	1.11 (0.09)	0.271
Mitral A (m/s)				
Birth	0.57 (0.11)	0.56 (0.11)	0.52 (0.13)	0.081
At term	"	0.92 (0.22)	0.91 (0.15)	<0.001[§§, §§§]
1 month	0.90 (0.20)	1.00 (0.22)	0.94 (0.14)	0.270
1 year	0.88 (0.16)	0.92 (0.18)	0.79 (0.19)	0.106
Mitral E:A				
Birth	1.13 (0.23)	0.95 (0.18)	0.92 (0.22)	**<0.001**[§§, §§§]
At term	"	1.03 (0.13)	1.02 (0.21)	0.054
1 month	1.14 (0.18)	1.06 (0.18)	1.10 (0.17)	0.293
1 year	1.36 (0.22)	1.23 (0.21)	1.44 (0.22)	**0.030**[†]
Mitral Vé (cm/s)				
Birth	7.3 (1.3)	6.3 (0.9)	5.1 (0.9)	**<0.001**[§, §§, §§§]
At term	"	9.2 (2.1)	7.9 (1.3)	<0.001[†,§§§]
1 month	11.7 (2.5)	11.0 (2.1)	10.5 (1.4)	0.215
1 year	14.9 (2.9)	13.7 (2.7)	13.1 (2.2)	0.284
Mitral E:Vé				
Birth	9.0 (1.8)	8.4 (1.9)	9.3 (2.5)	0.226
At term	"	10.8 (3.2)	12.1 (2.3)	<0.001[§§, §§§]
1 month	9.11(1.9)	10.1 (1.9)	10.6 (2.5)	**0.031**[††]
1 year	8.2 (1.9)	8.9 (3.0)	8.0 (1.1)	0.432

Results are presented as mean (SD)
[§] p <0.001 (PT RDS V PT control), [§§] p <0.001 (PT RDS V Term control), [§§§] p <0.001 (PT control V Term control), [†] p <0.05 (PT RDS V PT control), [††] p <0.05 (PT RDS V Term control)

3.3.2.4 Left ventricular regional function

Left ventricular basal lateral and basal septal systolic myocardial velocities (LV Vsbl and LV Vsbs) were lowest in the preterm RDS group and highest in the term control group at birth. The left ventricular velocities of the preterm groups increased when assessed at term compared to their velocities at birth. LV Vsbl and LV Vsbs of the preterm groups at term scan were higher than the term control group at birth but only LV Vsbs was significantly different. By one month there was no difference in LV Vsbl and LV Vsbs between the groups and by one year, LV Vsbs of the preterm RDS group was found to be significantly lower than the term control group. In all groups, LV Vsbl increased from birth until the last follow up scan at one year. LV Vsbs peaked at one month in the preterm groups but was found to be highest in the term group at one year (Table 3.14).

Left ventricular early and late diastolic myocardial velocities, both basal lateral and basal septal, were highest in the term control group and lowest in the preterm RDS group. The diastolic velocities in both walls of the left ventricle of the preterm groups increased significantly by the time they reached term corrected age and were significantly higher than the term control group at birth. However, by one month and one year corrected age, the diastolic velocities of the term control group were highest between the groups although the differences were not statistically significant. Both LV Vebl and LV Vebs increased from the lowest values at birth to the highest at one year. The LV Vabl and LV Vabs in the preterm groups were highest at term corrected age and then decreased with age, whereas in the term control group, the late diastolic velocities were highest at one month corrected age (Table 3.14).

Table 3.14 LV regional myocardial velocities at follow up scans

	Term Control (A)	PT Control (B)	PT RDS (C)	ANOVA p value
LV Vsbl (cm/s)				
Birth	3.0 (0.8)	2.1 (0.7)	1.7 (0.8)	**<0.001**[§§,§§§]
At term	"	3.4 (0.8)	3.1 (1.0)	0.121
1 month	4.3 (0.9)	4.3 (1.2)	3.9 (1.1)	0.481
1 year	4.8 (1.0)	4.7 (1.0)	4.7 (0.7)	0.861
LV Vebl (cm/s)				
Birth	4.5 (1.1)	3.5 (1.1)	2.52 (1.2)	**<0.001**[‡,§§,§§§]
At term	"	6.8 (1.5)	5.9 (1.9)	<0.001[§§,§§§]
1 month	9.1 (2.4)	8.3 (2.6)	8.2 (2.5)	0.292
1 year	11.7 (2.1)	11.0 (1.9)	10.8 (1.2)	0.190
LV Vabl (cm/s)				
Birth	3.7 (1.4)	3.1 (1.1)	2.8 (1.2)	**0.003**[‡‡]
At term	"	4.9 (1.0)	4.2 (0.9)	0.015[†††]
1 month	5.2 (1.1)	4.8 (1.2)	4.0 (1.9)	0.178
1 year	3.7 (1.6)	3.6 (1.0)	3.4 (0.8)	0.850
LV Vsbs (cm/s)				
Birth	3.0 (0.7)	2.6 (0.8)	1.9 (0.6)	**<0.001**[‡,§§,†††]
At term	"	3.8 (0.6)	3.7 (0.7)	<0.001[§§,§§§]
1 month	4.2 (0.7)	4.3 (0.6)	4.3 (0.6)	0.831
1 year	4.6 (0.8)	4.1 (0.6)	3.8 (0.7)	**0.007**[‡‡]
LV Vebs (cm/s)				
Birth	3.8 (0.9)	3.4 (1.5)	2.8 (1.0)	**<0.001**[§§]
At term	"	6.6 (1.7)	6.0 (2.1)	<0.001[§§, §§§]
1 month	8.6 (2.2)	7.8 (1.5)	8.1 (1.8)	0.308
1 year	9.0 (2.0)	8.2 (1.8)	8.0 (1.8)	0.119
LV Vabs (cm/s)				
Birth	3.7 (1.1)	3.8 (0.8)	3.1 (0.9)	**0.016**[†,††]
At term	"	5.0 (1.1)	5.0 (1.1)	<0.001[‡‡,‡‡‡]
1 month	5.6 (1.7)	4.6 (0.8)	4.4 (0.6)	0.123
1 year	4.4 (1.2)	4.2 (1.0)	3.7 (1.1)	0.236

Results are presented as mean (SD)
[§§] p <0.001 (PT RDS V Term control), [§§§] p <0.001 (PT control V Term control), [‡] p <0.01 (PT RDS V PT control), [‡‡] p <0.01 (PT RDS V Term control), [‡‡‡] p <0.01 (PT control V Term control), [†] p <0.05 (PT RDS V PT control), [††] p <0.05 (PT RDS V Term control), [†††] p <0.05 (PT control V Term control)

Peak systolic strain of the left ventricular lateral and septal walls (LV Ssl and LV Sss) were lowest in the preterm RDS group at birth but at term, LV Ssl increased to a similar value as the term control group and LV Sss increased significantly higher than the control group. The LV Ssl and LV Sss of the preterm control group were similar to the term control group at birth but these increased significantly by the time they reach term corrected age. By one month and one year corrected age, there were no differences in the LV Ssl and LV Sss between the groups. In all groups, the LV peak systolic strain in both walls increased with age; lowest at birth and peaking at one year (Table 3.15).

Left ventricular systolic strain rate in both lateral and septal walls (LV SRsl and LV SRss) were similar between the groups at birth. At term, there was no difference in LV SRsl between the groups but LV SRss in both preterm groups were significantly higher than the term control group at birth. At one month corrected age, there was no difference in both LV SRsl and LV SRss between the groups. At one year of age, the only difference in LV systolic strain rates between the groups was found in LV SRss between the term control group and preterm RDS group ($p=0.043$). Both LV SRsl and LV SRss in all groups increased with age (Table 3.16).

In summary:

- LV regional myocardial systolic velocities (LV Vsbl and LV Vsbs) and early diastolic velocity at the basal lateral wall were lowest in the preterm RDS group at birth suggesting some element of LV regional myocardial systolic and diastolic dysfunction at birth. These velocities increased with age and attained the velocities of their term counterparts by one month of age.

- LV regional systolic strain was lowest in preterm RDS group at birth but this was only significantly different compared to the term control group. By one month and one year of age, the LV regional systolic strain was similar between groups.
- There was no difference in LV regional SR between the groups at birth, one month and one year of age.

Table 3.15 Left ventricular mid-segment myocardial peak systolic longitudinal strain at follow up scans

	Term Control (A)	**PT Control (B)**	**PT RDS (C)**	**ANOVA p value**
LV lateral wall mid-segment longitudinal peak systolic strain, Ssl (- %)				
Birth	22.8 (3.9)	21.2 (3.8)	18.9 (4.9)	**<0.001**[§§]
At term	"	25.5 (5.1)	22.8 (4.7)	0.041[†††]
1 month	27.7 (5.3)	27.2 (3.1)	27.5 (4.7)	0.928
1 year	31.7 (4.0)	31.0 (3.6)	29.1 (3.2)	0.079
LV septal wall mid-segment longitudinal peak systolic strain, Sss (- %)				
Birth	19.8 (3.8)	19.5 (3.2)	17.5 (3.9)	**0.027**[††]
At term	"	25.2 (5.5)	24.6 (4.2)	<0.001[§§,§§§]
1 month	24.0 (3.8)	25.9 (4.0)	25.3 (3.5)	0.154
1 year	30.3 (2.6)	28.8 (1.9)	28.5 (3.1)	**0.034**

Results are presented as mean (SD), (- %) negative value of peak systolic strain denotes longitudinal shortening of myocardial fibres
[§§] *p* <0.001 (PT RDS V Term control), [§§§] *p* <0.001 (PT control V Term control[††], p <0.05 (PT RDS V Term control), [†††] p <0.05 (PT control V Term control)

Table 3.16 Left ventricular mid-segment myocardial strain rate at follow up scans

	Term Control (A)	PT Control (B)	PT RDS (C)	ANOVA p value
LV SRsl (/s)				
Birth	2.2 (0.8)	1.9 (0.5)	2.0 (0.8)	0.116
At term	"	2.4 (0.7)	2.3 (0.9)	0.758
1 month	2.5 (1.1)	2.9 (0.6)	2.4 (1.0)	0.370
1 year	3.4 (1.2)	3.1 (1.0)	3.3 (1.1)	0.627
LV SRel (/s)				
Birth	2.7 (0.9)	3.1 (0.9)	2.6 (0.9)	0.172
At term	"	4.5 (1.4)	3.8 (1.3)	<0.001§§,§§§
1 month	5.0 (1.3)	4.6 (1.2)	5.4 (1.2)	0.178
1 year	6.0 (1.5)	5.6 (1.1)	5.1 (0.7)	0.068
LV SRal (/s)				
Birth	2.4 (1.0)	2.5 (0.8)	2.8 (0.9)	0.188
At term	"	3.0 (0.8)	2.9 (1.1)	0.123
1 month	3.5 (1.2)	3.1 (1.4)	2.9 (1.3)	0.394
1 year	2.7 (1.1)	2.3 (0.7)	2.1 (0.7)	0.135
LV SRss (/s)				
Birth	2.0 (0.7)	2.0 (0.6)	2.0 (1.0)	0.952
At term	"	2.6 (0.6)	2.4 (0.6)	0.001††,‡‡‡
1 month	2.5 (0.9)	2.7 (0.8)	2.6 (0.8)	0.677
1 year	3.2 (0.7)	2.8 (0.5)	2.7 (0.6)	**0.027**
LV SRes (/s)				
Birth	2.2 (0.7)	2.1 (0.6)	2.3 (0.9)	0.6
At term	"	3.3 (1.2)	3.0 (1.3)	<0.001‡‡,‡‡‡
1 month	3.7 (1.2)	3.5 (1.1)	3.3 (1.2)	0.471
1 year	4.5 (1.1)	3.9 (1.0)	4.2 (1.5)	0.229
LV SRas (/s)				
Birth	2.0 (0.7)	2.3 (0.9)	2.6 (0.8)	**0.014**††
At term	"	3.0 (1.1)	2.8 (1.0)	<0.001‡‡,‡‡‡
1 month	3.0 (1.6)	2.3 (0.5)	2.7 (0.8)	0.385
1 year	2.4 (0.8)	2.4 (0.7)	2.1 (0.5)	0.390

Results are presented as mean (SD).
§§ p <0.001 (PT RDS V Term control), §§§ p <0.001 (PT control V Term control), ‡‡ p <0.01 (PT RDS V Term control), ‡‡‡ p <0.01 (PT control V Term control), †† p <0.05 (PT RDS V Term control).

3.3.2.5 Right ventricular global function

Tricuspid annular systolic excursion was highest in the term control and lowest in the preterm RDS groups at birth. However, the tricuspid annular systolic excursion of the preterm groups increased when they reached a corrected gestational age at term. The values were higher than the term control group's value at birth but these were not significant. At one month and one year corrected age, the tricuspid annular systolic excursion was similar between the groups.

The right ventricular global function was assessed by dividing tricuspid annular systolic excursion by right ventricular chamber length to reflect the right ventricular longitudinal axis shortening presented as a %. I found the RV longitudinal axis shortening was lowest in the preterm RDS group compared to the two control groups ($p=0.003$) at birth. The difference between the preterm groups disappeared by term age (preterm RDS group 35.7 ± 6.8 vs. preterm control group 35.6 ± 4.3) but were significantly higher than the term control group at birth (28.7 ± 4.5), $p < 0.001$. Although the difference between the preterm groups and term control group persisted until one month of age, this was not statistically significant. At one year of age, the RV longitudinal axis shortening was similar between the groups (Table 3.17).

In summary:

- The preterm RDS group had RV global systolic dysfunction at birth with the lowest RV Ds' and RV long axis shortening. The RV global systolic dysfunction resolved by term corrected age and there was no difference in the RV systolic function at one month and one year of age.

Table 3.17 Right ventricular global function at follow up scans

	Term Control (A)	PT Control (B)	PT RDS (C)	ANOVA p value
RV Ds' (mm)				
Birth	7.6 (1.3)	5.9 (1.1)	4.4 (1.3)	**<0.001**[§, §§, §§§]
At term	"	8.4 (1.7)	8.4 (1.2)	0.030
1 month	9.6 (1.4)	10.4 (1.7)	10.2 (1.3)	0.119
1 year	14.4 (1.8)	14.6 (2.0)	13.4 (2.0)	0.113
RV long axis shortening (%)				
Birth	28.7 (4.5)	29.2 (4.4)	25.1 (6.6)	**0.003**[‡,‡‡]
At term	"	35.6 (4.3)	35.7 (6.8)	<0.001[§§, §§§]
1 month	31.9 (4.3)	34.1 (3.6)	34.6 (3.8)	**0.037**
1 year	37.0 (4.9)	37.6 (3.6)	34.8 (4.6)	0.169

Results are presented as mean (SD).
[§] *p* <0.001 (PT RDS V PT control), [§§] *p* <0.001 (PT RDS V Term control), [§§§] *p* <0.001 (PT control V Term control), [‡] p <0.01 (PT RDS V PT control), [‡‡] p <0.01 (PT RDS V Term control), [‡‡‡] p <0.01 (PT control V Term control), [†] p <0.05 (PT RDS V PT control), [††] p <0.05 (PT RDS V Term control), [†††] p <0.05 (PT control V Term control)

3.3.2.6 Right ventricular regional function

Right ventricular regional function was assessed using myocardial velocity measurements, myocardial longitudinal deformation (also known as myocardial strain) and myocardial strain rate. Both regional systolic and diastolic functions were assessed.

RV myocardial systolic and diastolic velocities were measured at the base of the right ventricular free wall. The RV systolic velocity (RV Vsbl) was lowest in the preterm RDS group and highest in the term control group at birth. By the time the preterm groups reach term corrected gestational age, their RV Vsbl had increased to become similar to the term control group's value at birth. RV Vsbl continued to increase with age within the groups and the highest values were seen at one year corrected age but there was no difference between the groups at one month and one year of age (Table 3,18).

RV early diastolic velocity (RV Vebl) was lowest in the preterm groups at birth compared to the term control. By term corrected age, RV Vebl was highest in the preterm control group and was significantly higher than the term control group at birth. RV Vebl continued to increase with age within the groups until follow up at one year. There was no difference in RV Vebl between the groups at one month and at one year. RV Vabl was lowest in the preterm RDS group at birth and was only significantly lower than term control group, 5.7 ± 1.2 vs 4.5 ± 1.4 respectively. RV Vabl in the preterm groups increased significantly at term corrected age but there was no difference between the groups at term. RV Vabl seemed to plateau at term and the values at one month and one year were similar within the groups and between groups (Table 3.18).

Right ventricular peak systolic longitudinal strain (RV Ss) was lowest in the preterm RDS group at birth and this was significantly lower than the term control group, $p<0.01$. RV Ss in the preterm groups increased significantly from birth to term corrected age and this was significantly higher than term control at birth. RV Ss continued to increase with time to reach their maximum values at one year of age. There was no difference in RV Ss between the groups at one month and one year.

There was no difference in right ventricular systolic strain rate (RV SRs) between the groups at birth. RV SRs of the preterm groups increased significantly from birth to term and were significantly higher when compared to the term group at birth. RV SRs only increased modestly with time with no difference noted between the groups at one month. At one year, RV SRs of the preterm RDS group was found to be lower than the preterm control group only.

The right ventricular early and late diastolic strain rates (RV SRe and SRa respectively) were similar at birth. At term, RV SRe and RV SRa in the preterm groups were significantly higher than the term group at birth. There was no difference in RV SRe and RV SRa between the groups at one month and one year. RV SRe increased with time and was highest at one year in all groups whereas RV SRa was highest in the preterm groups at term and highest in the term control group at one month of age.

In summary:

- The only RV regional function parameter to show a significant difference between the groups at birth was RV myocardial systolic velocity; suggesting possible RV regional systolic dysfunction in the preterm RDS group at birth. However, RV

systolic strain was similar between the groups at birth. There was no difference in RV regional function in all parameters at other time frames except when compared to the control groups at term.

- Table 3.18 Right ventricular regional function at follow up scans

	Term Control (A)	PT Control (B)	PT RDS (C)	ANOVA p value
RV Vsbl (cm/s)				
Birth	4.3 (0.9)	3.7 (0.8)	2.7 (0.8)	**<0.001**[§,§§,‡‡‡]
At term	"	4.9 (1.5)	4.7 (1.1)	0.059
1 month	5.4 (1.3)	6.0 (1.1)	5.8 (1.1)	0.283
1 year	7.7 (1.9)	7.9 (2.0)	7.2 (1.9)	0.525
RV Vebl (cm/s)				
Birth	6.1 (1.8)	4.4 (1.8)	4.3 (2.3)	**<0.001**[§§,§§§]
At term	"	8.9 (3.8)	7.4 (3.0)	<0.001[§§§]
1 month	11.2 (4.2)	9.7 (3.1)	12.1 (4.9)	0.257
1 year	12.9 (4.0)	11.2 (3.2)	12.6 (4.4)	0.331
RV Vabl (cm/s)				
Birth	5.7 (1.2)	5.3 (1.2)	4.5 (1.4	**0.002**[‡‡]
At term	"	7.0 (2.1)	6.1 (1.8)	0.030
1 month	5.3 (1.7)	6.5 (2.0)	5.5 (1.0)	0.238
1 year	6.4 (2.5)	7.0 (2.4)	6.3 (1.4)	0.627
RV Ss (- %)				
Birth	27.6 (5.8)	25.0 (5.5)	23.2 (6.7)	**0.004**[‡‡]
At term	"	34.2 (5.1)	34.9 (5.6)	<0.001[§§,§§§]
1 month	34.2 (4.4)	34.2 (3.7)	34.4 (5.3)	0.989
1 year	40.9 (3.9)	40.3 (3.2)	39.1 (4.5)	0.315
RV SRs (/s)				
Birth	2.4 (0.7)	2.3 (0.7)	2.2 (0.8)	0.490
At term	"	3.4 (0.8)	3.5 (0.6)	<0.001[§§,§§§]
1 month	4.1 (0.9)	3.9 (1.0)	3.5 (0.9)	0.095
1 year	4.4 (1.0)	4.5 (1.0)	3.7 (0.9)	**0.032**[†]
RV SRe (/s)				
Birth	2.7 (0.9)	2.4 (0.8)	2.8 (1.2)	0.182
At term	"	5.0 (1.6)	3.9 (1.7)	<0.001[†,‡‡,§§§]
1 month	5.8 (1.9)	5.0 (1.6)	5.5 (1.9)	0.359
1 year	6.2 (1.2)	6.1 (1.5)	5.4 (1.1)	0.113
RV SRa (/s)				
Birth	2.9 (0.9)	3.1 (0.8)	3.0 (1.3)	0.556
At term	"	5.4 (1.1)	4.2 (0.9)	<0.001[‡,§§,§§§]
1 month	4.6 (1.7)	3.5 (1.0)	3.6 (1.6)	0.062
1 year	3.9 (1.3)	3.4 (1.4)	2.9 (0.9)	0.077

Results are presented as mean (SD).
[§] p <0.001 (PT RDS V PT control), [§§] p <0.001 (PT RDS V Term control), [§§§] p <0.001 (PT control V Term control), [‡] p <0.01 (PT RDS V PT control), [‡‡] p <0.01 (PT RDS V Term control), [‡‡‡] p <0.01 (PT control V Term control), [†] p <0.05 (PT RDS V PT control), [††] p <0.05 (PT RDS V Term control), [†††] p <0.05 (PT control V Term control)

3.3.2.7 Surrogate markers of PA pressure

Tricuspid regurgitation (TR) was highest in the preterm RDS group at birth. By term corrected age, TR in the preterm RDS group was similar to those in the preterm control group. A TR jet was only detected in approximately 38% (range 30% – 48%) in the term control group, 25% (range 11% - 40%) in the preterm control group and 53% (26% - 83%) in preterm RDS groups (Table 3.19) in the whole study from birth to one year follow up. There was no difference in TR jet detection rate between groups at one month and one year.

Pulmonary regurgitation was only detected in small number of subjects in each group in all scans. The numbers were small and although ANOVA analysis showed some significant differences between the groups, it is difficult to interpret the significance of the mildly raised diastolic pulmonary pressure.

Right ventricular pre-ejection period (RV PEP) was longest in the term control group compared to the preterm groups at birth ($p=0.005$). This difference is more marked when the preterm groups were assessed at term ($p<0.001$). However, by one month of age, RV PEP in the term control group was found to be lower than the preterm groups. By one year of age, there were no differences between the groups.

Pulmonary artery acceleration time (PA AT) (also known as time to peak velocity in the pulmonary blood flow) was shortest in the preterm RDS group at birth and at term compared to the control groups. By one month, PA AT in the preterm groups was lower than the term control group and by one year, there were no differences between the groups. Pulmonary ejection times (PA ET) of the term control were longer than the

preterm groups at birth and at term. By one month and one year, PA ET was similar between the groups. The PA AT:ET ratio was noted to be the lowest in the preterm RDS group at birth compared to the control groups. This difference persisted at term corrected age. By one month of age, the PA AT:ET ratio of the preterm RDS groups was still significantly lower than that of the term control. By one year of age, the PA AT:ET ratios were similar between the groups.

In summary:

- The preterm RDS group had increased PA pressures at birth as noted by their significantly higher TR and significantly lower PA AT:ET.

Table 3.19 Tricuspid regurgitation and pulmonary regurgitation at follow up scans

	Term Control (A)	PT Control (B)	PT RDS (C)	ANOVA p value
TR (m/s) (assuming TR=0 if not detected)				
Birth [n/total]	1.0 (1.1) [29/60]	0.8 (1.1) [12/30]	1.7 (1.0) [25/30]	**0.005**‡,††
At term [n/total]	"	0.5 (0.8) [6/22]	0.5 (0.9) [4/19]	0.042
1 month [n/total]	0.6 (1.0) [14/45]	0.2 (0.7) [2/17]	1.0 (1.1) [7/15]	0.084
1 year [n/total]	0.6 (1.0) [10/33]	0.2 (0.7) [2/18]	1.0 (1.2) [7/16]	0.079
PR (m/s) (assuming PR=0 if not detected)				
Birth [n/total]	0.1 (0.2) [8/60]	0.3 (0.5) [12/30]	0.2 (0.3) [8/30]	**0.008**‡‡‡
At term [n/total]	"	0.2 (0.4) [4/22]	0.2 (0.5) [4/19]	0.187
1 month [n/total]	0.1 (0.3) [3/45]	0.5 (0.6) [7/17]	0.4 (0.6) [5/15]	**0.002**‡‡‡
1 year [n/total]	0.2 (0.3) [7/33]	0.5 (0.5) [/18]	0.3 (0.6) [/16]	**0.031**†††

Results are presented as mean (SD).
‡ p <0.01 (PT RDS V PT control), ‡‡‡ p <0.01 (PT control V Term control), †† p <0.05 (PT RDS V Term control), ††† p <0.05 (PT control V Term control)

Table 3.20 Surrogate markers of PA pressure at follow up scans

	Term Control (A)	PT Control (B)	PT RDS (C)	ANOVA p value
RV PEP (ms)				
Birth	53.7 (13.1)	46.2 (12.3)	45.7 (12.4)	**0.005**††,†††
At term	"	36.7 (9.5)	40.0 (10.0)	**<0.001**§§,§§§
1 month	36.9 (7.4)	45.0 (8.7)	45.6 (7.4)	**<0.001**‡‡,‡‡‡
1 year	41.7 (8.2)	41.6 (10.6)	40.8 (8.7)	0.939
PA AT (ms)				
Birth	70.3 (11.9)	64.2 (15.1)	52.6 (11.3)	**<0.001**‡,§§
At term	"	57.3 (10.2)	49.5 (11.2)	**<0.001**§§,§§§
1 month	61.1 (8.9)	54.8 (6.5)	54.2 (7.6)	**0.005**††,†††
1 year	79.5 (10.9)	83.1 (10.4)	84.7 (15.8)	0.316
PA ET (ms)				
Birth	224.6 (20.7)	208.2 (19.7)	198.1 (26.3)	**<0.001**§§,‡‡‡
At term	"	197.4 (15.9)	202.0 (15.8)	**<0.001**§§,§§§
1 month	199.2 (16.0)	193.8 (14.9)	197.4 (13.5)	0.479
1 year	236.3 (20.2)	234.6 (19.0)	238.3 (24.5)	0.874
PA AT:ET ratio				
Birth	0.31 (0.04)	0.31 (0.06)	0.27 (0.04)	**<0.001**‡,§§,
At term	"	0.29 (0.06)	0.25 (0.06)	**<0.001**†,§§
1 month	0.31 (0.05)	0.28 (0.03)	0.27 (0.03)	**0.015**††
1 year	0.34 (0.05)	0.35 (0.03)	0.35 (0.05)	0.287

Results are presented as mean (SD).
§§ *p* <0.001 (PT RDS V Term control), §§§ *p* <0.001 (PT control V Term control), ‡ p <0.01 (PT RDS V PT control), ‡‡ p <0.01 (PT RDS V Term control), ‡‡‡ p <0.01 (PT control V Term control), † p <0.05 (PT RDS V PT control), †† p <0.05 (PT RDS V Term control), ††† p <0.05 (PT control V Term control)

3.4 Discussion

3.4.1 All scans (at birth, at term, one month and one year)

3.4.1.1 Demographics and general characteristics

This is the first large study that has evaluated the global and regional myocardial function of preterm infants with RDS compared to preterm infants without RDS and term controls to determine the usefulness of tissue Doppler parameters such as myocardial velocities, strain and strain rate. I recruited 120 infants (60 term control, 30 preterm control, and 30 preterm RDS) into the study and assessed their cardiac function at birth (within 72 hours) until they reached one year of age with one additional scan at term corrected age for the preterm groups and another at one month corrected age for all groups. I have managed to preserve the 2:1:1 ratio between the groups throughout the study period with a dropout rate of fewer than 50%. At the last assessment at one year, there were 33 term controls, 18 preterm controls and 16 preterm RDS subjects assessed.

Preterm RDS subjects were born at an earlier gestation compared to the control groups and was therefore also smaller compared to the control groups. Despite my best efforts to study the subjects at a similar time frame, the preterm RDS group was assessed at an earlier age at term, one month and one year compared to the control groups. The preterm RDS group weighed least compared to both control groups and this persisted at term and at one year assessments. There was no difference in weight between the groups at one month. Correspondingly the preterm groups' ventricular chamber lengths (a measurement of cardiac size) were smaller compared to the term control group. I am uncertain of how the difference in ventricular size would affect the results of the measured parameters especially the values of myocardial velocities. Ventricular size

would not have any effects on the measurements of myocardial strain and strain rate since these parameters are measured as a relative change in deformation or rate of deformation within a small sample area of the ventricles.

Systolic and diastolic blood pressures in the preterm RDS group were significantly lower than the control groups at birth and at term. By one month corrected age, there was no difference in both systolic and diastolic blood pressures between the groups, which persisted until one year of age.

3.4.1.2 Left ventricular global function

The LV stroke volume and left ventricular output increased with age as the LVOT diameter increased with growth along with higher LVOT VTI with time. The marked difference seen in stroke volume and cardiac output were most likely due to the difference in cardiac size (LVOT d and larger LV chamber). Oberhänsli et al also noted the increase in LV diameter soon after birth due to increased blood flow into the left atrium and subsequent increases in LV chamber associated with increased body weight (Oberhänsli 1980). LV PEP:ET were highest at birth and decreased at term and continued to decrease to become lowest at one year follow up. This was consistent with the results reported by Oberhänsli et al, where it was postulated to be due to a sudden increase in systemic vascular resistance following the exclusion of placental circulation as a result of clamping of the umbilical cord (Oberhänsli 1980). The increase in LV afterload, pulmonary blood flow and LV preload are most likely to be responsible for changes in the LV systolic time intervals.

LV Ds'bl and LV Ds'bs were highest in the term control group at birth and this was thought to be an effect secondary to differences in LV size. When the peak systolic displacement (or excursion) was divided by the LV chamber length, which is represented by the longitudinal axis shortening parameter, the differences disappeared except in the LV basal lateral longitudinal axis shortening between term control and preterm RDS groups, $p<0.05$. The differences in LV Ds' and LV longitudinal axis shortening between the preterm groups at term and term group at birth are largely due to the transition of the postnatal circulation observed in the term group soon after birth. The preterm groups had undergone weeks of postnatal adaptation which would have changed the LV mechanics and function which were not afforded to the term group at birth. The differences seen at term disappeared at one month after the term infants had undergone their postnatal adaptation and changes in the LV mechanics. It is interesting to note that at one year follow up, the LV global function parameters were found to be significantly higher in the term control groups than the preterm groups both in the systolic displacement of the mitral annulus and the 'corrected' LV longitudinal axis shortening. This could not be explained by differences in preload and afterload seen in the preterm groups as ventricular filling and both the systolic and diastolic blood pressures were similar in all groups.

Left ventricular filling pattern (E:A) reflects early diastolic changes and the ratio of early diastolic mitral inflow velocity to early diastolic velocity of the mitral annular motion, E:Ve' has been shown to correlate well with mean ventricular filling pressure. This has been validated in adults as a useful tool to assess LV diastolic function in adults (Sohn 1997, Ommen 2000). In one adult study, E:Ve' >10 was shown to correlate with raised filling pressure when lateral Ve' was used (Nagueh 1997) whereas another

study has shown that E:Ve' ratio of >15 correlated with elevated filling pressure when medial Ve' was used (Ommen 2000). As it is not yet clear whether the medial or the lateral mitral annular velocity is more useful for diagnosing diastolic dysfunction, I opted to measure both medial and lateral mitral annular velocities and used the average of the medial and lateral mitral annular e' velocities as mean Ve' to calculate the ratio E:Ve'. Mitral E was lowest at birth in all groups and increased with time within the groups with a significant difference seen between the groups at birth and at term. Mitral E was highest at the one year assessment and this finding is consistent with those reported by Schmitz et al (Schmitz 2004c). In another longitudinal study over the first three months of life comparing small for gestational age against appropriately grown infants, similar observations were seen in mitral E in the appropriately grown infants although their mitral E values were lower than ours (Gurses 2013). Elkiran et al investigated infants of different age groups from 36-37 weeks gestation up to 3 months old infants, they found mitral E increased with increasing age with the highest mitral E velocity in the 3 months old group (Elkiran 2013). My finding of mitral A velocity increasing from birth and peaking at one month old in all groups has also been reported by the above studies (Elkiran 2013, Gurses 2013).

Mitral E:A in the preterm infant groups were significantly lower than their term counterparts. A similar finding had been report in a study on left ventricular filling patterns in fetuses of different gestations (Harada 1997, Chan 2005). This could be due to the less compliant left ventricle as a result of relative higher content of collagen within the myocytes and the higher ratio of type I to type III collagen resulting in a more rigid, less compliant heart in neonates (Marijianowski 1994). By the time the preterm groups reach term corrected age, mitral E:A were similar to the term group.

Mitral E:A continue to increase with age until the last follow up at one year. My findings are in agreement with a study by Schmitz et al who looked into the diastolic LV function in preterm infants <1500g comparing with term infants (Schmitz 2004b). The changes seen in the improvement of diastolic functions of the left ventricle with age is due to a combination of improvement in left ventricular compliance and relaxation (Kozák-Bárány 2000, Kozák-Bárány 2001).

Mitral E:Ve' peaked at term corrected age in the preterm infant groups and at one month in the term group. After this, mitral E:Ve' decreased and was similar between the groups at one year of age. The decrease in the E:Ve' ratio with age was primarily a result of increased early diastolic DTI velocity during the study period. Eidem et al found in their study that mitral E:Ve' was to be significantly associated with age, heart rate, LV end-diastolic dimension and LV mass (Eidem 2004). Following multiple regression analysis, only LV end-diastolic dimension and LV mass correlated independently with mitral E:Ve' (Eidem 2004).

3.4.1.3 Left ventricular regional function

I have found LV systolic and diastolic myocardial velocities, in both lateral and septal walls, to be lowest in the preterm RDS group, which was also the most preterm and had the smallest ventricular chamber length amongst the groups. The LV systolic and diastolic myocardial velocities increased with increasing gestation. A similar result was reported in other neonatal and fetal studies (Chan 2005, Ciccone 2011). Chan et al noted a 1.6-1.8 fold increase in systolic myocardial velocity and a 1.5-2 fold increase in early diastolic myocardial velocity from mid-trimester to term, in their study of 302 normal fetal hearts from 19 to 37 weeks gestation (Chan 2005). This suggests the LV systolic

function and ventricular relaxation improve with fetal maturity. I found that LV systolic and diastolic function continue to improve postnatally, especially in the preterm groups where both LV systolic and diastolic velocities caught up with the term control group at one month and one year corrected age despite being significantly lower at birth. Klitsie el al also reported a significant increase in LV systolic and diastolic TDi parameters from 1-3 days of life to 6-7 weeks after birth in term infants (Klitsie 2013). They suggested continued improvement of LV performance and cardiac growth as possible causes for the increase in the TDi parameters.

LV myocardial strain was lowest in the preterm RDS group at both the lateral and septal walls. The LV longitudinal strain values in my study is comparable to those reported by de Waal et al (LV Ssl 18.9% ± 4.9% vs 15.7% ± 4.3%; LV Sss 17.5% ± 3.9% vs 16.2% ± 3.5%) although they used speckle tracking echocardiography to measure the longitudinal strain (de Waal 2014). All of my RDS subjects were ventilated while most of de Waal's subjects (81%) were on CPAP. The lower systolic strain in the preterm RDS group could be due to reduced preload secondary to pulmonary disease. There was no evidence of increased afterload in the preterm RDS group as their systolic blood pressure was significantly lower than the control groups. The term control LV longitudinal strain value of 22.8% ± 3.9% is comparable to that reported by other studies using TDi in term newborns assessed in the first 3 days of life (Nestass 2009, Pena 2009). As the preterm RDS subjects got older, their LV peak systolic strain increased and matched those seen in the preterm groups at one month and one year of life. It is reassuring that the LV systolic function improves with age and catches up with the control groups by one month of age.

LV systolic strain rate was similar between the groups. The strain rate did not increase significantly up to one month corrected age in all groups. This has led to some authors suggesting that strain rate measurements are not affected by cardiac growth and could be used for evaluation of LV systolic performance during the neonatal period (Boettler 2005, Klitsie 2013). In a separate study comparing strain and strain rate measurements on healthy newborns and infants (36 weeks preterm neonates to 3 month old infants), there was no difference in LV SR between the preterm and 3 month old infants (Elkiran 2013). This group also concluded that neither strain nor strain rate values were markedly affected by volume and pressure loadings during the first month of life.

3.4.1.4 Right ventricular global and regional functions

RV annular displacement (RV Ds') is lowest in the smallest preterm RDS subjects at birth. However, the RV long axis shortening, which was corrected for RV size and represents RV global function, was still significantly lower than the control groups. There was also evidence of regional myocardial dysfunction in the preterm RDS group where RV systolic velocity was also lower than the control groups and RV systolic strain lower than the term control both reflecting increased afterload in these subjects. These differences disappeared by the time the preterm RDS subjects reached term corrected age. There was no difference in systolic strain rates between the groups, which could suggest preservation of regional contractile function. There is right ventricular regional diastolic dysfunction in the preterm groups at birth but by one month and one year corrected age the RV regional diastolic function normalised. This finding was similar to that in the left ventricle.

3.4.1.5 Surrogate markers of PA pressure

In my study, TR was only detected in 66% of all subjects at birth, with 83% of preterm RDS subjects noted to have TR. TR was significantly higher in the preterm RDS group compared to the control groups. The proportion of TR detection in all subjects at term, one month and one year was low and comparison performed between the groups with the relatively small numbers did not show any significant difference. The raised TR in the preterm RDS group confirmed raised pulmonary vascular resistance which results in higher RV afterload. This is reflected by the lower RV myocardial systolic velocity and systolic strain.

I have also noted a shorter pulmonary artery acceleration time (PA AT) and a lower pulmonary artery acceleration time to ejection time ratio (PA AT:ET) in the preterm RDS group compared to the control groups. Both these parameters have been shown to correlate with increased pulmonary pressures (Evans 1991b, Fitzgerald 1994). This confirms the result of the higher TR jet, lower systolic strain and systolic velocity values in the preterm RDS group at birth.

It has been shown that PA AT can be significantly affected by changes in heart rate without any change in PA pressures (Gardin 1988, Mallery 1991). However, Gardin et al found PA AT:ET does not change with alterations in heart rate in his porcine model which led him to suggest using PA AT:ET as a more useful measurement for estimating PA pressure (Gardin 1988).

The PA AT:ET of the preterm RDS subjects was still significantly lower than the preterm control group at term corrected age suggesting the pulmonary arterial pressure

had not normalised at that stage. However, there were no differences in other surrogate markers of PA pressures between the groups at term.

3.4.1.6 Normalisation of left and right regional myocardial velocities and strain

There was a correlation between regional myocardial systolic and diastolic velocities with infants' weight and heart size at birth. I had wondered if the differences seen between the groups were due to the effects of ventricular size rather than prematurity and / or RDS. I had, therefore, performed a non-standardised normalisation of myocardial velocities by dividing the myocardial velocities by the respective ventricular chamber length and found that after ventricular length normalisation, the differences in myocardial systolic and diastolic velocities and strain in both ventricles noted without normalisation had disappeared. This was an interesting finding and raised the question if ventricular size does affect myocardial velocities in the preterm population. Similar observations were noted on myocardial strain.

I was unable in my study to prove or dispel this effect of heart size on myocardial velocities and strain as this was not the main objective of the study nor was it powered to investigate this effect. The relatively small sample size in this study was not sufficient for me to produce z-scores for myocardial velocities or strain for different gestations in the preterm infants. Chan et al reported increased systolic myocardial velocity and early diastolic myocardial velocity in normal fetal hearts from 19 to 37 weeks gestation and suggested that these increments in systolic and diastolic myocardial velocities are secondary to normal maturation processes in the fetal heart (Chan 2005).

3.4.1.7 Study limitations

This was a prospective longitudinal study of preterm and term neonates involving 120 infants at the beginning of the study. The numbers of subjects studied at subsequent scans at term, one month and one year fell to just over 50% of the number at the beginning of the study. Unfortunately, despite efforts to track and recall subjects for follow up scans, the dropout rate was high. In spite of this, the ratio between the groups had been maintained at 2:1:1 throughout the different scan times.

I only recruited preterm infants of ≤34 weeks who were ventilated when the first echocardiogram was done to ensure infants with significant RDS were studied. However, the practice of early use of pulmonary surfactant and antenatal glucocorticoid administrations would have reduced the severity of RDS and progression to developing bronchopulmonary dysplasia (or chronic lung disease of prematurity).

Although myocardial velocity and strain imaging can provide accurate measures of regional myocardial function, they are associated with a number of technical problems. Strain images may be characterised by signal noise compromising image quality. Strain profiles and curves do not always return to baseline at the end of systole. This may be in part due to the mathematical integration algorithm, but may also be caused by the fact that the wall itself does not return to exactly the same state of deformation at the end of the cycle as was the case at the start. This aspect could be related to several factors, including normal beat to beat variation in stroke volume. It is also angle dependent and tissue direction should be within 30° of the beam for meaningful measurements to be made.

3.4.1.8 Summary and conclusion

In summary, preterm infants with RDS have a higher PA pressure at birth as reflected by a higher TR jet and a lower PA AT:ET. RV global function (RV longitudinal axis shortening) was lower in this group at birth but the only RV regional myocardial parameter that was significantly lower compared to other groups was the myocardial systolic velocity. LV regional myocardial systolic velocity was lowest in the preterm RDS group at birth. Otherwise, there was no difference in LV global and regional systolic functions at birth between the groups. Both preterm infant groups have LV diastolic dysfunction at birth. These differences noted at birth in the preterm groups disappeared by the time they were assessed at term, which indicate postnatal maturation of cardiac function. The preterm infants' left and right global and regional myocardial functions were similar to the term infant group when assessed at one month and one year.

PA AT:ET is a good alternative and possibly a more sensitive surrogate marker of PAP in the event that TR cannot be measured because this parameter can be easily measured in all infants, including extremely preterm infants. Both PA AT:ET and TR jet were significantly different in the preterm RDS group compared to the control groups but the PAP measured by TR jet showed no evidence of increased PAP in the preterm RDS infants. This could suggest milder form of RDS in the preterm RDS group due to routine use of antenatal corticosteroid and exogenous surfactant.

There was evidence of RV global dysfunction (RV longitudinal axis shortening) and RV regional myocardial dysfunction (RV Vsbl) in preterm RDS infants. The newer TDi parameter of RV regional systolic strain and strain rate in the preterm RDS groups was

similar to the control groups. I could only postulate that these newer parameters were either not sensitive enough to detect this difference in regional myocardial dysfunction in the RV of this population or there could be some limitations in applying this parameter in this population.

I have shown that preterm infants continue the myocardial maturation postnatally with improvement in both systolic and diastolic functions and that this process reflects the changes in cardiac haemodynamics associated with ex-utero conditions. The fact that the global and regional myocardial function of both ventricles in the preterm infants caught up with that of term infants at one month and one year of age shows the adaptability of the myocardium to preterm birth provided that there are no significant respiratory complications.

3.4.1.9 Recommendations

- PA AT:ET to be routinely used in the assessment of PAP in both preterm and term infants due to the ease of measurement.
- Longitudinal axis shortening is a sensitive method to assess global dysfunction and can be used in addition to the current more established methods.
- Regional myocardial velocity measurement can be used to assess regional myocardial function but care must be taken in interpreting this value between subjects with different heart size. The establishment of z-scores for myocardial velocities for corrected gestations or infant weight would allow more meaningful interpretation of this parameter in the assessment of regional myocardial function.

- Preterm or term newborn infants are known to have biventricular diastolic dysfunction in the first week of life. An understanding of this fact would avoid unnecessary investigations or treatments to be instituted.
- Even though I have shown the resolution of RV global and regional dysfunction along with improvement of neonatal lung disease, there will be a cohort of preterm infants who develop severe chronic lung disease of prematurity as a result of RDS who may have residual or worsening RV global and regional function. In this cohort of patients, it would be prudent to monitor their cardiac status regularly and institute therapy should the RV function be significantly affected by their lung disease.

Chapter Four

Feasibility of estimating pulmonary artery pulse wave velocity in children using velocity-encoded magnetic resonance imaging (MRI Pilot study)

4.1 Introduction

Pulmonary hypertension is the result of failure of the pulmonary circulation to buffer the pulsatile flow generated by the right ventricle (RV) leading to high flow and pressure from the RV reaching the smaller pulmonary vessels. The loss of pulmonary artery (PA) compliance or increased PA stiffness is thought to be the early precursor to the development of pulmonary arterial hypertension (PAH). In adults with PAH, measures of PA stiffness are increased (Ley 2007) and this is associated with increased mortality (Mahapatra 2006, Gan 2007).

As discussed in section 1.5.1, an inverse relationship between resistance and compliance of the PA circulation has been reported in subjects with or without pulmonary hypertension (Lankhaar 2008). Prompt introduction of targeted therapies can be initiated if changes in PA stiffness are detected earlier. Reliable assessment of PA stiffness permits treatment planning and monitoring.

Recent developments in cardiac magnetic resonance imaging (MRI) techniques allow accurate non-invasive measurements of pulse wave velocity, another measure of arterial stiffness, of the PA in adults without the need for invasive right heart catheterization to measure PA pressures (Peng 2006, Bradlow 2007). Techniques utilizing the flow area (QA) and transit time methods, have been compared showing similar PA PWV values (Ibrahim 2011).

Pulmonary hypertension is relatively common in children and causes include PAH associated with congenital heart disease, connective tissue disease and lung disease such as cystic fibrosis or chronic lung disease of prematurity (Naeije 1987). Early targeted

therapy can delay the onset of PAH, thus improving the quality of life and survival of these children. Thus far, we are not aware of any studies that measured PA PWV in children.

Furthermore, acute exposure to hypoxia causes pulmonary vasoconstriction at the arteriolar level, thus increasing pulmonary vascular resistance, PA pressure and stiffness. Adults who have suffered transient perinatal hypoxic pulmonary hypertension demonstrate significantly higher systolic pulmonary arterial pressure compared to controls at high altitudes (Sartori 1999). However, there is very little data on the effects of acute hypoxia on large vessel stiffness in normal children or indeed, in vulnerable individuals including those with cardiac and respiratory conditions where the risk of PAH is high.

The main objective of this study was to establish the feasibility of measuring PA PWV in children using the QA MRI method and administering a hypoxic challenge to children within the MRI scanner as well as assessing intra- and inter-observer image analysis variability in measuring PA PWV values.

4.2 Methods

In order to establish the feasibility of measuring PA PWV in children, fifteen, 9 – 12 years old children, who were born between 23 - 42 weeks of gestation, were recruited into the study. Written informed consent and assent were obtained from parents and children, respectively. The study was approved by the South East Wales Regional Ethics Committee (REC reference number: 09/WSE02/31) and Cardiff and Vale NHS Trust Research and Development department (R&D study reference: 09/RPM/4554).

Details of subjects' neonatal and medical histories were obtained from their parents and medical records by JME or CYP. Subjects who had patent ductus arteriosus corrected by occlusion coils or clips, ventricular septal defects or had any cardiovascular surgery to correct any congenital structural cardiac defects were excluded from the study, in addition to the other absolute contraindications to having an MRI scan.

4.2.1 Echocardiographic examination

All subjects underwent echocardiographic examination, performed either by JME or CYP, to confirm normality of cardiac structure and function before the MRI scan. The standard echocardiographic assessment using subcostal, parasternal short and long axes, apical four chamber and suprasternal views were used (Appendix A2.2). Pulmonary arterial blood flow acceleration time, ejection time, and tricuspid regurgitation peak velocity, if present, were measured to approximate systolic pulmonary arterial pressure, using the modified Bernoulli equation (Yock 1984).

4.2.2 MRI scanning setup

MRI scans were performed using a 3.0T GE Signa HDx MRI scanner with an 8-channel phased-array cardiac coil (GE Healthcare, Bucks, UK) located in Cardiff University Brain Research Imaging Centre (CUBRIC). Every subject was initially exposed to a practice run in a mock MRI scanner lying within the scanner with simulated background noise, prior to the actual MRI examination. Each subject was scanned twice to acquire cine images of the PA cross section, first while breathing room air and again after breathing 12% inspired oxygen (balance nitrogen) for 20 minutes. The subjects

continued breathing the hypoxic inspirate during the second MRI scan. Using MRI-compatible prisms spectacles, subjects were able to watch a film on a projector screen during the scanning. Parents were permitted to comfort the child as necessary during the scanning after appropriate screening procedures.

4.2.3 MRI protocol

The protocol included three-plane localizers followed by cine images of the PA in long axis and cross-sectional view using a steady-state free precession sequence. Retrospective ECG-gated phase-contrast velocity-encoded images were obtained approximately 0.5cm above the pulmonary valve using 2-dimension gradient-echo sequence. The cine sequence parameters were: slice thickness=7mm, TR=4.7ms, TE=2.9ms, number of averages=2, no. of reconstructed phases=65, no. of acquired phases between 35 – 58 phases depending on heart rate, V_{enc}=150 cm/s, acquisition matrix=192 x 192, FOV=350 mm, flip angle=20° (Appendix A2.3). The MRI examination was performed under free breathing conditions with instructions to maintain shallow breathing during image acquisition to minimize translational movement of the heart associated with respiration and to obtain normal physiological pulmonary arterial blood flow.

4.2.4 Hypoxic challenge

Premixed cylinders of 12% oxygen/nitrogen mixture and 100% oxygen, situated at the MR control room were obtained from British Oxygen Company Limited (BOC, UK). A closed respiratory circuit was used to deliver the hypoxic challenge and supplemental oxygen. Anaesthetic tubing from these two cylinders formed the inspiratory limbs that

delivered humidified gases into a small mixing chamber before being inhaled by the subject via an anaesthetic face mask. The excess gases and expired breaths from subjects exited the circuit through the expiratory limb, which also acted as a rebreathing reservoir necessary for when the peak inspiratory flow instantaneously exceeded the gas flow rate. A high flow rate of 20L/min was used to deliver the hypoxic oxygen mixture to prevent significant rebreathing of the previous breath.

4.2.5 Monitoring during the MRI scan

Subjects heart rate, oxygen saturation, inspired oxygen and end-tidal carbon dioxide levels were monitored continuously by both JME and CYP, who were both trained in basic life support and required to be present during the hypoxic challenge. 100% oxygen was titrated into the circuit to maintain the oxygen saturations between 80–85% if oxygen saturations decreased to below 80%. Each subject received at least 20 minutes of hypoxic challenge before the repeat PWV assessment.

4.2.6 MRI analysis

The MRI images were anonymised and transferred to a personal computer and analysed using the freely available software Segment version 1.8 R1145 (http://segment.heiberg.se) (Heiberg 2010). The region of interest outlining the PA was defined manually on the magnitude images (Figure 4.1). After outlining the PA, the software calculated the cross-sectional area of the PA and the flow within the cross section from the magnitude and phase (velocity-encoded) images, respectively for each acquired phase of the cardiac cycle. Flow rate was plotted against measured cross-sectional area of the PA during early systole. Pulse wave velocity was derived from the

slope of the line fitted to the flow-area data, which represents the ratio of flow change (ΔQ) and area change (ΔA) during early systole (Peng 2006) (Figure 4.2).

The images were analysed by two different observers (JME and CYP) and repeated by one of the observers (CYP), at least two weeks between analyses to measure intra- and inter-observer variability and repeatability. The observers were blinded during analysis to whether images were acquired during normoxia or hypoxia.

4.2.7 Statistical analysis

As this was a pilot study carried out to establish the feasibility of obtaining good quality MRI images for the measurement of PA PWV in young children, the decision to perform on 15 children was to assess the robustness of the MRI acquisition protocol and the MRI analysis of PA PWV. I did not aim to compare PA PWV between different groups of children examined; therefore, sample size calculation was not considered necessary for this study.

Statistical analyses were performed using the Statistics Package for Social Science (SPSS) version 16.0 (Chicago, Illinois, USA). The paired Student's *t*-test was used to compare parameters before and during hypoxic challenge. A p-value of less than 0.05 was considered significant.

Intra- and inter-observer repeatability are reported as the mean coefficients of variation (CV, in %) of all subjects, where individual subject CV was calculated using the formula: CV = (standard deviation of measurements 1 and 2 / mean of the

measurements) x 100. Correlation and Bland–Altman analyses were also used to report intra- and inter-observer variability.

Figure 4.1 - Magnitude images of main PA during early systole

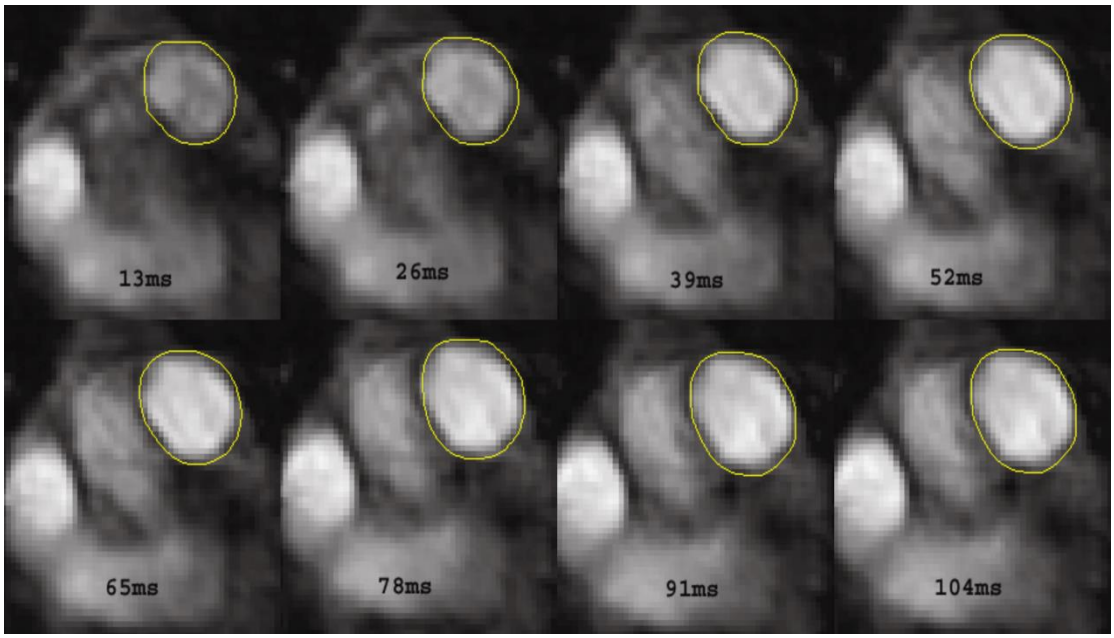

A succession of cross-sectional images showing main PA (circled in yellow) distending during early systole. The vessel cross-sectional area and flow rate are measured at each frame during early systole.

PA=pulmonary artery.

Figure 4.2 - Derivation of PA PWV from flow rate versus cross-sectional area graph

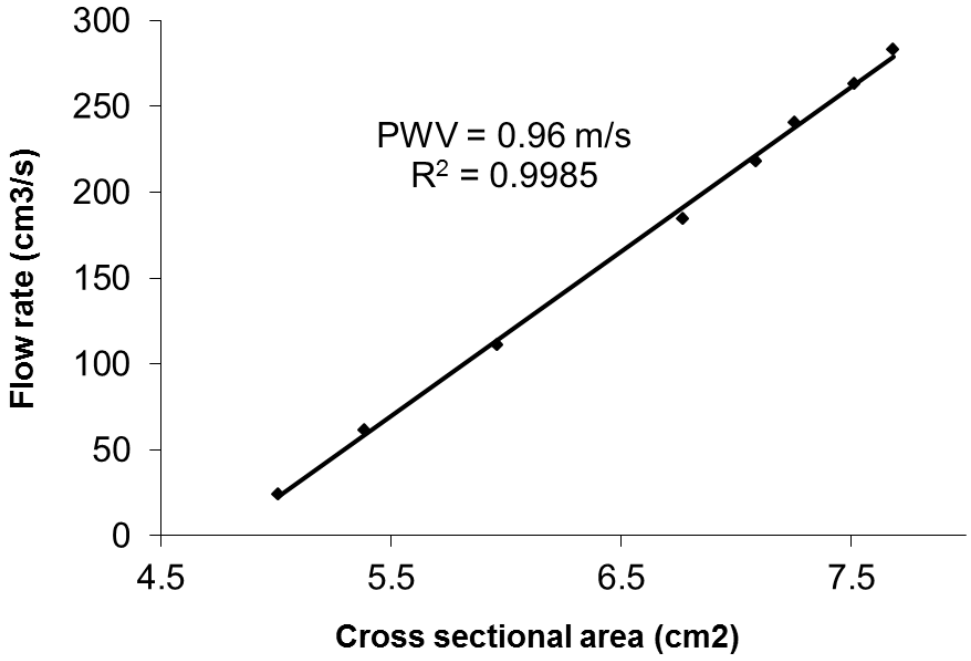

A line is fitted to the plotted data, where PWV is determined as the line slope (change in flow over change in area).

cm^3/s=centrimetre^3 per second, cm^2=centimetre^2, PWV=pulse wave velocity.

4.3 Results

Subject characteristics and baseline measurements of vital signs are given in Table 4.1. All fifteen subjects (ten males and five females) tolerated and successfully completed the MRI scanning and hypoxia challenge. The youngest subject in the study was nine years and eight months and the mean (SD) age of the study population was 11.7 (0.9) years.

All subjects had normal cardiac structure and function on echocardiogram. None of the subjects had evidence of increased right atrial or PA pressure. 11/15 (73%) had detectable tricuspid regurgitation with velocities between 1.3 – 2.2 m/s (estimated systolic pulmonary arterial pressures 11.8 – 24.4 mmHg). Mean (SD) pulmonary acceleration/ejection time ratio was 0.418 (0.044) seconds.

4.3.1 PA PWV measurements using velocity encoded MRI

The MRI examination lasted approximately 90 minutes including the 20 minutes hypoxic exposure. PA PWV measurements were successfully derived from the 15 children, both in air and during hypoxic challenge. Mean (SD) PA PWV increased significantly from 1.32 (0.32) m/s in air to 1.61 (0.58) m/s during hypoxic challenge ($p = 0.03$) (Figure 4.3). Table 4.2 shows PA PWV values in each subject in air and during hypoxic challenge.

4.3.2 Hypoxic challenge

Effective hypoxic challenge was successfully delivered to all children with oxygen saturations decreasing within 2-3 minutes, reaching a nadir and stabilizing within 10 minutes of starting the hypoxic challenge. The mean (SD) inspired O_2 was 11.2 ± 0.6 % and end-tidal CO_2 was 4.7 ± 0.6 %. The oxygen saturations decreased significantly from a mean (SD) of 98.3% (1.6%) in air to 84.5% (3.6%) after 12% oxygen administration (mean difference 13.7%, 95% CI 11 to 16%, $p<0.001$). The monitored heart rate increased by a mean of 17 bpm (95% CI 11 to 23 bpm, $p<0.001$) during hypoxia from baseline (Table 4.3).

4.3.3 Reproducibility and variability

Intra- and inter-observer CV were 9.0% and 15.6% with good intra- and inter-observer correlations between measurements, r=0.92 and r=0.72 respectively (Figure 4.4). Mean (95% limit of agreement) intra- and inter-observer disagreement on Bland-Altman analysis were -0.02 m/s (-0.41 – 0.38 m/s) and -0.28 m/s (-1.06 – 0.49 m/s) (Figure 4.5).

Table 4.1 – Subject characteristics, baseline vital signs and echocardiographic findings

Parameter	**Mean ± SD**
Sex	10 males, 5 females
Gestation (wks)	33.2 ± 5.8
Birth weight (kg)	2.2 ± 1.1
Age (yrs)	11.7 ± 0.9
Weight (kg)	39.3 ± 6.3
Height (cm)	148.5 ± 9.4
Heart rate (bpm)	72 ± 10
Systolic/diastolic blood pressure in air (mmHg)	119 ± 12 / 64 ± 8
Oxygen saturations (%)	98.3 ± 1.6
Tricuspid regurgitation jet (m/s)	1.9 ± 0.4
Pulmonary acceleration time ejection time ratio	0.418 ± 0.044

bpm=beats per minute, cm=centimetre, kg=kilogram, m/s=metre per second, SD=standard deviation, wks=weeks, yrs= years

Table 4.2– Individual PA PWV values in air and during hypoxic challenge

Subject	Age (yrs)	Gestation (wks)	PWV in air (m/s)	PWV in 12% (m/s)
Subject 1	11.8	40.0	1.24	1.75
Subject 2	11.8	40.0	1.19	1.22
Subject 3	11.6	39.4	0.96	1.45
Subject 4	11.4	32.0	1.87	1.79
Subject 5	11.5	31.3	1.45	1.81
Subject 6	12.5	27.0	0.92	1.04
Subject 7	10.8	31.6	1.10	1.73
Subject 8	12.4	30.1	1.98	2.09
Subject 9	9.8	41.0	1.47	1.26
Subject 10	11.3	32.0	1.27	2.12
Subject 11	12.6	42.0	1.27	2.01
Subject 12	12.3	28.0	1.13	1.36
Subject 13	10.8	23.0	1.57	2.98
Subject 14	12.9	31.0	1.30	0.74
Subject 15	10.9	29.6	0.88	0.81

m/s= metre per second, wks= weeks, yrs= years

Table 4.3 - Measurements before and during hypoxic challenge

Parameters	**Normoxia** (Mean ± SD)	**Hypoxia** (Mean ± SD)
Heart rate in air (bpm)	73 ± 10	90 ± 12
Oxygen saturations in air (%)	98.3 ± 1.6	84.5 ± 3.6
Inspired O_2 (%)	-	11.2 ± 0.6
End-tidal CO_2 (%)	-	4.7 ± 0.6

bpm= beats per minute, SD= standard deviation

Figure 4.3 - Change in PA PWV in normoxia and following hypoxic challenge

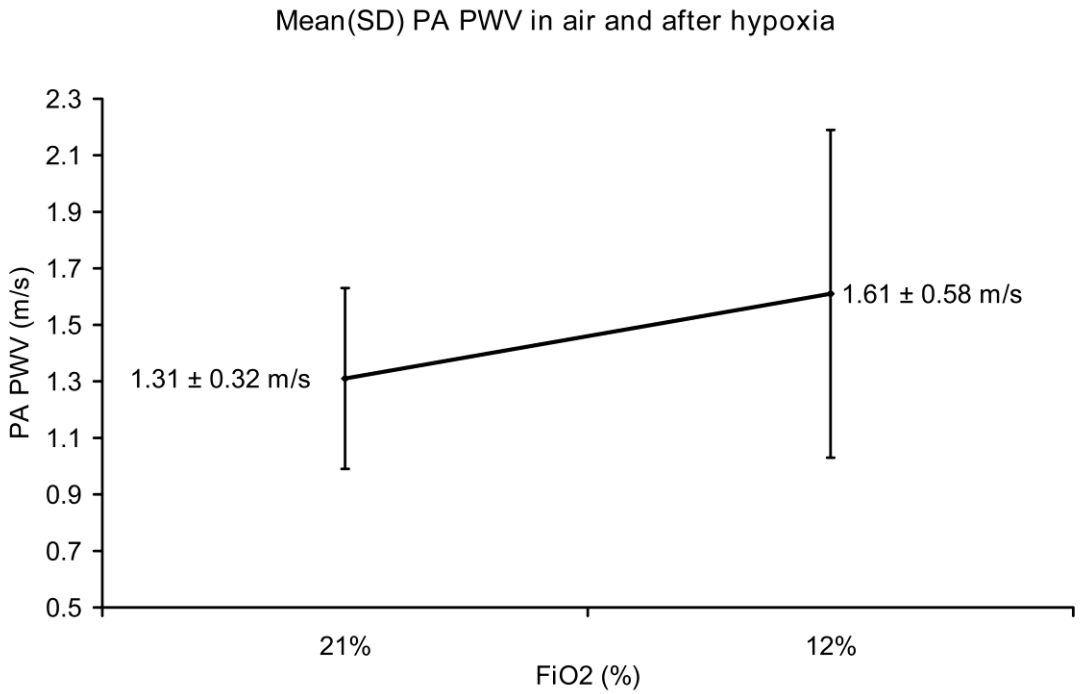

Mean PA PWV increased significantly from 1.32 (0.32) m/s in air to 1.61 (0.58) m/s following hypoxic challenge (p = 0.03).

FiO_2=inspired oxygen, m/s=metre per second, PA=pulmonary artery, PWV=pulse wave velocity, SD=standard deviation.

Figure 4.4 - Intra- and inter-observer correlation analysis

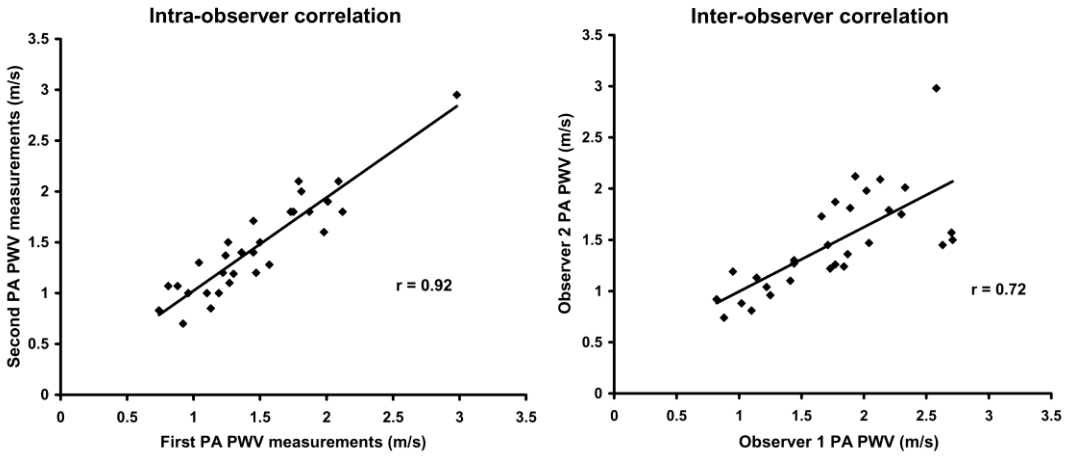

Good intra-observer correlation (r=0.92) and reasonable correlation between observers (r=0.72).

m/s=metre per second, PA=pulmonary artery, PWV=pulse wave velocity

Figure 4.5 - Intra- and inter-observer Bland-Altman analysis

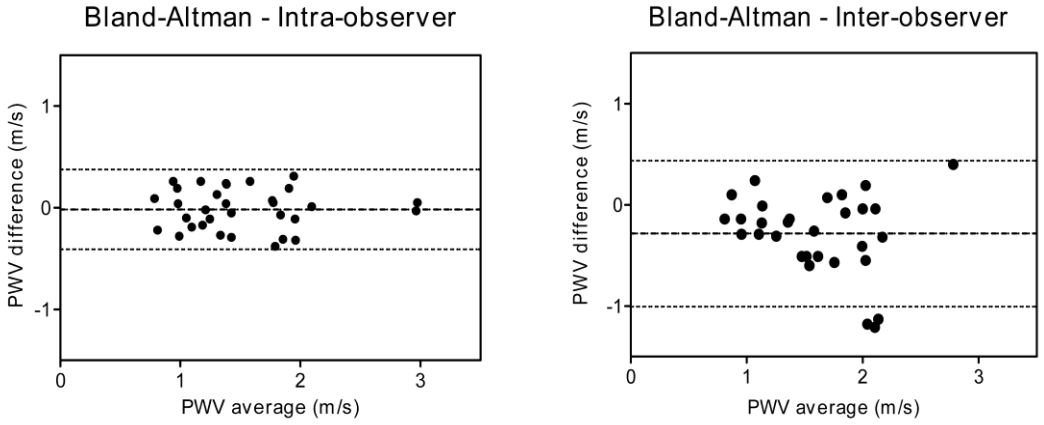

Mean (95% limits of agreement) intra- and inter-observer differences were -0.02 (-0.41 – 0.38) m/s and -0.28 (-1.06 – 0.49) m/s, respectively. Dashed line is the mean difference and dotted lines the 95% limits of agreement.

m/s=metre per second, PWV=pulse wave velocity

4.4 Discussion

This is the first MRI study to successfully measure PA PWV non-invasively in children. I have demonstrated that using the QA method, PA PWV can be measured in children as young as 9 years of age. The facility for children to watch a film during the MRI scan is likely to have contributed significantly to the success in distracting and prevented gross movement of the child during the scanning and certainly during the 3 - 5 minutes duration of cine imaging of the PA. The ability to perform practice runs in a mock scanner was another factor that diminished the fear and anxiety associated with MRI scanning.

4.4.1 PA PWV measurements using velocity encoded MRI

PA PWV was successfully measured in fifteen children in normoxia and after hypoxia. The QA method was chosen to measure main PA PWV in children because of the smaller size and shorter length of their main PA as the latter may introduce more errors if the transit time method had been used. Furthermore, the need for a much longer acquisition time, as reported previously (Ibrahim 2011), is highly impractical in young subjects.

The PA PWVs measured in all fifteen children, aged between 9 – 12 years were between 0.88m/s and 1.98 m/s, with a mean of 1.3 m/s. The PA PWV values were less than the 1.96m/s reported by Peng et al in adults without PAH (Peng 2006). The difference in the observations in children is likely to be due to the more compliant PA than their adult counterparts as has been shown in studies of children and adults assessing the arterial stiffness in the systemic circulation. The aortic PWV measured in

11 year-old children by McEniery and colleagues was 4.7 m/s (McEniery 2011) and the aortic PWV in healthy 26 – 41 years healthy adults studied by Koivistoinen and colleague were 7.7 m/s in males and 7.0 m/s in females (Koivistoinen 2007). If the arterial stiffness changes with age in the pulmonary circulation were assumed to be similar to those in the systemic circulation, then the PA PWV of 1.3 m/s measured in this study is likely to be representative in children without pulmonary hypertension.

PA PWV was found to be significantly higher during hypoxic challenge. This is as predicted since hypoxia promotes arteriolar vasoconstriction resulting in increased pulmonary vascular resistance and decreased pulmonary compliance. The PA PWV during hypoxic challenge was noted to be lower than that in air in four subjects. The differences between the two measurements in three subjects were 0.06 m/s, 0.07 m/s, 0.21 m/s and 0.56 m/s. There are several sources of variability in the measurements. The manual outlining of the MPA can be subjective and may distort PWV estimations. Significant movement of the PA was noted in this young population during scanning due to marked cardiac contraction and respiration possibly due to greater heart and respiratory rates in children; the PA movements were worse during hypoxia due to increased heart and respiratory rate. The heart rate is generally higher in children and increased further following hypoxic challenge. The heart would be contracting more hyper-dynamically under hypoxic conditions and this would result in lower spatial resolution of the PA for manual outlining. It was not possible to avoid the movement effects due to respiration as the cine imaging of the PA cross-section takes 3 – 5 minutes to complete using our protocol. Despite the above, I obtained excellent R^2 values for each PA PWV for each child before and after hypoxia challenge as shown in Figure 4.2.

4.4.2 Reproducibility and variability

Despite the above observations, good repeatability in image analysis as reflected by the good CV of 9% for intra-observer measurements and low variability as the mean difference between measurements was -0.02 m/s (95% CI -0.41 m/s to 0.38 m/s) on the Bland-Altman plots with a correlation coefficient, r=0.92. The inter-observer repeatability was reasonable with CV of 15.6%. PA PWV measurements obtained by JME were generally higher than CYP as the Bland-Altman plots showed the mean difference to be -0.28 m/s (95% CI -1.06 m/s – 0.49 m/s), although the PA PWV values had relatively good correlation, r=0.72. It is noted that JME generally under-detected the change in PA cross-sectional area resulting in a higher PWV value.

An experience echocardiographer (JME) with experience in off-line echocardiographic images post-processing but had limited experience off-line post-processing of cardiac MRI images was used to compare inter-observer repeatability. Despite receiving training on manual outlining of the PA prior to performing the analysis, a higher but acceptable variability and CV was observed. This reaffirms the importance of involving a highly trained operator in cardiac MRI analysis to analyse the images obtained using this technique.

Ibrahim and colleague reported low intra- and inter-observer variability in both transit time and QA methods but found the standard deviations of differences between measurements in the QA method to be greater than the transit time method, albeit not significantly different (Ibrahim 2011). In their study, the MRI images were outlined semi-automatically by bespoke computer software after the operator had marked the vessel cross-section boundary, thus minimizing errors that may occur after manual

delineation of the PA cross-sectional area. Peng and colleagues reported percentage inter-scan differences to be around 10% but it is ethically difficult to envisage repeated scanning in such a young population (Peng 2006).

4.4.3 Hypoxic challenge

Normobaric hypoxia was successfully delivered to all children using a 12% oxygen/balance nitrogen cylinder mixture via anaesthetic tubing, a small mixing chamber and anatomical face mask. A previous study that administered 18% and 15% oxygen did not significantly decrease oxygen saturations to below 85%; hence we opted to use a 12% hypoxic challenge (personal communication with Professor S Kotecha who performed the study in Leicester, unpublished data). This level of hypoxia was tolerated well by all the subjects and there were no significant side effects experienced except the expected ones of mild dizziness, headache, tachycardia, and tachypnoea. We set the lower limit of 80% for oxygen saturations as hypoxemia below this level was considered unethical and unacceptable.

The success of the hypoxic challenge was confirmed by the measured inspired oxygen of 11.2%. The normal range of end-tidal CO_2 recorded in our subjects reassured us that the effects observed were due to hypoxia rather than changes in CO_2 levels.

In three children oxygen saturations remained above 86% during hypoxic challenge. This may have been due to poor fit of the anaesthetic face mask. Nevertheless, the heart rate in these subjects increased from the baseline during hypoxia but it is uncertain if the PA PWV values were affected.

4.4.4 Conclusion

In conclusion, I have demonstrated the feasibility of measuring PA PWV in children with phase-contrast velocity-encoded MRI using the QA method under normal and hypoxic conditions. This method was found to be reproducible with low variation in this young population. Phase-contrast velocity-encoded MRI has the potential to detect early changes in pulmonary arterial stiffness and can be used to non-invasively screen for sub-clinical pulmonary arterial hypertension in children.

This study has been published in the Magnetic Resonance Imaging journal (Poon 2013a) (Appendix H3).

Chapter Five

Exaggerated pulmonary artery response to hypoxia in survivors of chronic lung disease of prematurity

(MRI Study)

5.1 Introduction

Children born preterm have impaired lung function and increased respiratory morbidity that persist into childhood (Fawke 2010, Kotecha 2012b). Few studies have investigated the effects of prematurity on the pulmonary circulation, specifically pulmonary vascular reactivity and pulmonary artery (PA) compliance beyond infancy (Poon 2013b). One of the reasons for this is the need for invasive cardiac catheterisation to assess the PA circulation and this limits the procedure to be ethically performed in children born preterm with echocardiographic evidence of pulmonary arterial hypertension (PAH).

Acute exposure to hypoxia causes pulmonary vasoconstriction at the arteriolar level, thus increasing pulmonary vascular resistance, PA pressure and stiffness. It has been shown that in the pulmonary circulation of patients with or without pulmonary hypertension there is an inverse relationship between resistance and compliance (Lankhaar 2008). However, there are very little data on the effects of acute hypoxia on large vessel stiffness in normal children or indeed, in vulnerable individuals including those with cardiac and respiratory conditions where the risk of PAH is high. Adults who had persistent pulmonary hypertension of the newborn demonstrate significantly higher systolic pulmonary arterial pressure, measured by echocardiography, compared to controls at high altitudes suggesting the increased pulmonary vascular reactivity persists into adulthood (Sartori 1999). Mourani et al studied the acute effects of changing oxygen tension in 10 patients (aged 4 months – 27 years, median 5 years) with bronchopulmonary dysplasia that underwent cardiac catheterization for evaluation of pulmonary hypertension. They reported that mean PA pressure increased by more than 20% following acute hypoxia, thus suggesting increased pulmonary vascular reactivity to hypoxia in this group of patients (Mourani 2004). Both these studies show increased

pulmonary vascular reactivity to hypoxia but it is unknown whether children who had CLD in infancy have similar PA hyper-reactivity.

Although systolic PA pressure can be estimated from tricuspid regurgitant (TR) jet flow by using the modified Bernoulli equation and appears to have a good correlation with cardiac catheterization (Skinner 1993), TR jet flow can only be measured in 61% of young children with CLD (Mourani 2008). Cardiac MRI offers a highly accurate assessment of cardiac structures including ventricular volume, mass, function and blood flow through the cardiac valves and major vessels. MRI-derived average blood velocity is strongly correlated to pulmonary pressures ($r = -0.73$) measured from right heart catheterisation (Sanz 2007), thus potentially allowing non-invasive diagnosis of pulmonary arterial hypertension. Capacitance and distensibility, both measures of arterial stiffness, when measured using velocity-encoded phase-contrast MRI were found to be inversely related to mean pulmonary arterial pressure measured from right heart catheterisation in patients with pulmonary arterial hypertension (Mahapatra 2006, Sanz 2009) Unfortunately the calculation of capacitance and distensibility require invasive pressure measurements. Peng et al used velocity-encoded phase-contrast MRI to measure PA pulse wave velocity (PWV), another measure of arterial stiffness, from the instantaneous changes in blood flow with cross sectional area of the PA during early systole, without the need for invasive pulmonary arterial pressure measurements (Peng 2006).

Our department had previously studied a similar group of children on the effects of hypoxia (15% and 12% inspired oxygen) on the pulmonary circulation using echocardiography (both conventional and myocardial velocity imaging techniques)

which did not show any difference in the echocardiographic parameters of PAP before or after hypoxia between the groups (Joshi 2014). Since velocity-encoded MRI is more sensitive at measuring PA compliance with relatively minor changes in PA resistance, this method may be more sensitive at detecting the changes in PA compliance with hypoxia challenge in these subjects.

The main objective of this study was to measure PA PWV in normoxia and under hypoxic conditions using this novel MRI technique in children born preterm who had chronic lung disease of infancy (CLD group) and compare the results against children born preterm (Preterm group) and at term (Term group) without lung disease during infancy. As this is a follow-on study from the feasibility study, this study included subjects from the study described in the previous chapter. I hypothesised that children born preterm who had CLD of infancy would have a significant increase in PA PWV with hypoxia compared to the two control groups.

5.2 Methods

5.2.1 Recruitment

Both Mourani et al and Sartori et al found children who had CLD and adults who recovered from transient perinatal hypoxic pulmonary hypertension had exaggerated increase in their PAP after a hypoxic challenge compared to the control groups (Sartori 1999, Mourani 2004). The differences in PAP between the groups were between 20-33%. Based on their data, I calculated that I would need to study at least 30 children in each arm to be 90% certain of a difference of 30% in pulmonary arterial pressure at a $p < 0.05$ between the groups.

In this cross-sectional study, sixty seven (15 CLD, 24 Preterm and 28 Term), 9–12 years old children, who were born between 23–42 weeks of gestation, responded to the invitation and recruited to participate in the study. Preterm-born children who were born ≤32 weeks gestation were identified from the Cardiff and Vale NHS trust neonatal database initially but towards the latter part of the study, recruitment of the preterm-born children was extended to include those born in Gwent Healthcare NHS trust due to poor response from the individuals identified from Cardiff and Vale NHS trust. Preterm children who were supplemental oxygen-dependent at 28 days of age or beyond were classified into the CLD group. Term-born children (≥37 weeks' gestation) were recruited from local outpatient clinics and from school friends of included preterm-born subjects. Children who had patent ductus arteriosus corrected by occlusion coils or clips, ventricular septal defects or had any cardiovascular surgery to correct any congenital structural cardiac defects were excluded from the study; in addition to the other absolute contraindications to having an MRI scan. All subjects were clinically well at the time of study.

The study was approved by the South East Wales Regional Ethics Committee (REC reference number: 09/WSE02/31), Cardiff and Vale NHS Trust Research and Development department (R&D study reference: 09/RPM/4554) and Gwent Healthcare NHS Trust Research and Development department (Reference number: RD/833/10). Written informed consent and assent were obtained from parents and children respectively.

Details of subjects' neonatal and medical histories were obtained from their parents and medical records by JME or CYP.

5.2.2 Echocardiographic examination

Echocardiographic examination was performed on all subjects by JME and CYP to confirm normal cardiac structure and function prior to the MRI scan. Subjects who had patent ductus arteriosus corrected by occlusion coils or clips, ventricular septal defects or had any cardiovascular surgery to correct any congenital structural cardiac defects were excluded from the study, in addition to the other absolute contraindications to having an MRI scan. Pulmonary arterial blood flow acceleration time, ejection time, and tricuspid regurgitation peak velocity, if present, were measured to approximate systolic pulmonary arterial pressure prior to hypoxia challenge.

5.2.3 Imaging technique

All MRI scans were performed using a 3.0T GE Signa HDx MRI scanner with an 8-channel phased-array cardiac coil (GE Healthcare, Bucks, UK). The MRI protocol described in section 4.2.3 was used in this study.

Each subject was initially given a practice run in a mock MRI scanner; lying within the scanner with simulated noise being played in the background, prior to the actual MRI examination (Figure 5.1). Each subject was scanned twice to acquire cine images of the PA cross section, first while breathing room air and again after breathing 12% inspired oxygen (balance nitrogen) for 20 minutes, using the same scanning protocol. The subjects continued breathing the hypoxic inspirate during the second MRI scan. During

the whole scanning procedure, subjects were able to watch a film on a projector screen within the scanner by wearing MRI-compatible prisms spectacles. The subject's parents were allowed to stay in the MRI scanner room during the scanning session, after appropriate screening procedures.

Figure 5.1 – Photograph showing subject in the mock MRI scanner

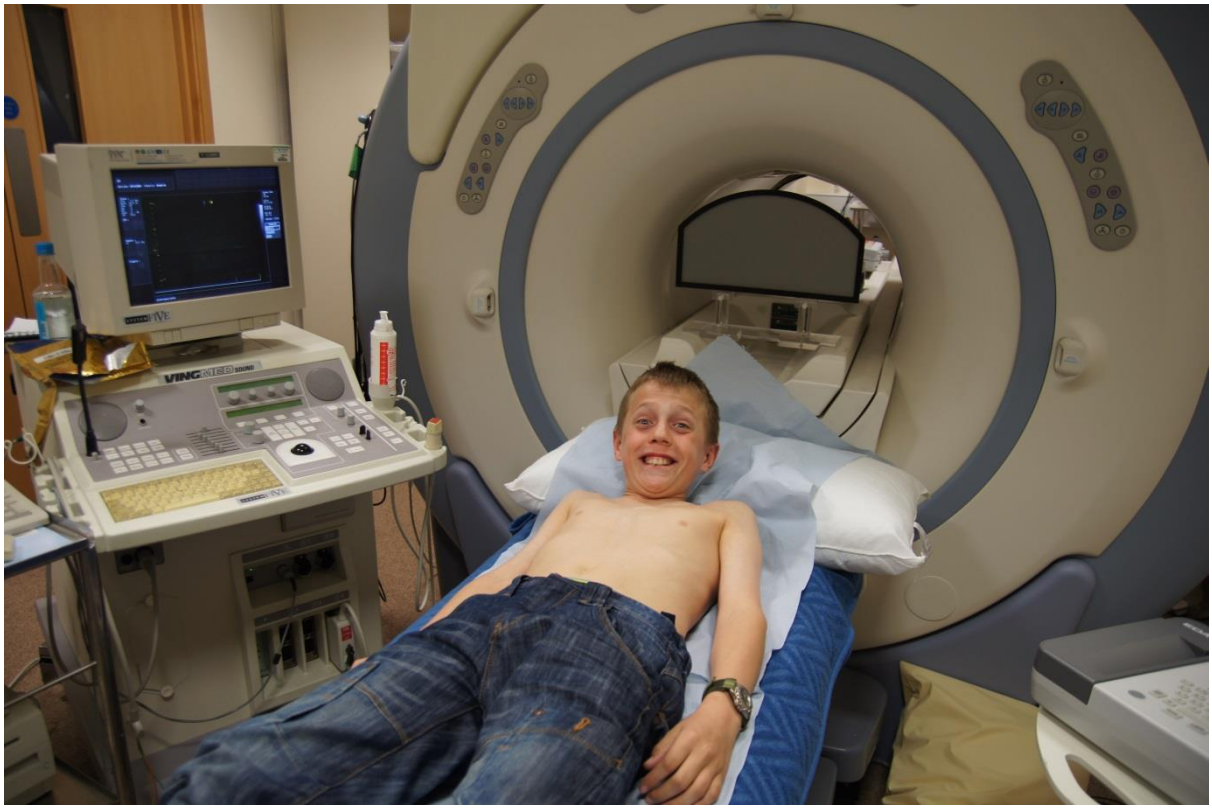

(Informed consent was obtained for the reproduction of this photograph in this thesis)

5.2.4 Hypoxic challenge

The same protocol and apparatus used in the MRI pilot study described in section 4.2.4 were used in this study. Figure 5.2 shows the subject wearing the mask connected to the oxygen cylinder delivering the hypoxic admixture via the respiratory circuit.

5.2.5 Monitoring during the MRI scan

The subjects heart rate, oxygen saturation, inspired oxygen and end-tidal carbon dioxide levels were monitored continuously during the hypoxic challenge. 100% oxygen was titrated into the circuit to maintain the oxygen saturations between 80–85% if oxygen saturations decreased to below 80%. Each subject received at least 20 minutes of hypoxic challenge before the repeat PWV assessment. CYP and JME were present throughout the whole MRI scanning procedure as part of the safety protocol agreed with ethics committee and both Cardiff and Vale NHS trust and Gwent Healthcare NHS trust research and development departments.

5.2.6 Image analysis

The images were anonymised and transferred to a personal computer and analysed using the freely available software Segment version 1.8 R1145 (http://segment.heiberg.se) (Heiberg 2010). The series of both magnitude and phase images showing the magnified view of the PA cross section throughout one cardiac cycle were displayed one at a time. The region of interest outlining the PA was defined manually on the magnitude images. After outlining the PA, the software calculated the cross-sectional area of the PA and the flow within the cross section from the magnitude and phase (velocity-encoded) images, respectively for each acquired phase of the cardiac cycle. Flow rate was plotted

against measured cross sectional area of the PA during early systole using the data generated by the software. Pulse wave velocity was derived from the slope of the line fitted to the flow-area data, which represents the ratio of flow change (ΔQ) and area change (ΔA) during early systole (Peng 2006) (Figure 5.3).

The images were analysed by a single observer (CYP), who was blinded to which group the images belonged to and whether the images were acquired during normoxia or hypoxia.

Figure 5.2 – Subject wearing mask and receiving hypoxia mixture from the cylinder via respiratory circuit

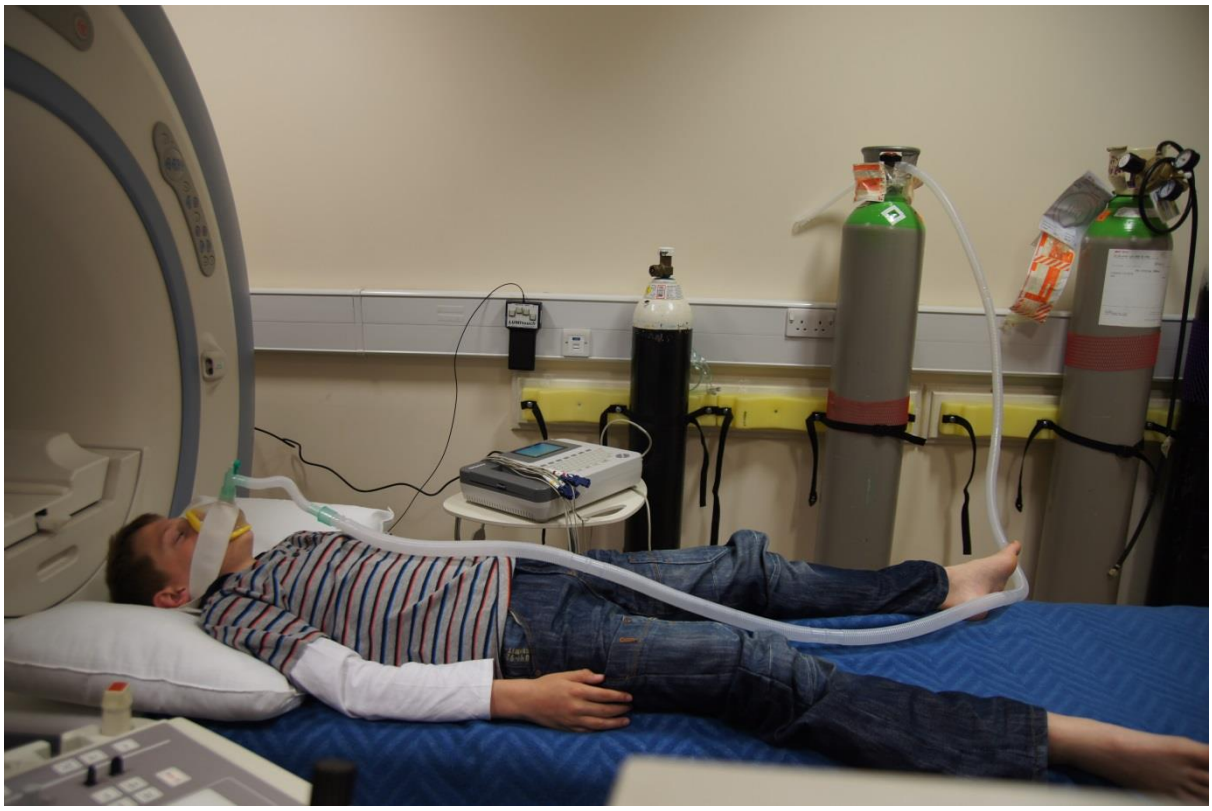

Respiratory circuit showed in this photograph is a simplified version used for the purpose of the practice run and does not represent the actual circuit use in this study

(Informed consent was obtained for the reproduction of this photograph in this thesis)

Figure 5.3 - Early systolic MRI images shows linear increase in PA flow and PA cross sectional area with data plotted onto a graph.

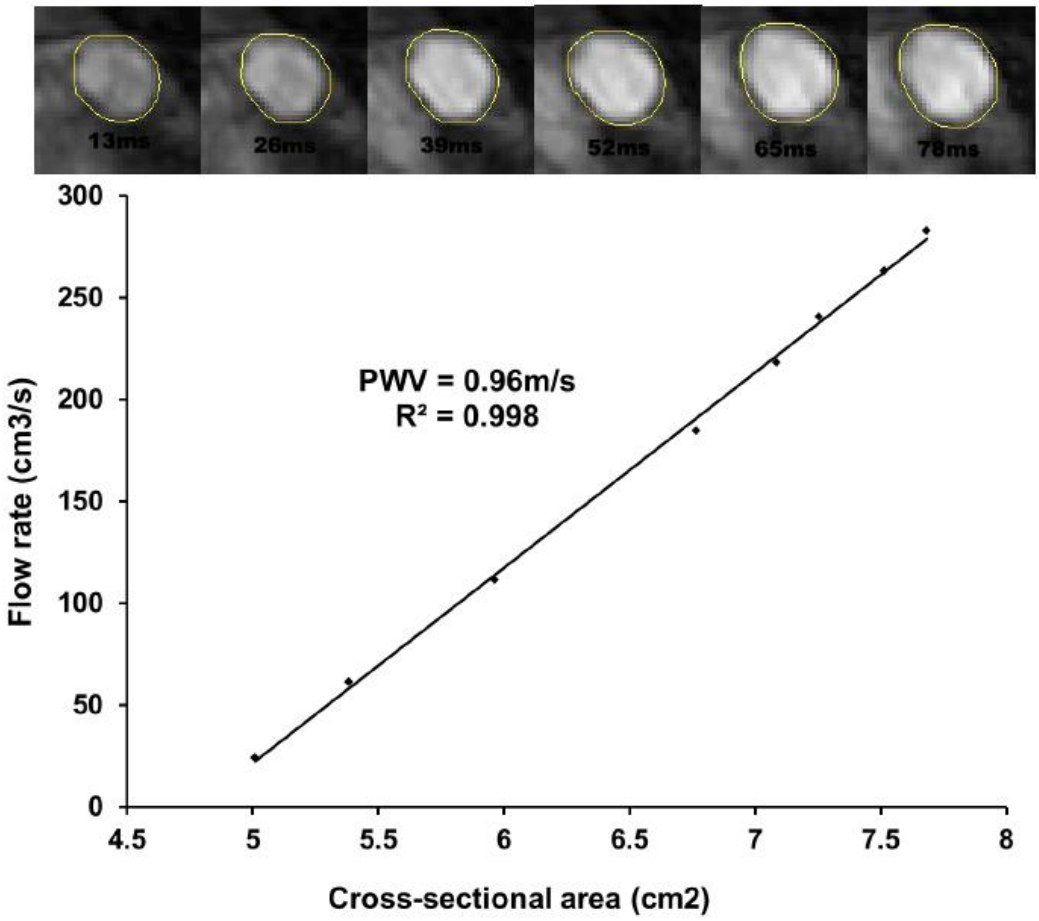

A succession of cross-sectional images showing MPA (delineated in yellow) distending during early systole. The vessel cross-sectional area and flow are measured at each frame during early systole. The graph shows the measured flow rate versus cross-sectional area. A line is fitted to the measured data, where PWV is determined as the gradient of the line (change in flow over change in area). A very high R^2 value showed a good fit of the plots in the linear regression line.

cm^3/s=centrimetre^3 per second, cm^2=centimetre^2, PWV=pulse wave velocity.

5.2.7 Statistical analysis

Statistical analyses were performed using IBM SPSS Statistics for Windows, version 21.0 (Armonk, NY: IBM Corp). The Shapiro-Wilk test was used to test the normality of the measured parameters. Paired Student's *t*-test was used to compare PA PWV before and during hypoxia within each individual group. A two-tailed one-way ANOVA with post-hoc Tukey test was used to compare demographics, echocardiographic and physiological data before and after hypoxic challenge between the three groups ($P<0.05$ was considered significant). Additional non-parametric bootstrap analysis was performed for the non-normally distributed change of PA PWV following hypoxia between the three groups. These results are presented as 95% confidence intervals.

5.3 Results

5.3.1 Subject characteristics and echocardiographic data

Eight subjects (12%; 2 CLD, 4 Preterm and 2 Term) were unable to complete the MRI protocol due to claustrophobia or inability to tolerate the hypoxic challenge. The remaining 59 subjects (13 CLD, 21 Preterm and 25 Term) completed both normoxia and hypoxia protocols. Subject characteristics and echocardiographic data are given in Table 5.1 and Table 5.2.

All subjects had normal cardiac structure and function on echocardiogram. None of the subjects had evidence of increased right atrial or PA pressure. Tricuspid regurgitation was detectable in 10 CLD (77%), 16 Preterm (76%) and 21 Term (84%) subjects with estimated mean systolic pulmonary arterial pressures of 22.6 mmHg in all three groups.

There were also no differences in pulmonary acceleration/ejection time ratio between the groups.

Table 5.1: Subject demographics and respiratory support during neonatal period

Parameters	CLD (Mean ± SD)	Preterm (Mean ± SD)	Term (Mean ± SD)	p-value
Number, n	13	21	25	
Gestation, wks	27.2 ± 1.0	30.5 ± 1.1	40.2 ± 1.2	<0.001
Birth weight, kg	11.5 ± 1.0	12.0 ± 0.8	11.5 ± 1.0	NS
Apgar score				
1 min	5 ± 2	7 ± 2	9 ± 1	<0.001
5 min	8 ± 2	9 ± 1	9 ± 1	0.005
Antenatal steroids, n	12	17	0	
Respiratory support, days	45.9 ± 19.1	3.3 ± 4.6	0	<0.001
Mechanical ventilation, days	21.8 ± 13.7	1.6 ± 2.8	0	<0.001
CPAP, days	24.2 ± 10.3	1.3 ± 1.8	0	<0.001
Oxygen dependency, days	147.5 ± 75.6	6.8 ± 9.5	0	<0.001

Expressed as mean (SD). wks=weeks, kg=kilograms, n=total number. ANOVA test used for gestation, birth weight and Apgar scores. T-test used for respiratory support, mechanical ventilation, CPAP and oxygen dependency.

Table 5.2: Subject demographics and echocardiographic data at the time of assessment

Parameters	CLD (Mean ± SD)	Preterm (Mean ± SD)	Term (Mean ± SD)	p-value
Number	13	21	25	
Male, number (%)	8 (62%)	10 (48%)	16 (64%)	
Age at study, yrs	11.5 ± 1.0	12.0 ± 0.8	11.5 ± 1.0	NS
Weight, kg	33.7 ± 4.6	50.2 ± 16.5	44.0 ±13.4	NS
Height, cm	141.3 ± 5.6	149.6 ±10.3	149.2 ± 10.6	NS
Systolic BP, mmHg	113 ± 12	113 ± 8.2	109 ± 11	NS
Diastolic BP, mmHg	70 ± 14	63 ± 6.5	60 ± 14	NS
Tricuspid jet velocity, m/s	2.1 ± 0.3	2.1 ± 0.3	2.1 ± 0.4	NS
AT:ET ratio	0.40 ± 0.01	0.41 ± 0.03	0.40 ± 0.04	NS

Expressed as mean (SD). wks=weeks, yrs=years, kg=kilograms, m/s=metre per second;

5.3.2 Hypoxic challenge

Three subjects (1 CLD and 2 Term) were unable to tolerate the hypoxic challenge and were excluded from the study. Effective hypoxic challenge was successfully delivered to the remaining 59 subjects with oxygen saturations decreasing within 2-3 minutes, reaching a nadir and stabilising within 10 minutes of starting the hypoxic challenge. All subjects had significant changes in heart rate, respiratory rate and oxygen saturations in all three groups ($p<0.001$). Table 5.3 highlights the changes in measured vital signs before and during the hypoxic challenge. Although there was a significant increase in respiratory rate following the hypoxic challenge, the normal range of end-tidal CO_2 recorded in my subjects reassured me that the effects observed were due to hypoxia rather than changes in CO_2 levels.

Table 5.3: Measurements before and during the hypoxic challenge

Parameters	CLD (Mean ± SD)	Preterm (Mean ± SD)	Term (Mean ± SD)	p-value
HR in air, bpm	74 ± 7	75 ± 12	82 ± 13	NS
HR under hypoxia, bpm	88 ± 13	87 ± 14	90 ± 9	NS
RR in air, /min	19 ± 4	23 ± 4	23 ± 4.4	NS
RR under hypoxia, /min	23 ± 3	26 ± 5	24 ± 3.1	NS
Oxygen saturation in air, %	98 ± 2	98 ± 1	98 ± 2	NS
Oxygen saturation under hypoxia, %	83 ± 2	83 ± 5	85 ± 4	NS
Inspired O_2, %	10.9 ± 1.4	11.3 ± 1.4	11.2 ± 0.7	NS
etCO_2, %	4.4 ± 0.9	4.4 ± 0.7	4.3 ± 0.8	NS

bpm=beats per minute, etCO_2=end-tidal CO_2

5.3.3 PA PWV measurements using velocity encoded MRI

The MRI examination lasted approximately 90 minutes including the 20 minutes hypoxic exposure. Fifty nine subjects successfully completed the MRI protocols in both normoxic and hypoxic conditions.

PA PWV measurements were successfully derived from the 59 subjects, both in air and during hypoxic challenge. Figure 5.4 shows the PA PWV for individual subjects at normoxia and during the hypoxia in all three groups. There were no differences in mean PA PWV between the groups breathing air [CLD=1.3 (0.4) m/s, preterm control=1.3 (0.4) m/s, term control=1.3 (0.3) m/s]. However, PA PWV increased significantly following hypoxia in all groups following hypoxia [CLD=1.9 (0.7) m/s, preterm control=1.5 (0.6) m/s and term=1.5 (0.5) m/s]. Using non-parametric bootstrap within ANOVA with Tukey correction, the mean differences (95% confidence interval) between the CLD and the preterm and term control groups were 0.37 (0.08, 0.70) and 0.34 (0.05, 0.70) respectively suggesting a significant difference in PA PWV changes following hypoxia between the CLD group and the two control groups. There was no difference in PA PWV change with hypoxia between the two control groups, mean difference 0.23 (-0.2, 0.3).

Figure 5.4 – PA PWV for individual subjects at normoxia and during hypoxia

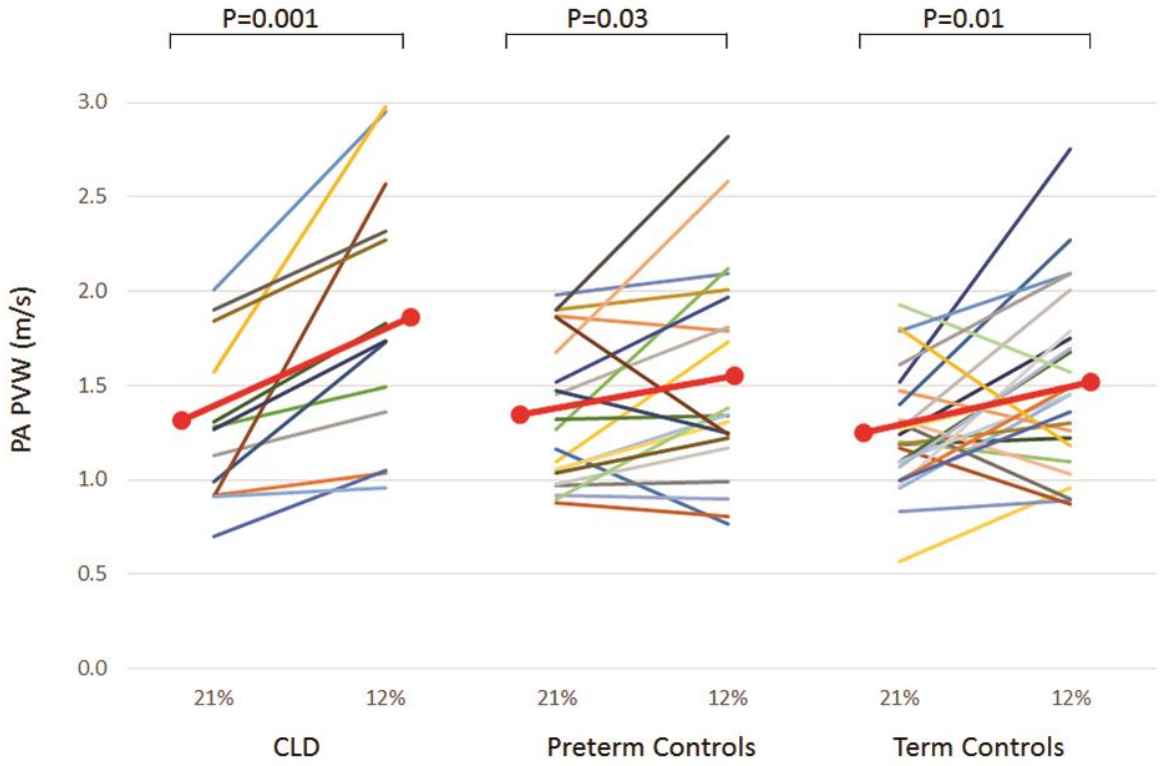

Graph showed PA PWV for individual subjects at normoxia and during hypoxia in the CLD, preterm control and term controls. The solid red line shows the mean change in PA PWV before and after hypoxia in each group.

PA=pulmonary artery, PWV=pulse wave velocity, CLD=chronic lung disease group

5.4 Discussion

I have managed to be the first to apply this new novel MRI technique in the assessment of PA PWV (or changes in compliance) in children who suffered CLD of infancy. I have successfully measured PA PWV non-invasively and compared PA PWV changes with hypoxia in children born preterm who suffered CLD of infancy and preterm and term children without CLD of infancy. All subjects were clinically well and did not have evidence of pulmonary hypertension at the time of study. Using this MRI technique, we were able to measure PA PWV in children as young as 9 years of age.

5.4.1 Hypoxic challenge

Normobaric hypoxia was successfully delivered to the subjects using a 12% oxygen/balance nitrogen cylinder mixture via our specially-designed respiratory circuit. 12% hypoxia was generally well tolerated by the subjects with no significant side effects experienced except the expected ones of mild dizziness, headache, tachycardia, and tachypnoea. The three subjects who could not tolerate the hypoxic challenge reported difficulty in breathing and chest discomfort and did not want to continue with the hypoxic challenge. Interestingly, two of these subjects were from the term control group and the desaturations following the hypoxia challenge in these two subjects were not greater than the rest of subjects who completed the whole protocol. The remaining subject who could not tolerate the hypoxia challenge was from the CLD group and complained of difficulty in breathing with chest discomfort during which oxygen saturations were in the low 90s. I could only postulate this subject had an exaggerated response to hypoxia leading to the symptoms experienced. The lower limit for oxygen

saturations was set to 80% as hypoxaemia below this level was considered unethical and unacceptable.

5.4.2 PA PWV measurements using velocity encoded MRI

Mean baseline PA PWV in all three groups were between 1.25 – 1.35 m/s. These values were lower than the values (1.96 m/s and 2.3 – 2.8m/s) reported in two other adult studies in the literature that used the same technique to measure PA PWV (Peng 2006, Ibrahim 2011). The great arteries in the body stiffen with increasing age, therefore, I expected the PA PWV in my cohort to be lower than those reported in the other two studies. This was illustrated in studies assessing aortic stiffness of children and adults (Koivistoinen 2007, Gurses 2013).

Although there was no difference in PA PWV between the groups following hypoxic challenge, the change in PA PWV, which reflects on the increase in pulmonary vascular resistance as a result of pulmonary vasoconstriction, is marginally greater in the CLD group than in the preterm and term control groups. My finding echoes the findings of Mourani et al where significant increases in PA pressure and pulmonary vascular resistance was found with hypoxia in subjects who suffered from CLD (Mourani 2004); thus implying these subjects have increased pulmonary vascular reactivity and are at higher risk of developing pulmonary hypertension. Sartori et al reported similar finding in young adults who had transient perinatal hypoxic pulmonary hypertension when exposed to altitude-induced hypoxaemia (Sartori 1999).

The underlying mechanism of the exaggerated pulmonary vasoconstrictor responsiveness in these subjects is unknown. It is hypothesised that there is a disruption

of normal lung angiogenesis in preterm infants with CLD that leads to dysregulated alveolarisation (Thebaud 2007). The impaired angiogenesis results in a reduction in the number and size of intra-acinar pulmonary arteries and total cross-sectional area of the pulmonary vascular bed, thus increasing pulmonary vascular resistance (Bush 1990). In addition, there is also evidence of increased muscularisation of the pulmonary arteries, along with a reduction of alveoli numbers, in infants who died from CLD (Hislop 1990, Margraf 1991). Extremely preterm infants with CLD are at high risk of developing pulmonary arterial hypertension due to the combination of an increase in pulmonary arterial medial thickness and pulmonary vascular resistance as a result of dysregulated angiogenesis.

Children who have CLD in infancy, are well-recognised to have dysregulated lung growth (Joshi 2007) and lung function abnormalities in childhood and beyond (Joshi 2013, Kotecha 2013). There is increasing concern that these subjects may be at risk of developing future lung disease such as COPD. COPD is closely linked to the development of pulmonary hypertension with an estimated 2-6/1000 COPD patients with pulmonary hypertension developing cor pulmonale (Naeije 2005). Furthermore, COPD is also associated with a higher prevalence of coronary artery disease (33.6% vs 27.1%) (Maclay 2013). Taken together with the increased respiratory deficits in preterm infants especially those with CLD (Kotecha 2013), it will be important to monitor not only respiratory function (Kotecha 2012a) but also cardiovascular outcomes in preterm infants (McEniery 2011, Bolton 2012).

Study Limitation

The number of subjects recruited for the study was less than the intended 30 subjects in each group. This is due to the poor response to the invitation to participate in the study. In view of the poor recruitment, recruitment of children who were born preterm was extended to another NHS trust towards the latter part of the study. Despite this, I still could not recruit the intended number of subjects for the study due to time constraints in completing my PhD degree and the financial implications for extending this study further. The reason for the poor response could be due to subject having moved out of the area as the contact details were obtained from admission details 9-12 years previously. This less than intended sample size could account for the borderline significant results seen in the CLD group.

I used oxygen dependency beyond 28 days postnatal age as the definition of CLD based on the current definition as proposed by Jobe and Bancalari and thus included subjects with milder forms of CLD / BPD (Jobe 2001). Whether using the CLD definition based on oxygen dependency beyond 36 weeks corrected gestation would have shown greater differences between the CLD group and the control groups is not known as I had only recruited 8 subjects who fulfill the CLD definition of oxygen dependency beyond 36 weeks corrected gestation but their PA PWV were similar to the others in the CLD group. Ideally, I would prefer to have recruited more subjects in the CLD group as the number of subjects recruited in the CLD group was less than intended. As such, there may be some degree of selection bias as the CLD cohort may have been at the less severe end of the disease spectrum.

There was significant movement of the PA in the slice plane between end-diastole to end-systole, especially during hypoxic challenge when the heart and respiratory rates

increased. This could be a source of error to estimate PA PWV as suggested by Ibrahim et al (Lee 2014). Manual outlining of the PA was required in all of the scans in my study. Although this can be subjective, I noted good repeatability and low variability in my feasibility study (Poon 2013a) and a very high regression value for each PA PWV value was obtained for each child. However, a robust, automated vessel outlining tool based on active contouring could possibly minimise this error by avoiding operator dependency.

In conclusion, I demonstrated that children born preterm who suffered from CLD in infancy have increased pulmonary vascular reactivity to hypoxia using velocity-encoded phase-contrast MRI to measure PA PWV. Although these children may be clinically well in normoxic conditions, they still have pulmonary vascular hyper-reactivity to hypoxia and reduced pulmonary function especially forced expiratory volume in the first second (FEV_1) (Kotecha 2013) at school age and possibly into adulthood. The human lungs continue to form alveoli during childhood and adolescence (Narayanan 2012) and recently, it has been reported that ex-preterm children with or without CLD of infancy also display catch up alveolarisation (Narayanan 2013). However, exposure to cigarette smoking, diseases and other environmental toxins may adversely affect alveolarisation in later life or even worse, damage normal lung parenchyma leading to chronic obstructive pulmonary disease, pulmonary hypertension and eventually right heart failure.

Chapter Six

Summary and Conclusions

6.1 Overview

Improvements in antenatal and neonatal care in the last two decades have changed the pathology, morbidity and mortality of chronic lung disease of prematurity. With increasing numbers of preterm births every decade (Field 2009) and increased survival of the extremely preterm population (Costeloe 2008), the proportion of conditions related to prematurity treated has increased. It is, therefore, important to detect any potential associated cardiac and pulmonary conditions in this population (Kotecha 2013, Poon 2013b) and instigate early prevention and /or treatment strategies.

In this thesis, I have presented the optimal technical settings for offline post-processing of myocardial longitudinal strain (ε) measurement in term and preterm infants. I have also presented the findings of the cardiovascular changes using both conventional and tissue Doppler echocardiography in preterm infants with respiratory distress syndrome and compared the findings with preterm and term–born control populations at birth until one year corrected age. I have also studied the pulmonary arterial stiffness and the effects of acute hypoxia on pulmonary vascular reactivity of 8-12 years old children who were born preterm and had chronic lung disease of infancy and compared this with age matched preterm and term-born control populations using a novel MRI technique. All preterm-born infants and children studied in this thesis that required mechanical ventilation support received surfactant and therefore, represent the modern or latest population of the surfactant era.

6.2 Summary of key findings

6.2.1 Optimisation of myocardial deformation imaging in term and preterm infants – a technical study (Chapter 2)

- In smaller preterm infant with smaller ventricles, using a computational distance or strain length of 6mm for the off-line analysis of segmental strain in myocardial velocity imaging is most reproducible.
- In term infants with larger hearts, both computational distances of 6mm and 10mm are optimal and similarly reproducible.
- All myocardial velocity loops should be acquired at frame rates above 180 fps.

6.2.2 Regional and global myocardial assessment in preterm neonates with respiratory distress syndrome at birth and maturation of myocardial function during the first year (Chapter 3)

- Pulmonary arterial pressure was raised in preterm infants with RDS at birth. Pulmonary artery acceleration to ejection time ratio was the most reliable surrogate marker of pulmonary arterial pressure as this could be calculated in all infants compared to tricuspid regurgitation which could only be measured in 39% of subjects.
- Right ventricular longitudinal axis shortening, a surrogate marker of RV global function, and right basal myocardial systolic velocity, a regional myocardial parameter were lower in preterm infants with RDS at birth.

- There were no differences in LV global and regional function between the groups at birth except LV myocardial systolic velocity being lowest in preterm infants with RDS.
- Preterm infants with and without RDS had left ventricular diastolic dysfunction at birth, which normalised by the time they reach 36-40 weeks corrected gestational age.
- The differences noted at birth between the groups mostly disappeared by term and by one month and one year of age, the regional and global function of both ventricles in the preterm infants with RDS had caught up with the control groups. This indicated postnatal maturation of cardiac function in the preterm groups, especially in those with RDS.

6.2.3 Pulse wave velocity in the pulmonary artery measurement and response to hypoxia in children who had CLD in infancy (Chapter 4 and 5)

- In the feasibility study, I have established that PA PWV can be assessed in children as young as 9 – 12 years old using velocity-encoded phase contrast MRI. I have then successfully applied it to measure PA PWV at baseline and after hypoxia challenge in children who had CLD in infancy.
- At baseline, pulmonary arterial stiffness (as measured by pulse wave velocity) was similar in children who had CLD in infancy and the control groups.
- In response to hypoxia, the pulse wave velocity in the pulmonary artery in all three groups of children (age 8-12 years) increased as expected as a result of increased pulmonary arterial resistance secondary to pulmonary hypoxic vasoconstriction.

- The increase in pulmonary arterial pulse wave velocity in children who had CLD in infancy was significantly higher than those of the control groups, thus suggestive of increased pulmonary vasoreactivity in this cohort.

6.3 Importance and clinical implications of findings

6.3.1 Neonatal tissue Doppler study

At the start of the study, there were limited published studies on using myocardial velocity imaging on newborn term and preterm infants (Ekici 2007, Nestass 2009, Wei 2009, Joshi 2010). These studies assessed different tissue Doppler parameters in the newborn term infants and term neonates who suffered asphyxia at birth. There was no published study on the optimal settings for assessment of myocardial deformation in the preterm population and definitely no publications on the preterm population suffering from RDS. Whilst my study was on-going, a few studies with longitudinal follow-up of healthy preterm infants were reported (Kozák-Bárány 2001, Eriksen 2013, Gurses 2013, Helfer 2014) but none had as large a population as this study or followed the same cohort for as long a period of time.

This study confirmed that despite the use of surfactant in preterm infants with RDS, the pulmonary arterial pressure was still elevated at birth as evidenced from decreased pulmonary artery acceleration to ejection time ratio (PA AT:ET) and increased tricuspid regurgitation in this group of infants compared to the controls. Pulmonary artery flow time analysis is simple, reproducible and could be reliably measured in most, if not all of the subjects compared to tricuspid regurgitation. PA AT:ET can be used to assess

raised pulmonary artery pressure in preterm infants with RDS if tricuspid regurgitation could not be obtained.

Infants with RDS have reduced RV global function and reduced RV myocardial systolic velocity measurement as a result of the raised pulmonary pressure at birth. RV longitudinal axis shortening, which is corrected for ventricular size should be used to assess global function instead of using isolated tricuspid annular excursion without z-scores normalised for infants' weight. I have found that myocardial systolic velocity is more sensitive than myocardial deformation in detecting regional myocardial dysfunction in the right ventricle in this cohort of extremely preterm infants with RDS. The abnormal RV global and regional parameters in the preterm RDS group at birth resolved following resolution of their respiratory condition.

In this study, I have noted both systolic and diastolic myocardial velocities to correlate positively to infant heart size. After I normalised the myocardial velocities to the heart size by dividing the myocardial velocity values by the chamber size, the difference in myocardial systolic velocity between the groups disappeared. This raises the question whether myocardial velocity could be influenced by heart size and may influence the result of the findings of the study. Producing a z-score for myocardial velocity for this cohort of preterm infants of various gestations would resolve this question but I was unable to address this issue due to the low number of subjects recruited into the study.

Preterm infants had LV diastolic dysfunction at birth but this normalised by the time they reached term. Preterm infants displayed catch up growth in cardiac size and maturation of cardiac function postnatally when compared to their term counterparts at

one month and one year of age. This can be used to guide or discourage unnecessary intervention in view of the natural history of initial diastolic dysfunction in the preterm population.

In this study, I have found longitudinal axis shortening and myocardial systolic velocity to be the most sensitive parameters among the parameters used in myocardial velocity imaging to assess global and regional function, respectively, of infants with RDS. Pulmonary arterial flow time analysis used to obtain PA AT:ET still has a role in the assessment of pulmonary artery hypertension amidst other new emerging parameters.

6.3.2 Pulmonary arterial pulse wave velocity MRI study

The evidence of long term respiratory sequelae of CLD in infancy is irrefutable (Hennessy 2008, Baraldi 2009, Kotecha 2013). However, the evidence of long term consequences of CLD in infancy on the pulmonary artery and its reactivity to hypoxia is lacking. Mourani et al studied the acute effects of oxygen tension in 10 patients (aged 4 months – 27 years, median 5 years) with bronchopulmonary dysplasia that underwent cardiac catheterization for evaluation of pulmonary hypertension (Mourani 2004) and another adult study reported the effects of high altitude on systolic pulmonary arterial pressure, measured by echocardiography on those who suffered transient perinatal hypoxic pulmonary hypertension (Sartori 1999). Our group has previously studied a similar group of children using conventional and tissue Doppler echocardiography to detect any long term consequences of CLD on the right heart and pulmonary arterial reactivity following hypoxic challenge (Joshi 2014). There was no difference in pulmonary arterial pressure using echocardiographic parameters between the groups following hypoxic challenge. MRI-based assessments of the right heart and pulmonary

artery are increasingly used on adults with pulmonary hypertension (Mahapatra 2006, Peng 2006, Gan 2007) and early changes of the pulmonary artery compliance seen in pulmonary hypertension could be detected using newer MRI techniques (Lankhaar 2006) prior to clinical manifestations of pulmonary hypertension.

As expected, the children with CLD in infancy who were clinically well and asymptomatic had the same baseline pulmonary arterial stiffness as measured by pulse wave velocity estimation on MRI compared to controls, in keeping with the findings by Korhonen et al (Korhonen 2005). However, following hypoxic challenge, we found that children who had CLD in infancy had a greater increase in pulmonary arterial PWV compared to the control groups. This suggests persistence of increased pulmonary vascular reactivity to hypoxia in this cohort at the age of 8-12 years. This result also suggests MRI is more sensitive in assessing pre-clinical changes in pulmonary arterial compliance prior to clinical manifestations of pulmonary hypertension. Children with previous CLD may be at higher risk of developing pulmonary hypertension if they were to be exposed to recurrent chest infections and should be discouraged from smoking tobacco.

In view of the risk of children with CLD in infancy developing right ventricular dysfunction secondary to pulmonary disease, these children should have a right sided cardiac assessment if pulmonary function deteriorates even if they are asymptomatic from the cardiac point of view. There may be a role for using this MRI technique to non-invasively assess these children's PA compliance or PWV longitudinally when MRI scanners become more readily available in the clinical setting.

6.4 Future and on-going research

- I have identified diastolic dysfunction in preterm infants at birth and normalisation of the diastolic function by the time they reach term corrected gestation. This finding was also reported by two other studies (Kozák-Bárány 2001, Eriksen 2013) with similar intervals (at birth and at term). At the time of doing this thesis, there was no study looking at the natural history of this improvement at such a short interval. This would improve our understanding of the maturation of the cardiac function of the preterm population.

- I was unable to address the question whether regional myocardial velocities are affected by heart size in my study. A larger study to obtain regional myocardial velocities of preterm infants of various gestations with and without RDS to address this relationship and also produce the z-scores for different gestations would help determine the suitability of this parameter in the assessment of regional myocardial function in the preterm population.

- Speckle tracking echocardiography has been used in the preterm population (Elkiran 2013, Schubert 2013, de Waal 2014) and has a potential advantage over myocardial velocity imaging or tissue Doppler echocardiography in the assessment of ventricular deformation. Speckle tracking echocardiography is not affected by the translation and stretching of neighbouring myocardial segments, has less angle dependency, is more reproducible and requires less post-processing time (Elkiran 2013). However, more studies will need to be carried out to using this technique to ascertain the usefulness of regional myocardial deformation in the assessment of

clinical or subclinical pulmonary hypertension in the preterm population with or without RDS.

- MRI assessment of the pulmonary artery and right ventricle has the potential for the detecting subclinical changes of pulmonary hypertension. A more robust automated vessel outlining tool based on active contouring in outlining the pulmonary artery would decrease the time to post-process images tremendously and increase the chances of this technique being used in the future.

- Future research investigating pulmonary vascular reactivity should include larger numbers of children with more severe CLD in infancy in order to compare the findings reported in this thesis.

- This cohort should be followed up longitudinally to monitor for any change or worsening of PA PWV especially if they smoke cigarettes or have poor lung function in later life.

6.5 Challenges of the study

6.5.1 Recruitment

6.5.1.1 Neonatal tissue Doppler studies

The parents of the preterm subjects in the study were approached and recruited following admission to the neonatal unit. Sixty seven out of 90 (35 preterm control and 32 preterm RDS) approached consented to participate in the study. The term controls were recruited from the postnatal ward and 60 out of 135 term controls identified were recruited over 3 years. The parents of the term infants were less keen to participate in

the study due to personal reasons, the potential delay at discharge from the postnatal ward and inability to attend follow-up scans at one month and one year of age.

6.5.1.2 Pulmonary artery pulse wave velocity MRI study

The preterm-born subjects in this study were identified from the contact details of the children at the time of birth and from their hospital records. The parents of these children were contacted only after confirmation with their general practitioner of their survival following their preterm births. Out of 336 preterm-born children identified to be eligible for the studies, only 189 (56%) could be traced with confirmation of them being alive with their general practitioner as most had moved out of the area. Out of 147 that were contacted by invitation letter (Appendix C2.1), only 50% (73/147) responded to participate in the study. The reasons for the non-response were unknown and this could have caused unintentional and unavoidable selection bias in the study.

6.5.2 Sample size

As there were no previous studies on tissue Doppler echocardiography changes in preterm infants with RDS and pulmonary vascular response to hypoxia in ex-preterm children, I based my sample size on a study by Sartori et al (Sartori 1999). Sartori and colleagues had studied term-born young adults who had persistent pulmonary hypertension rather than those with CLD of prematurity. Thus, the sample size was based on a study that had a different study population with regards to their disease pathology. The sample size in the MRI study was less than intended due to poor recruitment response from identified subjects despite extension of recruitment duration and recruitment centre.

6.5.3 Neonatal tissue Doppler study

This was a prospective study and there was a 50% drop out rate (as a result of missed follow-up and also death in the neonatal period) in the one month and one year follow-up assessment. However, the ratio of 2:1:1 (term control: preterm control: preterm with RDS) was maintained throughout the study and the dropout was not felt to have influenced the result of the study.

6.5.3.1 The challenges of tissue Doppler echocardiography

Measurement of myocardial velocity and deformation by ultrasound are associated with a number of technical problems such as angle dependency of ultrasound beam, artefacts from reverberations and shadows, sampling rate, out of plane motion, and random noise. Strain images may be characterised by signal noise compromising image quality. Strain profiles and curves do not always return to baseline at the end of systole. This may be in part due to the mathematical integration algorithm, but may also be caused by the fact that the wall itself does not return to exactly the same state of deformation at the end of the cycle as was the case at the start. This aspect could be related to several factors, including normal beat to beat variation in stroke volume. RV isovolumic acceleration and isovolumetric relaxation time were assessed in the study in view of the high inter-observer variability in our group's reproducibility study (Joshi 2010).

6.5.4 Pulmonary artery pulse wave velocity MRI study

6.4.4.1 Definition of CLD used (28 days oxygen dependency)

Oxygen dependency beyond 28 days postnatal age was used as the definition of CLD in this study as recommended by Jobe and Bancalari (Jobe 2001). Because of this, the cohort recruited into this study may represent milder CLD and potentially display less pulmonary vascular reactivity than those who were oxygen dependent at 36 weeks corrected gestation.

6.5.4.2 MRI scan: Challenges

Five subjects were unable to tolerate the claustrophobic environment within the MRI scanner and were excluded from the study. The MRI scanning time initially lasted approximately 90 minutes (including 20 minutes hypoxic challenge) but with more practice and familiarity of the protocol, MRI scanning time was reduced to 60 minutes per subject. Distraction by using optic prisms to enable subject to watch DVD during the scanning procedure greatly reduced the failure of non-completion of the protocol. Manual outlining of the pulmonary artery was required during post-processing of the MRI images. Although this can be subjective, I noted good repeatability and low variability in my methodology study. However, I do suggest a more robust, automated vessel outlining tool based on active contouring could possibly minimise this error by avoiding operator dependency. The process of moving the subjects out of the MRI scanner to place the face mask to deliver the hypoxic challenge and then repeat localisation of the pulmonary artery could introduce errors. This was performed in order to improve the success of completing the MRI scanning protocol by reducing the time subjects breathed via the face mask.

6.5.4.3 Challenges of hypoxic challenge test

Three subjects were unable to tolerate the hypoxic challenge whilst having the MRI scan and had to be excluded from the study. This was due to the use of an anatomical anaesthetic face mask which exaggerated the claustrophobic experience in addition to the MRI scanning. A closed respiratory circuit was used to deliver the normobaric hypoxic challenge (12%) from oxygen/nitrogen mixture and 100% oxygen cylinder. Humidified gases delivered at a high flow rate (20L/min) were delivered into a small mixing chamber, to prevent rebreathing of the previous breath, before being inhaled by

the subject. The excess gases and expired breaths from subjects exited the circuit through the expiratory limb, which also acted as a rebreathing reservoir necessary for when the peak inspiratory flow instantaneously exceeded the gas flow rate. Normobaric hypoxic challenge was used because the MRI assessment could not be performed alongside the hypoxic chamber; hence the use of my methodology in this study. In some of the subjects studied, the hypoxic challenge caused the subjects' oxygen saturations to fall to below 80%. This would undoubtedly cause more significant changes in pulmonary arterial pulse wave velocity but in order to abide to the criteria agreed with the ethics committee, supplemental oxygen was given to maintain oxygen saturation to above 80%.

6.6 Conclusion

This thesis includes two detailed studies on the cardiovascular effects of RDS in preterm infants and long term effects of CLD in infancy on the pulmonary artery reactivity in children aged 8-12 years. The study population represents both infants and children born in the surfactant era. All parameters measured in the studies were compared between subjects affected by their respective respiratory conditions and the preterm and term control population.

In this thesis, I have demonstrated preterm infants with RDS have impaired RV global systolic function and impaired myocardial velocities. Preterm infants, both with and without RDS have diastolic dysfunction which improves by the time they reach term corrected gestation. I have also showed that preterm infants displayed catch up growth in cardiac size and maturation of cardiac function postnatally when compared to their term counterparts at one month and one year of age.

Using velocity-encoded MRI assessment of the pulmonary artery stiffness, I demonstrated that children who had CLD in infancy had normal baseline pulmonary artery pulse wave velocity but displayed an exaggerated response in pulmonary vascular reactivity to hypoxic challenge. This could be suggestive that the increased pulmonary vascular reactivity may persist well into adulthood in this population, similar to Sartori et al's cohort of young adults who had suffered transient perinatal hypoxic pulmonary hypertension (Sartori 1999).

More research is required on this growing population of teenagers and young adults who had CLD in infancy to identify their risk of developing pulmonary hypertension at an earlier age and ensure appropriate follow up and active management.

Bibliography

Abman S H. (2001). Bronchopulmonary dysplasia: "A vascular hypothesis". *Am J Respir Crit Care Med,* 164**,** 1755-1756.

Abman S H, Shanley P F & Accurso F J. (1989). Failure of postnatal adaptation of the pulmonary circulation after chronic intrauterine pulmonary hypertension in fetal lambs. *J Clin Invest,* 83**,** 1849-1858.

Abman S H, Wolfe R R, Accurso F J, Koops B L, Bowman C M & Wiggins J W, Jr. (1985). Pulmonary vascular response to oxygen in infants with severe bronchopulmonary dysplasia. *Pediatrics,* 75**,** 80-84.

Akiba T, Yoshikawa M, Otaki S, Kobayashi Y, Nakasato M, Suzuki H, et al. (1988). Prediction of peak pulmonary artery pressure by continuous-wave doppler echocardiography in infants and children. *Pediatr Cardiol,* 9**,** 225-229.

An H S, Bae E J, Kim G B, Kwon B S, Beak J S, Kim E K, et al. (2010). Pulmonary hypertension in preterm infants with bronchopulmonary dysplasia. *Korean Circ J,* 40**,** 131-136.

Anderson P A W. (1996). The heart and development. *Semin Perinatol,* 20**,** 482-509.

Anderson R H, Webb S & Brown N A. (1999). Clinical anatomy of the atrial septum with reference to its developmental components. *Clin Anat,* 12**,** 362-74.

Avery M E & Mead J. (1959). Surface properties in relation to atelectasis and hyaline membrane disease. *AMA J Dis Child,* 97**,** 517-23.

Ballard P L & Ballard R A. (1972). Glucocorticoid receptors and the role of glucocorticoids in fetal lung development. *Proc Natl Acad Sci U S A,* 69**,** 2668-2672.

Baraldi E, Carraro S & Filippone M. (2009). Bronchopulmonary dysplasia: Definitions and long-term respiratory outcome. *Early Hum Dev,* 85**,** S1-S3.

Bartram U & Speer C P. (2004). The role of transforming growth factor beta in lung development and disease. *Chest,* 125**,** 754-65.

Baum M, Benzer H, Lempert J, Regele H, Stuhlinger W & Tolle W. (1971). The surface tension properties of the lungs of newborn babies. Investigations from autopsies on stillborn and premature infants and babies dying from hyaline membrane disease 'respiratory distress' syndrome. *Respiration,* 28**,** 409-28.

Bellotti M, Pennati G, De Gasperi C, Battaglia F C & Ferrazzi E. (2000). Role of ductus venosus in distribution of umbilical blood flow in human fetuses during second half of pregnancy. *Am J Physiol Heart Circ Physiol,* 279**,** H1256-63.

Benatar A, Clarke J & Silverman M. (1995). Pulmonary hypertension in infants with chronic lung disease: Non-invasive evaluation and short term effect of oxygen treatment. *Arch Dis Child Fetal Neonatal Ed,* 72**,** F14-F19.

Benstein B D, Crouse D T, Shanklin D R & Ourth D D. (2003). Ureaplasma in lung: 2. Association with bronchopulmonary dysplasia in premature newborns. *Exp Mol Pathol,* 75**,** 171-7.

Bhandari V, Hussain N, Rosenkrantz T & Kresch M. (1998). Respiratory tract colonization with mycoplasma species increases the severity of bronchopulmonary dysplasia. *J Perinat Med,* 26**,** 37-42.

Bhat R, Salas A A, Foster C, Carlo W A & Ambalavanan N. (2012). Prospective analysis of pulmonary hypertension in extremely low birth weight infants. *Pediatrics,* 129**,** e682-e689.

Bhatt A J, Pryhuber G S, Huyck H, Watkins R H, Metlay L A & Maniscalco W M. (2001a). Disrupted pulmonary vasculature and decreased vascular endothelial growth factor, flt-1, and tie-2 in human infants dying with bronchopulmonary dysplasia. *Am J Respir Crit Care Med,* 164**,** 1971-80.

Bhatt A J, Pryhuber G S, Huyck H, Watkins R H, Metlay L A & Maniscalco W M. (2001b). Disrupted pulmonary vasculature and decreased vascular endothelial growth factor, flt-1, and tie-2 in human infants dying with bronchopulmonary dysplasia. *Am J Respir Crit Care Med,* 164**,** 1971-1980.

Bland R D, Ling C Y, Albertine K H, Carlton D P, MacRitchie A J, Day R W, et al. (2003). Pulmonary vascular dysfunction in preterm lambs with chronic lung disease. *Am J Physiol Lung Cell Mol Physiol,* 285**,** L76-85.

Boettler P, Hartmann M, Watzl K, Maroula E, Schulte-Moenting J, Knirsch W, et al. (2005). Heart rate effects on strain and strain rate in healthy children. *J Am Soc Echocardiogr,* 18**,** 1121-1130.

Bolton C E, Stocks J, Hennessy E, Cockcroft J R, Fawke J, Lum S, et al. (2012). The epicure study: Association between hemodynamics and lung function at 11 years after extremely preterm birth. *J Pediatr,* 161**,** 595-601.e2.

Bossley C & Balfour-Lynn I M. (2008). Taking young children on aeroplanes: What are the risks? *Arch Dis Child,* 93**,** 528-33.

Bove A A & Santamore W P. (1981). Ventricular interdependence. *Prog Cardiovasc Dis,* 23**,** 365-388.

Bradlow W M, gatehouse P D, Hughes R L, O'Brien A B, Gibbs J S, Firmin D N, et al. (2007). Assessing normal pulse wave velocity in the proximal pulmonary arteries using transit time: A feasibility, repeatability, and observer reproducibility study by cardiovascular magnetic resonance. *J Magn Reson Imaging,* 25**,** 974 - 981.

Bréchot N, Gambotti L, Lafitte S & Roudaut R. (2008). Usefulness of right ventricular isovolumic relaxation time in predicting systolic pulmonary artery pressure. *Eur J Echocardiogr,* 9**,** 547-554.

Burri P H. (1984). Fetal and postnatal development of the lung. *Annu Rev Physiol,* 46**,** 617-628.

Bush A, Busst C M, Knight W B, Hislop A A, Haworth S G & Shinebourne E A. (1990). Changes in pulmonary circulation in severe bronchopulmonary dysplasia. *Arch Dis Child,* 65**,** 739-745.

Chakraborty M, McGreal E P & Kotecha S. (2010). Acute lung injury in preterm newborn infants: Mechanisms and management. *Paediatr Respir Rev,* 11**,** 162-70; quiz 170.

Chan L Y S, Wing Y F, John T H W, Cheuk M Y, Tse N L & Tze K L. (2005). Reference charts of gestation-specific tissue doppler imaging indices of systolic and diastolic functions in the normal fetal heart. *Am Heart J,* 150**,** 750-755.

Ciccone M M, Scicchitano P, Zito A, Gesualdo M, Sassara M, Calderoni G, et al. (2011). Different functional cardiac characteristics observed in term/preterm neonates by echocardiography and tissue doppler imaging. *Early Hum Dev,* 87**,** 555-558.

Coalson J J. (2003). Pathology of new bronchopulmonary dysplasia. *Semin Neonatol,* 8**,** 73-81.

Coker R K, Shiner R & Partridge M R. (2008). Is air travel safe for those with lung disease? *Eur Respir J,* 32**,** 1423-4.

Cornish J D, Dreyer G L, Snyder G E, Kuehl T J, Gerstmann D R, Null D M J, et al. (1994). Failure of acute perinatal asphyxia or meconium aspiration to produce persistent pulmonary hypertension in a neonatal baboon model. *Am J Obstet Gynecol,* 171**,** 43-9.

Costeloe K, Hennessy E, Myles J & Draper E. (2008). Epicure 2: Survival and early morbidity of extremely preterm babies in england: Changes since 1995. *Arch Dis Child,* 93**,** A32-A34.

Cunha G S, Mezzacappa-Filho F & Ribeiro J D. (2005). Risk factors for bronchopulmonary dysplasia in very low birth weight newborns treated with mechanical ventilation in the first week of life. *J Trop Pediatr,* 51**,** 334-40.

Currie A E, Vyas J R, MacDonald J, Field D & Kotecha S. (2001). Epidermal growth factor in the lungs of infants developing chronic lung disease. *Eur Respir J,* 18**,** 796-800.

Dambrauskaite V, Delcroix M, Claus P, Herbots L, D'Hooge J, Bijnens B, et al. (2007). Regional right ventricular dysfunction in chronic pulmonary hypertension. *J Am Soc Echocardiogr,* 20**,** 1172-1180.

Darlow B A, Cust A E & Donoghue D A. (2003). Improved outcomes for very low birthweight infants: Evidence from new zealand national population based data. *Arch Dis Child Fetal Neonatal Ed,* 88**,** F23-F28.

Dawes G S, Mott J C & Widdicombe J G. (1954). The foetal circulation in the lamb. *J Physiol,* 126**,** 563-587.

de Waal K, Lakkundi A & Othman F. (2014). Speckle tracking echocardiography in very preterm infants: Feasibility and reference values. *Early Hum Dev,* 90**,** 275-279.

deMello D E, Sawyer D, Galvin N & Reid L M. (1997). Early fetal development of lung vasculature. *Am J Respir Cell Mol Biol,* 16**,** 568-81.

DiFiore J W & Wilson J M. (1994). Lung development. *Semin Pediatr Surg,* 3**,** 221-32.

Dillard T A, Berg B W, Rajagopal K R, Dooley J W & Mehm W J. (1989). Hypoxemia during air travel in patients with chronic obstructive pulmonary disease. *Ann Intern Med,* 111**,** 362-7.

Dillard T A, Moores L K, Bilello K L & Phillips Y Y. (1995). The preflight evaluation. A comparison of the hypoxia inhalation test with hypobaric exposure. *Chest,* 107**,** 352-7.

Edelstone D I & Rudolph A M. (1979). Preferential streaming of ductus venosus blood to the brain and heart in fetal lambs. *Am J Physiol,* 237**,** H724-9.

Eidem B W, McMahon C J, Cohen R R, Wu J, Finkelshteyn I, Kovalchin J P, et al. (2004). Impact of cardiac growth on doppler tissue imaging velocities: A study in healthy children. *J Am Soc Echocardiogr,* 17**,** 212-221.

Ekici F, Atalay S, Ozcelik N, Ucar T, Yilmaz E & Tutar E. (2007). Myocardial tissue velocities in neonates. *Echocardiography,* 24**,** 61-67.

Elkiran O, Karakurt C, Kocak G & Karadag A. (2013). Tissue doppler, strain, and strain rate measurements assessed by two-dimensional speckle-tracking echocardiography in healthy newborns and infants. *Cardiol Young,* 24**,** 201-211.

Eriksen B H, Nestaas E, Hole T, Liestøl K, Støylen A & Fugelseth D. (2013). Myocardial function in premature infants: A longitudinal observational study. *BMJ Open,* 3.

Evans N J & Archer L N. (1991a). Doppler assessment of pulmonary artery pressure and extrapulmonary shunting in the acute phase of hyaline membrane disease. *Arch Dis Child,* 66**,** 6-11.

Evans N J & Archer L N. (1991b). Doppler assessment of pulmonary artery pressure during recovery from hyaline membrane disease. *Arch Dis Child,* 66**,** 802-804.

Farquhar M & Fitzgerald D A. (2010). Pulmonary hypertension in chronic neonatal lung disease. *Paediatr Respir Rev,* 11**,** 149-53.

Farstad T, Bratlid D, Medbo S & Markestad T. (2011). Bronchopulmonary dysplasia - prevalence, severity and predictive factors in a national cohort of extremely premature infants. *Acta Paediatr,* 100**,** 53-8.

Fawke J, Lum S, Kirkby J, Hennessy E, Marlow N, Rowell V, et al. (2010). Lung function and respiratory symptoms at 11 years in children born extremely preterm: The epicure study. *Am J Respir Crit Care Med,* 182**,** 237-45.

Field D, Draper E S, Fenton A, Papiernik E, Zeitlin J, Blondel B, et al. (2009). Rates of very preterm birth in europe and neonatal mortality rates. *Arch Dis Child Fetal Neonatal Ed,* 94**,** F253-F256.

Fine N M, Chen L, Bastiansen P M, Frantz R P, Pellikka P A, Oh J K, et al. (2013). Outcome prediction by quantitative right ventricular function assessment in 575 subjects evaluated for pulmonary hypertension. *Circulation Cardiol Imaging,* 6**,** 711-721.

Fitzgerald D, Evans N, Van Asperen P & Henderson-Smart D. (1994). Subclinical persisting pulmonary hypertension in chronic neonatal lung disease. *Arch Dis Child Fetal Neonatal Ed,* 70**,** F118-F122.

Friedman W F. (1972). The intrinsic physiologic properties of the developing heart. *Prog Cardiovasc Dis,* 15**,** 87-111.

Frommelt P C, Ballweg J A, Whitstone B N & Frommelt M A. (2002). Usefulness of doppler tissue imaging analysis of tricuspid annular motion for determination of right ventricular function in normal infants and children. *Am J Cardiol,* 89**,** 610-613.

Galie N, Hoeper M M, Humbert M, Torbicki A, Vachiery J L, Barbera J A, et al. (2009). Guidelines for the diagnosis and treatment of pulmonary hypertension: The task force for the diagnosis and treatment of pulmonary hypertension of the european society of cardiology (esc) and the european respiratory society (ers), endorsed by the international society of heart and lung transplantation (ishlt). *Eur Heart J,* 30**,** 2493-537.

Gan C T, Lankhaar J W, Westerhof N, Marcus J T, Becker A, Twisk J W, et al. (2007). Noninvasively assessed pulmonary artery stiffness predicts mortality in pulmonary arterial hypertension. *Chest,* 132**,** 1906-12.

Gardin J M, Sato D A, Rohan M K, Shu V W, Allfie A, Gardin S K, et al. (1988). Effect of acute changes in heart rate on doppler pulmonary artery acceleration time in a porcine model. *Chest,* 94**,** 994-7.

Ge Z, Zhang Y, Ji X, Fan D & Duran C M. (1992). Pulmonary artery diastolic pressure: A simultaneous doppler echocardiography and catheterization study. *Clin Cardiol,* 15**,** 818-24.

Gonzalez A, Sosenko I R S, Chandar J, Hummler H, Claure N & Bancalari E. (1996). Influence of infection on patent ductus arteriosus and chronic lung disease in premature infants weighing 1000 grams or less. *J Pediatr,* 128**,** 470-478.

Grande J P. (1997). Role of transforming growth factor-β in tissue injury and repair. *Exp Biol Med,* 214**,** 27-40.

Groneck P & Speer C P. (1995). Inflammatory mediators and bronchopulmonary dysplasia. *Arch Dis Child Fetal Neonatal Ed,* 73**,** F1-F3.

Groves A M, Kuschel C A, Knight D B & Skinner J R. (2008). Does retrograde diastolic flow in the descending aorta signify impaired systemic perfusion in preterm infants? *Pediatr Res,* 63**,** 89-94.

Gurses D & Seyhan B. (2013). Evaluation of cardiac systolic and diastolic functions in small for gestational age babies during the first months of life: A prospective follow-up study. *Cardiol Young,* 23**,** 597-605.

Harada K, Orino T, Yasuoka K, Tamura M & Takada G. (2000). Tissue doppler imaging of left and right ventricles in normal children. *Tohoku J Exp Med,* 191**,** 21-29.

Harada M D K, Rice M D M J, Shiota M D T, Ishii M D M, McDonald R R R W, Reller M D M D, et al. (1997). Gestational age- and growth-related alterations in fetal right and left ventricular diastolic filling patterns. *Am J Cardiol,* 79**,** 173-177.

Haworth S G. (1988). Pulmonary vascular remodeling in neonatal pulmonary hypertension. State of the art. *Chest,* 93**,** 133S-138S.

Haworth S G. (2008). The management of pulmonary hypertension in children. *Arch Dis Child,* 93**,** 620-625.

Heiberg E, Sjögren J, Ugander M, Carlsson M, Engblom H & Arheden H. (2010). Design and validation of segment - freely available software for cardiovascular image analysis. *BMC Med Imaging,* 10**,** 1-13.

Helfer S, Schmitz L, Bührer C & Czernik C. (2014). Tissue doppler–derived strain and strain rate during the first 28 days of life in very low birth weight infants. *Echocardiography,* 31**,** 765-772.

Hennessy E M, Bracewell M A, Wood N, Wolke D, Costeloe K, Gibson A, et al. (2008). Respiratory health in pre-school and school age children following extremely preterm birth. *Arch Dis Child,* 93**,** 1037-1043.

Hislop A. (2005). Developmental biology of the pulmonary circulation. *Paediatr Respir Rev,* 6**,** 35-43.

Hislop A A. (2002). Airway and blood vessel interaction during lung development. *J Anat,* 201**,** 325-34.

Hislop A A & Haworth S G. (1990). Pulmonary vascular damage and the development of cor pulmonale following hyaline membrane disease. *Pediatr Pulmonol,* 9**,** 152-61.

Hislop A A, Wigglesworth J S, Desai R & Aber V. (1987). The effects of preterm delivery and mechanical ventilation on human lung growth. *Early Hum Dev,* 15**,** 147-64.

Hooper S B & Harding R. (2005). Role of aeration in the physiological adaptation of the lung to air- breathing at birth. *Current Respiratory Medicine Reviews,* 1**,** 185-195.

Humphreys S, Deyermond R, Bali I, Stevenson M & Fee J P. (2005). The effect of high altitude commercial air travel on oxygen saturation. *Anaesthesia,* 60**,** 458-60.

Hunt R W, Evans N, Rieger I & Kluckow M. (2004). Low superior vena cava flow and neurodevelopment at 3 years in very preterm infants. *J Pediatr,* 145**,** 588-92.

Husain A N, Siddiqui N H & Stocker J T. (1998). Pathology of arrested acinar development in postsurfactant bronchopulmonary dysplasia. *Hum Pathol,* 29**,** 710-717.

Ibrahim E-S H, Shaffer J M & White R D. (2011). Assessment of pulmonary artery stiffness using velocity-encoding magnetic resonance imaging: Evaluation of techniques. *Magn Reson Imaging,* 29**,** 966-974.

Jakkula M, Le Cras T D, Gebb S, Hirth K P, Tuder R M, Voelkel N F, et al. (2000). Inhibition of angiogenesis decreases alveolarization in the developing rat lung. *Am J Physiol Lung Cell Mol Physiol,* 279**,** L600-7.

Jobe A & Ikegami M. (1987). Surfactant for the treatment of respiratory distress syndrome. *Am Rev Respir Dis,* 136**,** 1256-75.

Jobe A H & Bancalari E. (2001). Bronchopulmonary dysplasia. *Am J Respir Crit Care Med,* 163**,** 1723-9.

Jobe A J. (1999). The new bpd: An arrest of lung development. *Pediatr Res,* 46**,** 641-3.

Johnson J W, Mitzner W, Beck J C, London W T, Sly D L, Lee P A, et al. (1981). Long-term effects of betamethasone on fetal development. *Am J Obstet Gynecol,* 141**,** 1053-64.

Joshi S, Edwards J M, Wilson D G, Wong J K, Kotecha S & Fraser A G. (2010). Reproducibility of myocardial velocity and deformation imaging in term and preterm infants. *Eur J Echocardiogr,* 11**,** 44-50.

Joshi S & Kotecha S. (2007). Lung growth and development. *Early Hum Dev,* 83**,** 789-794.

Joshi S, Powell T, Watkins W J, Drayton M, Williams E M & Kotecha S. (2013). Exercise-induced bronchoconstriction in school-aged children who had chronic lung disease in infancy. *J Pediatr,* 162**,** 813-818.e1.

Joshi S, Wilson D G, Kotecha S, Pickerd N, Fraser A G & Kotecha S. (2014). Cardiovascular function in children who had chronic lung disease of prematurity. *Arch Dis Child Fetal Neonatal Ed,* 99**,** F373-F379.

Joulin O, Petillot P, Labalette M, Lancel S & Neviere R. (2007). Cytokine profile of human septic shock serum inducing cardiomyocyte contractile dysfunction. *Physiol Res,* 56**,** 291-7.

Kallapur S G, Bachurski C J, Le Cras T D, Joshi S N, Ikegami M & Jobe A H. (2004). Vascular changes after intra-amniotic endotoxin in preterm lamb lungs. *Am J Physiol Lung Cell Mol Physiol,* 287**,** L1178-85.

Kapusta L, Thijssen J M, Cuypers M H M, Peer P G M & Daniëls O. (2000). Assessment of myocardial velocities in healthy children using tissue doppler imaging. *Ultrasound Med Biol,* 26**,** 229-237.

Kitabatake A, Inoue M, Asao M, Masuyama T, Tanouchi J, Morita T, et al. (1983). Noninvasive evaluation of pulmonary hypertension by a pulsed doppler technique. *Circulation,* 68**,** 302-309.

Klitsie L M, Roest A A W, Haak M C, Blom N A & Ten Harkel A D J. (2013). Longitudinal follow-up of ventricular performance in healthy neonates. *Early Hum Dev,* 89**,** 993-997.

Kluckow M & Evans N. (2000a). Ductal shunting, high pulmonary blood flow, and pulmonary hemorrhage. *J Pediatr,* 137**,** 68-72.

Kluckow M & Evans N. (2000b). Low superior vena cava flow and intraventricular haemorrhage in preterm infants. *Arch Dis Child Fetal Neonatal Ed,* 82**,** F188-94.

Koenig J M, Stegner J J, Schmeck A C, Saxonhouse M A & Kenigsberg L E. (2005). Neonatal neutrophils with prolonged survival exhibit enhanced inflammatory and cytotoxic responsiveness. *Pediatr Res,* 57**,** 424-429.

Koivistoinen T, Koobi T, Jula A, Hutri-Kahonen N, Raitakari O T, Majahalme S, et al. (2007). Pulse wave velocity reference values in healthy adults aged 26-75 years. *Clin Physiol Funct Imaging,* 27**,** 191-6.

Korhonen P, Hyödynmaa E, Lautamatti V, Iivainen T & Tammela O. (2005). Cardiovascular findings in very low birthweight schoolchildren with and without bronchopulmonary dysplasia. *Early Hum Dev,* 81**,** 497-505.

Kosturakis D, Goldberg S J, Allen H D & Loeber C. (1984). Doppler echocardiographic prediction of pulmonary arterial hypertension in congenital heart disease. *Am J Cardiol,* 53**,** 1110-5.

Kotecha S. (1996a). Cytokines in chronic lung disease of prematurity. *Eur J Pediatr,* 155 Suppl 2**,** S14-7.

Kotecha S & Allen J. (2002). Oxygen therapy for infants with chronic lung disease. *Arch Dis Child Fetal Neonatal Ed,* 87**,** F11-F14.

Kotecha S, Chan B, Azam N, Silverman M & Shaw R J. (1995). Increase in interleukin-8 and soluble intercellular adhesion molecule-1 in bronchoalveolar lavage fluid from premature infants who develop chronic lung disease. *Arch Dis Child Fetal Neonatal Ed,* 72**,** F90-6.

Kotecha S, Mildner R J, Prince L R, Vyas J R, Currie A E, Lawson R A, et al. (2003). The role of neutrophil apoptosis in the resolution of acute lung injury in newborn infants. *Thorax,* 58**,** 961-967.

Kotecha S, Wangoo A, Silverman M & Shaw R J. (1996b). Increase in the concentration of transforming growth factor beta-1 in bronchoalveolar lavage fluid before development of chronic lung disease of prematurity. *J Pediatr,* 128**,** 464-9.

Kotecha S J, Dunstan F D & Kotecha S. (2012a). Long term respiratory outcomes of late preterm-born infants. *Semin Fetal Neonatal Med,* 17**,** 77-81.

Kotecha S J, Edwards M O, Watkins W J, Henderson A J, Paranjothy S, Dunstan F D, et al. (2013). Effect of preterm birth on later fev1: A systematic review and meta-analysis. *Thorax,* 68**,** 760-766.

Kotecha S J, Watkins W J, Paranjothy S, Dunstan F D, Henderson A J & Kotecha S. (2012b). Effect of late preterm birth on longitudinal lung spirometry in school age children and adolescents. *Thorax,* 67**,** 54-61.

Kozák-Bárány A, Jokinen E, Rantonen T, Saraste M, Tuominen J, Jalonen J, et al. (2000). Efficiency of left ventricular diastolic function increases in healthy full-term infants during the first months of life: A prospective follow-up study. *Early Hum Dev,* 57**,** 49-59.

Kozák-Bárány A, Jokinen E, Saraste M, Tuominen J & Välimäki I. (2001). Development of left ventricular systolic and diastolic function in preterm infants during the first month of life: A prospective follow-up study. *J Pediatr,* 139**,** 539-545.

Kutty S, Deatsman S L, Nugent M L, Russell D & Frommelt P C. (2008). Assessment of regional right ventricular velocities, strain, and displacement in normal children using velocity vector imaging. *Echocardiography,* 25**,** 294-307.

Lankhaar J-W, Westerhof N, Faes T J C, Marques K M J, Marcus J T, Postmus P E, et al. (2006). Quantification of right ventricular afterload in patients with and without pulmonary hypertension. *Am J Physiol Heart Circ Physiol,* 291**,** H1731-1737.

Lankhaar J-W, Westerhof N, Faes T J C, Tji-Joong Gan C, Marques K M, Boonstra A, et al. (2008). Pulmonary vascular resistance and compliance stay inversely related during treatment of pulmonary hypertension. *Eur Heart J,* 29**,** 1688-1695.

Lassus P, Turanlahti M, Heikkila P, Andersson L C, Nupponen I, Sarnesto A, et al. (2001a). Pulmonary vascular endothelial growth factor and flt-1 in fetuses, in acute and chronic lung disease, and in persistent pulmonary hypertension of the newborn. *Am J Respir Crit Care Med,* 164**,** 1981-7.

Lassus P, Turanlahti M, HeikkilÄ P, Andersson L C, Nupponen I, Sarnesto A, et al. (2001b). Pulmonary vascular endothelial growth factor and flt-1 in fetuses, in acute and chronic lung disease, and in persistent pulmonary hypertension of the newborn. *Am J Respir Crit Care Med,* 164**,** 1981-1987.

Le Cras T D, Markham N E, Tuder R M, Voelkel N F & Abman S H. (2002). Treatment of newborn rats with a vegf receptor inhibitor causes pulmonary hypertension and abnormal lung structure. *Am J Physiol Lung Cell Mol Physiol,* 283**,** L555-62.

Lee A, Nestaas E, Liestol K, Brunvand L, Lindemann R & Fugelseth D. (2014). Tissue doppler imaging in very preterm infants during the first 24 h of life: An observational study. *Arch Dis Child Fetal Neonatal Ed,* 99**,** F64-F69.

Lee A P, Yamamoto L G & Relles N L. (2002). Commercial airline travel decreases oxygen saturation in children. *Pediatr Emerg Care,* 18**,** 78-80.

Lemons J A, Bauer C R, Oh W, Korones S B, Papile L A, Stoll B J, et al. (2001). Very low birth weight outcomes of the national institute of child health and human development neonatal research network, january 1995 through december 1996. Nichd neonatal research network. *Pediatrics,* 107**,** E1.

Ley S, Mereles D, Puderbach M, Gruenig E, Schöck H, Eichinger M, et al. (2007). Value of mr phase-contrast flow measurements for functional assessment of pulmonary arterial hypertension. *Eur Radiol,* 17**,** 1892-1897.

Liggins G C & Howie R N. (1972). A controlled trial of antepartum glucocorticoid treatment for prevention of the respiratory distress syndrome in premature infants. *Pediatrics,* 50**,** 515-525.

Lindqvist P, Waldenstrom A, Wikstrom G & Kazzam E. (2006). Right ventricular myocardial isovolumic relaxation time and pulmonary pressure. *Clin Physiol Funct Imaging,* 26**,** 1-8.

Lopez-Candales A, Rajagopalan N, Dohi K, Edelman K & Gulyasy B. (2008). Normal range of mechanical variables in pulmonary hypertension: A tissue doppler imaging study. *Echocardiography,* 25**,** 864-72.

Maclay J D & MacNee W. (2013). Cardiovascular disease in copd: Mechanisms. *Chest,* 143**,** 798-807.

MacRitchie A N, Albertine K H, Sun J, Lei P S, Jensen S C, Freestone A A, et al. (2001). Reduced endothelial nitric oxide synthase in lungs of chronically ventilated preterm lambs. *Am J Physiol Lung Cell Mol Physiol,* 281**,** L1011-20.

Mahapatra S, Nishimura R A, Sorajja P, Cha S & McGoon M D. (2006). Relationship of pulmonary arterial capacitance and mortality in idiopathic pulmonary arterial hypertension. *J Am Coll Cardiol,* 47**,** 799-803.

Mallery J A, Gardin J M, King S W, Ey S & Henry W L. (1991). Effects of heart rate and pulmonary artery pressure on doppler pulmonary artery acceleration time in experimental acute pulmonary hypertension. *Chest,* 100**,** 470-3.

Margraf L R, Tomashefski Jr J F, Bruce M C & Dahms B B. (1991). Morphometric analysis of the lung in bronchopulmonary dysplasia. *Am Rev Respir Dis,* 143**,** 391-400.

Marijianowski M M H, van der Loos C M, Mohrschladt M F & Becker A E. (1994). The neonatal heart has a relatively high content of total collagen and type i collagen, a condition that may explain the less compliant state. *J Am Coll Cardiol,* 23**,** 1204-1208.

Marshall D D, Kotelchuck M, Young T E, Bose C L, Kruyer L & O'Shea T M. (1999). Risk factors for chronic lung disease in the surfactant era: A north carolina population-based study of very low birth weight infants. North carolina neonatologists association. *Pediatrics,* 104**,** 1345-50.

Marwick T H. (2006). Measurement of strain and strain rate by echocardiography: Ready for prime time? *J Am Coll Cardiol,* 47**,** 1313-1327.

Masuyama T, Kodama K, Kitabatake A, Sato H, Nanto S & Inoue M. (1986). Continuous-wave doppler echocardiographic detection of pulmonary regurgitation and its application to noninvasive estimation of pulmonary artery pressure. *Circulation,* 74**,** 484-492.

McEniery C M, Bolton C E, Fawke J, Hennessy E, Stocks J, Wilkinson I B, et al. (2011). Cardiovascular consequences of extreme prematurity: The epicure study. *J Hypertens,* 29**,** 1367-1373.

McGoon M, Gutterman D, Steen V, Barst R, McCrory D C, Fortin T A, et al. (2004). Screening, early detection, and diagnosis of pulmonary arterial hypertension: Accp evidence-based clinical practice guidelines. *Chest,* 126**,** 14S-34S.

Mielke G & Benda N. (2001). Cardiac output and central distribution of blood flow in the human fetus. *Circulation,* 103**,** 1662-8.

Moorman A F & Christoffels V M. (2003). Cardiac chamber formation: Development, genes, and evolution. *Physiol Rev,* 83**,** 1223-67.

Mori K, Nakagawa R, Nii M, Edagawa T, Takehara Y, Inoue M, et al. (2004). Pulsed wave doppler tissue echocardiography assessment of the long axis function of the right and left ventricles during the early neonatal period. *Heart,* 90**,** 175-180.

Moudgil R, Michelakis E D & Archer S L. (2005). Hypoxic pulmonary vasoconstriction. *J Appl Physiol,* 98**,** 390-403.

Mourani P M, Ivy D D, Gao D & Abman S H. (2004). Pulmonary vascular effects of inhaled nitric oxide and oxygen tension in bronchopulmonary dysplasia. *Am J Respir Crit Care Med,* 170**,** 1006-1013.

Mourani P M, Mullen M & Abman S H. (2009a). Pulmonary hypertension in bronchopulmonary dysplasia. *Prog Pediatr Cardiol,* 27**,** 43-48.

Mourani P M, Sontag M K, Ivy D D & Abman S H. (2009b). Effects of long-term sildenafil treatment for pulmonary hypertension in infants with chronic lung disease. *J Pediatr,* 154**,** 379-84, 384 e1-2.

Mourani P M, Sontag M K, Younoszai A, Ivy D D & Abman S H. (2008). Clinical utility of echocardiography for the diagnosis and management of pulmonary vascular disease in young children with chronic lung disease. *Pediatrics,* 121**,** 317-325.

Murray D R & Freeman G L. (1996). Tumor necrosis factor-alpha induces a biphasic effect on myocardial contractility in conscious dogs. *Circ Res,* 78**,** 154-60.

Muscedere J G, Mullen J B, Gan K & Slutsky A S. (1994). Tidal ventilation at low airway pressures can augment lung injury. *Am J Respir Crit Care Med,* 149**,** 1327-1334.

Naderi N, Ojaghi Haghighi Z, Amin A, Naghashzadeh F, Bakhshandeh H, Taghavi S, et al. (2013). Utility of right ventricular strain imaging in predicting pulmonary vascular resistance in patients with pulmonary hypertension. *Congest Heart Fail,* 19**,** 116-122.

Naeije R. (2005). Pulmonary hypertension and right heart failure in chronic obstructive pulmonary disease. *Proc Am Thorac Soc,* 2**,** 20-22.

Naeije R, Hallemans R, Melot C, Boeynaems J M, Mols P, Lejeune P, et al. (1987). Eicosanoids and hypoxic pulmonary vasoconstriction in normal man. *Bull Eur Physiopathol Respir,* 23**,** 613-7.

Nagueh M D S F, Middleton K J, Kopelen H A, Zoghbi W A & Quinones M A. (1997). Doppler tissue imaging: A noninvasive technique for evaluation of left ventricular relaxation and estimation of filling pressures. *J Am Coll Cardiol,* 30**,** 1527-1533.

Narayanan M, Beardsmore C S, Owers-Bradley J, Dogaru C M, Mada M, Ball I, et al. (2013). Catch-up alveolarization in ex-preterm children. Evidence from 3he magnetic resonance. *Am J Respir Crit Care Med,* 187**,** 1104-1109.

Narayanan M, Owers-Bradley J, Beardsmore C S, Mada M, Ball I, Garipov R, et al. (2012). Alveolarization continues during childhood and adolescence: New evidence from helium-3 magnetic resonance. *Am J Respir Crit Care Med,* 185**,** 186-191.

Negrine R J S, Chikermane A, Wright J G C & Ewer A K. (2012). Assessment of myocardial function in neonates using tissue doppler imaging. *Arch Dis Child Fetal Neonatal Ed,* 97**,** F304-F306.

Nestaas E, Stoylen A, Brunvand L & Fugelseth D. (2011). Longitudinal strain and strain rate by tissue doppler are more sensitive indices than fractional shortening for assessing the reduced myocardial function in asphyxiated neonates. *Cardiol Young,* 21**,** 1-7.

Nestaas E, Stoylen A & Fugelseth D. (2008). Optimal types of probe, and tissue doppler frame rates, for use during tissue doppler recording and off-line analysis of strain and strain rate in neonates at term. *Cardiol Young,* 18**,** 502-511.

Nestaas E, Stoylen A & Fugelseth D. (2012). Myocardial performance assessment in neonates by one-segment strain and strain rate analysis by tissue doppler - a quality improvement cohort study. *BMJ Open,* 2.

Nestaas E, Stoylen A, Sandvik L, Brunvand L & Fugelseth D. (2007). Feasibility and reliability of strain and strain rate measurement in neonates by optimizing the analysis parameters settings. *Ultrasound Med Biol,* 33**,** 270-8.

Nestass E, Stoylen A, Brunvand L & Fugelseth D. (2009). Tissue doppler derived longitudinal strain and strain rate during the first 3 days of life in healthy term neonates. *Pediatr Res,* 65**,** 357-362 10.1203/PDR.0b013e318193f149.

Nielsen H C. (1985). Androgen receptors influence the production of pulmonary surfactant in the testicular feminization mouse fetus. *The Journal of Clinical Investigation,* 76**,** 177-181.

Northway W H, Jr., Rosan R C & Porter D Y. (1967). Pulmonary disease following respirator therapy of hyaline-membrane disease. Bronchopulmonary dysplasia. *N Engl J Med,* 276**,** 357-68.

Oberhänsli I, Brandon G, Lacourt G & Friedli B. (1980). Growth patterns of cardiac structures and changes in systolic time intervals in the newborn and infant: A longitudinal echocardiographic study. *Acta Paediatr Scand,* 69**,** 239-247.

Ommen S R, Nishimura R A, Appleton C P, Miller F A, Oh J K, Redfield M M, et al. (2000). Clinical utility of doppler echocardiography and tissue doppler imaging in the estimation of left ventricular filling pressures : A comparative simultaneous doppler-catheterization study. *Circulation,* 102**,** 1788-1794.

Oparil S, Bishop S P & Clubb F J, Jr. (1984). Myocardial cell hypertrophy or hyperplasia. *Hypertension,* 6**,** III38-43.

Osborn D A, Evans N & Kluckow M. (2003). Hemodynamic and antecedent risk factors of early and late periventricular/intraventricular hemorrhage in premature infants. *Pediatrics,* 112**,** 33-9.

Patel N, Mills J & Cheung M. (2009). Use of the myocardial performance index to assess right ventricular function in infants with pulmonary hypertension. *Pediatr Cardiol,* 30**,** 133-137.

Peacock A J. (1998). Abc of oxygen: Oxygen at high altitude. *BMJ,* 317**,** 1063-6.

Pena J L B, Silva M G d, Faria S C C, Salemi V M C, Mady C, Baltabaeva A, et al. (2009). Quantification of regional left and right ventricular deformation indices in healthy neonates by using strain rate and strain imaging. *J Am Soc Echocardiogr,* 22**,** 369-375.

Peng H-H, Chung H-W, Hsi-Yu Y & Wen-Yih I T. (2006). Estimation of pulse wave velocity in main pulmonary artery with phase contrast mri: Preliminary investigation. *J Magn Reson Imaging,* 24**,** 1303-1310.

Pickerd N & Kotecha S. (2009). Pathophysiology of respiratory distress syndrome. *Paediatr Child Health,* 19**,** 153-157.

Poon C Y, Edwards J M, Evans C J, Harris A D, Tsai-Goodman B, Bolton C E, et al. (2013a). Assessment of pulmonary artery pulse wave velocity in children: An mri pilot study. *Magn Reson Imaging,* 31**,** 1690-1694.

Poon C Y, Edwards J M, Joshi S, Kotecha S & Fraser A G. (2011). Optimization of myocardial deformation imaging in term and preterm infants. *Eur Heart J Cardiovasc Imaging,* 12**,** 247-254.

Poon C Y, Edwards M O & Kotecha S. (2013b). Long term cardiovascular consequences of chronic lung disease of prematurity. *Paediatr Respir Rev,* 14**,** 242-249.

Rajagopalan N, Simon M A, Shah H, Mathier M A & López-Candales A. (2008). Utility of right ventricular tissue doppler imaging: Correlation with right heart catheterization. *Echocardiography,* 25**,** 706-711.

Rasanen J, Wood D C, Weiner S, Ludomirski A & Huhta J C. (1996). Role of the pulmonary circulation in the distribution of human fetal cardiac output during the second half of pregnancy. *Circulation,* 94**,** 1068-73.

Reiser P J, Westfall M V, Schiaffino S & Solaro R J. (1994). Tension production and thin-filament protein isoforms in developing rat myocardium. *Am J Physiol Heart Circ Physiol,* 267**,** H1589-H1596.

Reynolds E O. (1970). Hyaline membrane disease. *Am J Obstet Gynecol,* 106**,** 780-97.

Roberson D A, Cui W, Chen Z, Madronero L F & Cuneo B F. (2007). Annular and septal doppler tissue imaging in children: Normal z-score tables and effects of age, heart rate, and body surface area. *J Am Soc Echocardiogr,* 20**,** 1276-1284.

Romero T, Covell J & Friedman W F. (1972). A comparison of pressure-volume relations of the fetal, newborn, and adult heart. *Am J Physiol,* 222**,** 1285-90.

Rozycki H J, Comber P G & Huff T F. (2002). Cytokines and oxygen radicals after hyperoxia in preterm and term alveolar macrophages. *American Journal of Physiology - Lung Cellular and Molecular Physiology,* 282**,** L1222-L1228.

Rudolph A M. (1979). Fetal and neonatal pulmonary circulation. *Annu Rev Physiol,* 41**,** 383-95.

Rudolph A M. (2000). Myocardial growth before and after birth: Clinical implications. *Acta Paediatr,* 89**,** 129-33.

Sachdev A, Villarraga H R, Frantz R P, McGoon M D, Hsiao J-F, Maalouf J F, et al. (2011). Right ventricular strain for prediction of survival in patients with pulmonary arterial hypertension. *Chest,* 139**,** 1299-1309.

Samuels M P. (2004). The effects of flight and altitude. *Arch Dis Child,* 89**,** 448-455.

Sanz J, Kariisa M, Dellegrottaglie S, Prat-Gonzalez S, Garcia M J, Fuster V, et al. (2009). Evaluation of pulmonary artery stiffness in pulmonary hypertension with cardiac magnetic resonance. *J Am Coll Cardiol Img,* 2**,** 286-295.

Sanz J, Kuschnir P, Rius T, Salguero R, Sulica R, Einstein A J, et al. (2007). Pulmonary arterial hypertension: Noninvasive detection with phase-contrast mr imaging. *Radiology,* 243**,** 70-79.

Sartori C, Allemann Y, Trueb L, Delabays A, Nicod P & Scherrer U. (1999). Augmented vasoreactivity in adult life associated with perinatal vascular insult. *Lancet,* 353**,** 2205-2207.

Saunders R A & Milner A D. (1978). Pulmonary pressure/volume relationships during the last phase of delivery and the first postnatal breaths in human subjects. *J Pediatr,* 93**,** 667-73.

Savourey G, Launay J C, Besnard Y, Guinet A & Travers S. (2003). Normo- and hypobaric hypoxia: Are there any physiological differences? *Eur J Appl Physiol,* 89**,** 122-6.

Sawyer M H, Edwards D K & Spector S A. (1987). Cytomegalovirus infection and bronchopulmonary dysplasia in premature infants. *Am J Dis Child,* 141**,** 303-5.

Schmidt B, Cao L, Mackensen-Haen S, Kendziorra H, Klingel K & Speer C P. (2001a). Chorioamnionitis and inflammation of the fetal lung. *Am J Obstet Gynecol,* 185**,** 173-177.

Schmidt B, Davis P, Moddemann D, Ohlsson A, Roberts R S, Saigal S, et al. (2001b). Long-term effects of indomethacin prophylaxis in extremely-low-birth-weight infants. *N Engl J Med,* 344**,** 1966-72.

Schmitz L, Stiller B, Koch H, Koehne P & Lange P. (2004a). Diastolic left ventricular function in preterm infants with a patent ductus arteriosus: A serial doppler echocardiography study. *Early Hum Dev,* 76**,** 91-100.

Schmitz L, Stiller B, Pees C, Koch H, Xanthopoulos A & Lange P. (2004b). Doppler-derived parameters of diastolic left ventricular function in preterm infants with a birth weight <1500 g: Reference values and differences to term infants. *Early Hum Dev,* 76**,** 101-114.

Schmitz L, Xanthopoulos A, Koch H & Lange P E. (2004c). Doppler flow parameters of left ventricular filling in infants: How long does it take for the maturation of the diastolic function in a normal left ventricle to occur? *Pediatr Cardiol,* 25**,** 482-491.

Schubert U, Muller M, Norman M & Abdul-Khaliq H. (2013). Transition from fetal to neonatal life: Changes in cardiac function assessed by speckle-tracking echocardiography. *Early Hum Dev,* 89**,** 803-808.

Scrase E, Laverty A, Gavlak J C, Sonnappa S, Levett D Z, Martin D, et al. (2009). The young everest study: Effects of hypoxia at high altitude on cardiorespiratory function and general well-being in healthy children. *Arch Dis Child,* 94**,** 621-6.

Sehgal A, Mak W, Dunn M, Kelly E, Whyte H, McCrindle B, et al. (2010). Haemodynamic changes after delivery room surfactant administration to very low birth weight infants. *Arch Dis Child Fetal Neonatal Ed,* 95**,** F345-F351.

Serri K, Reant P, Lafitte M, Berhouet M, Le Bouffos V, Roudaut R, et al. (2006). Global and regional myocardial function quantification by two-dimensional strain: Application in hypertrophic cardiomyopathy. *J Am Coll Cardiol,* 47**,** 1175-1181.

Shimada S, Kasai T, Hoshi A, Murata A & Chida S. (2003). Cardiocirculatory effects of patent ductus arteriosus in extremely low-birth-weight infants with respiratory distress syndrome. *Pediatr Int,* 45**,** 255-62.

Sinkin R A, Cox C & Phelps D L. (1990). Predicting risk for bronchopulmonary dysplasia: Selection criteria for clinical trials. *Pediatrics,* 86**,** 728-36.

Sitaru A G, Holzhauer S, Speer C P, Singer D, Obergfell A, Walter U, et al. (2005). Neonatal platelets from cord blood and peripheral blood. *Platelets,* 16**,** 203-10.

Skinner J R, Boys R J, Hunter S & Hey E N. (1991). Non-invasive assessment of pulmonary arterial pressure in healthy neonates. *Arch Dis Child,* 66**,** 386-90.

Skinner J R, Boys R J, Hunter S & Hey E N. (1992). Pulmonary and systemic arterial pressure in hyaline membrane disease. *Arch Dis Child,* 67**,** 366-373.

Skinner J R, Stuart A G, O'Sullivan J, Heads A, Boys R J & Hunter S. (1993). Right heart pressure determination by doppler in infants with tricuspid regurgitation. *Arch Dis Child,* 69**,** 216-220.

Skjaerpe T & Hatle L. (1986). Noninvasive estimation of systolic pressure in the right ventricle in patients with tricuspid regurgitation. *Eur Heart J,* 7**,** 704-10.

Slinker B K & Glantz S A. (1986). End-systolic and end-diastolic ventricular interaction. *Am J Physiol,* 251**,** H1062-75.

Smith V C, Zupancic J A F, McCormick M C, Croen L A, Greene J, Escobar G J, et al. (2005). Trends in severe bronchopulmonary dysplasia rates between 1994 and 2002. *J Pediatr,* 146**,** 469-473.

Smolich J J, Walker A M, Campbell G R & Adamson T M. (1989). Left and right ventricular myocardial morphometry in fetal, neonatal, and adult sheep. *Am J Physiol Heart Circ Physiol,* 257**,** H1-H9.

Sohn D W, Chai I H, Lee D J, Kim H C, Kim H S, Oh B H, et al. (1997). Assessment of mitral annulus velocity by doppler tissue imaging in the evaluation of left ventricular diastolic function. *J Am Coll Cardiol,* 30**,** 474-480.

Speer C P. (2006). Inflammation and bronchopulmonary dysplasia: A continuing story. *Semin Fetal Neonatal Med,* 11**,** 354-62.

Stenmark K R & Abman S H. (2005). Lung vascular development: Implications for the pathogenesis of bronchopulmonary dysplasia. *Annu Rev Physiol,* 67**,** 623-661.

Stenmark K R, Orton E C, Reeves J T, Voelkel N F, Crouch E C, Parks W C, et al. (1988). Vascular remodeling in neonatal pulmonary hypertension. Role of the smooth muscle cell. *Chest,* 93**,** 127S-133S.

Stoelhorst G M, Rijken M, Martens S E, Brand R, den Ouden A L, Wit J M, et al. (2005). Changes in neonatology: Comparison of two cohorts of very preterm infants (gestational age <32 weeks): The project on preterm and small for gestational age infants 1983 and the leiden follow-up project on prematurity 1996-1997. *Pediatrics,* 115**,** 396-405.

Subhedar N V & Shaw N J. (2000). Changes in pulmonary arterial pressure in preterm infants with chronic lung disease. *Arch Dis Child Fetal Neonatal Ed,* 82**,** F243-247.

Sutherland G R, Di Salvo G, Claus P, D'Hooge J & Bijnens B. (2004). Strain and strain rate imaging: A new clinical approach to quantifying regional myocardial function. *J Am Soc Echocardiogr,* 17**,** 788-802.

Talbot N P, Balanos G M, Dorrington K L & Robbins P A. (2005). Two temporal components within the human pulmonary vascular response to approximately 2 h of isocapnic hypoxia. *J Appl Physiol,* 98**,** 1125-39.

te Pas A B, Davis P G, Hooper S B & Morley C J. (2008). From liquid to air: Breathing after birth. *J Pediatr,* 152**,** 607-11.

Teitel D F, Iwamoto H S & Rudolph A M. (1990). Changes in the pulmonary circulation during birth-related events. *Pediatr Res,* 27**,** 372-8.

Thebaud B & Abman S H. (2007). Bronchopulmonary dysplasia: Where have all the vessels gone? Roles of angiogenic growth factors in chronic lung disease. *Am J Respir Crit Care Med,* 175**,** 978-985.

Thomas J D & Popovic Z B. (2006). Assessment of left ventricular function by cardiac ultrasound. *J Am Coll Cardiol,* 48**,** 2012-25.

Thornburg K L & Morton M J. (1983). Filling and arterial pressures as determinants of rv stroke volume in the sheep fetus. *Am J Physiol,* 244**,** H656-63.

Thornburg K L & Morton M J. (1986). Filling and arterial pressures as determinants of left ventricular stroke volume in fetal lambs. *Am J Physiol,* 251**,** H961-8.

Toubas P L, Hof R P, Heymann M A & Rudolph A M. (1978). Effects of hypothermia and rewarming on the neonatal circulation. *Arch Fr Pediatr,* 35**,** 84-92.

Tremblay L, Valenza F, Ribeiro S P, Li J & Slutsky A S. (1997). Injurious ventilatory strategies increase cytokines and c-fos m-rna expression in an isolated rat lung model. *The Journal of Clinical Investigation,* 99**,** 944-952.

Trevisanuto D, Zaninotto M, Altinier S, Plebani M & Zanardo V. (2000). High serum cardiac troponin t concentrations in preterm infants with respiratory distress syndrome. *Acta Paediatr,* 89**,** 1134-1136.

van den Hoff M J, Kruithof B P, Moorman A F, Markwald R R & Wessels A. (2001). Formation of myocardium after the initial development of the linear heart tube. *Dev Biol,* 240**,** 61-76.

Ventolini G, Neiger R, Mathews L, Adragna N & Belcastro M. (2008). Incidence of respiratory disorders in neonates born between 34 and 36 weeks of gestation following exposure to antenatal corticosteroids between 24 and 34 weeks of gestation. *Am J Perinatol,* 25**,** 79-83.

Vulliémoz S, Stergiopulos N & Meuli R. (2002). Estimation of local aortic elastic properties with mri. *Magn Reson Med,* 47**,** 649-654.

Wagenaar G T M, ter Horst S A J, van Gastelen M A, Leijser L M, Mauad T, van der Velden P A, et al. (2004). Gene expression profile and histopathology of experimental bronchopulmonary dysplasia induced by prolonged oxidative stress. *Free Radic Biol Med,* 36**,** 782-801.

Walther F J, Benders M J & Leighton J O. (1992). Persistent pulmonary hypertension in premature neonates with severe respiratory distress syndrome. *Pediatrics,* 90**,** 899-904.

Walther F J, Benders M J & Leighton J O. (1993). Early changes in the neonatal circulatory transition. *J Pediatr,* 123**,** 625-632.

Walther F J, Siassi B, Ramadan N A, Ananda A K & Wu P Y. (1985). Pulsed doppler determinations of cardiac output in neonates: Normal standards for clinical use. *Pediatrics,* 76**,** 829-33.

Wei Y, Xu J, Xu T, Fan J & Tao S. (2009). Left ventricular systolic function of newborns with asphyxia evaluated by tissue doppler imaging. *Pediatr Cardiol,* 30**,** 741-746.

Weidemann F, Eyskens B, Jamal F, Mertens L, Kowalski M, D'Hooge J, et al. (2002). Quantification of regional left and right ventricular radial and longitudinal function in healthy children using ultrasound-based strain rate and strain imaging. *J Am Soc Echocardiogr,* 15**,** 20-28.

Winck J C, Drummond M, Almeida J & Marques J A. (2008). Air travel and hypoxaemia in real life. *Eur Respir J,* 32**,** 236-7.

Yaron M & Niermeyer S. (2008). Travel to high altitude with young children: An approach for clinicians. *High Alt Med Biol,* 9**,** 265-9.

Yock P G & Popp R L. (1984). Noninvasive estimation of right ventricular systolic pressure by doppler ultrasound in patients with tricuspid regurgitation. *Circulation,* 70**,** 657-62.

Young K C, Del Moral T, Claure N, Vanbuskirk S & Bancalari E. (2005). The association between early tracheal colonization and bronchopulmonary dysplasia. *J Perinatol,* 25**,** 403-7.

Yu S H & Possmayer F. (1990). Role of bovine pulmonary surfactant-associated proteins in the surface-active property of phospholipid mixtures. *Biochim Biophys Acta,* 1046**,** 233-41.

Zeitlin J, Draper E S, Kollée L, Milligan D, Boerch K, Agostino R, et al. (2008). Differences in rates and short-term outcome of live births before 32 weeks of gestation in europe in 2003: Results from the mosaic cohort. *Pediatrics,* 121**,** e936-e944.

Zeltner T B & Burri P H. (1987). The postnatal development and growth of the human lung. Ii. Morphology. *Respir Physiol,* 67**,** 269-82.

Zhao L, Mason N A, Morrell N W, Kojonazarov B, Sadykov A, Maripov A, et al. (2001). Sildenafil inhibits hypoxia-induced pulmonary hypertension. *Circulation,* 104**,** 424-428.

Appendices

Appendix A – Study protocols

A1.1 TDi study protocol

A1.2 TDi study echocardiogram acquisition protocol

A1.3 TDi Study analysis protocol

A2.1 MRI study protocol

A2.2 MRI study echocardiogram acquisition protocol

A2.3 MRI Study - MRI acquisition protocol

A1.1 TDi study protocol

Cardiff and Vale NHS Trust
Ymddiriedolaeth GIG Caerdydd a'r Fro

University Hospital of Wales
Ysbyty Athrofaol Cymru

1948-2008

Eich cyf/Your ref
Ein cyf/Our ref
Welsh Health Telephone Network 1872
Direct Line/Llinell uniongyrchol

Heath Park
Cardiff CF14 4XW
Phone (029) 2074 7747
Minicom (029) 2074 3632

Parc Y Mynydd Bychan,
Caerdydd CF14 4XW
Ffôn (029) 2074 7747
Minicom (029) 2074 3632

Tissue Doppler Assessment of Longitudinal Right and Left Ventricular Strain and Strain Rate in Term and Preterm Infants

Investigators: Dr S Joshi[1], Ms J Edwards[2], Dr AG Fraser[2], Dr DG Wilson[1], Dr O Uzun[1], Dr M Drayton[1] and Professor S Kotecha[1]
1. Department of Child Health, University Hospital of Wales, Cardiff University
2. Department of Cardiology, University Hospital of Wales, Cardiff University

Funded by: Departmental Funds

Start date: October 2007

Duration of Study: 4 years

Background:
Infants undergo significant haemodynamic changes during the transition from their foetal to neonatal life. During foetal life, less than 10% of flow from the right ventricle passes through the lungs. The pulmonary arterial wall is thick, the lumen is narrow and resistance to pulmonary vascular flow is high. Immediately after birth, the pulmonary vascular resistance falls and blood flow increases. Within the first few days of life, the ductus arteriosus closes and pulmonary blood flow increases further. As a result of these changes, the preload and the afterload of the left ventricle increase. In the right ventricle, as pulmonary hypertension is attenuated, the afterload of the right ventricle gradually decreases. Apart from these physiological changes, the contractility and the histological structure of the ventricular myocardium also changes after birth [Hislop 2005].

Failure of the natural postnatal adaptation of pulmonary vascular resistance and right ventricular haemodynamics may occur due to various perinatal conditions, including respiratory distress syndrome (RDS) or other hypoxic respiratory diseases which increase pulmonary arterial pressure. In an experiment with newborn lambs, RDS was shown to have resulted in a two-fold increase in pulmonary arterial pressure and significant increase in right ventricular systolic function to maintain cardiac output in the face of increased right ventricular afterload [De et al. 2001]. Ventricular function may also be altered in other neonatal disease processes such as sepsis, haemolytic disease, persistent pulmonary hypertension and transient tachypnoea of newborn. Furthermore, according to Barker Hypothesis, foetal under nutrition and disproportionate foetal growth also contributes to cardiovascular disease [Barker 1995]. Better understanding of left and right ventricular function and their natural adaptation to postnatal life is essential, in order to understand the contribution of retardation of normal myocardial development to haemodynamics instability or circulatory disease in the newborn. Therefore, there is a need for a good method to assess regional and global ventricular function in detail and also to assess markers of pulmonary arterial hypertension. This is vital for the logical management of these infants specially, for important clinical decisions such as appropriate use of inhaled nitric oxide which can act as a potent vasodilator and improve pulmonary haemodynamics and gas exchange in infants with pulmonary arterial hypertension. [Kinsela et al 2007]

Accurate methods to assess ventricular function in newborn infants are currently lacking. M-mode echocardiography is often used as a non-invasive measure of quantitative assessment of left ventricular function in the neonates. However, due to its irregular shape, quantitative evaluation of right ventricular function by M-mode is inaccurate. Assessment of the pulmonary arterial pressures by using either the tricuspid regurgitation or AT/ET ratio has limitations in clinical practice. In recent years, tissue Doppler imaging (TDI) is increasingly being utilized for the assessment of regional myocardial function and assessment of pulmonary arterial hypertension in adults [Rajdev et al. 2006]. TDI has also been used to evaluate myocardial tissue velocities in foetuses [Harada et al. 1999], preterm [Clark et al. 2004] and term neonates [Mori et al. 2004, Ekici F et al. 2007] and older children [Harada et al. 2000, Frommelt et al. 2002]. It has not yet been used to study subclinical myocardial dysfunction in neonates, or to investigate continuous relationship between arterial oxygen saturation and right ventricular function such as we have recently demonstrated in adults [Sabit et al. 2007]

Measurement of the magnitude of ventricular tissue deformation (strain) and the time course of this deformation (strain rate) is a novel, non invasive method of quantitative analysis of regional myocardial function, which has been described in adult populations [Marwick TH 2006]. Although measurement of strain and strain rate appears to be feasible in and reliable in neonates [Nestaas et al 2007] to detect local changes in both RV and LV, it has not been applied to relevant diseases of newborn infants e.g. respiratory distress syndrome, RDS.

The purpose of this study is to assess the left and right ventricular strain (S) and strain rate (SR) by tissue Doppler imaging, in healthy term infants and preterm infants and to compare these values with ventilated preterm infants with RDS and term infants who are born small for dates. We will test the hypothesis that neonates with RDS have impaired right and left ventricular function, compared with healthy term infants, and we will explore its relationship with gestational age and birth weight.

Aims:
Specific aim 1: To assess longitudinal right and left ventricular strain and strain rate in healthy, term newborn infants and in term infants who are small for dates.

Specific aim 2: To assess longitudinal right and left ventricular strain and strain rate in ventilated preterm infants with RDS and in preterm infants without RDS

Specific aim 3: To assess the relationship between the gestational age, birth weight and the myocardial function in newborn infants

Methodology:
Population:

Group1A: Full term newborn infants (≥ 37 complete weeks of gestational age) who are appropriate for dates
Group 1B: Full term newborn infants (≥ 37 complete weeks of gestational age) who are small for dates (birth weight <10th Centile)

Group 2A: Preterm infants (≤ 34 weeks of gestational age) without RDS
Group 2B: Preterm infants (≤ 34 weeks of gestational age) with RDS

Exclusion criteria:

Exclusion criteria:
1. Significant congenital heart disease but expected heart conditions called Patent Ductus Arteriosus (PDA) or Persistent Foramen Ovale (PFO) will not be excluded as these are normal early in newborn babies.
2. Lack of parental consent.
3. If the Consultant in charge of the baby thinks that the baby is not be suitable for the study due to any clinical or social reason.

Recruitment:
Groups 1A and 1B: Healthy newborn babies born on time with an appropriate birth weight of small for dates birth weight (SFD) will be invited to join the study from the Post-Natal Wards at the University Hospital of Wales. Gestational age of the infants will be re-confirmed by checking either the last day of the menstrual period (LMP) or estimated gestational age according to the 6-8 weeks ultrasound scan (USS). According to their birth weight, those infants who are appropriate for dates will be included in group 1A and those who are small for dates will be included in group 1B. Informed written consent will be obtained from the parents prior to the recruitment of the newborn infants.

Groups 2A and 2B: Preterm infants of less than or equal to 34 weeks of gestational age will be identified from the Neonatal Unit at the University Hospital of Wales. Infants who do not have clinical signs of lung disease, and hence do not require assistance with their breathing will be included in Group 2A and those who have clinical signs of lung disease, requiring assisted mechanical ventilation/breathing will be included in Group 2B. Informed written consent will be obtained from the parents prior to the recruitment of the newborn infants.

Prior to contacting the parents for the 3-6 weeks and 1 year follow up studies, we will first contact the infant's General Practitioner by letter or telephone to ensure suitability of the infant for the follow up studies.

Sample size and statistical analysis:
As there are no previous data on newborn infants, on which we could base our sample size, we are opting to study 100 infants in Group 1A and 50 infants in each of the groups 1B, 2A and 2B. We opted for this sample size as 50 Vs 100 will detect a shift of 0.5 SDs in any parameter at the conventional 5% alpha level with 80% power.

The infants will have the following series of echocardiograms:

Full term infants (Groups 1A and 1B)	1st scan: 1-3 days of age 2nd scan: 3-6 weeks of age 3rd scan: 1 year of age (± 1 month)
Preterm infants (Groups 2A and 2B)	1st scan: 1-3 days of age 2nd scan: 7-14 days of age 3rd scan: 3-6weeks of age and weekly until discharge Final scan: 1 year of age (± 1 month)

We will use 2-tailed non-parametric tests including Kruskal-Wallis and Mann-Whitney U tests to compare the multiple groups. $P<0.05$ will be considered significant.

Echocardiography methods:
Relevant antenatal and perinatal details will be obtained from the clinical notes of the mother and the baby. Baby's gestational age and birth weight will also be noted.

The initial scans will be done by either Dr S Joshi or Ms J Edwards, in either the Postnatal Ward or the Neonatal Unit. If the infant is discharged home before the second week of life, the infant will be invited to attend the Wales Heart Research Institute (WHRI), for the subsequent scans.

Initially, the infant will have cardiovascular examination and measurement of baseline heart rate as a part of routine post-natal check-up, followed by blood pressure, ECG, and oxygen saturation measurements.

The infant will then have a transthoracic echocardiographic study, to confirm normal cardiac anatomy and to exclude significant structural cardiac defects. If these are normal, then further studies will be performed to document global and regional right ventricular (RV) and left ventricular (LV) function (see below). Studies will be performed with a commercially available ultrasound scanner (GE Vivid 7) with neonatal transthoracic probes (7 MHz or 10 MHz). If the infant is unsettled during the echocardiogram, with

parental consent, we will use oral sucrose, which is routinely used as a pacifier for infants, during procedures in the Neonatal Unit.

Echocardiographic recordings will be obtained from conventional windows (sub-costal, apical, parasternal, and suprasternal) and 3-beat loops will be stored digitally for post-processing:

Tissue Doppler Imaging:

a) Global and regional **LV systolic function** will be assessed from end-diastolic and end-systolic volumes, ejection fraction, stroke volume, stroke distance / cardiac output, fractional shortening, mean long-axis excursion, myocardial velocities and deformation indices (strain and strain rate), and isovolumetric acceleration.

b) Global and regional **LV diastolic function** will be assessed from mitral filling velocities, E/A ratio, isovolumetric relaxation time, pulmonary venous flow, and myocardial tissue Doppler (including estimated filling pressure from the E/Ve ratio).

c) **RV function** will be measured from tricuspid annular excursion, fractional area change; RV free wall myocardial velocities and deformation indices; and tricuspid, pulmonary arterial and hepatic venous flow.

Acquisition and analysis of strain and strain rate:
Images will be acquired with the infant lying on the back. Standard apical views (apical 4 chamber, 2 chamber and apical long axis views) will be acquired using appropriate neonatal transthoracic transducer. Single walls, including high frame rate septal images will also be obtained.

The raw TDI data will be stored and analysed off line. Systolic strain (SS), diastolic strain (DS), systolic strain rate (SSR) and diastolic strain rate (DSR) will be displayed in a graphic format.

If any unexpected findings are noted in the echocardiogram, that may be relevant to the clinical care of the infant, this will be drawn to the attention of the Neonatal Consultant responsible for the infant's clinical care and the infant's GP. Dr Wilson, Paediatric Cardiologist, who is part of the research team, or his colleagues will assess any significant condition urgently.

Potential adverse effects:
Tissue Doppler imaging is a non-invasive method of echocardiography and we do not anticipate any adverse effect directly related to the imaging procedure. The principle of echocardiography is based on ultrasound waves and there is no radiation hazard involved in this imaging modality. Each heart scan will take approximately 15-20 minutes.

Importance of the study:
Assessment of right ventricular function in infants with respiratory distress syndrome, chronic lung disease of infancy and other hypoxic conditions leading to pulmonary hypertension would be extremely useful to direct therapy including the use of oxygen and pulmonary vasodilators such as nitric oxide. Use of tissue Doppler imaging to measure longitudinal right and left ventricular strain and strain rate is a promising method of non-invasive measurement of regional ventricular function that may be a useful diagnostic tool in the optimal management of infants with pulmonary hypertension.

References:

1. Abman SH, Wolfe RR, Accurso FJ, Koops BL, Bowman CM, Wiggins, JW Jr. Pulmonary vascular response to oxygen in infants with severe bronchopulmonary dysplasia. Pediatrics 1985; **75**:80-4
2. Abman SH. Monitoring cardiovascular function in infants with chronic lung disease of prematurity. Arch Dis Child 2002; 87:F15-F18
3. Barker DPJ. Fetal origins of coronary heart disease. BMJ 1995;311:171-174
4. Benatar A, Clarke J, Silverman M. Pulmonary hypertension in infants with chronic lung disease: non-invasive evaluation and short term effect of oxygen treatment. Arch Dis Child fetal Neonatal Ed. 1995 Jan; 72(1):F14-9
5. Clark SJ et al. Right ventricular volume measurements in ventilated preterm neonates. Paediatr Cardiol. 2004 Mar-Apr;25(2):149-53
6. De VM et al. Enhanced systolic function of the right ventricle during respiratory distress syndrome in newborn lambs. Am J physiol heart Circ Physiol. 2001 Jan;280(1):H392-400
7. Ekici F et al. Myocardial tissue velocities in neonates. Echocardiography 2007; 24(1): 61-7
8. Fraser AG et al. Feasibility and reproducibility of off-line tissue Doppler measurement of regional myocardial function during Dopamine stress echocardiography. Eur J Echocardiogr 2003;4(1):43-53
9. Frommelt PC et al. Usefulness of Doppler tissue imaging Analysis of Tricuspid annular motion for determination of right ventricular function in normal infants and children. The American Journal of Cardiology 2002 Mar; 89: 610-13
10. Harada k et al. Tissue Doppler imaging of left and right ventricles in normal children. Exp. Med. 2000;191:21-9
11. Haraka K et al. Tissue Doppler imaging in the normal fetus. *Int J Cardiol* 1999 Dec ; 71(3): 227-34
12. Hislop A. Developmental biology of the pulmonary circulation. Paediatric Respiratory Reviews 2005; 6:35-43
13. Kinsella J P et al. Inhaled nitric oxide in the premature newborn. J Pediatr 2007; 151: 10-5
14. Marwick TH. Measurement of strain and strain rate by echocardiography. Journal of American college of echocardiography 2006; 47 (7): 1313-27
15. Mori et al. Pulsed wave Doppler tissue echocardiography assessment of the long axis function of the right and left ventricles during the early neonatal period. Heart 2004; 90:175-80
16. Nestaas E et al. Feasibility and reliability of strain and strain rate measurement in neonates by optimizing the analysis parameters settings. Ultrasound in Med. & Biol.2007; 33: 270-278
17. Rajdev S et al. Tissue Doppler assessment of longitudinal right and left ventricular strain and strain rate in Pulmonary artery hypertension. Echocardiography 2006; 23(10):872-79
18. Sabit R et al. Sub-clinical left and right ventricular dysfunction in chronic obstructive pulmonary disease. [Circulation AHA, submitted for publication]

A1.2 TDi study echocardiogram acquisition protocol

Tissue Doppler Assessment of Longitudinal Right and Left Ventricular Strain and Strain Rate in Term and Preterm Infants
(Echo Acquisition Protocol)

A. Subcostal window

1. PWD of hepatic venous flow
2. 2D- IVC (sniff test)
3. CFD of atrial septum

B. Apical window

A4C

1. CFD of ventricular septum
2. PWD of MV flow (CFD)
3. CWD of TV flow (if TR is present in CFD)
4. PWD (TDI) of lateral tricuspid annulus
5. PWD (TDI) of lateral mitral annulus
6. PWD (TDI) of medial mitral annulus
7. A4C –2D
8. A4C – TD
9. TD – RV only
10. TD – LV only
11. TD – Septum only

A5C

12. PWD of LVOT (CFD)

C. Parasternal long axis window

1. Conventional 2D grey scale (for LVOT diameter)
2. CFD- AV
3. CFD of ventricular septum

D. Parasternal short axis window

1. PWD of PA (CFD)
2. PWD at RVOT (if PR is present)
3. PWD of LPA flow
4. PWD of RPA flow
5. PWD of PDA flow (if present)
6. CWD of TV (if TR is present in CFD)
7. 2 D grey scale- Mid- papillary level (CFD to r/o VSD)

Neonatal TDI Study- Data Analysis

Serial No: Patient ID: Gender:

DOB: Scan Date: Age at scan: Scan No:

Image	Measurement	Result	Image No
PLAX	LVOT diameter (d) cm		
	LVOT CSA (a) = πr^2 cm^2		
LVOT PWD	LVOT Peak velocity		
	Stroke distance (VTI) cm		
	Stroke Volume (SV) = a X VTI ml		
	Heart Rate (HR) /min		
	Cardiac output = SV X HR		
Length (cm)	Weight in Kg		
BSA = √Ht(cm)xWt(kg)/3600	Cardiac output ml/kg/min (CO)		
BSA =	Cardiac index (ml/kg/m^2)		
LVOT PWD	QRS to onset of aortic flow time interval (LV PEP) ms		
	LV ejection time (LVET) ms		
	****AV event timing****		
MV inflow PWD	Mitral E velocity (E) m/s		
	Mitral A velocity (A) m/s		
	E/A ratio (EAR)		
	****MV event timing****		
Real time mitral annular TD (Lateral)	Early diastolic velocity (LMA Ve') m/s		
Real time mitral annular TD (Medial)	Early diastolic velocity (MMA Ve') m/s		
Average early diastolic velocity	Ve' = (MMA Ve' + LMA Ve')/2		
	E/Ve'		
PV PWD (PSAX)	Heart rate (HR) / min		
RVOT	QRS to pulm flow time interval (RV PEP) ms		
	PA acceleration time (PA AT) ms		
	PA ejection time (PA ET) ms		
	AT : ET ratio		
PSAX	PR end diastolic velocity (m/s)		
	PR end diastolic pressure (mmHg)		
	PDA peak velocity (m/s)		
	PDA peak pressure (mmHg)		
TV inflow CWD	TR peak velocity (m/s)		
	TR peak pressure (mmHg)		

Image	Measurement	Result	Image No
LV (lateral wall) Tissue Doppler	Heart rate (HR) / min		
	Frame rate (FR) / sec		
	LV (LMA - TT) Displacement (LV Ds) mm		
	Peak systolic (s) velocity (LV Vsbl) cm/s		
	Early diastolic (e) velocity (LV Vebl) cm/s		
	Late diastolic (a) velocity (LV Vabl) cm/s		
SL= 6 mm	Strain- LV lateral mid wall (LV Ssal) %	End-systolic Post systolic PSSI	
	Strain Rate /s	Peak S Peak E Peak A	
	****PV event timing****		
RV Tissue Doppler	HR / min		
	FR / sec		
	RV (LTA – TT) Displacement (RV Ds) mm		
	Peak systolic (s) velocity (RV Vsbl) cm/s		
	Early diastolic (e) velocity (RV Vebl) cm/s		
	Late diastolic (a) velocity (RV Vabl) cm/s		
SL= 6 mm	Strain- RV lateral mid wall (RV Ssbl) %	End-systolic Post systolic PSSI	
	Strain Rate /s	Peak S Peak E Peak A	

Image	Measurement	Result	Image No
	****AV&MV event timing****		
Septum TD	HR / min		
	FR / sec		
	Septal (MMA – TT) Displacement (S Ds) mm		
	Peak systolic (s) velocity (S Vsbs) cm/s		
	Early diastolic (e) velocity (S Vebs) cm/s		
	Late diastolic (a) velocity (S Vabs) cm/s		

SL= 6 mm	Strain- Mid Septal (S Ssms) %	End-systolic Post systolic PSSI	
	Strain Rate /s	Peak S Peak E Peak A	

LV longitudinal function measurements	Longitudinal length of LV (apex to MV) cm (L_{LV})		
	LV Ds (cm) / L_{LV} x 100 (%)		
	S Ds (cm) / L_{LV} x 100 (%)		
RV longitudinal function measurements	Longitudinal length of RV (apex to TV) cm (L_{RV})		
	RV Ds (cm) / L_{RV} x 100 (%)		

Pulmonary and systemic haemodynamics in children born preterm: an MRI study

Serial No: **Participant ID:** **DOB:** **Date of study:**

** Neonatal history from case notes □**

General history □ (5-10min during echo/ECG)
Including:- Maternal history during pregnancy
Examination □
Baseline HR _____, BP_____, O2 sats_____ □
Weight _____(kg) and height_____(m) □

Calibrate all equipment and check resuscitation equipment □
Set predicted values to 'Paediatric' □

Checklist □
- Nose clip
- Mouthpiece between teeth
- Filter

1. Spirometry- Demonstration and Practice □ (5min)
→ Exhale to RV
→ Inhale to TLC
→ Breathe out fast and hard

Start.....
Finish.....

Rest for 2 minutes

Checklist □
- Nose clip
- Mouthpiece between teeth
- Filter

Spirometry □ (5min)
→ Inhale to TLC
→ Exhale quickly to RV and maintain flow for >6 secs
** Repeat at least 3 times **
- Calculate and display (F7)
- Save and exit (F12)

Start.....
Finish.....

Checklist □
- Ensure that the child doesn't have pacemaker or any other internal medical devise
-Empty pockets (e.g. mobile, keys phones, wallet/purse, coins etc.)
- Remove all metal objects (e.g. belts, earrings, piercing, rings etc)
-ECG leads (4)
-Chest coil
-Vicorder cuffs

Practice MRI + screening (30min)
Lie on the table with face mask and chest coil
Practice run

Start
Finish

PuSH Flowchart version 1.7 23rd Mar 2010

MRI Scan and Hypoxia challenge

Add 100% O2-if oxygen saturation drops < 85% for more than 30seconds
Add 100% O2- If oxygen saturation drops <80%
Add 100% O2- if oxygen saturation drops to 85% less than 30 seconds on 3 occasions.

Checklist □
- Ensure that the child doesn't have pacemaker or any other internal medical devise
-Empty pockets (e.g. mobile, keys phones, wallet/purse, coins etc.)
-Remove all metal objects (e.g. belts, earrings, piercing, rings etc)
-ECG leads (4)
-Chest coil
-Vicorder cuffs

ECG & Echocardiography (15-20min)
– check for normal cardiac structure and function and to assess pulmonary arterial pressure

Start
Finish

Baseline MRI (in room air) (20-25min)
Localising scans – sagittal, oblique-sagittal, MPA X-section (1-2cm above PV)

Start
Finish

12% oxygen inhalation
O2 sats and (HR) at
5 min…….....10 min.....……
15 min……..20 min.....……
25 min……...30 min…….....
35 min…….....40 min……
Occasions when oxygen saturation dropped <85%
Sats (%) duration (min) time

Max HR during hypoxia -

12% oxygen inhalation for 20 minutes □
(20L/min - increase if rebreathing CO2)

Start

Flow rate:

Checklist
- Holes on either sides of the mask are closed
- Bag remains inflated throughout

MRI during hypoxia (12% oxygen)
MPA X-section (1-2cm above PV)
(20-25min)

Finish

Checklist □
- Nose clip
- Mouthpiece between teeth
- Filter

Spirometry (right after hypoxia, in mock scanner) □
→ Inhale to TLC
→ Exhale quickly to RV and maintain flow for >6 secs
** Repeat at least 3 times **
- Calculate and display (F7)
- Save and exit (F12) (5min)

Start.....
Finish.....

Procedural time – 125min
Time in scanner – 60-70min
Preparation time for scanning – 15-20 min
Time in CUBRIC – 160-180min

Study complete

PuSH Flowchart version 1.7 23rd Mar 2010

A2.2 MRI study echocardiogram acquisition protocol

Pulmonary and Systemic Haemodynamics in Children born Preterm: an MRI Study (PuSH MRI)
(Echo Acquisition Protocol)

Assessment for cardiac structure and raised pulmonary arterial pressure

A. Subcostal view
   1. Assess situs – position of aorta and IVC in relation to vertebra
   2. Sniff test on IVC – to approximate CVP / RA pressure

B. Subcostal 4 chamber view
   1. Look for ASD and VSD using colour flow Doppler (CFD)

C. Parasternal long axis view
   1. Look for VSD using CFD

D. Parasternal short axis view
   1. Assess aortic and mitral valves
   2. Assess PA flow velocity using pulsed wave Doppler (PWD)
   3. Look for PR using PWD
   4. Look for TR using continuous wave Doppler (CWD)

E. Apical 4 (and 5) chamber view
   1. Look for VSD using CFD
   2. Look for TR jet using CWD
   3. Assess LVOT flow velocity using PWD

F. Suprasternal view
   1. Assess the arch of aorta – CFD (turbulence) and PWD (velocity) at descending aorta

A2.3 MRI Study - MRI acquisition protocol

Pulmonary and Systemic Haemodynamics in Children born Preterm: an MRI Study (PuSH MRI)
(MRI Acquisition Protocol)

Baseline scan

	Scanning sequence
1	3 plane localiser
2	Asset calibration
3	Shimming with localisation with shallow breathing
4	Scan along the main pulmonary artery – to identify pulmonary valve (PV)
5	Cross sectional image of PA (perpendicular to 4) 1-2cm above PV FIESTA cine of PA (Venc depends on PA flow velocity from echo, default 90cm/s) - Sequence to be determined / calculated - Preferably 10-12ms between images

Following hypoxic challenge (after 20 minute of 12% O2)

	Scanning sequence
1	3 plane localiser
2	Asset calibration
3	Shimming with localisation with shallow breathing
4	Scan along the main pulmonary artery – to identify pulmonary valve (PV)
5	Cross sectional image of PA (perpendicular to 4) 1-2cm above PV FIESTA cine of PA (Venc depends on PA flow velocity from echo, default 90cm/s) - Sequence to be determined / calculated - Preferably 10-12ms between images

Appendix B – History proforma

B1.1 TDi study history proforma

B2.1 MRI study history proforma

Tissue Doppler Assessment of Longitudinal Right and Left Ventricular Strain and Strain Rate in Term and Preterm Infants

History and General Examination: Proforma **Date:**

Participant ID: [study (N= Neonatal), group, serial number, name initials, visit e.g. N1A01SJ1]

Visit: 1 2 3 4

Study group: Circle as appropriate
1A: Full term newborn infants (≥ 37 complete weeks of gestational age) who are appropriate for dates (≥ 10th Centile)
1B: Full term small for dates (birth weight <10th Centile) infants
2A: Preterm infants (≤ 34 weeks of gestational age) without RDS
2B: Preterm infants (≤ 34 weeks of gestational age) with RDS

Demographics:

Date of birth: Date of Discharge:
Gender:
Age in days:
Current Gestational age in weeks:
Multiple birth: Yes / No Twin 1 2 Triplet 1 2 3

Nutritional History:

Current weight ……..…kg ……..Centile
Current length ……..cm ……..Centile
Current OFC ……cm ……..Centile

Current Feeding:

Feeding route PN /oral/ tube
Fluid volume available for feeding.....ml/kg

Type of milk breast/ formula/ mixed feeding
If mixed feeding roughly what percentage of breast milk/ breast feeds …….
Type of formula.....

Supplementation of milk Yes/No
Supplement used ..... dose.....

Vitamin supplements given Yes/No
Duration ....Days Dose.....

Gastroesophageal reflux disease Yes / No
Treatment for GORD Medical Yes / No Surgical Yes / No

Tissue Doppler Assessment of Longitudinal Right and Left Ventricular Strain and Strain Rate in Term and Preterm Infants

Respiratory system:

Spontaneously breathing Yes/ No
Assisted ventilation Yes/ No
CPAP Days…….. Maximum PEEP……
SIMV/ SIPPV Days…….. Maximum PIP……
HFOV Days…….. Maximum delta P…… Maximum MAP……..

Supplemental oxygen Yes/ No Days so far…… Maximum FiO2……

Dexamethasone Yes/ No

Airleak Yes/ No

Cardiovascular system:

Oxygen saturation (%) ……
Heart rate ……
Blood pressure Current…… Lowest so far……
Ionotropic support Yes/ No
Dopamine……
Dobutamine……
Hydrocortisone……
Heart murmur Yes/ No
Normal femoral pulses Yes/ No

Gastrointestinal system:

Necrotising enterocolitis Yes/ No
Medical management Yes/ No
Surgical management Yes/ No

Neonatal sepsis Yes/ No

Positive culture 1…… Source……
Positive culture 2…… Source……
Positive culture 3…… Source……

Cranial USS
IVH Yes / No Worst grade …….

Was sucrose used for echocardiography ? Yes / No

History and General Examination: Proforma **Date:**

Participant ID: [study (PUSH), serial number e.g. PUSH01]
Serial Number:
Visit: CUBRIC □ Date:

Group: (circle as appropriate)

A. Children who were born prematurely at ≤ 32 weeks of gestational age and who had oxygen dependency beyond 36 weeks of corrected gestational age
B. Children who were born prematurely at ≤ 32 weeks of gestational age but did not have oxygen dependency beyond 36 weeks of corrected gestational age
C. Age and gender matched healthy control children who were born at full term (37 complete weeks or more)

Demographics

Date of birth:
Age in years:
Gender: M/ F
Height in cm …….. Centile …….
Weight in kg …… Centile …….
Multiple birth Yes/ No Twin 1 2 Triplet 1 2 3

History

Birth and Neonatal History: (Hospital case notes)

Maternal smoking during pregnancy Y/N How many:
Gestational age at birth in weeks…….
Antenatal steroids Y/ N
Surfactant Y/ N

Assisted ventilation Y/ N
Total duration of assisted ventilation …….days
SIMV/ SIPPV…….days
HFOV……days
CPAP……..days

Duration of oxygen dependency:
Corrected gestational age ……. weeks
Days of life ……days
Maximum FiO2 at any stage after birth……..

Respiratory status at 36 weeks of corrected gestational age:
Maximum FiO2 Room air □ < 30% □ >30% □
Ventilatory status Spontaneous □ CPAP □ SIMV/SIPPV/ HFOV □

Respiratory status at 28 days of life:
Maximum FiO2 Room air □ < 30% □ >30% □
Ventilatory status Spontaneous □ CPAP □ SIMV/SIPPV/HFOV □

Air leaks Y/ N
Postnatal steroids Y/ N

Neonatal sepsis Y/ N
Positive culture 1…….. Source……
Positive culture 2…… Source……
Positive culture 2…… Source……

High risk for GBS infection Y/ N
Prolonged rupture of membrane Y*/ N (*duration in hours……)
Intrapartum fever (>37.5 degrees) Y/ N
GBS isolated in high vaginal swab Y*/ N (*date……)
Previous child with GBS Y/ N
Intrapartum antibiotics for GBS Y/ N

Persistent pulmonary hypertension of newborn (PPHN) Y/ N
Treatment 1…….. 2…… 3……

Intraventricular haemorrhage Y/ N
Worst grade…….
Grade at discharge……

Family History: (first- degree relatives)

Cigarette smoking Y/ N Not sure
Asthma Y/ N Not sure
Eczema Y/ N Not sure
Hay fever Y/ N Not sure
Sudden death Y*/ N * ……age in years

Medical history:

Asthma Has the child ever been diagnosed with Asthma? Y*/ N Not sure
*Age at diagnosis……..
*Last episode of asthmatic attack requiring treatment……years of age
*Last episode of asthmatic attack requiring hospital admission…..years of age

Wheeze H/O wheeze at any time since birth Y*/ N Not sure
*First episode of wheeze at ……..years of age
*Last episode of wheeze at……years of age
*Number of attacks of wheezing in the past 1 year ……..
*Number of attacks requiring 'rescue inhaler' in the past 1 year…….
*Number of attacks requiring hospital admission in the past 1 year …….
*Exercise induced wheeze in the past 1 year Y/ N Not sure
*Dry cough at night (not cold/flu associated) in the past 1 year Y/ N Not sure

Rhinitis H/O hay fever at any time since birth Y/ N Not sure
H/O a problem with sneezing, or a runny, or a blocked nose without having cold or the flu At any time since birth Y/ N Not sure
In the past 1 year Y/ N Not sure

Eczema H/O eczema at any time since birth Y/ N Not sure
H/O itchy rash at any time in the past 1 year Y*/ N Not sure
* Itchy rash affecting the folds of the elbow, behind the knees, in front of the ankles, under the buttocks, or around the neck, ears or eyes Y/ N Not sure

Exercise Periods of activity at school (longer than 30 minutes) i.e. walking to school, break time, lunchtime, PE (mean periods per day)……
After school, in the evenings or at weekends does the child play sport/or participate in any activities (e.g. dancing) Y/N
If yes, estimate of how many hours a week does he/she do this sport/activity for? ……hours
How does the child consider his/ her daily activity compared to friends or siblings?
More active □ Less active □ Same as friends/ siblings □

Cardiac H/O structural congenital heart disease Y*/ N Not sure
Diagnosis ……..
Surgical correction Y/ N Not sure
Medical treatment Y/ N Not sure

H/O cardiac disease any time since birth (not structural defect) Y*N Not sure
*Diagnosis ……
Medical treatment Y/ N Not sure
Surgical treatment Y/ N Not sure
Cardiology follow-up in the last 1 year Y/ N Not sure

Symptoms in the past 1 year
Chest pain requiring medical attention Y*/ N * At rest/ exercise
Breathlessness requiring medical attention Y*/N * At rest/ exercise
Palpitation requiring medical attention Y*/ N * At rest/ exercise
Snoring Y/ N
Undue tiredness Y/ N
Fainting episodes Y/ N

H/O treatment with oxygen in the past 1 year for any reason Y*/ N Not sure
*Diagnosis……
Regular medication Y/N (details if yes)……
Any ongoing medical problem Y/ N (details if yes)……
Number of hospital admissions since birth ……

<u>Nutritional History:</u>

Birth weight ……Kg ……C
OFC at birth……cm ……C

Weight at discharge ……Kg ……C
OFC at discharge ……cm ……C

Weight at 36 weeks of corrected gestational age ……Kg ……C
OFC at 36 weeks of corrected gestational age ……cm ……C

Feeding at birth Breast*/ formula/ mixed fed *Duration of breast feeding……..weeks
Weight at 6 weeks of age ……Kg ……..C
Mother's height ……m Father's height ……m
Child's estimated adult height ……m ……C
Has the child ever been a fussy eater? Y/ N
Has the child ever struggled with lumpy food? Y/ N
?? Food diary

Clinical signs and baseline observations:

Pallor Y/ N
Clubbing Y/ N
Cyanosis Y/ N
Ankle oedema Y/ N

Respiratory rate at rest ……../min
Heart rate at rest ……../ min

Shape of the chest Normal/ Abnormal ……
Subcostal/ intercostal recessions Y/ N
Harrison's sulcus Y/ N
Wheeze Y/ N
Breath sounds
Equal Y/ N* *……
Vesicular Y/ N* *……
Added sounds Y*/ N *Crepitations □ Ronchi □

Pulse rate ……. / min
Regular Y/ N* *Details if irregular ……
Heart sounds S1……. S2……. S3 …….
Murmur Y*/ N *Details if yes……..
Left parasternal heave Y/ N

Ascites Y/ N
Palpable hepatomegaly Y/ N

Blood pressure measurement at rest1: Blood pressure measurement 2:
Oxygen saturation in room air at rest:
ECG Normal/Abnormal (details if abnormal)……..

Appendix C – Invitation letter to parents

C1.1 TDi study invitation letter to parents

C2.1 MRI study invitation letter to parents

C1.1 TDi study invitation letter to parents

School of Medicine
Department of Child Health

Professor Sailesh Kotecha
Professor of Child Health and Head of Department

Ysgol Meddygaeth
Adran Iechyd Plant

Yr Athro Sailesh Kotecha
Athro Iechyd Plant a Phennaeth Adran

1883-2008 125 YEARS BLYNEDD

CARDIFF UNIVERSITY
PRIFYSGOL CAERDYDD

Cardiff University
School of Medicine
Heath Park
Cardiff CF14 4XN
Tel *Ffon* +44(0)29 2074 3375
Fax *Ffacs* +44(0)29 2074 4283
Prifysgol Caerdydd
Ysgol Meddygaeth
Mynydd Bychan
Caerdydd CF14 4XN

Dear Parent/Guardian

Re: Tissue Doppler Assessment of Longitudinal Right and Left Ventricular Strain and Strain Rate in Term and Preterm Infants (Neo- TDI)

Thank you for participating in the above study at Cardiff University. We are writing to invite [Name] for the 3-6 week/1 year [delete as necessary] follow-up scan at the Wales Heart Research Institute (WHRI). We have enclosed directions to the WHRI.

We would be most grateful if you could fill in the enclosed slip and send it in the enclosed envelope to let us know if you are or are not able to attend the WHRI with your baby [Name] for the follow-up scan. Alternatively, please let us know by telephone or email. If the arranged date or time is not suitable for you, please contact us at the following address and we will re-arrange the appointment for a more convenient time for you.

Please do not hesitate to contact us if there are any questions that you may have regarding the study.

We would very much like to thank you for participating in our study.

Yours sincerely,

Dr Kevin Poon
Clinical Fellow
Cardiff University
Heath Park
Cardiff, CF14 4XN
02920743438
pooncy@cardiff.ac.uk.

C2.1 MRI study invitation letter to parents

NHS WALES GIG CYMRU
1948-2008

Cardiff and Vale NHS Trust
Ymddiriedolaeth GIG Caerdydd a'r Fro

University Hospital of Wales
Ysbyty Athrofaol Cymru

Eich cyf/Your ref
Ein cyf/Our ref
Welsh Health Telephone Network 1872
Direct Line/Llinell uniongyrchol

Heath Park
Cardiff CF14 4XW
Phone (029) 2074 7747
Minicom (029) 2074 3632

Parc Y Mynydd Bychan,
Caerdydd CF14 4XW
Ffôn (029) 2074 7747
Minicom (029) 2074 3632

Parent / Guardian of
(Name and address)

18/01/2010

Dear Parent/Guardian

Re: Pulmonary and Systemic Haemodynamics in Children born Preterm: an MRI Study

I am writing because ……..was on the baby unit after he/she was born. I hope he/she is keeping well. We are keen to learn more about how our ex-neonatal unit babies do as they grow up so we can improve our care in the future. I would like to invite …….to join the above study at Cardiff University. We have enclosed information leaflets which give more details of the study.

The study will involve spending one morning or afternoon at the 'Cardiff University Brain Research Imaging Centre', Park Place, Cardiff. We would be most grateful if you could fill in the enclosed slip and send it in the enclosed envelope to let us know if you are or are not able to join our study. If there are any questions that we may answer before you can make a decision, please contact Dr Kevin Poon on 029 20 74 8965 or email us on pooncy@cardiff.ac.uk.

We would very much like to thank you for taking time to consider our study.

Yours sincerely,

Dr Mark Drayton
Consultant Neonatologist
University Hospital of Wales
Heath Park
Cardiff, CF14 4XN

Letter to parents Version 1.1 15th May 2009

Appendix D – Information leaflet for parents

D1.1 TDi study - information leaflet for parents of ventilated preterm infants

D1.2 TDi study - information leaflet for parents of non-ventilated preterm infants

D1.3 TDi study - information leaflet for parents of term born infants

(D1.2 and D1.3 were provided separately to parents of the preterm and term control groups respectively and contain similar information as D1.1)

D2.1 MRI study – information leaflet for parents of children born preterm with CLD

D2.2 MRI study – information leaflet for parents of children born preterm without CLD

D2.3 MRI study – information leaflet for parents of healthy children born at term

(D2.2 and D2.3 were provided separately to parents of the preterm and term control groups respectively and contain similar information as D2.1)

Cardiff and Vale NHS Trust
Ymddiriedolaeth GIG Caerdydd a'r Fro

University Hospital of Wales
Ysbyty Athrofaol Cymru

1948-2008

Eich cyf/Your ref
Ein cyf/Our ref
Welsh Health Telephone Network 1872
Direct Line/Llinell uniongyrchol

Heath Park
Cardiff CF14 4XW
Phone (029) 2074 7747
Minicom (029) 2074 3632

Parc Y Mynydd Bychan,
Caerdydd CF14 4XW
Ffôn (029) 2074 7747
Minicom (029) 2074 3632

Parent Information Leaflet – Ventilated Preterm

Tissue Doppler Assessment of Longitudinal Right and Left Ventricular Strain and Strain Rate in Term and Preterm Infants or Neo-TDI

Principal investigator: Professor Sailesh Kotecha
Department of Child Health
Cardiff University
Cardiff, CF14 4XN

Dear Parents

We would like to invite your baby to take part in our research study at the University Hospital of Wales, Cardiff University. Before you decide whether or not you wish your baby to participate in the study, it is important for you to understand why the research is being done and what it involves. Please take time to read the following information and please feel free to ask any questions that you may have. Thank you for reading this leaflet.

1. **What is the purpose of the study?**
   When babies are born, there are lots of important changes that take place in the way their heart work. It is important that these changes occur for the heart and the lungs to work effectively. In some babies, who are born early or those who are small or sick, these natural changes may not occur. In these situations, it is important to know how well their heart is working in order to make appropriate decisions in the treatment of these babies. At present, we do not have a good tool to assess heart function in detail in newborn babies.

   In this study, we wish to use a new method of scanning the heart by ultrasound to assess how different parts of the heart muscles work in babies born on time or babies born prematurely and how they change during the first year of life. We will also use the tool in babies born on time with a lower than expected birth weight and in premature babies with lung disease needing breathing machines to help their breathing.

2. **Why has my baby been invited?**
   Your baby has been invited to participate in this study because he/she was born prematurely and has breathing problems that sometimes occur in babies born before their due date.

3. **What does it involve?**
   To study the function of your baby's heart, we will do a series of heart scans which are similar to the scans that you had during your pregnancy. This involves applying jelly (same as the gel used during antenatal scans) on your baby's chest and recording pictures of different parts of your baby's heart. We will also check your baby's blood pressure, oxygen levels (with a probe on the wrist or hand) and heart tracing (ECG) before we do the scans.

If the baby is unsettled during the scan, with your permission, we shall give your baby about half a tea spoonful of sucrose (sugar). Sucrose is a liquid form of sugar that is often used in babies to pacify them during medical procedures. We will not use it if the baby stays calm during the scans or if you would not like us to give sucrose to your baby.

We would like to do the following series of scans:
1st scan: within the first 3 days of your baby's birth
2nd scan: between 7-14 days of age
3rd scan: between 3-6 weeks of age

Thereafter, only if your baby is still in the hospital, we will repeat the scan every week until your baby is discharged from the hospital.

As most babies are discharged from hospital after the first few days of age, we would like to invite your baby to the Wales Heart Research Institute (WHRI) at the Heath between 3-6 weeks of age and again at about 1 year of age for further scans. This will help us understand how the heart function changes during the first year of life.

With your consent, we would also like to access maternal or baby's medical records to note important events during pregnancy and birth e.g., expected date of delivery (to calculate gestational age), history of infection, time of rupture of membrane, pregnancy related complications, etc. None of the personal or identifiable maternal details will be noted.

4. **What are the possible benefits of taking part?**
   We do not anticipate any direct benefits or any abnormalities for your baby but in the unlikely event of any unusual finding, we shall inform the doctors looking after your baby and shall arrange for the baby to be seen quickly.

5. **Is my baby likely to experience any discomfort or distress during this study?**
   We do not anticipate any distress to the baby due to the heart scan.

6. **What if my child is harmed by the study?**
   Medical research is covered for mishaps in the same way as for patients undergoing treatment in the NHS i.e. compensation is only available if negligence occurs.

7. **Will information obtained in the study be confidential?**
   Any identifiable information about your child will be handled in confidence. No identifiable information will be used in the presentation or the publication of the results of this study.

8. **Will I receive out of pocket expenses for taking part in the study?**
   We will reimburse any travelling expenses that you may incur by bringing your baby to the hospital for this study.

9. **What happens if I do not wish my child to participate in the study or wish to withdraw from the study?**
   If you do not wish your child to participate in this study or if you wish to withdraw your child from the study you may do so without justifying your decision and your child's future treatment will not be affected.

10. **Who is funding the study?**
    This study is being funded by the Department of Child Health, Cardiff University.

11. **Who has reviewed the study?**
    This project has been reviewed by the South East Wales Research Ethics Committee.

Thank you for taking the time to read this information leaflet. Please feel free to ask us any questions that you may have or if you would like more information about this study.

Dr Suchita Joshi
Walport Academic Clinical Fellow
Department of Child Health
Cardiff University
Joshis3@cardiff.ac.uk
02920743438

Prof Sailesh Kotecha
Professor of Paediatrics and Child Health
Cardiff University
kotechas@cardiff.ac.uk
02920744187

Cardiff and Vale NHS Trust
Ymddiriedolaeth GIG Caerdydd a'r Fro

University Hospital of Wales
Ysbyty Athrofaol Cymru

1948-2008

Eich cyf/Your ref
Ein cyf/Our ref
Welsh Health Telephone Network 1872
Direct Line/Llinell uniongyrchol

Heath Park
Cardiff CF14 4XW
Phone (029) 2074 7747
Minicom (029) 2074 3632

Parc Y Mynydd Bychan,
Caerdydd CF14 4XW
Ffôn (029) 2074 7747
Minicom (029) 2074 3632

Information Sheet for Parents (Group A)
(For parents of preterm children who had lung disease in infancy)

'Pulmonary and Systemic Haemodynamics in Children born Preterm: an MRI Study'

Principal investigator: Professor Sailesh Kotecha
Department of Child Health
Cardiff University
Cardiff, CF14 4XN

Dear Parent/Guardian

We would like to invite to take part in our research study at Cardiff University. This study will be done in collaboration with the Cardiff University Brain Research Imaging Centre (CUBRIC). Before you and your child decide, whether or not to participate in the study, it is important for you to understand why this research is being done and what it involves. Please take time to read the following information carefully and feel free to ask any questions that you may have.

1. What is the purpose of the study?

Many babies who are born prematurely may develop breathing problems at birth. Some of these babies may develop lung disease called chronic lung disease of prematurity or CLD. The majority of children who had CLD as a baby go on to participate in play, exercise and other activities without having any problems. It is unknown if the lungs continue to behave normally as the children grow up.

We are trying to find out how the blood vessels that connects the heart to the lungs (pulmonary artery) and to the rest of the body (aorta) in these children react if they breathe air containing less oxygen than natural air, as happens when travelling an aeroplane or when climbing a mountain or skiing in high altitude ski resorts.

We will compare the results from children **A)** who were born early and had CLD, with results from **B)** those who were born early but did not develop any lung disease, and **C)** those who were born at full term without any lung disease. A total of 90 children will take part in this study.

2. Why has my child been invited?

We have invited your child to participate in this study because he/she was born early and had lung disease of infancy as a baby **(Group A)**.

3. Does my child have to take part?

No. It is up to you and your child to decide. Your child does not have to take part in this research if either you or your child does not wish to do so. We will describe the study and go through this information sheet, which we will then give to you. Your child will also be given his/her own information sheet. You and your child will have the opportunity to discuss any questions that you may have with the researcher after you have read the information sheets.

We will then ask you to sign a consent form if you agree for your child to take part in this research. Your child will also be asked to sign an assent form to show that he/she is happy to take part.

4. What will happen to my child if he/she takes part?

We would like to invite your child to the **"MRI Suite" in CUBRIC, Cardiff University, Park Place, Cardiff** for about two to three hours. You will be able to stay with your child at all times including when the scan is being performed. **Your child should not to drink tea, coffee, cola or any drinks containing caffeine at least 3 hours before the study.** We would like to collect a urine sample from your child after arrival to CUBRIC to check your child's exposure to other people's cigarette smoking. (We will discard the urine sample after this test and will not perform any DNA testing from the urine sample.)

We will ask you some questions regarding your child's birth details, relevant medical history and family history and record your child's height, weight, blood pressure and oxygen levels with a probe on a finger. We will test how fit his/her lungs are with the 'breathing and blowing' tests (spirometry). We will demonstrate the test to your child and let him/her practice it until he/she understands how to do the tests.

We will also do a standard blood pressure measurement on his/her upper arm using an inflatable cuff and scan the arteries in the wrist and neck using an ultrasound machine to estimate his/her blood pressure in the artery that delivers blood to the whole body called the aorta. We will then proceed to do an ultrasound of the heart to check if your child's heart has formed correctly and is working fine.

Because MRI uses a very strong magnet, you and your child will first be asked safety questions to make sure that your child does not have anything in their body that might be affected by the scans, such as a pacemaker, cochlear implants and other implanted devices, or metal in your child's body. Your child will be asked to remove all metal objects including keys, coins, jewellery, piercing, belt and watches. It might be best for your child to bring a change of clothes, or come in loose but warm clothes with no metal fixings – sweatshirt and jogging pants are ideal. We have a private changing room. Your child's valuables can be locked away securely if necessary.

The scanner consists of a large magnet with a tunnel, and your child will be asked to lie within the tunnel. A coil will be placed around your child's chest to scan the heart and lungs. An MRI machine does not use radiation like an x-ray or CT scanner and we are not aware of any risks to your child.

We will do a practice run so your child can get used to the scanning process and get used to the noise of the scanner. He or she will be able to watch a DVD to keep them occupied and to help keep them still during the scanning process.

Once your child is comfortable with the scanner surroundings and procedures, we will proceed to the MRI scanner room for the scan of the heart and lungs. The Research Team will be able to talk to your child and you via an intercom. Your child will be given an alarm bulb so that he/she can call us during the scan for any reason including if he/she does not wish to continue. You will be able to see the Research Team through the control room window at all times.

We will first perform a scan whilst your child is breathing air but will monitor his oxygen and carbon-dioxide (waste gas) levels. We will then ask your child to breathe 12% oxygen for 20 minutes whilst lying still in the scanner. The air we breathe is about 21% oxygen, the cabin in a long distance aeroplane is about 15% and skiing in highest mountains in Europe is about 12%. We will repeat the MRI scan to see if any changes in blood flow and vessel sizes with the decrease in oxygen. Each scan will take about 15 – 20 minutes.

At all times we will monitor your child closely to ensure that he/she is comfortable and will stop the scan if he/she is distressed in any way. We will also monitor his/her oxygen and carbon-dioxide levels at all times.

5. Can I stay with my child during the tests?

You will be able to stay with your child at all times. We will also ask you safety questions about being in the scanning room and ask you to remove any metal objects that you may have including ear-rings and any other jewellery.

6. How long will the different tests take?

We expect the study to take 2½ to 3 hours at CUBRIC, Cardiff University, Park Place, Cardiff. Approximately 30 minutes will be needed for taking a medical history and for the blowing (lung function) test, approximately 45 minutes for measuring the blood pressure (standard and using ultrasound), ultrasound of the heart and doing the practice MRI scanner run and about an hour to do the MRI scans.

7. Have similar studies been done in the past?

Often a low oxygen (15%) test is performed for 20 minutes in babies with lung disease who have recently come off their oxygen if they are likely to travel in an aeroplane to ensure that their oxygen levels do not drop when they fly. The scanning of the heart arteries by using an MRI scanner is new but has been applied to adult patients with lung and heart diseases without any problems reported.

8. What are the possible benefits of taking part?

This study may help identify whether children who are born early and had lung disease of infancy are more likely to have lung and heart disease earlier in adulthood and therefore benefit with early monitoring and treatment.

The MRI scans done in this study are designed to look at the blood vessels from the heart to the lungs and body only; not to diagnose other heart or lung disorders. Although it is unlikely that we will find any abnormalities, if we do then we shall explain the findings to you and ask Dr Wilson, children's heart specialist, or Dr Doull, children's lung specialist to see your child to go through the findings in detail.

9. Is my child likely to experience any discomfort or distress during this study?

The concentration of oxygen that will be used in this study is similar to that found in high altitude ski resorts (12% oxygen) and we do not anticipate any serious side effects. Some children may temporarily breathe faster, similar to rates after exercise in the playground. Oxygen levels using a finger probe will be monitored at all times and the study will be discontinued if your child is unable to tolerate the tests or feels any discomfort or distress by breathing reduced oxygen level. The study will also be stopped if your child's oxygen level drops below 80% for more than 30 seconds or if it drops less than 80% for periods of less than 30 seconds on three or more occasions. We will have provisions for high oxygen (100%) should your child need it.

Some children may dislike the tunnel in the MRI scanner but most are comfortable especially as they will be distracted by watching a DVD whilst in the scanner. The practice run is to get used to the MRI scanner and we can help relax your child as much as we can. If he/she becomes distressed at any time we shall stop the study.

In very rare cases, some people have reported a 'tickling' sensation in their back or shoulders or hands. This may be slightly uncomfortable, but will not be painful, and is not in any way harmful. If your child does not like this feeling then we will stop the scan. The radiofrequency waves we use to create the MR scans can cause your child's head and body to warm up slightly. Usually this is not noticed but again if he is uncomfortable, we will stop the scan.

The magnetic field changes make an electric current flow through the body. Usually this is not felt but if two parts of the body are touching, e.g. crossing legs or arms then very rarely a burn can occur. We will ask your child to lie with their arms by their sides, and their legs uncrossed to stop this from happening.

10. What if my child is harmed by the study?

Medical research is covered for mishaps in the same way as for patients undergoing treatment in the NHS i.e. compensation is only available if negligence occurs.

11. Will information obtained in the study be confidential?

There will be no identifiable details of your child in any study information. All information about your child will be handled in confidence.

12. Will I or my child receive out of pocket expenses for taking part in the study?

We will provide any travelling expenses that you may incur. Your child will also receive two cinema vouchers as a 'thank you' for helping us with the project.

13. What happens if my child or I do not wish to participate in the study or wish to withdraw from the study?

If your child or you do not wish to participate in this study or if you wish to withdraw from the study you may do so without justifying your decision and your child's future treatment will not be affected.

14. Will my child's taking part in this study be kept confidential?

Yes. We will follow ethical and legal practice and all information about your child will be handled in confidence. With your permission, your GP will be informed of your child's participation in this study. None of your child's identifiable details will be stored or used in any publication or presentation in future.

15. Who is funding the study?

We are using departmental funds to fund the study.

16. Who has reviewed the study?

Before any research goes ahead it has to be reviewed by Research Ethics Committee. This project has been reviewed by the South East Wales Research Ethics Committee.

Thank you for reading this. Please feel free to ask us if there is anything that is not clear or if you would like more information about this study.

Dr Chuen Yeow Poon
Research Fellow
Cardiff University
pooncy@cardiff.ac.uk
Tel: 02920 748965

Prof Sailesh Kotecha
Professor of Child Heath
Cardiff University
kotechas@cardiff.ac.uk

Appendix E – Information sheet for children

E1.1 MRI study - information leaflet for children born preterm with CLD

E1.2 MRI study - information leaflet for children born preterm without CLD

E1.3 MRI study - information leaflet for well children born at term

(E1.2 and E1.3 were provided separately to parents of the preterm and term control groups respectively and contain similar information as D1.1)

Cardiff and Vale NHS Trust
Ymddiriedolaeth GIG Caerdydd a'r Fro

University Hospital of Wales
Ysbyty Athrofaol Cymru

1948-2008

Eich cyf/Your ref
Ein cyf/Our ref
Welsh Health Telephone Network 1872
Direct Line/Llinell uniongyrchol

Heath Park
Cardiff CF14 4XW
Phone (029) 2074 7747
Minicom (029) 2074 3632

Parc Y Mynydd Bychan,
Caerdydd CF14 4XW
Ffôn (029) 2074 7747
Minicom (029) 2074 3632

Information Sheet for Children – Group A
(For children who were born early and needed oxygen for a long time as babies)

'Pulmonary and Systemic Haemodynamics in Children born Preterm: an MRI Study'

Dear ,

We would like to invite you to take part in a research project on children who were born early. We would like to study children like you who were born earlier than expected and needed oxygen to help you breathe for a long time after you were born. Before you decide if you would like to take part, it's important that you understand why the research is being done and what you will be asked to do if you take part.

Please read this leaflet carefully with your mum or dad (or ask them to read it to you) and talk about it with them. If you do not understand anything or if you have any questions please let us know and we will try to answer them for you.

1. What is research?

Research is a way we try to find out the answers to questions.

2. Why is this project being done?

Some babies are born earlier than they should. Some of these babies need oxygen for a long time to help them breathe until their lungs are strong. In this research, we want to find out how the heart's blood vessels behave if they breathe oxygen which is less than in air – similar oxygen levels to the highest mountains in Europe.

To find out the answers to these questions, we will need to do different tests on children who were born early and compare the test results with children who were born on time.

This project will help us understand if children who were born early and needed oxygen for a long time as babies develop like children who were born on time when they grow up.

3. Why have I been asked to take part?

You have been asked to take part in this research because you were born early and you needed oxygen to help you breathe when you were a baby (Group A).

4. Did anyone else check the study is OK to do?

Before any research is allowed to happen, it has to be checked by a group of people called Research Ethics Committee (REC). They make sure that the research is fair. This project has been checked by South East Wales REC.

5. Do I have to take part?

No. It is up to you. You don't have to take part if you don't want to.

If you do, we will ask you to sign a form to say that you are happy to take part in this project. **You can ask the study to be stopped at any time if you do not wish to continue**. You do not have to give us any reason.

6. What will happen to me if I take part?

If you take part in this research, you will be asked to spend about 2 to3 hours with us at the Cardiff University Brain Research Imaging Centre (CUBRIC) at Cardiff University, Park Place, Cardiff for breathing test and heart scans. **Your mum or dad will stay with you throughout the tests.** On the morning of the test, **we will ask you not to drink any tea, coffee or cola for three hours before the scan.**

We will do following different tests to check how strong your heart has to work to pump blood to your lungs.

Arrive in the morning with your mum or dad
↓
We will ask you to provide a urine sample for us in a small bottle
↓
Your mum or dad will be asked some questions about you when you were young
↓

We will measure your height, weight, blood pressure and oxygen level and listen to your chest and heart. We will also do a special test using special gel and a machine to detect the pulse wave in your wrist and neck.

↓

After this, we will ask you to lie on a bed to relax while we do a heart scan. For this, we will put special gel on your chest and take pictures of your heart. You will be able to see how the inside of your heart looks like on a TV screen. This will take about 15 minutes. This will not cause you any pain or discomfort.

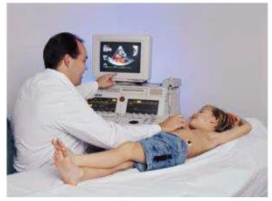

↓

We will then show you how to do some special breathing and blowing tests called spirometry. You can then practice the tests to make sure you understand what to do. Once you are sure that you have understood how to do the special breathing and blowing tests, we will do the tests.

↓

We will then show you the practice MRI scanner and ask you some questions to make sure you do not bring any metals with you into the scanning room. We will ask you to practice holding your breath to help get good scans.

↓

We will put some stickers and a pad on your chest. We will also put a band around your neck and another on your leg to measure blood pressure.

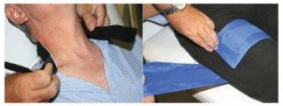

↓

We will then lay you on the table and practice having the scan with all equipments on you. You will have earplugs on as the machine makes noisy sounds. We will help you put on a mask over your nose and mouth as this will be used in the real scan to give you oxygen.

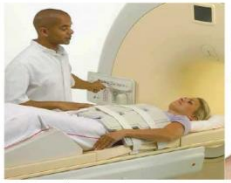

↓

Once you are happy and comfortable being in the scanner, we will go into the real scanner in another room. There will be a screen where you can watch your favourite DVD while lying inside the scanner. We will then ask you to lie comfortably on table and try to stay still for the scan. We will then take pictures of your heart. This will take about 15 minutes and should not cause you any pain or discomfort.

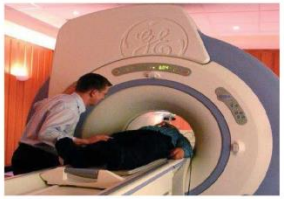

↓

After this scan, we will help you put on a mask over your nose and mouth. You will breathe lower level of oxygen for 20 minutes. This may make you breathe faster as if you have been running in a playground. The scan will be repeated. **If you feel uncomfortable and do not wish to continue we will stop the scan at any time.**

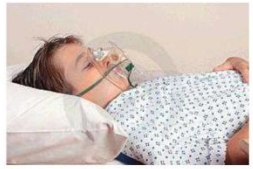

↓

Study is finished and you can go home

7. Might anything about the research upset me?

When you breathe lower level of oxygen, you may breathe faster as if you have been running in the playground. During this test, we will keep a very close eye on you and make sure you are fine. We will stop the scan if you feel uncomfortable.

The scanner is like a tunnel which sometimes may feel too small. If you feel uncomfortable we will stop the test. You can watch DVD to help you relax in the scanner.

8. Will joining in help me?

No. The study will not help you but the information we get might help us look after children who were born too early and who needed oxygen for a long time as babies.

9. What happens when the research stops?

We will write to your parents/ guardians to let them know the results of this research.

10. What if something goes wrong?

We do not expect anything to go wrong during this project and we will not ask you to do anything that maybe harmful to you. We will also keep a close eye on you throughout the tests and will stop the test immediately if we need to or if you want us to.

11. Will anyone else know I'm doing this?

With your mum or dad's permission, we will let your doctor (GP) know that you are taking part in this project. Apart from your GP and the research team, nobody else will have to know that you are taking part in this project.

12. What will happen to the urine samples that I give?

Once we have tested the urine sample, we will throw it away in a special hospital bin.

13. Who is organising and paying for this research?

This research is being organised by the Children's Department at Cardiff University.

14. What if I don't want to do the research anymore?

If at any time you don't want to do the research anymore, just tell us or your mum or dad and you can stop taking part. You do not have to continue if you do not want to do so.

Thank you for reading this leaflet and I hope I can meet you. If you do not understand anything that this leaflet says or if you have any questions for us, please ask your mum or dad to contact me and I will try to answer your questions.

Dr Chuen Yeow Poon (Kevin)
Department of Child Health
Cardiff University
02920748965
pooncy@cardiff.ac.uk

Appendix F – Consent form for parents

F1.1 TDi study consent form for parents

F2.1 MRI study consent form for parents

F1.1 TDi study consent form for parents

NHS WALES GIG CYMRU

Cardiff and Vale NHS Trust | Ymddiriedolaeth GIG Caerdydd a'r Fro

University Hospital of Wales
Ysbyty Athrofaol Cymru

1948-2008

Eich cyf/Your ref
Ein cyf/Our ref
Welsh Health Telephone Network 1872
Direct Line/Llinell uniongyrchol

Heath Park
Cardiff CF14 4XW
Phone (029) 2074 7747
Minicom (029) 2074 3632

Parc Y Mynydd Bychan,
Caerdydd CF14 4XW
Ffôn (029) 2074 7747
Minicom (029) 2074 3632

Patient label and identification number for this study.

CONSENT FORM

Title of Project: Tissue Doppler Assessment of Longitudinal Right and Left Ventricular Strain and Strain Rate in Term and Preterm Infants (Neo- TDI)

Name of the researchers: Professor S Kotecha, Dr A Fraser, Dr S Joshi and Ms J Edwards, Department of Child Health and Cardiology, Cardiff University.

Please initial box

1. I confirm that I have read and understand the information sheet dated 20th September 2007 (Version 3.0) for the above study. I have had the opportunity to consider the information, ask questions and have had these answered satisfactorily. ☐
2. I understand that my baby's participation is voluntary and that I am free to withdraw my baby from the study at any time, without giving any reason, without my baby's medical care or legal rights being affected. ☐
3. I understand that relevant sections of my or my baby's medical records and data collected during the study, maybe looked at by responsible individuals from Cardiff University, from regulatory authorities or from the NHS Trust, where it is relevant to my baby's taking part in this research. I give permission for these individuals to have access to my or my baby's medical records. [This section needs to be signed by the participant's mother] ☐
4. I agree to my baby's GP being informed of my baby's participation in the above study. ☐
5. I agree to my baby having ultrasound scans of the heart as the part of the above study. ☐
6. I agree to my baby having sucrose if the baby is not settled during the heart scans. ☐
7. I agree to being contacted in future for the follow up scans for my baby as a part of the above study. ☐

Name of the Parent	Date	Signature
Researcher	Date	Signature

Consent form Version 2.0 30th July 2007 (Neo-TDI)

F2.1 MRI study consent form for parents

NHS WALES GIG CYMRU

1948-2008

Eich cyf/Your ref
Ein cyf/Our ref
Welsh Health Telephone Network 1872
Direct Line/Llinell uniongyrchol

Cardiff and Vale NHS Trust
Ymddiriedolaeth GIG Caerdydd a'r Fro

University Hospital of Wales
Ysbyty Athrofaol Cymru

Heath Park
Cardiff CF14 4XW
Phone (029) 2074 7747
Minicom (029) 2074 3632

Parc Y Mynydd Bychan,
Caerdydd CF14 4XW
Ffôn (029) 2074 7747
Minicom (029) 2074 3632

Patient Identification Number for this study:

CONSENT FORM (Version 1.2 28th June 2009)

Title of Project: Pulmonary and Systemic Haemodynamics in Children born Preterm: an MRI Study

Name of the Researchers: Professor S Kotecha, Dr CY Poon

		Please initial box
1	I confirm that I have read and understand the information sheet dated 28th June 2009 (version 1.3) for the above study. I have had the opportunity to consider the information, ask questions and have had these answered satisfactorily.	☐
2	I understand that my child's participation is voluntary and that my child is free to withdraw at any time, without giving any reason, without my child's medical care or legal rights being affected.	☐
3	I understand that relevant sections of any of my child's medical notes and data collected during the study may be looked at by responsible individuals from Cardiff University, from regulatory authorities or from the NHS Trust, where it is relevant to my child's taking part in this research. I give permission for these individuals to have access to my child's records.	☐
4	I agree to my child's GP being informed of my child's participation in the study.	☐
5	I agree to my child having the lung function test (spirometry) as a part of the above study.	☐
6	I agree to my child having ultrasound scan on the arteries in the wrist and neck as part of the above study.	☐
7	I agree to my child having ultrasound scan of the heart as part of the above study.	☐
8	I agree to my child having MRI scans of the heart and lung as a part of the above study.	☐
9	I agree to my child having urine test as a part of the above study.	☐

Name of Parent	Date	Signature
Researcher	Date	Signature

Appendix G – Assent form for children

G1.1 MRI study assent form for children

G1.1 MRI study assent form for children

NHS WALES GIG CYMRU

Cardiff and Vale NHS Trust
Ymddiriedolaeth GIG Caerdydd a'r Fro

University Hospital of Wales
Ysbyty Athrofaol Cymru

1948-2008

Eich cyf/Your ref
Ein cyf/Our ref
Welsh Health Telephone Network 1872
Direct Line/Llinell uniongyrchol

Heath Park
Cardiff CF14 4XW
Phone (029) 2074 7747
Minicom (029) 2074 3632

Parc Y Mynydd Bychan,
Caerdydd CF14 4XW
Ffôn (029) 2074 7747
Minicom (029) 2074 3632

ASSENT FORM FOR CHILDREN

(To be completed by the child in presence of their parent/ guardian)

Project title: Pulmonary and Systemic Haemodynamics in Children born Preterm: an MRI Study

Child (or if unable, parents on their behalf) to circle all they agree with:

1.	Have you read (or had it read to you) about this project? (Child Information Sheet Group A Version 1.3 28th June 2009 or Child Information Sheet Group B Version 1.3 28th June 2009 or Child Information Sheet Group C Version 1.3 28th June 2009)	Yes/ No
2.	Has somebody else explained this project to you?	Yes/ No
3.	Do you understand what this project is about?	Yes/No
4.	Have you asked all the questions you want?	Yes/ No
5.	Have you had your questions answered in a way you understand?	Yes/ No
6.	Do you understand it is OK to stop taking part at any time?	Yes/ No
7.	Are you happy to take part?	Yes/ No
8.	Are you happy to have breathing and blowing tests as a part of this project?	Yes/ No
9.	Are you happy to have a scan on your wrist and neck as a part of this project?	Yes/ No
10.	Are you happy to have a heart scan (cold gel on your chest) as part of this project?	Yes/ No
11.	Are you happy to have MRI scan of the heart and lung as a part of this project?	Yes/ No
12.	Are you happy to have urine test as a part of this project?	Yes/ No

If any of the answers 1-11 are 'No' or you don't want to take part, don't sign your name!

If you do want to take part, you can write your name below:

Your name _____ Date _____

The doctor who explained this project to you needs to sign too:

Print name _____ Date _____

Sign _____

Thank you for your help.

Assent Form for Children Version 1.2 28th June 2009

Appendix H – Published papers

H1 Optimisation of myocardial deformation imaging in term and preterm infants

H2 Long term cardiovascular consequences of chronic lung disease of prematurity

H3 Assessment of pulmonary artery pulse wave velocity in children: an MRI pilot study

European Journal of Echocardiography (2011) **12**, 247–254
doi:10.1093/ejechocard/jeq192

Optimization of myocardial deformation imaging in term and preterm infants

Chuen Y. Poon[1], Julie M. Edwards[2], Suchita Joshi[1], Sailesh Kotecha[1], and Alan G. Fraser[2]*

[1]Department of Child Health, School of Medicine, Cardiff University, Cardiff, UK; and [2]Wales Heart Research Institute, School of Medicine, Cardiff University, Cardiff CF14 4XN, UK

Received 27 October 2010; accepted after revision 23 December 2010; online publish-ahead-of-print 21 January 2011

Aims Myocardial deformation imaging is now used to assess regional ventricular function in infants but their small size presents particular technical challenges. We therefore investigated the determinants of reproducibility of myocardial longitudinal strain (ε) in term and preterm infants, in order to determine optimal technical settings.

Methods and results Repeated longitudinal ε measurements of the mid-segments of the septum, and the left and right ventricular free walls, were performed using five different computation distances (CDs; also called strain length) in 20 infants. The coefficients of variation (CV) were calculated for each CD. Overall, ε measurements were most reproducible with a CD of 6 mm (CV 11.7%). In preterm infants (<34 weeks gestation; mean ± SD diastolic LV length, 20.3 ± 3.5 mm), ε measurements were most reproducible with CD of 6 mm (CV 7.2%); in term infants (>37 weeks gestation; mean ± SD diastolic LV length, 29.6 ± 3.0 mm), ε measurements were most reproducible with CD of 10 mm (CV 13.2%). The reproducibility of measuring ε increased with higher frame rates, from CV of 17.3% at frame rates <180 per s to 11.7% for frame rates >180 per s and 9.6% for rates >248 per s.

Conclusion In newborn infants, tissue Doppler loops should be acquired at frame rates above 180 per s. Myocardial deformation analysis of preterm infants should be performed using a CD of 6 mm, whereas a CD of 10 mm is more reproducible in term infants.

Keywords Infants • Preterm • Tissue Doppler • Myocardial velocity imaging • Strain length • Strain

Introduction

Myocardial velocity imaging (MVI) is now established as a tool for quantifying regional myocardial function in adults. The technique has been validated and established in children, infants, and neonates.[1–6] Reference values of parameters measured using MVI in healthy children and neonates have been published.[7–9] MVI has also been used to assess regional myocardial function in different neonatal conditions.[10,11] It has been proven to be both feasible and reproducible in preterm infants,[12] thus permitting the assessment and monitoring of regional myocardial function which can be affected by various respiratory and congenital cardiac conditions prevalent in this population.

MVI allows the measurements of velocities at any point in the ventricular wall during the cardiac cycle. Myocardial strain (ε), a measure of local contractile function, is a one-dimensional measurement of relative deformation of myocardial fibres. Strain rate is the rate by which deformation occurs and this is derived from the instantaneous velocity gradient between adjacent points of the myocardium. The instantaneous data on deformation (or ε) are then obtained by integrating the strain rate curve with time.[13]

The distance between two adjacent points used to calculate the velocity gradient is known as the computation distance (CD). A shorter CD is associated with greater noise since the gradient is estimated from fewer velocities. Regional ε is the average ε from all the points within a sample area or the region of interest (ROI). A larger ROI will include more points within that area to be averaged. Therefore, a longer CD and a larger ROI will give a better signal-to-noise ratio, hence a more consistent ε estimation.

There are only two published studies on the technical aspects of offline tissue Doppler deformation analysis in the neonatal population.[14,15] Nestaas *et al.*[14] recommended the ROI size of 1 mm long by 3 mm wide with a strain length (or CD) of 10 mm in a two-segment ε analysis of the term neonatal population. Pena *et al.*,[5] who used a computation length of 6 mm, suggested measuring ε in the middle segment of each wall as an initial screening parameter of local systolic function in the neonatal population, but no data are available for preterm infants.

The inter-observer reproducibility of myocardial deformation imaging in the neonatal population is 30%[12] compared with 10–15% in children[7] and adults.[16] This would need to be improved considerably if it was to be used in the clinical setting. However, the size of the heart in this population presents additional technical challenges in the acquisition and analysis of myocardial deformation images.

The aim of the study was to establish the parameters that improve the reproducibility of measuring ε in both term and preterm infants.

* Corresponding author. Tel: +44 29 2074 3489, Fax: +44 29 2074 3500, Email: fraserag@cardiff.ac.uk

Table 1 Subject demographics, heart rate, frame rate, and ventricular chamber lengths

Variable	Group A (term infants)	Group B (preterm infants without RDS)	Group C (preterm infants with RDS)	*P*-value
Number of infants	7	7	6	
Gestational age (week)	40.04 ± 0.83	33.02 ± 0.57	26.98 ± 2.65	$P^{\S} = <0.001^{*,+,\#}$
Birth weight (kg)	3.67 ± 0.31	1.87 ± 0.23	1.06 ± 0.37	$P^{\ddagger} = <0.001^{*}, 0.001^{+}, 0.005^{\#}$
Heart rate (b.p.m.)	120 ± 10	113 ± 24	144 ± 11	$P^{\S} = 0.703^{*}, 0.046^{+}, 0.009^{\#}$
Frame rate (frames/s)	201 ± 56	219 ± 53	256 ± 72	$P^{\ddagger} = 0.097^{*}, 0.022^{+}, 0.073^{\#}$
Ventricular length (mm)				
LV at systole	21.7 ± 2.3	16.7 ± 1.8	13.2 ± 2.5	$P^{\S} = <0.001^{*,+}, 0.025^{\#}$
LV at diastole	29.6 ± 3.0	22.8 ± 2.1	17.5 ± 2.4	$P^{\S} = <0.001^{*,+}, 0.004^{\#}$
RV at systole	20.3 ± 2.5	13.9 ± 2.2	12.4 ± 2.3	$P^{\S} = <0.001^{*,+}, 0.467^{\#}$
RV at diastole	27.5 ± 2.7	19.3 ± 1.8	16.3 ± 2.5	$P^{\S} = <0.001^{*,+}, 0.082^{\#}$

Data expressed as numbers or as mean ± standard deviation.
RDS, respiratory distress syndrome; LV, left ventricle; RV, right ventricle.
[‡]Denotes ANOVA test and [§]denotes Mann–Whitney *U*-test.
*A vs. B; [+]A vs. C; [#]B vs. C.

Methods

Population

Out of 108 sets of digitally stored echocardiographic images from a myocardial function study, 20 recent sets of images [recorded in 7 healthy term infants (Group A), 7 preterm infants without respiratory distress syndrome (Group B), and 6 preterm infants with respiratory distress syndrome (Group C)] were studied. Details of the infants are given in *Table 1*. The study was approved by the local research ethics committee, and written informed consent was obtained from parents.

All infants were scanned within 72 h after birth. The infants were screened for congenital cardiac defects and excluded from the study if there was any abnormality other than patent ductus arteriosus or patent foramen ovale.

Echocardiographic protocol

Images were obtained from infants in a supine or left lateral position using a standard commercial ultrasound machine (Vivid 7, GE Vingmed Ultrasound AS, Horten, Norway) with a 10 MHz or a 7.0 MHz transducer, by a single operator (J.M.E.).

Pulsed Doppler recordings of flow in the left ventricular outflow tract (LVOT) and the proximal pulmonary trunk were acquired from apical four-chamber and parasternal short-axis views, and used to determine the timing of the opening and closure of the aortic and pulmonary valves. Ventricular chamber lengths were measured from the apical four-chamber image.

Colour tissue Doppler images of the left ventricle (LV), right ventricle (RV), and septum were acquired separately using the apical four-chamber view. The sector width and depth of each image were adjusted to obtain for the highest frame rate possible with the optimum Nyquist limit to avoid aliasing. All images were stored as three-beat loops on magneto-optical disks for post-processing.

Offline analysis

Images were analysed using the commercial EchoPac software (GE Vingmed Ultrasound EchoPac 7.00, Horten, Norway) by the same operator (C.Y.P.). The heart rates and frame rates of each loop were recorded. The LV and RV chamber lengths in end-diastole and end-systole were measured from the midpoint of each atrioventricular junction (between the lateral mitral or tricuspid annulus and the septum) to the apex of the left or right ventricular cavity, respectively.

Myocardial ε was measured in the middle segment of the LV and RV free walls and the septum (*Figure 1*). Maximal negative ε during systole was measured, using the timings of opening and closure of the aortic and pulmonary valves. All parameters were measured in three beats and averaged, unless the signal from an individual beat was too noisy, in which case only two beats were averaged. Linear drift compensation and the default 40 ms Gaussian smoothing were used for all ε analyses.

Maximal end-systolic ε was analysed using five different CDs (also called strain length) (2, 4, 6, 8, and 10 mm) with the same ROI size (10 × 5 mm), in two ways. First, the stored loop from each subject was analysed by positioning the ROI within the middle segments of the septum, LV and RV free walls, at sites that gave similar strain waveforms for each beat. This process was performed for all subjects, using the same CD for all walls, and then repeated in all subjects using the other CDs; the order in which the CDs were tested was determined randomly. In the second method, a CD of 10 mm was used while

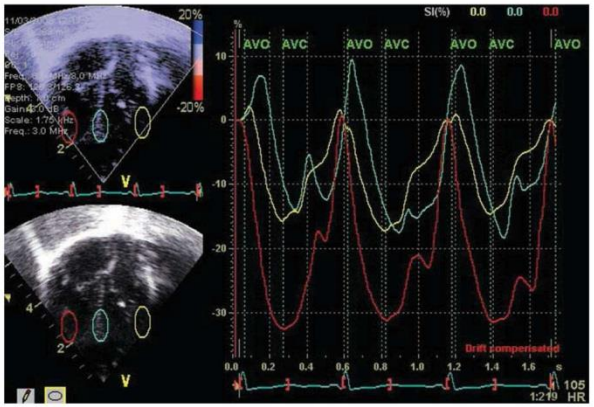

Figure 1 Comparison of longitudinal strain in midwall sites. Position of the ROI in the middle segments of each wall displaying the ε curves of each wall. Note the heterogeneity in the ε between the walls.

selecting the position within the middle segment of the RV free wall that gave the least noisy strain curve. The maximal ε for this CD was determined. Without changing the ROI position, the CD was then reduced to 8, 6, 4, and 2 mm and the maximal end-systolic longitudinal ε for the different CDs were documented. The same process was repeated separately on the LV free wall and septal wall. These methods were used in all subjects, twice, at an interval of 2 weeks.

Statistical analysis

Data were analysed using SPSS version 16.0 (SPSS Inc, Chicako, IL, USA). Values are presented as mean ± 2 SD. The Shapiro–Wilk test was used to test the normality of the measured parameters. Measurements between groups were compared by one-way ANOVA for normally distributed parameters and Tukey HSD was used for *post hoc* multiple comparison. For parameters that were not normally distributed, measurements between the groups were compared by the Mann–Whitney *U*-test.

Two sets of longitudinal ε measurements on 20 sets of images were obtained on all three walls using five different CD by each method. The two methods were analysed separately. For each method, the mean ε, standard deviation (SD), and coefficients of variation (CV, in %) were calculated for each CD. The CV was calculated using the formula: CV = (SD/arithmetic mean of measurements) × 100, where SD is the standard deviation of the differences between the two sets of measurements.

The CD with the smallest CV represents the highest reproducibility between measurements. The influences of other parameters such as frame rate, birth weight, and heart size (measured as ventricular length) on the reproducibility of measurements were also analysed by one-way ANOVA, where the means between groups were compared.

Results

As expected, infants who were born at an earlier gestational age weighed less at birth and had smaller hearts (*Table 1*). With increasing prematurity, there was a trend for the echocardiographic colour tissue Doppler loops to be recorded at higher frame rates, but the number of frames per heart beat was relatively constant (Group A 100 frames/beat, Group B 116 frames/beat, and Group C 107 frames/beat).

A total of 59 segments (20 RV free wall, 20 LV free wall, and 19 septum) were analysed, excluding only the septum in one infant in Group C. Measurements of these segments were averaged from three successive beats except for 7/59 (11.9%) (3 LV free wall and 4 septum).

Systolic ε was highest in the RV free wall, followed by the LV and then the septum, in all 20 infants. Longitudinal ε increased proportionally with the size of the infants: the average ε values for Group A (mean birth weight 3.7 kg), Group B (1.9 kg), and Group C (1.1 kg) were −23.5 ± 5.6%, −20.4 ± 7.4%, and −14.4 ± 5.8%, respectively, at CD of 6 mm (*Table 2*).

Using the first method (resampling the colour tissue Doppler loop for each measurement, to optimize each trace), the CD that gave the lowest CV was 6 mm (CV 11.7%). The least reproducible CD was 2 mm (CV 18.3%). Using the second method (when the ε measurements were done by reducing the CD without altering the position of the ROI within each wall, and without resampling the colour tissue Doppler loop), the differences in CV were minimal from CD of 2–10 mm (13.7 and 12.6%, respectively) (see Supplementary data online, *Table S1*). Further analyses were done using data obtained by the first method as this is a more realistic test of repeated measurements in clinical practice.

Table 2 Reproducibility of longitudinal systolic strain with each computation distance resampled within each wall

Computation distance	RV		LV		Septum		Combined (LV, RV, septum)	
	Mean ε ± SD (%)	CV (%)	Mean ε ± SD (%)	CV (%)	Mean ε ± SD (%)	CV (%)	Mean ε ± SD (%)	CV (%)
All groups								
2 mm	−21.4 ± 6.3	10.9	−21.1 ± 9.6	22.5	−18.7 ± 6.7	15.7	−20.4 ± 7.7	18.3
4 mm	−22.2 ± 5.8	8.8	−19.8 ± 8.5	19.3	−18.6 ± 7.0	11.7	−20.2 ± 7.2	14.0
6 mm	−21.6 ± 5.3	9.8	−19.3 ± 9.1	15.1	−18.3 ± 6.8	6.3	−19.6 ± 7.2	11.7
8 mm	−21.7 ± 5.4	8.8	−18.4 ± 8.6	16.5	−17.9 ± 6.3	14.5	−19.3 ± 7.0	13.8
10 mm	−21.1 ± 5.3	10.7	−17.0 ± 7.7	13.6	−17.4 ± 6.2	12	−18.5 ± 6.6	12.9
Group A (term infants)								
2 mm	−25.3 ± 6.8	12.2	−26.7 ± 11.6	22.8	−22.5 ± 5.9	11.4	−24.8 ± 8.2	20.0
4 mm	−25.8 ± 5.5	11.5	−24.6 ± 6.7	25.4	−22.9 ± 5.5	6.3	−24.4 ± 5.8	17.1
6 mm	−24.5 ± 5.2	12.8	−23.9 ± 6.8	19.5	−22.0 ± 5.3	7.4	−23.5 ± 5.6	14.8
8 mm	−25.2 ± 5.3	11.3	−23.4 ± 6.1	16.7	−21.6 ± 4.8	12.2	−23.4 ± 5.4	14.2
10 mm	−24.7 ± 5.3	12.0	−22.8 ± 5.5	15.0	−21.3 ± 5.1	8.4	−22.9 ± 5.3	13.2
Group B (preterm infants without RDS)								
2 mm	−21.0 ± 5.3	9.8	−21.4 ± 6.1	20.7	−19.2 ± 6.7	20.7	−20.5 ± 5.8	17.5
4 mm	−21.8 ± 4.6	3.2	−21.1 ± 9.0	8.2	−18.8 ± 7.3	17.7	−20.6 ± 6.9	10.5
6 mm	−21.4 ± 4.7	5.0	−20.7 ± 10.1	9.7	−19.0 ± 7.3	4.8	−20.4 ± 7.4	8.2
8 mm	−21.1 ± 4.4	6.2	−19.5 ± 9.1	16.3	−18.1 ± 6.8	19.6	−19.5 ± 6.8	15.6
10 mm	−20.6 ± 5.3	9.1	−16.9 ± 6.6	11.2	−17.4 ± 6.6	17.3	−18.3 ± 5.8	13.6
Group C (preterm infants with RDS)								
2 mm	−17.3 ± 4.5	10.4	−14.2 ± 6.6	5.6	−12.6 ± 3.5	17.0	−14.8 ± 5.2	11.2
4 mm	−18.3 ± 5.3	8.4	−12.8 ± 5.9	4.6	−12.5 ± 4.1	8.3	−14.7 ± 5.6	7.3
6 mm	−18.4 ± 4.9	3.0	−12.2 ± 6.4	3.9	−12.2 ± 3.8	4.9	−14.4 ± 5.8	3.6
8 mm	−18.3 ± 4.8	4.2	−11.3 ± 6.2	5.0	−12.5 ± 3.3	5.9	−14.1 ± 5.7	4.9
10 mm	−17.3 ± 4.6	9.5	−10.4 ± 6.1	8.0	−12.2 ± 3.1	9.6	−13.4 ± 5.5	9.2

RV, right ventricle; LV, left ventricle; ε, strain; SD, standard deviation; CV, coefficients of variation; RDS, respiratory distress syndrome.

Influence of computation distance (CD)

When the measurements were analysed collectively, ε was most reproducible when the CD was 6 mm. In the analysis between groups, a CD of 10 mm gave the most reproducible measurements (with CV 13.2%) in the infants who were heaviest at birth and had the largest ventricular chambers (Group A). In the preterm infants (Groups B and C), the ε measurements were most reproducible using a CD of 6 mm (CVs 8.2 and 3.6%, respectively). In the preterm groups, the poorest reproducibility was observed using CDs of 2 and 10 mm (*Figure 2*).

Influence of frame rate

In order to examine the influence of frame rate on the reproducibility of ε measurements, the data were sorted according to tertiles of frame rate, and within each tertile the CV for each CD was calculated. The average frame rate for all loops recorded in our study was 223 ± 63 frames per second (fps) and the mean for each group was >200 fps. There was an inverse relationship between frame rates and CV which decreased from 17.3% in the lowest tertile to 11.7% in the middle and 9.6% in the highest tertile (one-way ANOVA) (*Table 3*). At rates above 179 fps, in the middle and upper tertiles, repeated measurements of ε using a CD of 6 mm gave CVs of only 7.0 and 8.0%, respectively.

Influence of heart size (diastolic ventricular length)

The longitudinal ε measurements obtained from images with frame rates >180 fps were sorted according to tertiles of diastolic length of the respective ventricles where each ε measurement was derived. Repeated measurements of systolic ε were most reproducible for infants in the first, second, and third tertiles of diastolic ventricular lengths (smallest, average, and biggest hearts,

respectively) using CDs of 4 mm (5.8%), 6 mm (4.8%), and 8 mm (8.4%) (*Table 4*).

Discussion

We have confirmed that myocardial strain imaging is both feasible and reproducible even in preterm neonates. The overall CV of 11.7% for repeated measurements of ε in this study compares very well with the intra-observer reproducibility in another study.[12]

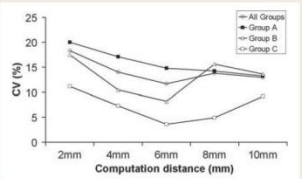

Figure 2 Reproducibility of longitudinal strain for different computation distances. Graph of coefficients of variation vs. computation distance according to groups.

The heterogeneity in the ε values seen between the three walls in our study is very similar to other studies,[5,6] albeit the mean RV ε values are lower. This may be explained by the inclusion in our study of preterm infants with respiratory distress syndrome, in whom RV function was impaired.

We used two different methods to test the reproducibility of different CDs for measuring systolic ε in neonatal hearts. In the first method, repeated measurements were made by the same observer who resampled the same digitally stored myocardial velocity loops; each new measurement was made using slightly different data because of the slightly different sampling site (or ROI) as well as the altered CD. The second method was employed with the aim to eliminate the intra-observer's inconsistencies of placing the ROI in different positions for the best ε curve. The differences in the measured ε values were related only to variations in the CD, and showed that there were no consistent variations resulting from the processing algorithm. In this study, a total of 590 offline measurements were taken, consisting of 295 paired measurements from 59 different segments in 20 infants, repeated 2 weeks apart, and used to test the reproducibility of five different CDs.

This study did not test the variability of repeated acquisitions or measurements by different observers, nor did it consider the

Table 3 Reproducibility of longitudinal strain sorted according to tertiles of frame rate

Computation distance	First (135–178 fps)		Second (179–247 fps)		Third (248–423 fps)	
	Mean $\varepsilon \pm$ SD (%)	CV (%)	Mean $\varepsilon \pm$ SD (%)	CV (%)	Mean $\varepsilon \pm$ SD (%)	CV (%)
2 mm	−23.3 ± 8.6	22.2	−17.1 ± 5.6	16.4	−20.5 ± 7.4	11.0
4 mm	−22.7 ± 7.6	17.5	−18.1 ± 6.6	10.7	−19.7 ± 7.0	9.5
6 mm	−22.4 ± 7.8	15.3	−17.2 ± 6.2	7.0	−19.4 ± 6.9	8.0
8 mm	−21.7 ± 7.3	16.6	−17.2 ± 6.0	11.6	−18.9 ± 7.1	9.7
10 mm	−20.4 ± 6.4	14.9	−16.5 ± 5.8	12.8	−18.5 ± 7.4	10.0
Mean CV		17.3 ± 2.9*		11.7 ± 3.4		9.6 ± 1.1

fps, frames per second; ε, strain; SD, standard deviation; CV, coefficients of variation.
*$P < 0.05$ ANOVA test, first vs. second tertiles and first vs. third tertiles.

Table 4 Reproducibility of longitudinal strain sorted according to tertiles of diastolic ventricular length (FR > 180 fps)

Computation distance	First (13.0–17.4 mm)		Second (17.5–23.0 mm)		Third (23.1–31.7 mm)	
	Mean $\varepsilon \pm$ SD (%)	CV (%)	Mean $\varepsilon \pm$ SD (%)	CV (%)	Mean $\varepsilon \pm$ SD (%)	CV (%)
2 mm	−16.0 ± 5.1	12.6	−18.5 ± 6.1	10.3	−25.0 ± 5.7	9.2
4 mm	−16.5 ± 6.2	5.8	−18.8 ± 6.4	7.9	−24.8 ± 4.2	9.6
6 mm	−16.0 ± 6.4	6.6	−17.9 ± 6.4	4.8	−23.8 ± 4.1	9.8
8 mm	−15.7 ± 6.8	13.2	−17.4 ± 6.0	10.9	−24.0 ± 4.9	8.4
10 mm	−14.8 ± 6.6	10.9	−16.5 ± 5.8	12.0	−23.5 ± 4.8	10.0
Mean CV		9.8 ± 3.4		9.2 ± 2.9		9.4 ± 0.6

$n = 25$. No statistical differences between all three mean CV on ANOVA testing.
FR, frame rate; fps, frames per second; ε, strain; SD, standard deviation; CV, coefficients of variation.

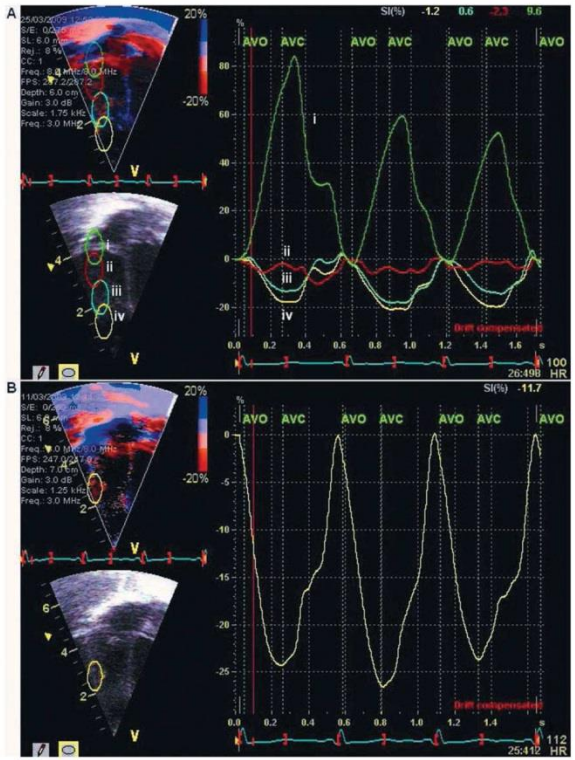

Figure 3 Variation of strain by sampling sites. (*A*) Examples of strain curves obtained at different sampling sites, all using a strain length (computation distance) of 6 mm. At site (i), longitudinal strain is positive because of the influence of the lateral wall of the right atrium, which elongates during systole. Sites (ii) and (iv) in mid and apex of the right ventricular free wall, respectively, give good-quality traces, whereas a sampling site at the base of the right ventricular wall (ii) show an intermediate pattern presumably because of contributions from both atrial and ventricular myocardium. (*B*) A good-quality strain curve obtained from the middle portion of the right ventricular free wall, as used in this study. N.B. In right ventricular strain measurements, 'AVO' and 'AVC' represent pulmonary valve opening and closing, respectively.

variability that can occur if different machines or echocardiographic systems are used. Each of these factors in clinical practice introduces more variability. We also did not test the reproducibility of strain rate which in a pilot study we found to be noisier than strain, in small infants, such that it may be difficult to use this parameter clinically.

Determinants of the reproducibility of myocardial strain

We have found that 6 mm is the most appropriate CD to be used when measuring myocardial longitudinal ε in preterm infants. Shorter CDs gave worse reproducibility, probably because of increased noise in the signals. Longer CDs were expected to be more reproducible because of more averaging and smoothing, but they also gave poorer reproducibility in repeated measurements, probably because the ROI included adjacent structures such as the papillary muscles, the mitral and tricuspid annuli, and atria (*Figure 3*). In the larger term infants with a mean birth weight of 3.7 kg, increasing the CD to 10 mm improved the reproducibility between measurements. This suggests that the CD to be used for measuring ε should be tailored to the size of the ventricle or infant.

Nestaas *et al.*[14] investigated the influence of different strain lengths (or CD) and ROI on two-segment ε and strain rate measurement in neonatal hearts. They found that the ROI size of 1 mm long by 3 mm wide with a CD of 10 mm gave the lowest beat-to-beat variation in a two-segment analysis of infants born at term. This is in keeping with our findings in the term infants. However, in the smaller preterm infants, 6 mm would be the optimal CD to be used in a single segment longitudinal ε analysis.

Our data have shown conclusively that the reproducibility of repeated measurements improved with higher frame rates, across all the CD tested. We think this is the most likely explanation for improvements in the reproducibility of measurements in the smaller ventricles seen in our study as images were acquired from the smaller infants at higher frame rates. We recommend acquiring tissue Doppler images at frame rates $>$180 fps, in order to optimize the reproducibility of myocardial deformation imaging, in keeping with the general consensus that frame rates $\geq$200 fps help reduce the random noise component of the post-processing of myocardial strain and strain rate.[16] It is particularly important to obtain high frame rates in neonates whose heart rates are higher than in the children and adults. The average frame rates in other neonatal myocardial deformation studies were between 190 and 300 fps.[5,14]

Limitations

The ROI size (10 $\times$ 5 mm) used in this study was larger than those used in other studies. The rationale for this was to obtain the best possible signal-to-noise ratio to highlight the differences between two measurements in comparing the different CD in the analysis of longitudinal ε in the middle segment of each wall. The total length used for ε calculation in this study ranged from 12 to 20 mm. Most computation lengths would not have exceeded the length of the ventricular walls, considering that the diastolic ventricular chamber lengths in this study were between 17.5 and 29.6 mm. However, we recognize that the ε values obtained are derived from the whole ventricular walls rather than the middle segment only. If a more accurate representation of segmental ε within each ventricle is required for clinical purposes, then the ROI length would have to be reduced. The ROI width could also be reduced in proportion to the thickness of the ventricular wall. The length and width of the ROI (1 $\times$ 3 mm) as recommended by Nestaas *et al.* may be applicable in this population.[14]

We found that the LV ε had the highest variation. One explanation could be difficulty in aligning the ultrasound beams to the motion of the LV free wall in neonates with suboptimal apical windows. Great care should be taken during image acquisition to ensure that the angle between the ultrasound beam and the direction of myocardial movement is less than 20%.

Conclusion

Myocardial deformation imaging is a practical and reproducible echocardiographic technique for assessing regional longitudinal LV and RV function in both term and preterm neonates. We recommend using a CD (strain length) of 6 mm for the offline analysis of segmental strain in preterm infants. A CD of 10 mm is appropriate in term infants with larger hearts. All myocardial velocity loops should be acquired at frame rates above 180 fps.

Supplementary data

Supplementary data are available at *European Journal of Echocardiography* online.

Conflict of interest: none declared.

Funding

This study was funded by departmental fund.

References

1. Harada K, Orino T, Yasuoka K, Tamura M, Takada G. Tissue Doppler imaging of left and right ventricles in normal children. *Tohoku J Exp Med* 2000;**191**:21–9.
2. Kapusta L, Thijssen JM, Cuypers MHM, Peer PGM, Daniëls O. Assessment of myocardial velocities in healthy children using tissue Doppler imaging. *Ultrasound Med Biol* 2000;**26**:229–37.
3. Frommelt PC, Ballweg JA, Whitstone BN, Frommelt MA. Usefulness of Doppler tissue imaging analysis of tricuspid annular motion for determination of right ventricular function in normal infants and children. *Am J Cardiol* 2002;**89**:610–3.
4. Mori K, Nakagawa R, Nii M, Edagawa T, Takehara Y, Inoue M *et al.* Pulsed wave Doppler tissue echocardiography assessment of the long axis function of the right and left ventricles during the early neonatal period. *Heart* 2004;**90**:175–80.
5. Pena JLB, da Silva MG, Faria SCC, Salemi VMC, Mady C, Baltabaeva A *et al.* Quantification of regional left and right ventricular deformation indices in healthy neonates by using strain rate and strain imaging. *J Am Soc Echocardiogr* 2009;**22**:369–75.
6. Nestass E, Stoylen A, Brunvand L, Fugelseth D. Tissue Doppler derived longitudinal strain and strain rate during the first 3 days of life in healthy term neonates. *Pediatr Res* 2009;**65**:357–62.
7. Weidemann F, Eyskens B, Jamal F, Mertens L, Kowalski M, D'Hooge J *et al.* Quantification of regional left and right ventricular radial and longitudinal function in healthy children using ultrasound-based strain rate and strain imaging. *J Am Soc Echocardiogr* 2002;**15**:20–8.
8. Roberson DA, Cui W, Chen Z, Madronero LF, Cuneo BF. Annular and septal Doppler tissue imaging in children: normal z-score tables and effects of age, heart rate, and body surface area. *J Am Soc Echocardiogr* 2007;**20**:1276–84.
9. Ekici F, Atalay S, Ozcelik N, Ucar T, Yilmaz E, Tutar E. Myocardial tissue velocities in neonates. *Echocardiography* 2007;**24**:61–7.

10. Patel N, Mills J, Cheung M. Assessment of right ventricular function using tissue Doppler imaging in infants with pulmonary hypertension. *Neonatology* 2009;**96**:193–9.
11. Wei Y, Xu J, Xu T, Fan J, Tao S. Left ventricular systolic function of newborns with asphyxia evaluated by tissue doppler imaging. *Pediatr Cardiol* 2009;**30**:741–6.
12. Joshi S, Edwards JM, Wilson DG, Wong JK, Kotecha S, Fraser AG. Reproducibility of myocardial velocity and deformation imaging in term and preterm infants. *Eur J Echocardiogr* 2010;**11**:44–50.
13. Marwick TH. Measurement of strain and strain rate by echocardiography: ready for prime time? *J Am Coll Cardiol* 2006;**47**:1313–27.
14. Nestaas E, Stoylen A, Sandvik L, Brunvand L, Fugelseth D. Feasibility and reliability of strain and strain rate measurement in neonates by optimizing the analysis parameters settings. *Ultrasound Med Biol* 2007;**33**:270–8.
15. Nestaas E, Stoylen A, Fugelseth D. Optimal types of probe, and tissue Doppler frame rates, for use during tissue Doppler recording and off-line analysis of strain and strain rate in neonates at term. *Cardiol Young* 2008;**18**:502–11.
16. Sutherland GR, Di Salvo G, Claus P, D'Hooge J, Bijnens B. Strain and strain rate imaging: a new clinical approach to quantifying regional myocardial function. *J Am Soc Echocardiogr* 2004;**17**:788–802.

Paediatric Respiratory Reviews 14 (2013) 242–249

Contents lists available at SciVerse ScienceDirect

Paediatric Respiratory Reviews

CME article

Long term cardiovascular consequences of chronic lung disease of prematurity

Chuen Yeow Poon, Martin Oliver Edwards, Sailesh Kotecha *

Department of Child Health, School of Medicine, Cardiff University, University Hospital of Wales, Heath Park, Cardiff CF14 4XN, UK

EDUCATIONAL AIMS THE READER WILL BE MORE FAMILIAR WITH

- The lung pathology of chronic lung disease of prematurity (CLD)
- The aetiology, clinical effects, investigations and treatment of pulmonary hypertension in neonates and infants with CLD
- The long term cardiovascular (pulmonary and systemic circulations) sequelae of CLD
- The association between airway disease and vascular dysfunction

ARTICLE INFO

Keywords:
Bronchopulmonary dysplasia
Chronic lung disease of prematurity
Arterial hypertension
Pulmonary arterial hypertension
Arterial stiffness
Lung development

SUMMARY

Pulmonary arterial (PA) hypertension in preterm infant is an important consequence of chronic lung disease of prematurity (CLD) arising mainly due to impaired alveolar development and dysregulated angiogenesis of the pulmonary circulation. Although PA pressure and resistance in these children normalise by school age, their pulmonary vasculature remains hyper-reactive to hypoxia until early childhood. Furthermore, there is evidence that systemic blood pressure in preterm born children with or without CLD is mildly increased at school age and in young adulthood when compared to term-born children. Arterial stiffness may be increased in CLD survivors due to increased smooth muscle tone of the pre-resistance and resistance vessels rather than the loss of elasticity in the large arteries. This review explores the long term effects of CLD on the pulmonary and systemic circulations along with their clinical correlates and therapeutic approaches.

INTRODUCTION

Advances in both perinatal and neonatal care over the past two decades have improved the survival of very preterm births but morbidity is significant among the survivors.[1–3] Chronic lung disease of prematurity (CLD), often also called bronchopulmonary dysplasia (BPD), is one of the most common sequelae in preterm births. Despite the improvements in neonatal care, the incidence of CLD has remained unchanged, although the incidence of severe CLD has decreased.[4] It has been reported that up to a fifth of infants born ≤ 32 weeks gestation progress to develop CLD.[5] CLD is prevalent in up to 40% of very low birth weight survivors and the incidence increases with decreasing birth weight affecting especially those born at less than 1 kg in birth weight.[6,7]

Survivors of CLD have been reported to have increased respiratory symptoms and abnormal pulmonary function in childhood and beyond when compared to preterm and term controls.[8–11] In this review, we will explore cardiovascular consequences of preterm birth and CLD from the neonatal period through to adulthood.

LUNG DEVELOPMENT AND GROWTH

The human lungs go through five different stages in their developments; embryonic (3–7 weeks), pseudoglandular (7–16 weeks), canalicular (16–26 weeks), saccular (26–36 weeks) and alveolar (36 weeks to 2 years).[12,13] The primary respiratory acini consisting of respiratory bronchioles, alveolar ducts and rudimentary alveoli develop during the late canalicular stage of lung development. During the saccular stage, the airspaces branch and expand to form saccules, surfactant is synthesized by type II cells and capillaries become closely associated with type I cells. Alveolar formation, maturation and proliferation occur during the alveolar stage resulting in a significant increase in the surface area for gas exchange.

The formation of primary respiratory acini is the critical period of lung development when gas exchange can occur and determines the limit of viability of preterm births. Infants born extremely preterm (≤28 weeks gestation) are at the late canalicular or early saccular stages of lung development, where gas exchange is inefficient, and are at risk of disrupted alveolarisation. Antenatal corticosteroids administration accelerates lung maturation and increases surfactant production[14] but caution is required for their long term consequences on lung growth and neurodevelopment especially after repeated courses of treatment.[15]

* Corresponding author. Tel.: +44 2920 744187; fax: +44 2920 744283.
E-mail addresses: pooncy@cardiff.ac.uk (C.Y. Poon), edwardsmo@cardiff.ac.uk (M.O. Edwards), kotechas@cardiff.ac.uk (S. Kotecha).

1526-0542/$ – see front matter © 2012 Elsevier Ltd. All rights reserved.
http://dx.doi.org/10.1016/j.prrv.2012.08.003

LUNG PATHOLOGY IN CHRONIC LUNG DISEASE OF PREMATURITY

The introduction of surfactant treatment has improved the survival of immature, extremely preterm infants and has changed the clinical and pathological course of CLD.[16] In post mortem of infants born in the surfactant era, an impairment of acinar development as evidenced by fewer and larger alveoli has been described.[17]

Animal studies have shown that vascular endothelial growth factor (VEGF), an angiogenic growth factor that is essential for vascular development, plays an important role in normal alveolar development.[18,19] Decreased levels of VEGF protein have been found in lung tissues of infants who died from CLD but not consistently.[20–22] These findings lead to the hypothesis that disruption of normal lung angiogenesis may contribute to dysregulated alveolarisation as observed in CLD; the "vascular hypothesis" of lung development.[23] The impairment of angiogenesis results in reduction in the number and size of intra-acinar pulmonary arteries and total cross-sectional area of the pulmonary vascular bed, thus increasing pulmonary vascular resistance.[24,25] In addition, there is also evidence of increased muscularisation of the pulmonary arteries, along with reduction of alveoli numbers, in infants who die from CLD.[26,27] Extremely preterm infants are at high risk of developing pulmonary arterial hypertension (PAH) due to the combination of increase in pulmonary arterial medial thickness and pulmonary vascular resistance as a result of dysregulated angiogenesis.

PULMONARY CIRCULATION CONSEQUENCES OF PRETERM BIRTHS

During the neonatal period to infancy

Newborn infants undergo significant haemodynamic changes during the transition from foetal to neonatal life. At birth, the aeration of the lungs and improved oxygenation of neonatal blood result in a dramatic fall in pulmonary vascular resistance and up to 10-fold increase in pulmonary blood flow. Any external stimuli such as hypoxia, hypercarbia, acidosis, cold or failure of lung expansion will disrupt or reverse the normal transition from foetal to neonatal circulation. Surfactant deficiency and immature pulmonary parenchyma and vessel development, as described above, may exacerbate the situation. Failure of this postnatal adaptation of the circulation can lead to pulmonary hypertension thus a vicious cycle of worsening hypoxia, acidosis and eventual cardiac failure.

Respiratory distress syndrome is the commonest cause of respiratory failure and pulmonary hypertension in extremely preterm infants. The pulmonary arterial (PA) pressure usually falls with the improvement of respiratory function. Surfactant administration, optimal ventilation management and maintenance of good alveolar and arterial oxygenation are essential in the management of acute RDS, also resulting in decreased PA pressure. Hypoxia, sepsis, pneumonia, hypothermia, pulmonary oedema secondary to patent ductus arteriosus or fluid overload among other risk factors can trigger a pulmonary hypertensive crisis in these infants. The acute increase in pulmonary vascular resistance can cause poor right ventricular function, impaired cardiac output and oxygen delivery, increased pulmonary oedema and the risk of sudden death.

PAH is defined as a mean PA pressure ≥ 25 mmHg at rest measured by cardiac catheterization or an estimated systolic PA pressure ≥ 40 mmHg on echocardiography.[28] Although the true prevalence of PAH in infants with CLD is unknown, a range between 17%–25% has been reported in individual studies.[29,30] The mean PA pressures of CLD infants with pulmonary hypertension were found to be around 43 mmHg by cardiac catheterization and these patients with severe pulmonary hypertension are at high risk of death during the first six months of diagnosis.[31,32]

Cardiac catheterization is the gold standard for the diagnosis of PAH. However, this procedure is very invasive and may not be available in all centres with neonatal intensive care units. Echocardiography, despite its limitations, is recommended as the main screening tool for pulmonary artery hypertension in CLD patients in many centres. Estimated systolic PA pressure can be derived from tricuspid regurgitant (TR) jet flow by using the modified Bernoulli equation and appears to have a good correlation with cardiac catheterization.[33] However, estimation of systolic PA pressure from TR jet flow is not always possible as only between 44% and 61% of infants and young children respectively with CLD have a measurable TR jet.[34,35] In the absence of TR jet flow, the ratio between pulmonary flow acceleration time (AT) and ejection time (ET) can be useful as it is inversely related to PA pressure estimated from TR jet or measured directly at cardiac catheterization.[34,36] Other qualitative echocardiographic findings such as right atrial enlargement, right ventricular hypertrophy and/or dilatation, septal flattening and pulmonary dilatation have been used to detect PAH but their predictive values are relatively poor.[37]

Inhaled nitric oxide (iNO) acts on guanylate cyclase to stimulate cyclic guanosine monophosphate formation which activates protein kinase-G to effect eventual smooth muscle relaxation within the pulmonary circulation. The reduction of pulmonary vascular resistance and improvement of pulmonary blood flow and oxygenation make iNO the ideal treatment for infants with pulmonary hypertension.

In addition to its pulmonary vasodilating effects, animal studies have shown iNO to upregulate VEGF and stimulate alveolar and pulmonary vascular growth in neonatal rats exposed to hyperoxia.[38] Similar alveolar development enhancement has been observed in preterm lambs with CLD treated with iNO.[39] In view of encouraging animal studies, it is reasonable to postulate that iNO may prevent development of CLD in preterm infants via promotion of alveolarisation. However, a systematic review of studies evaluating the use of iNO as an early rescue therapy for hypoxic respiratory failure in preterm infants at risk of developing CLD has not shown improved survival or decrease in rates of CLD.[40]

Supplemental oxygen reverses hypoxic pulmonary vasoconstriction, improving oxygen saturation, decreasing pulmonary vascular resistance and improving right ventricular performance.[41] Long term supplemental oxygen therapy is considered the standard treatment for PAH associated with CLD[25] and a target oxygen saturation range of 91–95% should be aimed for these patients.[42] Supplemental oxygen may reduce the pulmonary vascular resistance seen in CLD. Weaning of supplemental oxygen should be gradual while maintaining target oxygen saturation levels as hypoxia will potentiate proliferation of pulmonary vascular smooth muscle cells and trigger pulmonary vasoconstriction.[43]

It is assumed that the gradual fall in PA pressure in CLD infants indirectly reflects the gradual weaning of supplemental oxygen and that PA pressure normalise once the infants are successfully weaned to breathing in room air. Evans and Archer refuted this assumption by showing that up to a third of preterm infants recovering from hyaline membrane disease when discharged

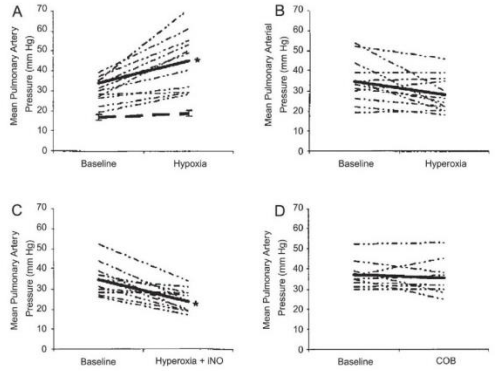

Figure 1. Individual effects of hypoxia (A), hyperoxia (B), hyperoxia + iNO (C), and calcium channel blockers (CCB) (D) on mean pulmonary artery pressure (PAP) compared with normoxic baseline measurements in children with CLD of prematurity. The mean PAP increased and decreased significantly ($p<0.01$) in response to hypoxia and hyperoxia + iNO, respectively, from normoxic baseline value. There was no change in mean PAP to either oxygen alone or CCB.
Light dashed lines represent measurements made in individual patients. The solid line displays mean values for the study group. (*Reproduced by kind permission of American Thoracic Society from Mourani et al*[49]).

home in air had evidence of raised PA pressure as assessed by Doppler echocardiography.[44] Another study reported that PA pressure in infants with CLD remains persistently increased until the end of first year of life.[45] These findings have led to the advice of monitoring PA pressure or its surrogate markers with serial echocardiography for persistent normalization after discontinuation of supplemental oxygen.[31]

From early childhood to adulthood

Fitzgerald et al studied the PA pressure of survivors of CLD (defined as oxygen dependence at 28 days with or without chest radiograph changes in the study) in early childhood by measuring PA AT:ET ratio.[46] They noted that nearly one quarter of CLD survivors have increased PA pressure, which was demonstrated across the range of severity of CLD in early childhood. These survivors of CLD from the pre-surfactant era with raised PA pressure often did not exhibit any clinical features of PAH; hence they may have been exposed to subclinical hypoxaemia. This study also noted an improving PA AT:ET ratio with increasing age in these children, suggesting improvement during childhood. In another study of CLD in the pre-surfactant era of children less than 2.5 years of age showed that up to one third of children have raised PA pressure assessed using PA AT:ET ratio and TR jet velocity, which were found to be inversely correlated.[34] Eight of 11 subjects with PAH responded to oxygen challenge with a decrease in PA pressure by at least 5 mmHg and it is postulated that increased muscularisation of the pulmonary arterioles may be the cause for the lack of response to the oxygen challenge.

Pre-school survivors of CLD from the post-surfactant have been noted to have higher PA pressures, estimated by TR jet velocity, compared to control subjects (30.4±6.9 mmHg vs 23.3±5.3 mmHg).[47] In the same study, CLD survivors had subclinical ventricular dysfunction using the myocardial performance index (also known as Tei index). A Finnish study on school-aged CLD survivors from the surfactant era did not find any evidence of raised PA pressure using echocardiographic Doppler assessment of TR jet and PA AT:ET ratio when compared to the term and preterm controls without CLD.[48] The findings from this study suggest that increased pulmonary vascular resistance associated with CLD resolves by school age.

Although pulmonary vascular resistance and PA pressures in CLD survivors appear to normalise by school age, pulmonary vascular reactivity to changes in oxygen tension and inhaled nitric oxide may persist into adolescence.[49] (Figure 1) Sartori et al found that term-born adults who were diagnosed with transient perinatal hypoxic pulmonary hypertension have significantly greater increases in their PA pressures at high altitude when compared to normal controls[50] but it is unknown whether children who had CLD in infancy have similar PA hyper-reactivity. Mourani et al reported that acute hypoxia increases mean pulmonary artery pressure by more than 20% in children who had severe CLD suggesting that the risk for pulmonary vasoconstriction due to hypoxia persists beyond 5 years of age.[49] Inhaled nitric oxide significantly augmented the vasodilator response of the PA to oxygen in children with CLD suggesting a marked reversible component. (Figure 2) The responsiveness to inhaled nitric oxide may indicate a likely response to a mechanistically similar agent such as sildenafil in the treatment of pulmonary artery hypertension associated with CLD.[51,52] Table 1 summarises the current and potential future treatments for established PAH in children.[53,54]

SYSTEMIC CIRCULATION CONSEQUENCES OF PRETERM BIRTHS

During the neonatal period to infancy

Preterm infants are particularly susceptible to haemodynamic instability and hypotension in the early neonatal period. The inability of the immature myocardium to cope with the sudden increase in peripheral vascular resistance of the extrauterine circulation during the transition period is associated with low systemic and cerebral blood flow, which may lead to intraventricular haemorrhage and adverse neurodevelopmental outcome.[55,56] In addition to the above, hypotension, generally

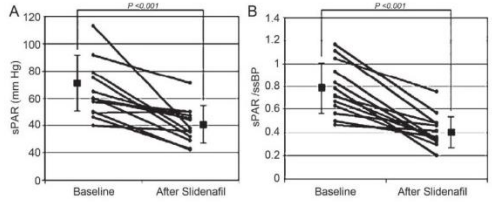

Figure 2. Changes in systolic pulmonary artery pressure (A) and pulmonary/systemic artery pressure (B) measured by echocardiogram after prolonged sildenafil treatment (range, 25-334 days) (*Reproduced by kind permission of Elsevier from Mourani et al*[52]).

accepted as the mean blood pressure (BP) less than the gestational age of the infant in weeks, could be secondary to patent ductus arteriosus, high ventilation pressure resulting in reduced preload, peripheral vasodilatation in infants born to mothers with chorioamnionitis, sepsis and relative adrenal insufficiency.

It is important to note that although BP is most commonly used indicator of circulatory status, it does not reflect systemic blood flow as studies have shown very weak or no association between BP and systemic blood flow.[57,58] Echocardiographic measurements of left and right ventricular output and superior vena cava flow are repeatable measures of systemic blood flow,[59,60] although care must be taken in the interpretation of ventricular output values with blood shunting at the ductal and atrial levels in the first few days of life. In addition, quantification of ductal and atrial size and flow, right ventricular systolic arterial pressure and myocardial performance would be valuable in eliciting possible aetiology for hypotension and/or poor perfusion and guiding treatment. However, due to lack of 24 hours availability of echocardiography in many neonatal intensive care units, blood pressure and other indirect measures such as urine output, capillary refill time, base deficit and serum lactate levels are still widely used to assess tissue perfusion.

Although inotropes such as dopamine, dobutamine, and adrenaline have been shown to be effective in the treatment of hypotension in preterm neonates, there is no evidence that shows any improvement in clinical outcome in response to specific

Table 1
Summary of the current and potential future treatments for established PAH.

Drug class (name)	Mechanism of action	Comment
Current therapies		
1. Calcium channel blockers Nifedipine, amlodipine	Blocks calcium influx into the smooth muscle cells peripheral arteries causing vasodilatation.	Therapeutic success depends on response to vasodilator challenge. High non-response rate (70-90%) to vasodilator challenge in children with severe PAH. Less commonly used now with other new targeted therapy emerging.
2. Prostacyclins Epoprostenol	Binding with prostacylin receptors increases cAMP and the activation of protein kinase A which leads to the cascade that eventually causes vasodilatation. Also activate other prostanoid receptors.	Continuous intravenous infusion limits use. Evidence of improved survival in children with PAH.
Iloprost		Inhaled form, up to eight administrations daily. Therapeutic success seen in post-operative congenital heart disease patients. Poor compliance and side effects limits use.
3. Endothelin receptor antagonist Bosentan	Blockade of endothelin-1 receptors. Endothelin-1 is a potent vasoconstrictor and mitogenic agent on vascular smooth muscle.	Lower PA pressure and resistance in adults with PAH. Safety profile and delay in disease progression proven in children.
4. Phosphodiesterase-5 inhibitors Sildenafil	Increases cGMP levels and promote pulmonary vasodilatation. Also inhibits both smooth muscle proliferation and platelet aggregation.	Useful in weaning of nitric oxide therapy and in PAH related to CLD. Approved for use in children with PAH in Europe. Improves mean PA pressure and pulmonary vascular resistance index.
Tadalafil		Once a day dosing, better compliance. Similar haemodynamic profile to sildenafil in children.
Novel/Potential therapies		
1. Tyrosine kinase inhibitors (also known as platelet-derived growth factor (PDGF) receptor antagonist) Imatinib	Blocks PDGF receptors. PDGF is involved in vascular remodelling, mitogenic signalling and smooth muscle recruitment.	Clinical and haemodynamic improvement in patients with severe refractory PAH. Phase III randomised, placebo-controlled clinical trial underway. Long term side effects include left ventricular dysfunction and heart failure.
2. Bone-derived endothelial progenitor cells (EPCs)	Repair and regenerate blood vessels	Injection of EPCs into pulmonary circulation results in regeneration of pulmonary arteriole endothelium. Animal trials underway.
Soluble guanylate cyclase (GC) stimulator Riociguat (BAY 63-2521)	Vasodilatation due to direct action on GC to increase cGMP without involving of nitric oxide pathway	Soluble GC expression and activity up-regulated in PAH and increases sensitivity of soluble GC to nitric oxide. Currently in Phase II trial for treating idiopathic PAH

inotropes.[61] Hydrocortisone has been shown to increase BP in inotrope resistant hypotension and permit weaning of other inotropic support.[62]

The use of corticosteroid therapy, especially with dexamethasone, for the treatment of CLD was a common practice. Short course dexamethasone use in preterm infants with CLD has been shown to cause acute transient left ventricular hypertrophy, which can lead to symptomatic left ventricular outflow tract obstruction or left ventricular diastolic dysfunction.[63,64]

From early childhood to adulthood

In 1989, Barker and colleagues identified an association between low birth weight (LBW) and increased risk of hypertension, carotid arteriosclerosis, and mortality from coronary heart disease in adulthood.[65] Many of these studies would have included subjects born prematurely, therefore it is reasonable to speculate that survivors of CLD may also be at risk of future cardiac disease. Many studies have since demonstrated an association between LBW and increased systemic blood pressure (BP) in later life, either with a higher systolic BP[66] or both systolic and diastolic BP.[67,68]

Besides LBW, preterm birth is also strongly related to elevated systolic BP in young men[69] and elevated systolic and diastolic BP in adolescents.[70] The mean systolic BP of teenagers and young adults born preterm were found to be 5 to 6 mmHg (range 0–15 mmHg) higher than those born at term. This magnitude of increase in BP on a population has been translated to an increase of 25% in cardiovascular deaths.[71] More recently, Bonamy et al noted that higher systolic BP in boys and higher diastolic BP in both boys and girls who were born extremely preterm at 2.5 years of age.[72] The prevalence of hypertension in ex-preterm school-aged children, adolescent and adults has been quoted to be in the range of 10–25%, 16% and 6–10% respectively.[73] Not all studies, however, reported a difference in systolic BP in pre-pubertal children born preterm compared to the control group.[74,75] A recent systematic review and meta-analysis of whether preterm birth predicts higher systolic BP in later life found that preterm birth is associated with a higher systolic BP (2.5 mmHg) than infants born at term.[76]

The findings above have led to the hypothesis that elastin synthesis is impaired as a result of foetal intra-uterine growth retardation causing the large elastic arteries to be stiff.[77] Extreme preterm birth itself may also affect elastin synthesis of the large artery. The incorporation of elastin into the large arterial vessel walls is greatest during the third trimester of pregnancy and falls rapidly after birth.[77] Extra-uterine growth in extremely preterm infants is usually sub-optimal when compared to uncomplicated in-utero growth due to inadequate nutrition and additional energy requirements associated with preterm births and its complications. Therefore, infants born extremely preterm may also suffer from impaired vascular elastogenesis leading to stiffer large arteries, an important risk factor for cardiovascular disease and predictor of cardiovascular mortality.[78]

There are other proposals to explain hypertension observed in ex-preterm infants, including impaired intra-uterine renal growth, impaired endothelium function and accelerated weight gain after birth.[79–81] Glomerulogenesis is markedly reduced in preterm infants compared to term controls as a result of interrupted renal development secondary to preterm birth.[80] Although there is continued renal growth postnatally, it may be impaired in preterm infants.[82,83] Subjects with systemic hypertension have decreased number of nephrons. Lazdam et al demonstrated that vascular structure and function are impaired in young adults born preterm that exhibit an increase in systolic BP in adult life.[79] Vohr et al found adolescents born preterm who exhibited accelerated weight gain between birth and 36 months also have higher systolic and diastolic BP.[81]

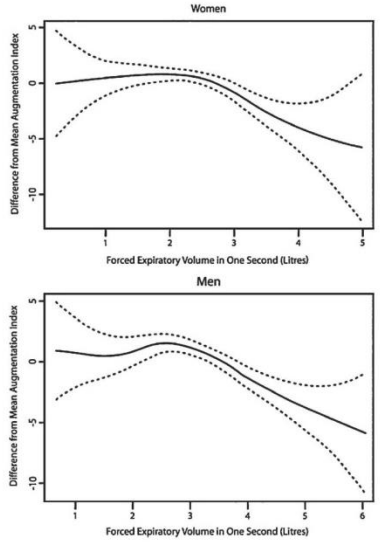

Figure 3. The association between augmentation index and FEV1 in men and women. (*Reproduced by kind permission of Elsevier from Janner et al*[85]).

Airway disease and vascular dysfunction

There is increasing interest and evidence to suggest that lung disease per se maybe a risk factor for arterial stiffness. In adults with chronic obstructive pulmonary disease (COPD) an association with increased risk of cardiovascular disease such as stroke, hypertension and myocardial infarction has been reported. There are several potential mechanisms for this association, including systemic inflammation, oxidative stress and hypoxia, reduced exercise tolerance and sympathetic activation.[84]

Janner et al reported that COPD (in men) is weakly associated with arterial stiffness and they showed a significant non-linear relationship between augmentation index and FEV_1 in men and women (see Figure 3).[85] Bolton et al have also reported an increased augmentation index in association with poor lung function in children born extremely preterm, independently of gestational age or birth weight.[86] Whether CLD is also a risk factor for vascular dysfunction in later life is unknown.

Arterial stiffness and arterial wave reflection

Pulse wave velocity (PWV) represents the speed of blood flow through the artery and augmentation index (AIx) is a measure of the enhancement of central aortic pressure by a reflected pulse wave. PWV is a direct measure of arterial stiffness and AIx, calculated as the ratio of augmented pressure to pulse pressure and expressed in percent, is an indirect surrogate measure of arterial stiffness with additional information concerning wave reflection. Both PWV and AIx are important predictor of cardiovascular mortality as both increased arterial stiffness and premature return of reflected waves in late systole increase systolic BP and thus the load on the LV.[87] AIx is found to be closely associated with traditional cardiovascular risk factors in younger individuals.[88] The main determinants of AIx are age, heart rate, height, gender, central BP and aortic PWV.

The relationship between prematurity alone and arterial stiffness has also been reviewed. Studies have demonstrated that both prematurity[89,90] and LBW[68,91] are inversely related to measures of large artery stiffness and wave reflection, both major determinants of large artery haemodynamics. The association between LBW and increased arterial stiffness is seen mainly in the preterm population as many studies do not demonstrate this association in children or adults born at term with LBW.[92–94] However there is considerable heterogeneity in the methods used to assess arterial stiffness and this is shown in the recent systematic review by Norman on LBW and vascular abnormalities although he concludes that the evidence does indicate there is an association between LBW and vascular pathology in later life.[95]

Arterial stiffness is associated with higher risk of cardiovascular disease and evidence from an adult population study showed that a 1 m/s increase in pulse wave velocity (PWV) relates to a 14% increase in total cardiovascular events.[78] The recent Enigma study of young adults aged 21 years with LBW and EPICure study of extremely preterm (≤25 weeks) 11 years old children did not show a difference in aortic PWV compared to control subjects.[88,92] However, McEniery and colleagues reported that extremely preterm children have significantly elevated aortic augmentation pressure and index. This finding suggests an increase in smooth muscular tone of the pre-resistance and resistance vessels, indicating an abnormally high peripheral vascular resistance.[88] This result echoes those found in Lurbe et al's study on LBW children[91] and Bonamy et al's study on preterm female adolescents.[67]

The finding by McEniery et al challenge the hypothesis of impaired elastin synthesis in extremely preterm infants and indicate that the problem may lie with the smaller, peripheral muscular vessels rather than the proximal large elastic arteries.[88] The precise mechanisms underlying the elevated AIx in extremely preterm children have yet to be fully understood. Studies on adults have shown that 3–6 months of aerobic exercise decreases AIx in elderly patients[96] and patients with coronary artery disease[97] but no such interventional studies have been done in children as yet.

Further work, however, is required to establish the extent of arterial stiffness and endothelial dysfunction in preterm born children who do and do not develop CLD and whether such findings have longer term consequences. The need for a standardised approach to the assessment of arterial stiffness and endothelial function in children is required.

FURTHER RESEARCH

The number of preterm infants who survive into adulthood will continue to rise with improved neonatal care. As survivors of CLD are at higher risk of developing PAH, new non-invasive methods to assess surrogate markers of PAH are required. Newer techniques such as myocardial deformation imaging and velocity-encoded magnetic resonance imaging are reproducible and may prove to be useful in the screening and assessment of PAH in CLD survivors of different ages.[98,99] Additionally, more studies involving infants and children with CLD to assess lung growth and vascular development are required. The use of hyperpolarised inert gases (helium, xenon) show promise but need careful evaluation and validation. Long term longitudinal studies of blood pressure, arterial stiffness and wave reflections monitoring are required to detect any changes and/or progress of hypertension and arterial stiffness in this group of subjects to understand the effects of LBW and/or prematurity on the systemic haemodynamics.

CONCLUSION

CLD survivors are at increased risk of early development of pulmonary hypertension due to dysregulated angiogenesis of the pulmonary circulation and impaired alveolarisation. Despite normalisation of PA pressure and resistance, their PA still exhibit hyper-reactivity to hypoxic stresses in adulthood. There is emerging evidence of mild increase in blood pressure and arterial stiffness in this population but until more longitudinal research is performed, a definitive cardiovascular risk of preterm birth and CLD cannot be quantified. Early detection and preventative measures such as smoking and obesity prevention programs are vital in this ever increasing population as they get older. There is no doubt that CLD survivors will contribute disproportionately to the burden of adult cardiovascular disease in the future and this calls for more research into the follow-up of the altered pulmonary and systemic haemodynamics in this population as well as early mechanisms and interventional strategies.

PRACTICE POINTS

- Pulmonary hypertension is common from the neonatal period until infancy in CLD survivors
- Targeted screening for pulmonary hypertension in CLD survivors is advocated in view of evidence of subclinical pulmonary hypertension and increased pulmonary vascular reactivity to hypoxia
- Adolescents and young adults who suffered from CLD have mildly elevated blood pressure, hence are at increased risk of cardiovascular events as they age compared to their counterparts born at term or without CLD.

RESEARCH DIRECTIONS

- Further research into new non-invasive techniques for earlier detection of pulmonary hypertension is essential to prevent or delay the condition
- Further research into targeting the repair, regeneration and prevention of abnormal proliferation of pulmonary vessel may lead to novel therapeutic strategies
- Longer term follow-up studies on the blood pressure and arterial stiffness in CLD survivors

References

1. Manktelow BN, Draper ES, Annamalai S, Field D. Factors affecting the incidence of chronic lung disease of prematurity in 1987, 1992, and 1997. *Arch Dis Child Fetal Neonatal Ed* 2001;**85**:F33–5.
2. De Kleine MJK, Den Ouden AL, Kollée LAA, et al. Lower mortality but higher neonatal morbidity over a decade in very preterm infants. *Paediatr Perinat Epidemiol* 2007;**21**:15–25.
3. Kotecha S, Allen J. Oxygen therapy for infants with chronic lung disease. *Arch Dis Child Fetal Neonatal Ed* 2002;**87**:F11–4.
4. Smith VC, Zupancic JAF, McCormick MC, et al. Trends in severe bronchopulmonary dysplasia rates between 1994 and 2002. *J Pediatr* 2005;**146**:469–73.
5. Zeitlin J, Draper ES, Kollée L, et al. Differences in rates and short-term outcome of live births before 32 weeks of gestation in europe in 2003: Results from the mosaic cohort. *Pediatrics* 2008;**121**:e936–44.
6. Darlow BA, Cust AE, Donoghue DA. Improved outcomes for very low birthweight infants: Evidence from new zealand national population based data. *Arch Dis Child Fetal Neonatal Ed* 2003;**88**:F23–8.
7. Farstad T, Bratlid D, Medbø S, Markestad T. The Norwegian Extreme Prematurity Study G. Bronchopulmonary dysplasia – prevalence, severity and predictive factors in a national cohort of extremely premature infants. *Acta Paediatr* 2011;**100**:53–8.
8. Vrijlandt EJLE, Boezen HM, Gerritsen J, Stremmelaar EF, Duiverman EJ. Respiratory health in prematurely born preschool children with and without bronchopulmonary dysplasia. *J Pediatr* 2007;**150**:256–61.

9. Hennessy EM, Bracewell MA, Wood N, et al. Respiratory health in pre-school and school age children following extremely preterm birth. *Arch Dis Child* 2008;**93**:1037–43.
10. Kairamkonda VR, Richardson J, Subhedar N, Bridge PD, Shaw NJ. Lung function measurement in prematurely born preschool children with and without chronic lung disease. *J Perinatol* 2008;**28**:199–204.
11. Doyle LW, Faber B, Callanan C, Freezer N, Ford GW, Davis NM. Bronchopulmonary dysplasia in very low birth weight subjects and lung function in late adolescence. *Pediatrics* 2006;**118**:108–13.
12. Kotecha S. Lung growth: Implications for the newborn infant. *Arch Dis Child Fetal Neonatal Ed* 2000;**82**:F69–74.
13. Joshi S, Kotecha S. Lung growth and development. *Early Hum Dev* 2007;**83**: 789–94.
14. Vyas J, Kotecha S. Effects of antenatal and postnatal corticosteroids on the preterm lung. *Arch Dis Child Fetal Neonatal Ed* 1997;**77**:F147–50.
15. Beck JC, Mitzner W, Johnson JWC, et al. Betamethasone and the rhesus fetus: Effect on lung morphometry and connective tissue. *Pediatr Res* 1981;**15**: 235–40.
16. Jobe AH, Bancalari E. Bronchopulmonary dysplasia. *Am J Respir Crit Care Med* 2001;**163**:1723–9.
17. Husain AN, Siddiqui NH, Stocker JT. Pathology of arrested acinar development in postsurfactant bronchopulmonary dysplasia. *Hum Pathol* 1998;**29**:710–7.
18. Jakkula M, Le Cras TD, Gebb S, et al. Inhibition of angiogenesis decreases alveolarization in the developing rat lung. *Am J Physiol Lung Cell Mol Physiol* 2000;**279**:L600–7.
19. Le Cras TD, Markham NE, Tuder RM, Voelkel NF, Abman SH. Treatment of newborn rats with a vegf receptor inhibitor causes pulmonary hypertension and abnormal lung structure. *Am J Physiol Lung Cell Mol Physiol* 2002;**283**:L555–62.
20. Bhatt AJ, Pryhuber GS, Huyck H, Watkins RH, Metlay LA, Maniscalco WM. Disrupted pulmonary vasculature and decreased vascular endothelial growth factor, flt-1, and tie-2 in human infants dying with bronchopulmonary dysplasia. *Am J Respir Crit Care Med* 2001;**164**:1971–80.
21. Lassus P, Turanlahti M, Heikkila P, et al. Pulmonary vascular endothelial growth factor and flt-1 in fetuses, in acute and chronic lung disease, and in persistent pulmonary hypertension of the newborn. *Am J Respir Crit Care Med* 2001;**164**:1981–7.
22. Currie AE, Vyas JR, MacDonald J, Field D, Kotecha S. Epidermal growth factor in the lungs of infants developing chronic lung disease. *Eur Respir J* 2001;**18**:796–800.
23. Thebaud B, Abman SH. Bronchopulmonary dysplasia: Where have all the vessels gone? Roles of angiogenic growth factors in chronic lung disease. *Am J Respir Crit Care Med* 2007;**175**:978–85.
24. Bush A, Busst CM, Knight WB, Hislop AA, Haworth SG, Shinebourne EA. Changes in pulmonary circulation in severe bronchopulmonary dysplasia. *Arch Dis Child* 1990;**65**:739–45.
25. Stenmark KR, Abman SH. Lung vascular development: Implications for the pathogenesis of bronchopulmonary dysplasia. *Annu Rev Physiol* 2005;**67**: 623–61.
26. Hislop AA, Haworth SG. Pulmonary vascular damage and the development of cor pulmonale following hyaline membrane disease. *Pediatr Pulmonol* 1990;**9**:152–61.
27. Margraf LR, Tomashefski Jr JF, Bruce MC, Dahms BB. Morphometric analysis of the lung in bronchopulmonary dysplasia. *Am Rev Respir Dis* 1991;**143**:391–400.
28. Haworth SG. The management of pulmonary hypertension in children. *Arch Dis Child* 2008;**93**:620–5.
29. Bhat R, Salas AA, Foster C, Carlo WA, Ambalavanan N. Prospective analysis of pulmonary hypertension in extremely low birth weight infants. *Pediatrics* 2012;**129**:e682–9.
30. An HS, Bae EJ, Kim GB, et al. Pulmonary hypertension in preterm infants with bronchopulmonary dysplasia. *Korean Circ J* 2010;**40**:131–6.
31. Khemani E, McElhinney DB, Rhein L, et al. Pulmonary artery hypertension in formerly premature infants with bronchopulmonary dysplasia: Clinical features and outcomes in the surfactant era. *Pediatrics* 2007;**120**:1260–9.
32. Slaughter JL, Pakrashi T, Jones DE, South AP, Shah TA. Echocardiographic detection of pulmonary hypertension in extremely low birth weight infants with bronchopulmonary dysplasia requiring prolonged positive pressure ventilation. *J Perinatol* 2011;**31**:635–40.
33. Skinner JR, Stuart AG, O'Sullivan J, Heads A, Boys RJ, Hunter S. Right heart pressure determination by doppler in infants with tricuspid regurgitation. *Arch Dis Child* 1993;**69**:216–20.
34. Benatar A, Clarke J, Silverman M. Pulmonary hypertension in infants with chronic lung disease: Non-invasive evaluation and short term effect of oxygen treatment. *Arch Dis Child Fetal Neonatal Ed* 1995;**72**:F14–9.
35. Mourani PM, Sontag MK, Younoszai A, Ivy DD, Abman SH. Clinical utility of echocardiography for the diagnosis and management of pulmonary vascular disease in young children with chronic lung disease. *Pediatrics* 2008;**121**: 317–25.
36. Kosturakis D, Goldberg SJ, Allen HD, Loeber C. Doppler echocardiographic prediction of pulmonary arterial hypertension in congenital heart disease. *Am J Cardiol* 1984;**53**:1110–5.
37. Mourani PM, Mullen M, Abman SH. Pulmonary hypertension in bronchopulmonary dysplasia. *Prog Pediatr Cardiol* 2009;**27**:43–8.
38. Lin YJ, Markham NE, Balasubramaniam V, et al. Inhaled nitric oxide enhances distal lung growth after exposure to hyperoxia in neonatal rats. *Pediatr Res* 2005;**58**:22–9.
39. Bland RD, Albertine KH, Carlton DP, MacRitchie AJ. Inhaled nitric oxide effects on lung structure and function in chronically ventilated preterm lambs. *Am J Respir Crit Care Med* 2005;**172**:899–906.
40. Barrington KJ, Finer N. Inhaled nitric oxide for respiratory failure in preterm infants. *Cochrane Database Syst Rev* 2010. CD000509.
41. Kotecha S, Allen J. Oxygen therapy for infants with chronic lung disease. *Archives of Disease in Childhood - Fetal and Neonatal Edition* 2002;**87**:F11–4.
42. Shaw NJ, Kotecha S. Management of infants with chronic lung disease of prematurity in the united kingdom. *Early Hum Dev* 2005;**81**:165–70.
43. Parker TA, Abman SH. The pulmonary circulation in bronchopulmonary dysplasia. *Semin Neonatol* 2003;**8**:51–61.
44. Evans NJ, Archer LN. Doppler assessment of pulmonary artery pressure during recovery from hyaline membrane disease. *Arch Dis Child* 1991;**66**(7 Spec No):802–4.
45. Subhedar NV, Shaw NJ. Changes in pulmonary arterial pressure in preterm infants with chronic lung disease. *Arch Dis Child Fetal Neonatal Ed* 2000;**82**:F243–7.
46. Fitzgerald D, Evans N, Van Asperen P, Henderson-Smart D. Subclinical persisting pulmonary hypertension in chronic neonatal lung disease. *Arch Dis Child Fetal Neonatal Ed* 1994;**70**:F118–22.
47. Kazanci E, Karagoz T, Tekinalp G, et al. Myocardial performance index by tissue doppler in bronchopulmonary dysplasia survivors. *Turk J Pediatr* 2011;**53**: 388–96.
48. Korhonen P, Hyödynmaa E, Lautamatti V, Iivainen T, Tammela O. Cardiovascular findings in very low birthweight schoolchildren with and without bronchopulmonary dysplasia. *Early Hum Dev* 2005;**81**:497–505.
49. Mourani PM, Ivy DD, Gao D, Abman SH. Pulmonary vascular effects of inhaled nitric oxide and oxygen tension in bronchopulmonary dysplasia. *Am J Respir Crit Care Med* 2004;**170**:1006–13.
50. Sartori C, Allemann Y, Trueb L, Delabays A, Nicod P, Scherrer U. Augmented vasoreactivity in adult life associated with perinatal vascular insult. *Lancet* 1999;**353**:2205–7.
51. Farquhar M, Fitzgerald DA. Pulmonary hypertension in chronic neonatal lung disease. *Paediatr Respir Rev* 2010;**11**:149–53.
52. Mourani PM, Sontag MK, Ivy DD, Abman SH. Effects of long-term sildenafil treatment for pulmonary hypertension in infants with chronic lung disease. *J Pediatr* 2009;**154**. 379–384.e372.
53. Ivy D. Advances in pediatric pulmonary arterial hypertension. *Curr Opin Cardiol* 2012;**27**:70–81.
54. Baliga RS, MacAllister RJ, Hobbs AJ. New perspectives for the treatment of pulmonary hypertension. *Br J Pharmacol* 2011;**163**:125–40.
55. Osborn DA, Evans N, Kluckow M. Hemodynamic and antecedent risk factors of early and late periventricular/intraventricular hemorrhage in premature infants. *Pediatrics* 2003;**112**:33–9.
56. Hunt RW, Evans N, Rieger I, Kluckow M. Low superior vena cava flow and neurodevelopment at 3 years in very preterm infants. *J Pediatr* 2004;**145**: 588–92.
57. Groves AM, Kuschel CA, Knight DB, Skinner JR. Relationship between blood pressure and blood flow in newborn preterm infants. *Arch Dis Child Fetal Neonatal Ed* 2008;**93**:F29–32.
58. Kluckow M, Evans N. Low superior vena cava flow and intraventricular haemorrhage in preterm infants. *Arch Dis Child Fetal Neonatal Ed* 2000;**82**:F188–94.
59. Groves AM, Kuschel CA, Knight DB, Skinner JR. Echocardiographic assessment of blood flow volume in the superior vena cava and descending aorta in the newborn infant. *Arch Dis Child Fetal Neonatal Ed* 2008;**93**:F24–8.
60. Evans N, Kluckow M. Early determinants of right and left ventricular output in ventilated preterm infants. *Arch Dis Child Fetal Neonatal Ed* 1996;**74**:F88–94.
61. Evans N. Which inotrope for which baby? *Arch Dis Child Fetal Neonatal Ed* 2006;**91**:F213–20.
62. Seri I, Tan R, Evans J. Cardiovascular effects of hydrocortisone in preterm infants with pressor-resistant hypotension. *Pediatrics* 2001;**107**:1070–4.
63. Skelton R, Gill AB, Parsons JM. Cardiac effects of short course dexamethasone in preterm infants. *Arch Dis Child Fetal Neonatal Ed* 1998;**78**:F133–7.
64. Mourani PM, Ivy DD, Rosenberg AA, Fagan TE, Abman SH. Left ventricular diastolic dysfunction in bronchopulmonary dysplasia. *J Pediatr* 2008;**152**: 291–3.
65. Barker DJ, Osmond C, Golding J, Kuh D, Wadsworth ME. Growth in utero, blood pressure in childhood and adult life, and mortality from cardiovascular disease. *BMJ* 1989;**298**:564–7.
66. Hack M, Schluchter M, Cartar L, Rahman M. Blood pressure among very low birth weight (<1.5 kg) young adults. *Pediatr Res* 2005;**58**:677–84.
67. Bonamy A-KE, Bendito ANA, Martin H, Andolf E, Sedin G, Norman M. Preterm birth contributes to increased vascular resistance and higher blood pressure in adolescent girls. *Pediatr Res* 2005;**58**:845–9.
68. Doyle LW, Faber B, Callanan C, Morley R. Blood pressure in late adolescence and very low birth weight. *Pediatrics* 2003;**111**:252–7.
69. Johansson S, Iliadou A, Bergvall N, Tuvemo T, Norman M, Cnattingius S. Risk of high blood pressure among young men increases with the degree of immaturity at birth. *Circulation* 2005;**112**:3430–6.
70. Edstedt Bonamy A-K, Bengtsson J, Nagy Z, De Keyzer H, Norman M. Preterm birth and maternal smoking in pregnancy are strong risk factors for aortic narrowing in adolescence. *Acta Pediatr* 2008;**97**:1080–5.
71. Norman M. Preterm birth: An emerging risk factor for adult hypertension? *Semin Perinatol* 2010;**34**:183–7.
72. Bonamy A-KE, Kallen K, Norman M. High blood pressure in 2.5-year-old children born extremely preterm. *Pediatrics* 2012;**129**:e1199–204.

73. Poplawska K, Dudek K, Koziarz M, et al. Prematurity-related hypertension in children and adolescents. *Int J Pediatr* 2012;**2012**:537936.
74. Mikkola K, Leipala J, Boldt T, Fellman V. Fetal growth restriction in preterm infants and cardiovascular function at five years of age. *J Pediatr* 2007;**151**. 494–499.e492.
75. Bracewell MA, Hennessy EM, Wolke D, Marlow N. The epicure study: Growth and blood pressure at 6 years of age following extremely preterm birth. *Arch Dis Child Fetal Neonatal Ed* 2008;**93**:F108–14.
76. de Jong F, Monuteaux MC, van Elburg RM, Gillman MW, Belfort MB. Systematic review and meta-analysis of preterm birth and later systolic blood pressure. *Hypertension* 2012;**59**:226–34.
77. Martyn CN, Greenwald SE. Impaired synthesis of elastin in walls of aorta and large conduit arteries during early development as an initiating event in pathogenesis of systemic hypertension. *Lancet* 1997;**350**:953–5.
78. Vlachopoulos C, Aznaouridis K, Stefanadis C. Prediction of cardiovascular events and all-cause mortality with arterial stiffness: A systematic review and meta-analysis. *J Am Coll Cardiol* 2010;**55**:1318–27.
79. Lazdam M, de la Horra A, Pitcher A, et al. Elevated blood pressure in offspring born premature to hypertensive pregnancy. *Hypertension* 2010;**56**:159–65.
80. Rodriguez MM, Gomez AH, Abitbol CL, Chandar JJ, Duara S, Zilleruelo GE. Histomorphometric analysis of postnatal glomerulogenesis in extremely preterm infants. *Pediatr Dev Pathol* 2004;**7**:17–25.
81. Vohr BR, Allan W, Katz KH, Schneider KC, Ment LR. Early predictors of hypertension in prematurely born adolescents. *Acta Pediatr* 2010;**99**:1812–8.
82. Schmidt IM, Chellakooty M, Boisen KA, et al. Impaired kidney growth in low-birth-weight children: Distinct effects of maturity and weight for gestational age. *Kidney Int* 2005;**68**:731–40.
83. Drougia A, Giapros V, Hotoura E, Papadopoulou F, Argyropoulou M, Andronikou S. The effects of gestational age and growth restriction on compensatory kidney growth. *Nephrol Dial Transplant* 2009;**24**:142–8.
84. Clarenbach CF, Thurnheer R, Kohler M. Vascular dysfunction in chronic obstructive pulmonary disease: Current evidence and perspectives. *Expert Rev Respir Med* 2012;**6**:37–43.
85. Janner JH, McAllister DA, Godtfredsen NS, Prescott E, Vestbo Jr. Is chronic obstructive pulmonary disease associated with increased arterial stiffness? *Respir Med* 2012;**106**:397–405.
86. Bolton CE, Stocks J, Hennessy E, et al. The epicure study: Association between hemodynamics and lung function at 11 years after extremely preterm birth. *J Pediatr* 2012.
87. Laurent S, Cockcroft J, Van Bortell L, et al. Expert consensus document on arterial stiffness: Methodological issues and clinical applications. *Eur Heart J* 2006;**27**:2588–605.
88. McEniery CM, Bolton CE, Fawke J, et al. Cardiovascular consequences of extreme prematurity: The epicure study. *J Hypertens* 2011;**29**:1367–73.
89. Keijzer-Veen MG, Finken MJJ, Nauta J, et al. Is blood pressure increased 19 years after intrauterine growth restriction and preterm birth? A prospective follow-up study in the netherlands. *Pediatrics* 2005;**116**:725–31.
90. Oren A, Vos LE, Bos W-JW, et al. Gestational age and birth weight in relation to aortic stiffness in healthy young adults: Two separate mechanisms? *Am J Hypertens* 2003;**16**:76–9.
91. Lurbe E, Torro MI, Carvajal E, Alvarez V, Redon J. Birth weight impacts on wave reflections in children and adolescents. *Hypertension* 2003;**41**:646–50.
92. Miles KL, McDonnell BJ, Maki-Petaja KM, et al. The impact of birth weight on blood pressure and arterial stiffness in later life: The enigma study. *J Hypertens* 2011;**29**:2324–31.
93. Bonamy A-KE, Andolf E, Martin H, Norman M. Preterm birth and carotid diameter and stiffness in childhood. *Acta Pediatr* 2008;**97**:434–7.
94. Schack-Nielsen L, Molgaard C, Larsen D, Martyn C, Michaelsen KF. Arterial stiffness in 10-year-old children: Current and early determinants. *Br J Nutr* 2005;**94**:1004–11.
95. Norman M. Low birth weight and the developing vascular tree: A systematic review. *Acta Pediatr* 2008;**97**:1165–72.
96. Tabara Y, Yuasa T, Oshiumi A, et al. Effect of acute and long-term aerobic exercise on arterial stiffness in the elderly. *Hypertens Res* 2007;**30**:895–902.
97. Edwards DG, Schofield RS, Magyari PM, Nichols WW, Braith RW. Effect of exercise training on central aortic pressure wave reflection in coronary artery disease. *Am J Hypertens* 2004;**17**:540–3.
98. Joshi S, Edwards JM, Wilson DG, Wong JK, Kotecha S, Fraser AG. Reproducibility of myocardial velocity and deformation imaging in term and preterm infants. *Eur J Echocardiogr* 2010;**11**:44–50.
99. Poon CY, Edwards JM, Joshi S, Kotecha S, Fraser AG. Optimization of myocardial deformation imaging in term and preterm infants. *Eur J Echocardiogr* 2011;**12**: 247–54.

CME SECTION

This article has been accredited for CME learning by the European Board for Accreditation in Pneumology (EBAP). You can receive 1 CME credit by successfully answering these questions online.

(A) Visit the journal CME site at http://www.prrjournal.com/.
(B) Complete the answers online, and receive your final score upon completion of the test.
(C) Should you successfully complete the test, you may download your accreditation certificate (subject to an administrative charge).

MULTIPLE CHOICE (EDUCATIONAL) QUESTIONS

Answer true or false to the following questions

1. Pulmonary arterial hypertension:
a. Is rare in infants with chronic lung disease of prematurity
b. Can be caused by patent ductus arteriosus in preterm infants
c. Can only be diagnosed by cardiac catheterisation
d. Can be present in asymptomatic children who had chronic lung disease of prematurity
e. Can be triggered by hypoxia in older children who suffered from severe chronic lung disease of prematurity
2. Pulmonary arterial hypertension can be diagnosed:
a. If systolic pulmonary artery pressure is estimated at 35 mmHg on echocardiography
b. If a tricuspid regurgitation velocity jet of 2.5 m/s was detected
c. Reliably if septal flattening or bowing into the left ventricle is detected
d. If mean pulmonary artery pressure is 25 mmHg at rest on cardiac catheterisation
e. Using the ratio of pulmonary flow acceleration time and ejection time
3. The following are effective in treating pulmonary arterial hypertension:
a. Calcium channel blockers
b. Prostacyclins
c. Inhaled nitrous oxide
d. Sildenafil
e. Bosentan
4. Chronic lung disease of prematurity survivors:
a. Have normal pulmonary artery pressure after weaning of home supplemental oxygen during infancy
b. Do not need any monitoring of pulmonary artery pressure after discontinuation of supplemental oxygen
c. Are at risk of developing acute pulmonary hypertension at high altitude
d. May have increased risk of developing hypertension in later life
e. May have increased arterial stiffness
5. Which of the following have been proposed to explain for hypertension observed in ex-preterm subjects?
a. Impaired elastin synthesis due to intra-uterine growth retardation and preterm birth
b. Impaired intra-uterine renal growth
c. Poor weight gain after birth
d. Accelerated weight gain after birth
e. Impaired endothelial function

Magnetic Resonance Imaging 31 (2013) 1690–1694

Contents lists available at ScienceDirect

Magnetic Resonance Imaging

journal homepage: www.mrijournal.com

Assessment of pulmonary artery pulse wave velocity in children: An MRI pilot study

Chuen Y. Poon [a], Julie M. Edwards [b], C. John Evans [c], Ashley D. Harris [c], Beverly Tsai-Goodman [d], Charlotte E. Bolton [e], John R. Cockcroft [b], Richard G. Wise [c], Sailesh Kotecha [a,*]

[a] Department of Child Health, School of Medicine, Cardiff University, Cardiff, UK
[b] Wales Heart Research Institute, School of Medicine, Cardiff University, Cardiff, UK
[c] Cardiff University Brain Research Imaging Centre, School of Psychology, Cardiff University, Cardiff, UK
[d] Department of Paediatric Cardiology, Bristol Children's Hospital, Bristol, UK
[e] Nottingham Respiratory Research Unit, University of Nottingham, UK

ARTICLE INFO

Article history:
Received 25 March 2013
Revised 6 August 2013
Accepted 20 August 2013

Keywords:
Velocity-encoded MRI
Pulse wave velocity
Pulmonary artery
Children
Hypoxia

ABSTRACT

Purpose: To assess the feasibility of measuring pulmonary artery (PA) pulse wave velocity (PWV) in children breathing ambient air and 12% oxygen.
Methods: Velocity-encoded phase-contrast MR images of the PA were acquired in 15 children, aged 9–12 years, without evidence of cardiac or pulmonary diseases. PWV was derived as the ratio of flow to area changes during early systole. Each child was scanned twice, in air and after at least 20 minutes into inspiratory hypoxic challenge. Intra-observer and inter-observer variability and repeatability were also compared.
Results: PA PWV, which was successfully measured in all subjects, increased from 1.31 ± 0.32 m/s in air to 1.61 ± 0.58 m/s under hypoxic challenge ($p = 0.03$). Intra- and inter-observer coefficients of variations were 9.0% and 15.6% respectively. Good correlation within and between observers of $r = 0.92$ and $r = 0.72$ respectively was noted for PA PWV measurements. Mean (95% limit of agreement) intra- and inter-observer agreement on Bland–Altman analysis were −0.02 m/s (−0.41–0.38 m/s) and -0.28 m/s (−1.06–0.49 m/s).
Conclusion: PA PWV measurement in children using velocity-encoded MRI is feasible, reproducible and sufficiently sensitive to detect differences in PA compliance between normoxia and hypoxia. This technique can be used to detect early changes of PA compliance and monitor PAH in children.

1. Introduction

Pulmonary hypertension is the result of failure of the pulmonary circulation to buffer the pulsatile flow generated by the right ventricle (RV) leading to high flow from the RV reaching the smaller pulmonary vessels [1,2]. The loss of pulmonary artery (PA) compliance or increased PA stiffness is thought to be the early precursor to the development of pulmonary arterial hypertension (PAH). In adults with PAH, measures of PA stiffness are increased [3] and this is associated with increased mortality [4,5].

An inverse relationship between resistance and compliance of the PA circulation has been reported in subjects with or without pulmonary hypertension [6]. Prompt introduction of targeted therapies can be initiated if changes in PA stiffness are detected earlier. Reliable assessment of PA stiffness permits treatment planning and monitoring.

Recent developments in cardiac magnetic resonance imaging (MRI) techniques allow accurate non-invasive measurements of pulse wave velocity, another measure of arterial stiffness, of the PA in adults without invasive PA pressure measurements [7,8]. Techniques utilizing the flow area (QA) and transit time methods have been compared showing similar PA PWV values [9].

Pulmonary hypertension is relatively rare in children and causes include PAH associated with congenital heart disease, connective tissue disease and lung disease such as cystic fibrosis or chronic lung disease of prematurity [10]. Early targeted therapy can delay the onset of PAH, thus improving the quality of life and survival of these children. Thus far, there are no studies that measured PA PWV in children.

Furthermore, acute exposure to hypoxia causes pulmonary vasoconstriction at the arteriolar level, thus increasing pulmonary vascular resistance, PA pressure and stiffness. Adults who have suffered transient perinatal hypoxic pulmonary hypertension demonstrate significantly higher systolic pulmonary arterial pressure compared to controls at high altitudes [11]. However, there is very little data on the effects of acute hypoxia on large vessel stiffness in normal children or in vulnerable individuals including those with cardiac and respiratory conditions where the risk of PAH is high.

The main objective of this study was to establish the feasibility of measuring PA PWV in children using the QA MRI method while administering a hypoxic challenge to children within the MRI scanner as well as assessing intra- and inter-observer image analysis variability in measuring PA PWV values. We hypothesized that PA PWV will increase with hypoxia.

2. Methods

2.1. Study population

Written informed consent and assent were obtained from parents and children, respectively. The study was approved by the local research ethics committee. Fifteen 9–12-year-old children, who were born between 23 and 42 weeks of gestation, were recruited into the study. Details of subjects' neonatal and medical histories were obtained from their parents and medical records. Subjects who had patent ductus arteriosus corrected by occlusion coils or clips, ventricular septal defects or had any cardiovascular surgery to correct any congenital structural cardiac defects were excluded from the study, in addition to the other absolute contraindications to having MRI scan.

2.2. Echocardiographic examination

All subjects underwent echocardiographic examination to confirm normality of cardiac structure and function before MRI scans. The standard echocardiographic assessment using subcostal, parasternal short and long axes, apical four chamber and suprasternal views were used. Pulmonary arterial blood flow acceleration time, ejection time, and tricuspid regurgitation peak velocity, if present, were measured to approximate systolic pulmonary arterial pressure, using the modified Bernoulli equation [12].

2.3. MRI scanning setup

Every subject was initially exposed to a practice scan in a mock MRI scanner lying within the scanner with simulated background noise, prior to the actual MRI examination. Each subject was scanned twice to acquire cine images of the PA cross section, first while breathing room air and again after breathing 12% inspired oxygen (balance nitrogen) for 20 minutes. The subjects continued breathing the hypoxic inspirate during the second MRI scan. Using MRI-compatible prisms spectacles, subjects were able to watch a film on a projector screen during the scanning. Parents were permitted to comfort the child as necessary during the scanning after appropriate screening procedures.

2.4. Imaging technique

Scans were performed using a 3.0 T GE Signa HDx MRI scanner with an 8-channel phased-array cardiac coil (GE Healthcare, Bucks, UK). The protocol included three-plane localizers followed by cine images of the PA in long axis and cross-sectional view using steady-state free precession sequence. Retrospective ECG-gated phase-contrast velocity-encoded images were obtained approximately 0.5 cm above the pulmonary valve using 2-dimension gradient-echo sequence. The cine sequence parameters were: slice thickness = 7 mm, TR = 4.7 ms, TE = 2.9 ms, number of averages = 2, no. of reconstructed phases = 65, no. of acquired phases between 35 and 58 phases depending on heart rate, V_{enc} = 150 cm/s, acquisition matrix = 192 × 192, FOV = 350 mm, flip angle = 20°. The MRI examination was performed under free breathing conditions with instructions to maintain shallow breathing during image acquisition to minimize translational movement of the heart associated with respiration and to obtain normal physiological pulmonary arterial blood flow.

2.5. Hypoxic challenge

Premixed cylinders of 12% oxygen/nitrogen mixture and 100% oxygen, situated at the MR control room were obtained from British Oxygen Company Limited (BOC, Port Talbot, UK). A closed respiratory circuit was used to deliver the hypoxic challenge and supplemental oxygen. Anesthetic tubing from these two cylinders formed the inspiratory limbs that delivered humidified gases into a small mixing chamber before being inhaled by the subject via an anesthetic face mask. The excess gases and expired breaths from subjects exited the circuit through the expiratory limb, which also acted as a rebreathing reservoir necessary when the peak inspiratory flow instantaneously exceeded the gas flow rate. A high flow rate of 20 L/min was used to deliver the hypoxic oxygen mixture to prevent significant rebreathing of the previous breath.

Subjects' heart rate, oxygen saturation, inspired oxygen and end-tidal carbon dioxide levels were monitored continuously during the hypoxic challenge; 100% oxygen was titrated into the circuit to maintain the oxygen saturations between 80% and 85% if oxygen saturations decreased to below 80%. Each subject received at least 20 minutes of hypoxic challenge before the repeat PWV assessment.

2.6. Image analysis

The images were anonymized and transferred to a personal computer and analyzed using the freely available software Segment version 1.8 R1145 (http://segment.heiberg.se) [13]. The series of both magnitude and phase images showing the magnified view of the PA cross section throughout one cardiac cycle were displayed one at a time. The region of interest outlining the PA was defined manually on the magnitude images (Fig. 1A). After outlining the PA, the software calculated the cross-sectional area of the PA and the flow within the cross section from the magnitude and phase (velocity-encoded) images, respectively for each acquired phase of the cardiac cycle. Flow rate was plotted against measured cross-sectional area of the PA during early systole, which is the time between onset of flow until peak flow. Pulse wave velocity was derived from the slope of the line fitted to the flow-area data, which represents the ratio of flow change (ΔQ) and area change (ΔA) during early systole [7] (Fig. 1B).

The images were analyzed by two different observers (JME and CYP) and repeated by one of the observers (CYP), at least two weeks between analyses to measure intra- and inter-observer variability and repeatability. The observers were blinded during analysis to whether images were acquired during normoxia or hypoxia.

2.7. Statistical analysis

Statistical analyses were performed using the Statistics Package for Social Science (SPSS) version 16.0 (Chicago, IL, USA). The paired Student's *t*-test was used to compare parameters before and during hypoxic challenge. *P* value of less than 0.05 was considered significant.

Intra- and inter-observer repeatability are reported as the mean coefficients of variation (CV, in %) of all subjects, where individual subject CV was calculated using the formula: CV = (standard deviation of measurements difference/mean of the measurements) × 100.

* Corresponding author. Department of Child Health, School of Medicine, Cardiff University, Heath Park, CF14 4XN Cardiff, UK. Tel.: +44 (0) 2920 74 4187; fax: +44 (0) 2920 74 4287.
E-mail address: kotechas@cardiff.ac.uk (S. Kotecha).

0730-725X/$ – see front matter © 2013 Elsevier Inc. All rights reserved.
http://dx.doi.org/10.1016/j.mri.2013.08.006

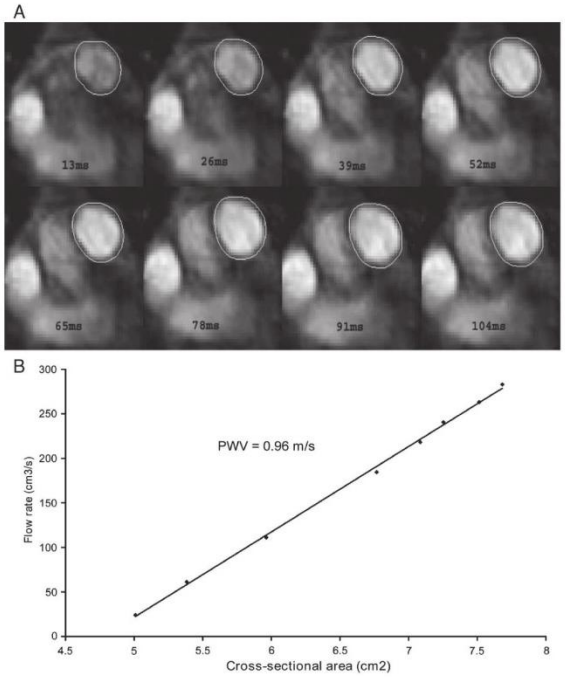

Fig. 1. (A) Magnitude images of main PA during early systole. A succession of cross-sectional images showing main PA (circled) distending during early systole. The vessel cross-sectional area and flow rate are measured at each frame during early systole. PA = pulmonary artery. (B) Derivation of PA PWV from flow rate versus cross-sectional area graph. A line is fitted to the plotted data, where PWV is determined as the line slope (change in flow over change in area). cm^3/s = centrimeter^3 per second, CSA = cross-sectional area, PA = pulmonary artery, PWV = pulse wave velocity.

Correlation and Bland–Altman analyses were also used to report intra- and inter-observer variability.

3. Results

3.1. Subject characteristics and echocardiographic data

Subject characteristics and baseline measurements of vital signs are given in Table 1. All fifteen subjects (ten males and five females) tolerated and successfully completed the MRI scanning and hypoxia challenge. The youngest subject in the study was nine years and eight months and the mean (SD) age of the study population was 11.7 (0.9) years.

None of the subjects had evidence of increased right atrial or PA pressure; 11/15 (73%) had detectable tricuspid regurgitation with velocities between 1.3 and 2.2 m/s (estimated systolic pulmonary arterial pressures 11.8–24.4 mmHg). Mean (SD) pulmonary acceleration/ejection time ratio was 0.418 (0.044) seconds.

3.2. PA PWV measurements using velocity encoded MRI

The MRI examination lasted for approximately 50–60 minutes including the 20 minutes hypoxic exposure. PA PWV measurements were successfully derived from the 15 children, both in air and during hypoxic challenge. Mean (SD) PA PWV increased significantly from 1.32 (0.32) m/s in air to 1.61 (0.58) m/s during hypoxic challenge ($P = 0.03$) (Fig. 2). The PA PWV during hypoxic challenge was noted to be lower than that in air in four subjects. The differences between the two measurements in four subjects were 0.06 m/s, 0.07 m/s, 0.21 m/s and 0.56 m/s.

3.3. Hypoxic challenge

Effective hypoxic challenge was successfully delivered to all children with oxygen saturations decreasing within 2–3 minutes, reaching a nadir and stabilizing within 10 minutes of starting the hypoxic challenge. The mean (SD) inspired O_2 was 11.2 ± 0.6 % and

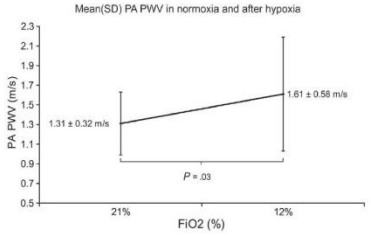

Fig. 2. Change in PA PWV in normoxia and following hypoxic challenge. Mean PA PWV increased significantly from 1.32 (0.32) m/s in air to 1.61 (0.58) m/s following hypoxic challenge ($P = 0.03$). FiO_2 = inspired oxygen, m/s = meter per second, PA = pulmonary artery, PWV = pulse wave velocity, SD = standard deviation.

end-tidal CO_2 was 4.7 ± 0.6 %. The oxygen saturations decreased significantly from a mean (SD) of 98.3% (1.6%) in air to 84.5% (3.6%) after 12% oxygen administration (mean difference 13.7%, 95% CI 11–16%, $P < 0.001$). The monitored heart rate increased by 17 bpm (95% CI 11–23 bpm, $P < 0.001$) during hypoxia from baseline.

3.4. Reproducibility and variability

Intra- and inter-observer CV were 9.0% and 15.6% with good intra- and inter-observer correlation between measurements, r = 0.92 and r = 0.72 respectively. Intra- and inter-observer measurements differences (95% limit of agreement) on Bland-Altman analysis were −0.02 m/s (−0.41–0.38 m/s) and −0.28 m/s (−1.06–0.49 m/s) (Fig. 3).

4. Discussion

This is the first MRI study to successfully measure PA PWV non-invasively in children. We have shown that using the QA method, PA PWV can be measured in children as young as 9 years of age. The facility for children to watch a film during the MRI scan is likely to have contributed significantly to the success in distracting and prevented gross movement of the child during the MRI scans. The ability to perform practice runs in a mock scanner was another factor that diminished the fear and anxiety associated with MRI scanning.

PA PWV was successfully measured in fifteen children in normoxia and after hypoxia. We chose to use the QA method in measuring main PA PWV in our children due to the smaller size and shorter length of their main PA as the latter may introduce more errors if the transit time method had been used. Furthermore, the need for much longer acquisition time, as reported previously [9], is highly impractical in our young subjects.

The mean PA PWVs of 1.3 m/s measured in our young subjects is less than the PA PWV in adults without PAH (1.96 m/s) reported by Peng et al. [7]. The difference in our observations in children could be due to the more compliant PA than their adult counterparts as have been shown in studies of healthy children and adults assessing the arterial stiffness in the systemic circulation. The aortic PWV measured in 11-year-old children by McEniery and colleagues was 4.7 m/s [14] and the aortic PWV in healthy 26–41 years healthy adults studied by Koivistoinen and colleague were 7.7 m/s in male and 7.0 m/s in females [15]. If the arterial stiffness changes with age in the pulmonary circulation were assumed to be similar to those in the systemic circulation, then our PA PWV of 1.3 m/s is likely to be representative in children without pulmonary hypertension.

PA PWV was found to be significantly higher during hypoxic challenge. This is as predicted since hypoxia promotes arteriolar vasoconstriction resulting in increased pulmonary vascular resistance and decreased pulmonary compliance. In four subjects, the PA PWV during hypoxic challenge was noted to be lower than that in air. There are several sources of variability in our measurements. The manual outlining of the MPA can be subjective and may distort PWV estimations. We also noted significant movement of the PA in our young population during scanning due to marked cardiac contraction and respiration possibly due to greater heart and respiratory rates in children; the PA movements were worse during hypoxia due to increased heart and respiratory rate. The heart rate is generally higher in children and increased further following hypoxic challenge. The heart would be contracting more hyper-dynamically under hypoxic condition and this would result in lower spatial resolution of the PA for manual outlining. It was not possible to avoid the movement effects due to respiration as the cine flow imaging of the PA cross-section takes 3–5 minutes to complete using our protocol.

Despite the above observations, we noted good repeatability in image analysis as reflected by the good CV of 9% for intra-observer measurements and low variability on the Bland-Altman analysis. The inter-observer repeatability was reasonable with CV of 15.6%. PA PWV measurements obtained by JME were generally higher than CYP with relatively good correlation, r = 0.72. We found that JME

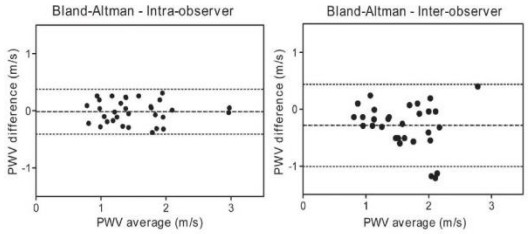

Fig. 3. Intra- and inter-observer Bland-Altman analyses. Mean (95% limits of agreement) intra- and inter-observer differences were −0.02 (−0.41–0.38) m/s and −0.28 (−1.06–0.49) m/s, respectively. Dashed line is the mean difference and dotted lines the 95% limits of agreement. m/s = meter per second, PWV = pulse wave velocity.

generally under-detected the change in PA cross-sectional area resulting in a higher PWV value.

We have used an experienced echocardiographer (JME) with experience in off-line echocardiographic images post-processing but had limited experience off-line post-processing of cardiac MRI images to compare inter-observer repeatability. Despite receiving training on manual outlining of the PA prior to performing the analysis, a higher variability and CV was observed. This reaffirms the importance of involving highly trained operator in cardiac MRI analysis to analyze the images obtained using this technique.

Ibrahim and colleague reported low intra- and inter-observer variability in both transit time and QA methods but found the standard deviations of differences between measurements in the QA method to be greater than the transit time method, albeit not significantly different [9]. In their study, the MRI images were outlined semi-automatically by bespoke computer software after the operator had marked the vessel cross-section boundary, thus minimizing errors that may occur after manual delineation of the PA cross-sectional area. Peng and colleagues reported percentage inter-scan differences to be around 10% but it is ethically difficult to envisage repeated scanning in such a young population [7].

Normobaric hypoxia was successfully delivered to all children using 12% oxygen/balance nitrogen cylinder mixture via anesthetic tubing, a small mixing chamber and anatomical face mask. In our previous study that administered 18% and 15% oxygen did not significantly decrease oxygen saturations to below 85%, hence we opted to use a 12% hypoxic challenge (manuscript in preparation). This level of hypoxia was tolerated well by all the subjects and there were no significant side effects experienced except the expected ones of mild dizziness, headache, tachycardia, and tachypnea. We set the lower limit of 80% for oxygen saturations as hypoxemia below this level was considered unethical and unacceptable.

The success of hypoxic challenge was confirmed by the measured inspired oxygen of 11.2%. The normal range of end-tidal CO_2 recorded in our subjects reassured us that the effects observed were due to hypoxia rather than changes in CO_2 levels.

In three children oxygen saturation remained above 86% during hypoxic challenge. This may be due to poor fit of the anesthetic face mask. Nevertheless, the heart rate in these subjects increased from the baseline during hypoxia but is uncertain if the PA PWV values were affected.

The main objective of this study was to establish the feasibility of measuring PA PWV in children using the QA method which we confirm is possible in children as young as 9 years of age. This study was not designed or powered to investigate differences between patient groups but clearly has the potential to non-invasively study PA PWV in children at risk of developing PAH.

There was significant movement of the PA in the slice plane between end-diastole to end-systole, especially during hypoxic challenge when the heart and respiratory rates increased. This could be a source of error to estimate PA PWV as suggested by Ibrahim et al. [9]. Manual outlining of the PA was required in all of the scans in our study. Although this can be subjective, we noted good repeatability and low variability in our study but a robust, automated vessel outlining tool based on active contouring could possibly minimize this error by avoiding operator dependency.

In conclusion, we demonstrated the feasibility of measuring PA PWV in children with phase-contrast velocity-encoded MRI using the QA method under normal and hypoxic conditions. This method was found to be reproducible with low variation in our young population. Phase-contrast velocity-encoded MRI has the potential to detect early changes in pulmonary arterial stiffness and can be used to non-invasively screen for sub-clinical pulmonary arterial hypertension in children.

References

[1] Greyson CR. The right ventricle and pulmonary circulation: basic concepts. Rev Esp Cardiol 2010;63(01):81–95.
[2] Lam C-F, Peterson TE, Croatt AJ, Nath KA, Katusic ZS. Functional adaptation and remodeling of pulmonary artery in flow-induced pulmonary hypertension. Am J Physiol Heart Circ Physiol 2005;289(6):H2334–41.
[3] Ley S, Mereles D, Puderbach M, Gruenig E, Schöck H, Eichinger M, et al. Value of MR phase-contrast flow measurements for functional assessment of pulmonary arterial hypertension. Eur Radiol 2007;17(7):1892–7.
[4] Mahapatra S, Nishimura RA, Sorajja P, Cha S, McGoon MD. Relationship of pulmonary arterial capacitance and mortality in idiopathic pulmonary arterial hypertension. J Am Coll Cardiol 2006;47(4):799–803.
[5] Gan CT, Lankhaar JW, Westerhof N, Marcus JT, Becker A, Twisk JW, et al. Noninvasively assessed pulmonary artery stiffness predicts mortality in pulmonary arterial hypertension. Chest 2007;132(6):1906–12.
[6] Lankhaar J-W, Westerhof N, Faes TJC, Tji-Joong Gan C, Marques KM, Boonstra A, et al. Pulmonary vascular resistance and compliance stay inversely related during treatment of pulmonary hypertension. Eur Heart J 2008;29(13):1688–95.
[7] Peng H-H, Chung H-W, Hsi-Yu Y, Wen-Yih IT. Estimation of pulse wave velocity in main pulmonary artery with phase contrast MRI: Preliminary investigation. J Magn Reson Imaging 2006;24(6):1303–10.
[8] Bradlow WM, Gatehouse PD, Hughes RL, O'Brien AB, Gibbs JS, Firmin DN, et al. Assessing normal pulse wave velocity in the proximal pulmonary arteries using transit time: a feasibility, repeatability, and observer reproducibility study by cardiovascular magnetic resonance. J Magn Reson Imaging 2007;25:974–81.
[9] Ibrahim E-SH, Shaffer JM, White RD. Assessment of pulmonary artery stiffness using velocity-encoding magnetic resonance imaging: evaluation of techniques. Magn Reson Imaging 2011;29(7):966–74.
[10] Berger RMF, Beghetti M, Humpl T, Raskob GE, Ivy DD, Jing Z-C, et al. Clinical features of paediatric pulmonary hypertension: a registry study. Lancet 2012;379(9815):537–46.
[11] Sartori C, Allemann Y, Trueb L, Delabays A, Nicod P, Scherrer U. Augmented vasoreactivity in adult life associated with perinatal vascular insult. Lancet 1999;353(9171):2205–7.
[12] Yock PG, Popp RL. Noninvasive estimation of right ventricular systolic pressure by Doppler ultrasound in patients with tricuspid regurgitation. Circulation 1984;70(4):657–62.
[13] Heiberg E, Sjogren J, Ugander M, Carlsson M, Engblom H, Arheden H. Design and validation of segment – freely available software for cardiovascular image analysis. BMC Med Imaging 2010;10:1.
[14] McEniery CM, Bolton CE, Fawke J, Hennessy E, Stocks J, Wilkinson IB, et al. Cardiovascular consequences of extreme prematurity: the EPICure study. J Hypertens 2011;29(7):1367–73.
[15] Koivistoinen T, Koobi T, Jula A, Hutri-Kahonen N, Raitakari OT, Majahalme S, et al. Pulse wave velocity reference values in healthy adults aged 26–75 years. Clin Physiol Funct Imaging 2007;27(3):191–6.

Appendix I – Posters presented

I1 Pulmonary and systemic haemodynamics in children born preterm: an MRI study

I2 Pulmonary artery stiffness assessment in children born preterm using velocity encoded MRI

I1 Pulmonary and systemic haemodynamics in children born preterm: an MRI study

Pulmonary and Systemic Haemodynamics in Children born Preterm: an MRI Study

Chuen Yeow Poon[1], Beverly Tsai-Goodman[4], Richard Wise[3], John R Cockcroft[2], Sailesh Kotecha[1]
[1]Department of Child Health, [2]Department of Cardiology, School of Medicine, [3]School of Psychology, Cardiff University, UK, [4]Bristol Children's Hospital, UK.

Background

- Extremely premature infants who survive the initial stormy neonatal course are at risk of developing pulmonary hypertension, systemic hypertension and atherosclerosis in adulthood.
- Cardiac MRI allows non-invasive measurements of distensibility, compliance and pulse wave velocity (PWV) of both major pulmonary and systemic arteries with good reproducibility and is able to detect subclinical changes compared to current conventional methods.
- Early detection of large artery changes as well as functional response to hypoxia may allow the development of intervention strategies to prevent the development of pulmonary hypertension and hypertension in such individuals.
- This is the first study to use cardiac MRI to investigate for subclinical changes of pulmonary hypertension and total and regional aortic stiffness in children born prematurely with and without CLD.

Aims

- To investigate if children born prematurely with CLD have lower pulmonary arterial compliance at baseline and have exaggerated response to hypoxia compared to health term controls and preterm controls who did not have CLD in infancy.
- To investigate if children born prematurely with CLD have higher total and regional aortic stiffness at baseline and have exaggerated response to hypoxia compared to health term controls and preterm controls who did not have CLD in infancy.

Methods

- Three groups (CLD group, Preterm Control group and Term Control group) of children, aged 8-12 years will be studied.
- Each child will have baseline peripheral blood pressure and non-invasive central blood pressure and pulse wave velocity measured with Sphygmocor®. Electrocardiograph and echocardiography will be done to ensure normality of cardiac structure and pulmonary pressures prior to baseline MR scan in air. After the baseline scan, the child will be exposed to 12% oxygen for 20 – 30 minutes whilst watching DVD within the MR scanner before a repeat MR scan. Oxygen saturations, end-tidal CO2 and heart rate will be constantly monitor whilst within the scanner.
- Three plane localisers will be performed with the child lying in the supine position. Pulmonary artery and aorta are identified in cine images.
- ECG-gated phase contrast images of cross sectional views are obtained 0.5 – 1cm above the pulmonary artery **(Figure 1)**. Image analysis is performed off line using cardiac image analysis software, Segment (http://segment.heiberg.se). The region of interest is semi-automatically generated around the pulmonary artery for flow and cross sectional area measurements **(Figure 2 and 3)**. The pulmonary arterial PWV (an index of compliance) is derived from early systolic instantaneous changes in blood flow with changes in the cross sectional area of the pulmonary artery.
- Aortic stiffness will be calculated using the difference in aortic cross sectional area at systole and diastole **(Figure 4)** and aortic pressure difference (reading from Sphygmocor®). Regional aortic PWV is calculated using the transit times of the systolic flow curves and the distance between two predetermined sites along the aorta **(Figures 5 and 6)**.

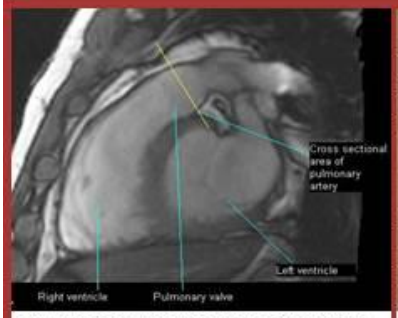

Figure 1: Pulmonary artery and position of cross sectional area as seen in Figure 2.

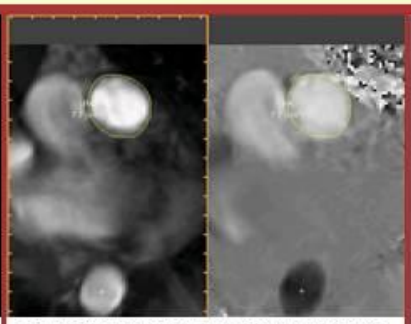

Figure 2: Magnitude and flow images of cross sectional area of pulmonary artery at systole.

Figure 3: Pulmonary artery flow curve versus time, as measured from cross sectional area in Figure 2.

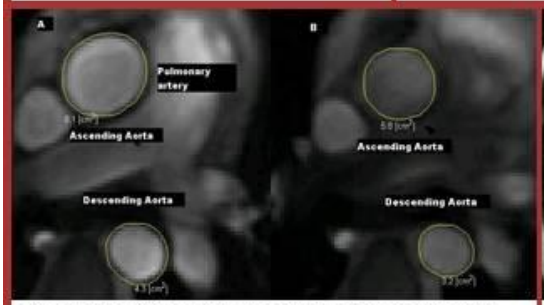

Figure 3: Cross sectional area of ascending and descending aorta at pulmonary artery bifurcation during systole (A) and diastole (B).

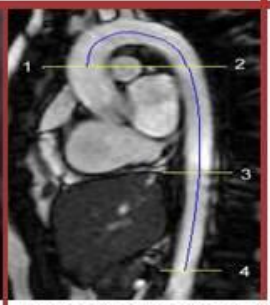

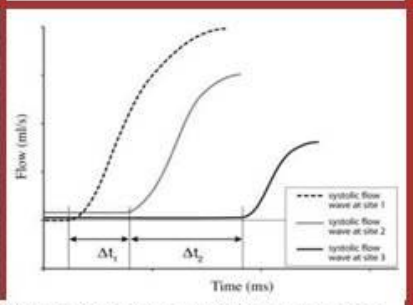

Figure 5 and 6: Regional aortic aortic PWV can be calculated but dividing the distance between 1 and 2 but the transit time, Δt. Other regions of the aorta can be calculated similiarly.

Acknowledgement

We are grateful for the Research Development Group funding from Children & Young People's Research Network for Wales for coordinating and establishing our MRI protocol for the pilot study and obtaining the data above.

I2 Pulmonary artery stiffness assessment in children born preterm using velocity encoded MRI

Pulmonary artery stiffness assessment in children born preterm using velocity-encoded MRI

Chuen Yeow Poon[1], John Evans[2], Charlotte E Bolton[3], John Cockcroft[1], Richard Wise[2], Sailesh Kotecha[1]
[1]School of Medicine, Cardiff University, Cardiff, UK, [2]School of Psychology, Cardiff University, UK,
[3]Nottingham Respiratory Biomedical Research Unit, University of Nottingham, UK.

Background

- Infants with pulmonary hypertension secondary to chronic lung disease of prematurity (CLD) have increased pulmonary arterial reactivity. It is uncertain if this persist into childhood following improvement of lung disease and normalisation of pulmonary arterial pressure.
- In the pulmonary circulation, an inverse relationship between pulmonary vascular resistance and compliance has been identified in subjects with or without pulmonary hypertension **(Figure 1)**.
- Velocity-encoded MRI allows non-invasive assessment of pulmonary artery (PA) pulse wave velocity (PWV), a measure of arterial stiffness, and detection of subclinical pulmonary hypertension.

Aim

- To assess and compare PA PWV in response to acute hypoxia in children born preterm with CLD compared to healthy preterm and term controls.

Methods

- Fifty-nine, 9-12 years old children (13 CLD, 21 Preterm Control and 25 Term Control), without any cardiac disease were recruited.
- Velocity-encoded phase-contrast MR images of the PA were acquired in air and after 20 minutes of 12% controlled hypoxia. Oxygen saturations, inspired O_2, end-tidal CO_2 and heart rate were monitored continuously during hypoxia challenge.
- ECG-gated phase-contrast images of cross sectional views of the PA were obtained 0.5 – 1cm above the pulmonary valve **(Figure 2)**.
- Offline analysis was performed using cardiac image analysis software, Segment (http://segment.heiberg.se).
- The region of interest was semi-automatically generated around the PA for flow and cross sectional area measurements, which were used to derive PA PWV (an index of compliance) as the ratio of instantaneous change in flow to cross sectional area during early systole **(Figure 3)**.

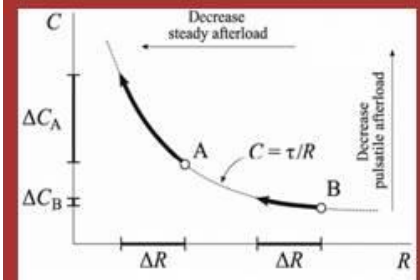

Figure 1: Resistance (R) and compliance (C) relationship in the pulmonary circulation.

The PA compliance in patient A with mild pulmonary hypertension (PH) improves more than patient B with severe PH with the same degree of reduction in R.

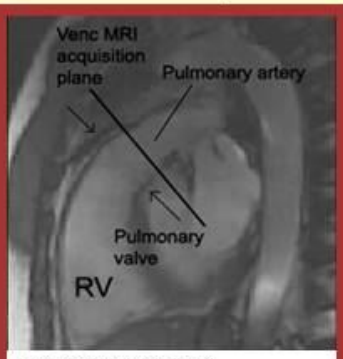

Figure 2: Oblique sagittal plane

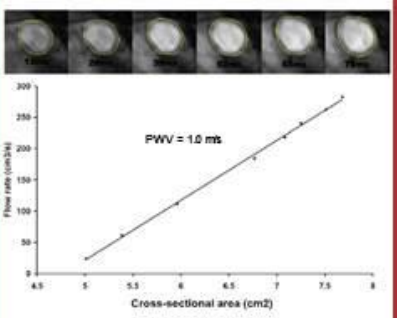

Figure 3: The graph shows flow rate against cross sectional area. PWV is determined from the gradient of the line.

Results

Parameters	CLD (Mean ± SD)	Preterm (Mean ± SD)	Term (Mean ± SD)	p-value
Number	13	21	25	
Male, number (%)	8 (62%)	10 (48%)	16 (64%)	
Gestation, wks	27.2 ± 1.0	30.5 ± 1.1	40.2 ± 1.2	<0.001
Age at study, yrs	11.5 ± 1.0	12.0 ± 0.8	11.5 ± 1.0	NS
Weight, kg	33.7 ± 4.6	50.2 ± 16.5	44.0 ±13.4	NS
Height, cm	141.3 ± 5.6	149.6 ±10.3	149.2 ± 10.6	NS
Tricuspid jet velocity, m/s	2.1 ± 0.3	2.1 ± 0.3	2.1 ± 0.4	NS
AT:ET ratio	0.40 ± 0.01	0.41 ± 0.03	0.40 ± 0.04	NS
HR in air, bpm	74 ± 7	75 ± 12	82 ± 13	NS
HR under hypoxia, bpm	88 ± 13	87 ± 14	90 ± 9	NS
RR in air, /min	19 ± 4	23 ± 4	23 ± 4.4	NS
RR under hypoxia, /min	23 ± 3	26 ± 5	24 ± 3.1	NS
Oxygen saturation in air, %	98 ± 2	98 ± 1	98 ± 2	NS
Oxygen saturation under hypoxia, %	83 ± 2	83 ± 5	85 ± 4	NS
Inspired O_2, %	10.9 ± 1.4	11.3 ± 1.4	11.2 ± 0.7	NS
PA PWV in air, m/s	1.29 ± 0.42	1.35 ± 0.38	1.25 ± 0.31	NS
PA PWV under hypoxia, m/s	1.87 ± 0.70	1.55 ± 0.56	1.51 ± 0.48	NS
PA PWV change with hypoxia, m/s	0.58 ± 0.50	0.21 ± 0.40	0.23 ± 0.47	*= 0.025 ‡= 0.043

*CLD vs. Preterm, ‡CLD vs. Term

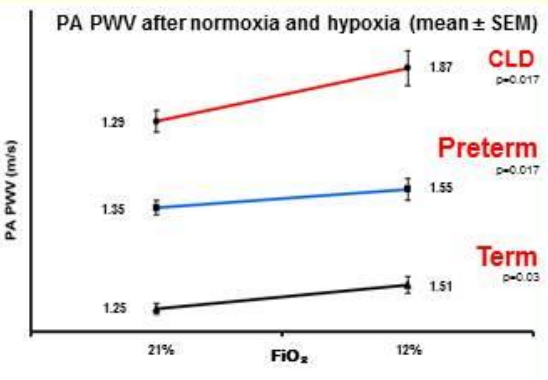

Conclusion

- The baseline PA PWV was very similar between the three groups but the children who had CLD in infancy had an exaggerated response to hypoxia, thus may be at higher risk of developing pulmonary hypertension in the future.

Acknowledgement

We are grateful to Children & Young People's Research Network for Wales and Mason's Medical Research Foundation for the grants received for the development and funding for the project.